

Prototype X

A Cost-Based Design Optimization of an Upper Stage Liquid Propulsion Module with Green-Storeable Propellants

Master Research Thesis

P.M.F. (Pepijn) Elferink

Prototype X Concept

A Cost-Based Design Optimization of an Upper Stage Liquid Propulsion Module with Green-Storable Propellants

by

P.M.F. (Pepijn) Elferink

to obtain the degree of Master of Science,
in the field of Aerospace Engineering,
at the Delft University of Technology,
to be defended publicly on Thursday May 12, 2022 at 13:00.

Student number: 4444582
Project duration: September 23, 2021 – May 12, 2022
Thesis committee: Dr. ir. B.V.S. Jyoti, TU Delft, supervisor, Ast. Prof. TU Delft
Prof. Dr. E.K.A. Gill, TU Delft, Chairman Committee
Ir. R. Noomen, TU Delft, External Committee Member
Ir. J. Quesada Mañas, SolvGE, Co-supervisor, Chief Technical Officer (CTO)
Dr. D. Mengü, SolvGE, Co-supervisor, Sr. Propulsion Eng.

This thesis is confidential and cannot be made public until May 12, 2023.

An electronJ.ic version of this thesis work is available at: <http://repository.tudelft.nl/>.

Cover image credited to the European Space Agency [1].

The work in this thesis was supported by SolvGE.
Their cooperation is hereby gratefully acknowledged.



Copyright © Department of Space System
Engineering (SSE)

All rights reserved.



Preface

The work presented in this Master's thesis is the culmination of six years of studying at the faculty of Aerospace Engineering and marks the end of a fantastic period in my life and brings a new chapter as a graduated Space Engineer. Over the past six years, through hard, stressful but mostly great times, I learned to tackle academic challenges while working in an exciting environment that the Technical University of Delft offers. Nonetheless, this all would not have been possible without the support of the great people around me that came along with me on my journey of becoming an Aerospace Engineer. I want to take this opportunity to show my gratitude and thank these people.

Direct acknowledgment for their contributions to this work in particular goes to B.V.S. Jyoti, Jaime and Dinesh. Their generous support, interest and feedback helped me to stay motivated at times when the academics of the whole endeavor seemed daunting. B.V.S. Jyoti, has been an involved, honest and enthusiastic supervisor with an energy that never failed to amaze me. Due to her perseverance and will to succeed it felt like a team effort. Your selfless guidance is something I will not forget. Jaime helped me to keep the quality of the work high through his guidance and his sharp eye for detail and nuance. Your critical but justified feedback provided the best conditions for me to succeed in this thesis. Dinesh has always been ready to meet, even though we had to cross through cyberspace and tackle the time zones. His understanding and positive attitude throughout this period helped me to keep the overview and direct me to the scope that sometimes was hard to find. Thank you for the positive impact you had on my thesis. Till we meet again, physically. Lastly, I would like to extend my gratitude to the entire SolvGE family. The melting-pot of different expertise's and passions helped me to keep the joy in working on this Master's thesis.

To my parents, Ellen and Rolf, that have been lovingly on my side throughout all phases of my life. Without them, I would not have been in a good place in the life I am in now. Both literally and figuratively. Although it is sometimes challenging to explain what I am doing on an academic level, they have always tried their hardest to understand. The way you selflessly support your children is something I have learned in life to be very special. My sister has always been my 'first stage' in life, boosting me and guiding me through challenges that make me a better person, engineer, and hopefully, brother. Kim suggested studying Aerospace Engineering, combining my love for air- and spacecraft, essentially being the foundation of this research work. Thank you for being my sister. Not least, I would like to thank my uncle Robbert for being a significant example in my life. With his experience, both in life, as well as in the engineering industry, he has been an important person to me. Your advice and support help me to always push for personal growth.

To Thijs, Philip and Bram, friends I consider closest in my life. I would like to thank you for being there also for the awesome times and the more delicate ones. You provided me with the distraction from studies and work that kept me sane.

Finally, to all the people I met in Delft during my studies that grew to become my friends, I would like to thank you for making the (sometimes) boring lectures and challenging assignments more fun. You know who you are.

"All designs are wrong, just how wrong?"

- Elon Musk

*P.M.F. (Pepijn) Elferink
Delft, April 2022*

Abstract

This paper investigates the cost-benefit, payload performance and technical feasibility of green storable upper stage design concepts on their potential implementation with existing launchers. Since the demand for reliable, safe, and cost-effective transport to space is growing, it is necessary to find sustainable rocket propellant solutions. Green fuels that react hypergolic with hydrogen peroxide as oxidisers can provide distinct advantages in the performance, complexity and reliability when integrated into systems with severe geometrical constraints, such as upper-stage propulsion modules.

This research aims to quantify the cost-effectiveness of green storable upper stage concepts on the commercial market prospect. This is done through detailed research into design concepts operating on various storable propellant combinations. These various design concepts for different propellant combinations are described by the hypothetical storable upper stage called the "Prototype X". As an oxidizer, concentrated hydrogen peroxide (HTP), combined with non-carcinogenic, non-toxic, and non-corrosive green storable fuels, can provide reliable and environmentally friendly propulsion solutions. Moreover, green hypergolic storable propellants will lower the operational cost, reduce system complexity and are safer to procure, store and handle. These "Prototype X" upper stage design concepts will be analysed and optimised on their cost-per-kg payload characteristic.

Detailed mass and cost optimization analysis was performed for a green storable launcher upper-stage concept. It was found that HTP together with screened storable fuels shows promising and acceptable performance characteristics in terms of specific impulse and density specific impulse. Implementation of these green storable propellants into the upper stage design *results in dry mass reductions of over 20%* compared to the conventional cryogenic hydrolox upper stage design. Although current 'green' storable propellants can reduce the cost-per-flight of the upper stage by 8.9%, resulting from constructive cost reductions in development, manufacturing and (pre-launch) operation phases, their wet mass burden reduces the payload performance by at least 308.09%. This is mainly due to the reduced performance of current 'green' storable propellants, compared to cryogenic propellants. Therefore, a cross-over analysis was conducted for the "Prototype X" storable design concept. Here the focus was on finding the required performance of a hypothetical storable "Fuel X" that would make the storable concept economically attractive. Calculations suggest that further development in storable propellant engineering can *improve the payload performance of the storable upper stage concept by +37.79%* for the same wet mass, compared to the cryogenic design, while *reducing the geometrical dimensions of the upper stage by roughly 33%*. Storable 'green' propellants significantly reduce complexity and add reliability and safety to the system, potentially improving the payload performance even further. Detailed analysis points out that a hybrid launch vehicle, comprised of a cryogenic first stage and a 'green' storable upper stage, would be *the most cost-effective expendable launch vehicle in the West having a payload performance of 3.80 k€/kg*. Taking into account the added safety, higher reliability and reduced complexity of the storable systems, it is expected that the proposed hybrid launch vehicle (either expendable or reusable) *will outperform all medium to heavy launch vehicles on the market today*. These findings indicate that the green (hypergolic) storable upper stage can be a cost-effective and reliable solution to future space flight applications.

Contents

Preface	iii
Abstract	v
List of Figures	ix
List of Tables	xi
Glossary	xv
Acronyms	xv
Symbols	xvii
1 Introduction	1
1.1 Thesis Scope	1
1.2 Partnership with SolvGE	2
2 Research Objectives and Questions	5
2.1 Research Goal	5
2.2 Research Objectives and Research Questions	5
3 Literature Study	7
3.1 Hydrogen Peroxide	7
3.1.1 Chemical Properties of Hydrogen Peroxide	7
3.2 Green Hypergolic Propellants	8
3.3 Upper Stage Designs	11
3.4 Upper Stage Propulsion Systems	11
3.5 Material Compatibility	12
3.5.1 Type of Materials	12
3.5.2 Material Capability with Hydrogen Peroxide	13
3.6 Executive Chapter Summary	13
4 Research Methodologies	15
4.1 Systems Engineering Framework	15
4.1.1 Analytical Models	18
4.1.2 Tool Architecture and Framework	18
4.2 Optimisation Tools and Strategy	19
4.3 Verification and Validation Methods	21
4.4 Executive Summary	22
5 Prototype X Model	23
5.1 Ariane 6 Launch Vehicle	23
5.2 The “Prototype X” Launcher Upper Liquid Propulsion Module (ULPM)	24
5.2.1 General Layout, Mass and Dimensions	24
5.2.2 Propulsion System	25
5.2.3 System Requirements	26
5.3 Launch Vehicle Model	27
5.3.1 Performance Model Assumptions & Requirements	27

5.3.2	Performance Model	27
5.3.3	Mass Model Assumptions & Requirements	31
5.3.4	Mass Model	31
5.4	Sensitivity Analysis	41
5.5	Verification and Validation	42
5.5.1	Performance Model Validation	43
5.5.2	Mass Model Validation	44
5.6	Executive Chapter Summary	45
6	Cost Model	47
6.1	Cost Breakdown	47
6.2	Cost Model Selection	48
6.2.1	Cost Model Justification	48
6.3	Cost Model Assumptions & Requirements	49
6.4	Cost Estimating Relationships	49
6.4.1	First Flight Unit Cost Estimate (T1)	50
6.4.2	OECD Inflation Correction	51
6.4.3	Development Cost Estimate	52
6.4.4	Manufacturing Cost Estimate	54
6.4.5	Operating Cost Estimate	55
6.4.6	Cost-per-Flight Estimate	56
6.5	Cost Modelling	57
6.5.1	Sensitivity Analysis	57
6.6	Verification and Validation	59
6.7	Ariane 6 Launch Vehicle Cost Estimate	59
6.7.1	First Unit Cost Estimate	60
6.7.2	Development Cost Estimate	60
6.7.3	Manufacturing Cost Estimate	61
6.7.4	Operation Cost Estimate	61
6.7.5	Cost-per-Flight Estimate	63
6.8	Executive Chapter Summary	66
7	Propellant Selection	69
7.1	Propellant Analysis Requirements & Assumptions	69
7.2	Conventional Cryogenic Propellants	69
7.3	Propellant Selection for Analysis	71
7.3.1	Green Storable Propellant Classification	71
7.3.2	Hydrocarbon Fuel Options	72
7.4	Criteria Selection	76
7.5	Propellant Combustion Analysis	79
7.6	Propellant Trade-Off	85
7.7	Executive Chapter Summary	88
8	Detailed Mass and Cost Analysis	91
8.1	Propellant Optimisation	91
8.1.1	Design Impact of Reactive Additives	91
8.1.2	Combustion Condition Optimisation	94
8.2	Prototype X - Mass & Cost Analysis	102
8.2.1	Prototype X Cost Estimation - H2O2/DMAZ	103
8.2.2	Prototype X Cost Estimation - H2O2/Ethanol	105
8.2.3	Prototype X Cost Estimation - H2O2/Dimethylamine	107
8.2.4	Sensitivity Analysis	109
8.3	Payload Capability and Mission Characteristics	111
8.4	Current Market Outlook Analysis	115
8.5	Executive Summary	117
9	Cross-Over Analysis	119

9.1	Propellant and Design Iterations	119
9.1.1	Cross-Over Analysis for Conventional Propellant Tank Material	120
9.1.2	Cross-Over Analysis for Advanced Propellant Tank Material	121
9.2	Mass & Cost Analysis	123
9.2.1	Mass & Cost Analysis for Conventional Propellant Tank Material	123
9.2.2	Mass & Cost Analysis for Advanced Propellant Tank Material	125
9.3	Cryogenic Performance Level Comparison	127
9.4	Payload Capability and Mission Characteristics	129
9.5	Geometrical Comparison	132
9.6	Market Outlook Analysis	134
9.7	Executive Chapter Summary	135
10	Subsystem Considerations and Re-design	139
10.1	Subsystems under Consideration	139
10.2	Propulsion Subsystem Considerations	139
10.2.1	Propellant Pump Design	141
10.2.2	Reliability Analysis	142
10.3	Propellant Storage and Feed Considerations	144
10.4	Thermal Control Considerations	145
10.5	Structural Considerations	147
10.6	Ground Operations and Handling	148
10.7	Re-Design Potential Cost Impact	151
10.8	Executive Chapter Summary	152
11	Conclusion	155
A	Inflation Charts	169
B	Hydrogen Peroxide Material Compatibility	171

List of Figures

1.1	Missions to LEO and GEO [6]	1
3.1	Theoretical Specific Impulse Performance for the Selected Fuels [45]	10
4.1	Model Based Systems Engineering Architecture	16
4.2	Thesis Research Framework	17
4.3	Schematic Depiction Optimisation Strategy between the Models Described	19
4.4	The Systems Engineering Process Described by the “V-Model” [81]	21
5.1	The Ariane 6 Launch Vehicle in Two Configurations [11]	24
5.2	Schematic Depiction of the Upper Liquid Propulsion Module Configuration [88]	25
5.3	Vinci Cryogenic Upper Stage Data [93]	26
5.4	Schematic of the Cylindrical Tank Layout	34
6.1	Cost Breakdown for Launch Vehicles	47
6.2	Drenthe’s SOLSTICE Cost Model [83]	50
6.3	Cost-per-Flight Breakdown for Ariane 6 Stages (Excluding Boosters) - Nominal Payload	63
6.4	Cost-per-Flight Breakdown for Ariane 6 Stages (Excluding Boosters) - Maximum Payload	64
6.5	Cost-per-Flight Breakdown for total Ariane 6 Launch Vehicle (excluding boosters) - Nominal Payload	65
6.6	Cost-per-Flight Breakdown for total Ariane 6 Launch Vehicle (excluding boosters) - Maximum Payload	65
7.1	Relative Weight of Criteria, based on Combined AHP Relative Expert Analysis	79
7.2	“Prototype X” Upper Stage Mass Breakdown per Propellant Combination	81
7.3	“Prototype X” Upper Stage Dry Mass per Propellant Combination	82
7.4	Required Volume for Oxidiser and Fuel	82
7.5	Relative Wet Mass Impact per Propellant Combination	83
7.6	“Prototype X” Upper Stage Absolute Wet Mass Increase per Propellant Combination vs. Payload Capability	84
7.7	“Prototype X” Upper Stage Available Payload per Propellant Combination - Nominal Payload Configuration	84
7.8	“Prototype X” Upper Stage Available Payload per Propellant Combination - Maximum Payload Configuration	85
8.1	Impact of DMAZ/Sodium Borohydride Fuel Mixtures on Specific Impulse and Wet Mass	92
8.2	Impact of Ethanol/Sodium Borohydride Fuel Mixtures on Specific Impulse and Wet Mass	93
8.3	Impact of Dimethylamine/Sodium Borohydride Fuel Mixtures on Specific Impulse and Wet Mass	93
8.4	DMAZ and H ₂ O ₂ Mass vs. O/F ratio under Fixed Combustion Chamber Pressure - P _c = 6 MPa	94
8.5	Specific Impulse, Combustion Chamber Temperature and Mass Behaviour vs. O/F ratio - DMAZ/H ₂ O ₂	95
8.6	Specific Impulse and Combustion Chamber Temperature vs. Combustion Chamber Pressure for various O/F ratio’s - DMAZ/H ₂ O ₂	96
8.7	Propellant Optimisation Analysis - DMAZ/H ₂ O ₂	97

8.8	Ethanol and H ₂ O ₂ Mass vs. O/F ratio under Fixed Combustion Chamber Pressure - P _c = 6 MPa	98
8.9	Specific Impulse, Combustion Chamber Temperature and Mass Behaviour vs. O/F ratio - Ethanol/H ₂ O ₂	98
8.10	Specific Impulse and Combustion Chamber Temperature vs. Combustion Chamber Pressure for various O/F ratio's - Ethanol/H ₂ O ₂	99
8.11	Propellant Optimisation Analysis - Ethanol/H ₂ O ₂	100
8.12	Dimethylamine and H ₂ O ₂ Mass vs. O/F ratio under Fixed Combustion Chamber Pressure - P _c = 6 MPa	100
8.13	Specific Impulse, Combustion Chamber Temperature and Mass Behaviour vs. O/F ratio - Dimethylamine/H ₂ O ₂	101
8.14	Specific Impulse and Combustion Chamber Temperature vs. Combustion Chamber Pressure for various O/F ratio's - Dimethylamine/H ₂ O ₂	102
8.15	Propellant Optimisation Analysis - Dimethylamine/H ₂ O ₂	102
8.16	Cost Breakdown Comparison for Selected Upper Stage Designs	112
8.17	C _p F Graphical Comparison Between Selected Upper Stage Designs	112
8.18	Wet Mass Increase and Available Payload Capability for Selected Propellant Combinations	113
8.19	Available Payload Capability for Selected Propellant Combinations, Compared to Conventional Hydrolox Combination	113
8.20	Graphical Comparison between the Cost-per-Kg of Upper Stage Designs	115
8.21	Current Medium/Heavy Launch Vehicle Market - Cost-per-Kg vs. Payload Capacity . .	117
9.1	Wet Mass and Dry Mass Cross-Over Analysis (H ₂ O ₂ /Fuel) - Conventional Aluminium Propellant Tanks	121
9.2	Wet Mass and Dry Mass Cross-Over Analysis (H ₂ O ₂ /Fuel) - Advance Carbon Fiber Composite Propellant Tanks	123
9.3	Cost Breakdown Comparison for Selected Upper Stage Designs	130
9.4	C _p F Graphical Comparison Between Selected Upper Stage Designs	131
9.5	Graphical Comparison between the Cost-per-Kg of Upper Stage Designs	132
9.6	Geometrical Comparison Analysis between the Cryogenic Upper Stage and Best Case "Prototype X" Concept - To Scale	133
9.7	Current Medium/Heavy Launch Vehicle Market - Cost-per-Kg vs. Payload Capacity . .	134
10.1	Temperature Distribution (in Celsius) of Ariane 6 ULPM [88]	146
11.1	Calculated Payload Performance for Various Prototype X Design Concepts Integrated with Ariane 6 First Stage	157
A.1	Average Monthly Inflation since 2015 in the European Union [115]	169

List of Tables

3.1	Chemical Properties of 100% Hydrogen Peroxide [19]	8
3.2	Promising Fuels that Hypergolically React with Hydrogen Peroxide. Compared on Type, Availability, Production Cost and Storability	11
3.3	Summary of the Upper Stage Designs [16]	11
3.4	Data Summary on the Upper Stage Propulsion Systems	12
5.1	General System Requirements	26
5.2	Prototype X Vehicle Requirements	27
5.3	Performance Model Assumptions	27
5.4	Performance Model Requirements	27
5.5	Mass Model Assumptions	31
5.6	Mass Model Requirements	31
5.7	Validation of Engine Mass Estimation Relationships [16], [102]–[104]	37
5.8	Sensitivity Analysis Performance Quality Factors - Vacuum Thrust	41
5.9	Sensitivity Analysis Performance Quality Factors - Vacuum Isp	41
5.10	Sensitivity Analysis - Isentropic Coefficient and Exit Pressure	41
5.11	Data Summary of First Stage Designs used for Validation	43
5.12	Validation of Performance Model	43
5.13	Performance Model Validation Results - Relative Differences	43
5.14	Performance Model Validation Results - Relative Error, Absolute Relative Error, Standard Deviation	43
5.15	Validation of Mass Model	44
5.16	Mass Model Validation Results - Relative Error, Absolute Relative Error, Standard Deviation	44
6.1	Cost Model Assumptions	49
6.2	Cost Model Requirements	49
6.3	Equipment Breakdown [83]	51
6.4	Cost Estimation Relationships for the Individual Subsystem Elements [83], [113]	51
6.5	ESA Costing Software (ECOS) Support Functions [116]	52
6.6	Learning Factor Slopes based on the Total Manufactured Units [82], [83], [117]	55
6.7	TRANSCOST Operations Cost Model with Variables, Assumptions and Fixed Values [82]	55
6.8	Sensitivity Analysis on Development Cost	58
6.9	Sensitivity Analysis on Manufacturing Cost	58
6.10	Sensitivity Analysis on Operation Cost	58
6.11	First Unit Cost Estimate for Ariane 6 Stages (Excluding Boosters)	60
6.12	Development Cost Estimate for Ariane 6 Stages (Excluding Boosters)	60
6.13	Manufacturing Cost Estimate for Ariane 6 First Stage (excluding boosters)	61
6.14	Manufacturing Cost Estimate for Ariane 6 Upper Stage (excluding boosters)	61
6.15	Operation Cost Estimate for Ariane 6 Stages (Excluding Boosters) - Nominal Payload	62
6.16	Operation Cost Estimate for Ariane 6 Stages (Excluding Boosters) - Maximum Payload	62
6.17	Operation Cost Estimate for total Ariane 6 Launch Vehicle (excluding boosters) - Nominal Payload	62
6.18	Operation Cost Estimate for total Ariane 6 Launch Vehicle (excluding boosters) - Maximum Payload	63
6.19	Cost-per-Flight Estimate for Ariane 6 Stages (Excluding Boosters) - Nominal Payload	63
6.20	Cost-per-Flight Estimate for Ariane 6 Stages (Excluding Boosters) - Maximum Payload	64

6.21	Cost-per-Flight Estimate for total Ariane 6 Launch Vehicle (excluding boosters) - Nominal Payload	64
6.22	Cost-per-Flight Estimate for total Ariane 6 Launch Vehicle (excluding boosters) - Maximum Payload	65
7.1	Propellant Selection Requirements	69
7.2	Propulsion Analysis Assumptions	70
7.3	Chemical Characteristics Liquid Oxygen [120]	70
7.4	Chemical Characteristics Liquid Hydrogen [120]	70
7.5	Chemical Characteristics Rocket Propellant-1 (RP-1) [120]	71
7.6	Chemical Characteristics Kerosene (T-1) [120]	71
7.7	Possible Green Propellants that have been Investigated by Project GRASP [122]	72
7.8	Chemical Characteristics Hydrogen Peroxide [120]	73
7.9	Chemical Characteristics Ethanol [120]	73
7.10	Chemical Characteristics DMAZ [123]	73
7.11	Chemical Characteristics MEA [120], [125]	74
7.12	Chemical Characteristics DETA [10], [120]	74
7.13	Chemical Characteristics Pyridine [120], [126]	74
7.14	Chemical Characteristics Isooctane [9], [120], [127]	75
7.15	Chemical Characteristics Dimethylamine [120], [129]	75
7.16	Chemical Characteristics Methanol [120]	75
7.17	Chemical Characteristics Isopropyl Alcohol [120], [131]	76
7.18	Chemical Characteristics Isoamyl Alcohol [120], [131]	76
7.19	Chemical Characteristics Triglyme [120], [132]	76
7.20	Scoring System used in the AHP Tool to assess relative expert weights [133]	78
7.21	The AHP Relative Expert Weights per Criterion	78
7.22	Combustion Analysis of Selected Propellant Combinations - $P_c = 6 \text{ MPa}$, $A_e/A_t = 240$	80
7.23	Trade-Off Table as input for the AHP Analysis	86
7.24	Propellant Analytical Hierarchy Process Trade-Off Analysis Results	87
8.1	Combustion Analysis for Different Fuel Mixtures with Sodium Borohydride - $P_c = 6 \text{ MPa}$	92
8.2	First Unit Cost and Development Cost - H2O2/DMAZ	103
8.3	“Prototype X” Manufacturing Cost - H2O2/DMAZ	104
8.4	“Prototype X” Operating Cost - H2O2/DMAZ	105
8.5	Cost-per-Flight Estimate for the Prototype X - H2O2/DMAZ	105
8.6	First Unit Cost and Development Cost - H2O2/Ethanol	106
8.7	“Prototype X” Manufacturing Cost - H2O2/Ethanol	106
8.8	“Prototype X” Operating Cost - H2O2/Ethanol	107
8.9	Cost-per-Flight Estimate for the Prototype X - H2O2/Ethanol	107
8.10	First Unit Cost and Development Cost - H2O2/Dimethylamine	108
8.11	“Prototype X” Manufacturing Cost - H2O2/Dimethylamine	108
8.12	“Prototype X” Operating Cost - H2O2/Dimethylamine	109
8.13	Cost-per-Flight Estimate for the Prototype X - H2O2/Dimethylamine	109
8.14	Sensitivity Analysis on Storable Upper Stage Dry Mass	110
8.15	Sensitivity Analysis on Storable Upper Stage Wet Mass	110
8.16	Sensitivity Analysis on Storable Upper Stage Cost-per-Flight	110
8.17	Cost Breakdown for Selected Upper Stage Designs	111
8.18	CpF Comparison Between Selected Upper Stage Designs	111
8.19	Sensitivity Analysis for Payload Capability	114
8.20	Cost-per-Kg per Upper Stage Design	115
8.21	Cost-per-Kg Analysis of Integrated Prototype X Designs	116
8.22	Current Medium/Heavy Launch Vehicle Market	116
9.1	Required Isp for Storable Propellants to Eliminate Wet Mass Growth - Conventional Storage System Material (Aluminium Alloy)	121
9.2	Required Isp for Storable Propellants to Eliminate Wet Mass Growth - Advanced Storage System Material (Carbon Fiber Composite)	122

9.3	First Unit Cost and Development Cost - H2O2/ Hypothetical Fuel - Conventional Aluminium Structure	124
9.4	“Prototype X” Manufacturing Cost - H2O2/ Hypothetical Fuel - Conventional Aluminium Structure	124
9.5	“Prototype X” Operating Cost - H2O2/ Hypothetical Fuel - Conventional Aluminium Structure	124
9.6	Cost-per-Flight Estimate for the Prototype X - H2O2/ Hypothetical Fuel - Conventional Aluminium Structure	125
9.7	First Unit Cost and Development Cost - H2O2/ Hypothetical Fuel - Advanced Carbon Fiber Composite Structure	125
9.8	“Prototype X” Manufacturing Cost - H2O2/ Hypothetical Fuel - Advanced Carbon Fiber Composite Structure	126
9.9	“Prototype X” Operating Cost - H2O2/ Hypothetical Fuel - Advanced Carbon Fiber Composite Structure	126
9.10	Cost-per-Flight Estimate for the Prototype X - H2O2/ Hypothetical Fuel - Advanced Carbon Fiber Composite Structure	127
9.11	Prototype X with Aluminium Structure, First Unit Cost for Cryogenic Performance Level - Isp = 463.53 seconds	128
9.12	Prototype X with Aluminium Structure, Cost-per-Flight for Cryogenic Performance Level - Isp = 463.53 seconds	128
9.13	Prototype X with Carbon Fiber Composite Structure, First Unit Cost for Cryogenic Performance Level - Isp = 463.53 seconds	128
9.14	Prototype X with Carbon Fiber Composite Structure, Cost-per-Flight for Cryogenic Performance Level - Isp = 463.53 seconds	129
9.15	Cost Breakdown for Selected Upper Stage Designs	129
9.16	CpF Comparison Between Selected Upper Stage Designs	130
9.17	Cost-per-Kg per Upper Stage Design	131
9.18	Cost-per-Kg Performance of Integrated Prototype X Designs - Excluding Boosters	134

Glossary

Acronyms

R^2	Coefficient of Determination
AHP	Analytical Hierarchy Process
AM	Additive Manufacturing
AMRDEC	Aviation and Missile Research and Development, and Engineering Center
APU	Auxiliary Power Unit
AvSS	Avionics Support Structure
CEA	Combustion Equilibrium Analysis
CERs	Cost Estimation Relationships
CFC	Carbon Fiber Composite
CFRP	Carbon Fiber Composite
CINCH	Competitive Impulse Non-Carcinogenic Hypergol
CpF	Cost-per-Flight
DETA	Diethylenetriamine
DMAZ	2-dimethylaminoethylazide
DOC	Direct Operating Cost
ECOS	ESA Costing Software
ELV	Expendable Launch Vehicle
ESA	European Space Agency
ESTEC	European Space Research and Technology Centre
FEP	Fluorinated Ethylene/Propylene
FM1	First Flight Model
FSW	Friction Stir Welding
FU	Theoretical First Unit
GEO	Geo Stationary Orbits
GLOW	Gross-Lift-Off-Weight
GRASP	GReen Advanced Space Propulsion
GTO	Geostationary Transfer Orbit
HIL	Hypergolic Ionic Liquids
HPHV	High Pressure Helium Vessels
HTP	High Test Peroxide
I&T	Integration and Testing
ICARUS	Innovative Carbon ARiane Upper Stage
IDT	Ignition Delay Time
INCOSE	International Council on Systems Engineering
IOC	Indirect Operating Cost

Isp	Specific Impulse
ITS	Inter Tank Structure
LCC	Life Cycle Cost
LEO	Low Earth Orbit
LH2	Liquid Hydrogen
LOX	Liquid Oxygen
LpA	Annual Launch Rate
LV	Launch Vehicle
LVA	Launch Vehicle Adapter
M/PA	Management and Product Assurance
MAE	Mean Absolute Error
MAIT	Manufacturing, Assembly, Integration and Test Cost
MBSE	Model Based Systems Engineering
MDA	Multidisciplinary Design Analysis
MDO	Multidisciplinary Design Optimisation
MEA	Ethanolamine
MEO	Medium Earth Orbit
MLI	Multi-Layer Insulation
MMH	Monomethylhydrazine
NAFCOM	NASA Air Force Cost Model
NASA	National Aeronautics and Space Agency
NPSP	Net Positive Suction Pressure
NTO	Dinitrogen Tetroxide
O/F	Oxidiser-to-Fuel Ratio
PAA	Payload, Avionics and Attitude Control
PaGMO	Parallel Global Multiobjective Optimizer
PHOEBUS	Prototype Highly OptimizEd Black Upper Stage
PO	Project Office
RFNA	Red Fuming Nitric Acid
RP1	Rocket Propellant-1
RSE	Relative Standard Error
SSCAG	Space Systems Cost Analysis Group
SSO	Sun Synchronous Orbits
T1	Theoretical First Unit
TEA-TEB	Triethylaluminium-Triethylborane
TRL	Technology Readiness Level
UDMH	Unsymmetrical Dimethylhydrazine
ULPM	Upper Liquid Propulsion Module
USCM	Unmanned Space Vehicle Cost Model
VITF	Vinci Thrust Frame
WFNA	White Fuming Nitric Acid

Symbols

Roman

$(O/F)_{ratio}$	Mixture Ratio	[-]
A_e	Nozzle Exit Area	$[m^2]$
A_t	Nozzle Throat Area	$[m^2]$
C_{Fid}	Ideal Thrust Coefficient	[-]
C_{Freal}	Corrected Thrust Coefficient	[-]
C_p	Profit Retention Cost Reduction Factor	[-]
D_{stage}	Stage Diameter	$[m]$
I_{sp}	Specific Impulse	$[s]$
L_R	Cylindrical Length of Tank	$[m]$
L_d	Development Learning Factor	[-]
M	Molecular Mass	$[g/mol]$
M_0	Initial Mass Launch Vehicle	$[kg]$
M_f	Final Mass Launch Vehicle	$[kg]$
M_{PL}	Payload Mass	$[kg]$
M_{dry}	Dry Mass	$[kg]$
P_a	Ambient Pressure	$[Pa]$
P_c	Combustion Chamber Pressure	$[Pa]$
P_e	Nozzle Exit Pressure	$[Pa]$
P_{rfuel}	Fuel Tank Pressure	$[Pa]$
P_{rox}	Oxidiser Tank Pressure	$[Pa]$
R	Specific Gas Constant	$[J \cdot kg \cdot K]$
R_a	Universal Gas Constant	$[8.314J \cdot K^{-1} \cdot mol^{-1}]$
SF_t	Tank Safety Coefficient	[-]
S_R	Propellant Tank Surface Area	$[m^2]$
S_{cap}	Tank Cap Surface Area	$[m^2]$
T_c	Combustion Chamber Temperature	$[K]$
T_e	Nozzle Exit Temperature	$[K]$
T_{vac}	Maximum Vacuum Thrust	$[N]$
V_e	Exhaust Velocity	$[m/s]$
V_{caps}	Volume of Caps	$[m^3]$
V_{fuel}	Fuel Volume	$[m^3]$
V_{ox}	Oxidiser Volume	$[m^3]$
\dot{m}	Mass Flow Rate	$[kg/s]$
b	Manufacturing Learning Exponent	[-]
c_f	Fuel Specific Cost-per-Kilogram	$[\text{€}/kg]$
c_o	Oxidizer Specific Cost-per-Kilogram	$[\text{€}/kg]$
c_{id}^*	Ideal Characteristic Velocity	$[m/s]$
c_{press}	Pressurizant Specific Cost-per-Kilogram	$[\text{€}/kg]$
c_{real}^*	Corrected Characteristic Velocity	$[m/s]$
f_t	Tank Thickness Safety Margin	[-]

g_0	Gravitational Acceleration	[9.81 m/s^2]
m_{prop}	Propellant Mass	[kg]
m_{tanks}	Propellant Tank Mass	[kg]
p	Manufacturing Learning Factor	[-]
q	Average Subcontractor Profit	[-]
S_{BAU}	Scope of Subcontracted Work (Business As Usual)	[-]
S_{COM}	Scope of Subcontracted Work (Commercial)	[-]
t	Tank Thickness	[m]

Greek

ΔV	Total Velocity Increment	[m/s]
Λ	Vandenkerckhove Function	[-]
ϵ_F	Nozzle Quality	[-]
ϵ_b	Combustion Quality	[-]
γ	Specific Heat Ratio	[-]
ρ_c	Chamber Density	[kg/m ³]
ρ_e	Exit Density	[kg/m ³]
ρ_{fuel}	Density Fuel	[kg/m ³]
ρ_{ox}	Density Oxidizer	[kg/m ³]
ρ_{tank}	Propellant Tank Material Density	[kg/m ³]
σ_t	Ultimate Strength of Tank Material	[MPa]

Introduction

1.1. Thesis Scope

As demand for reliable, safe and cost-effective transport to space rapidly increases [2], we are entering into a new era of spaceflight. This especially amounts to the capability of bringing payload into Low Earth Orbit (LEO) and Geostationary Orbit (GEO), this is illustrated by Figure 1.1. To provide for this expansion into space, society demands and requires sustainable solutions for rocket propulsion. While the conventional cryogenic propulsion systems (liquid hydrogen and liquid oxygen) are environmentally friendly, they effectuate large launch vehicle costs. The simpler and volume optimised storable propellants can reduce the complexity and dry mass of the launch vehicle while increasing the safety of operation [3]. In the past, the storable propellants were negatively impacting the environment, were toxic and carcinogenic. As a result of this, environmental restrictions and health regulations made the use of these conventional storable propellants very limited. To overcome this, a new rocket propellant is necessary to reduce the large impact conventional storable rocket propellants have on the environment and toxicity while allowing for beneficial launch vehicle design solutions [4], [5]. These environmentally friendly storable space propellants (also called “green” propellants) will be able to be handled safer, easier and more cost-effective, bringing down the risk and cost of the launch vehicle. Moreover, storable propellants are safer to store and on-ground operational cost is reduced while limiting peripheral subsystem complexity and increasing reliability of the overall launch vehicle system [3].

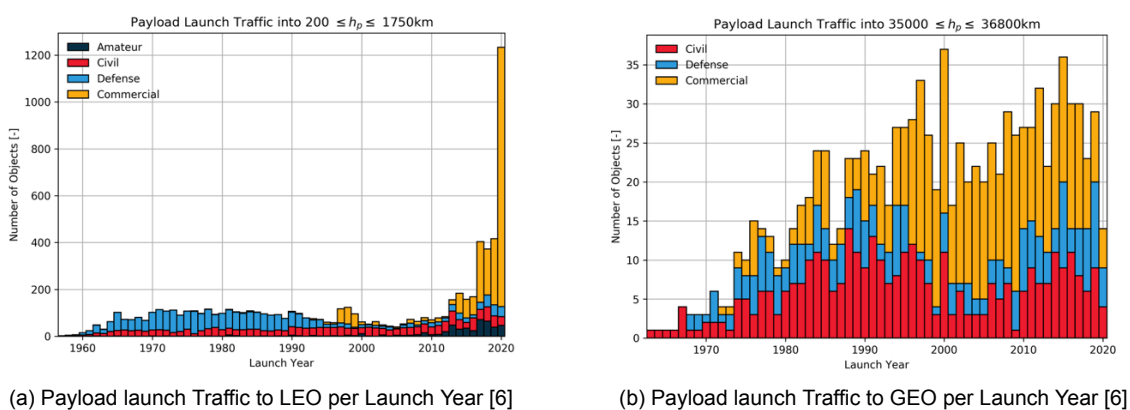


Figure 1.1: Missions to LEO and GEO [6]

Over the past decades development of bipropellant propulsion systems shifted from storable propellants to the use of cryogenics. The main reason for this paradigm shift was the typical toxic, carcinogenic and corrosive character of the storable propellants at the time. Cryogenic propellants, often the combination of liquid hydrogen and liquid oxygen, produce high specific impulse characteristics while

being environmentally friendly. However, cryogenic propellants have a significant impact on the overall launch vehicle design. The use of cryogenic propellants typically increases vehicle dimensions and adds significantly to the complexity of the system. Resulting in higher launch vehicle cost and lower reliability [3], [7], [8]. Apart from that, hydrolox systems (liquid hydrogen with liquid oxygen) are costly in production and operation, LH2 production is expensive and very energy consuming and LH2 storage requires costly cooling technologies and is hazardous to handle [9].

Through research conducted by H. Kang and S. Kwon it was shown that green hypergolic propellant combinations can provide distinct advantages on performance and reliability of the propulsion system restricted by geometrically severe constraints such as an upper stage and lunar descent/ascent modules [10]. Moreover, green storable propellants will lower the operational cost and is safer to procure, store and handle. The aim of this research is to investigate the commercial market prospect of green storable upper stage design concepts. This is done through detailed research into design concepts operating on various storable propellant combinations. These "Prototype X" upper stage design concepts will be analysed and optimised on their cost-per-kg payload characteristic. The "Prototype X" upper stage module is the name of the hypothetical storable design concept that will be used to compare the performance, in terms of combustion, mass and cost, with the cryogenic upper stage of the Ariane 6 launch vehicle. The Ariane 6, manufactured on behalf of the European Space Agency (ESA), is a new medium-heavy vehicle used to perform a wide range of missions of delivering payload to Geo Stationary Orbits (GEO), Polar and Sun Synchronous Orbits (SSO), Medium Earth Orbit (MEO) et cetera. The upper stage of the Ariane 6 – Upper Liquid Propulsion Module (ULPM) – is equipped with cryogenic engines that operate on liquid hydrogen and liquid oxygen [11].

In this thesis research the storable upper design concepts will be investigated in terms of propulsive performance characteristics, feed/storage system design and structural components. "Prototype X" will serve as a benchmark for future storable upper stage modules, having a wide variety of mission profiles and payload capabilities. During the design optimization it is key that the overall required propulsive performance characteristics of the cryogenic predecessor are met and maintained for the "Prototype X" upper stage module. In this case, the optimisation of storable upper stage concepts is focused on minimising the cost-per-kg characteristic. This is done by analysing design iterations that will minimise dry/wet mass and maximise the payload capability of the system. The market outlook will shed light on the cost-effectiveness of the proposed concepts. From this improvements and future recommendations can be formulated. Furthermore, it is important to investigate the upper module's material capability with the proposed storable propellants, in-space operation and the required peripheral subsystems redesigns, such as the propellant feed subsystem. A risk assessment will be performed on the individual redesign considerations as well as on the spacecraft system as a whole to verify and validate the reliability characteristics of the optimised design. This design optimization research will be conducted by the use of knowledge and tools from the fields of propulsion engineering, systems engineering chemical engineering and cost engineering.

1.2. Partnership with SolvGE

Over the past years hydrogen peroxide (H_2O_2) has become one of the most promising new "green" storable oxidiser for space applications [12]. Hydrogen peroxide has the advantageous characteristic that it can be used in either mono- or bipropellant propulsion systems. When hydrogen peroxide is used as a monopropellant the propulsion system will include a catalytic bed to decompose the hydrogen peroxide into superheated steam and oxygen. Depending on the configuration of the catalytic bed the experimental specific impulse for hydrogen peroxide monopropellant engines ranges between 140 and 170 seconds [13]. Hydrogen peroxide can also be used as an oxidizer in a bipropellant propulsion system where it will react with a fuel and can attain, depending on the type of fuel used, hypergolic characteristics. These types of systems will typically have a higher specific impulse than their monopropellant counterparts, the combination H_2O_2 /kerosene can produce a specific impulse between 310 and 330 seconds [14].

Recognising the fact that the storage and transportation of high concentration hydrogen peroxide is a very expensive undertaking, still some hurdles have to be taken to make hydrogen peroxide a cost-

effective “green” rocket propellant of the future. The company SolvGE took one of these hurdles as a challenge and developed the world’s first Hydrogen Peroxide Printer. This novel patented technology makes it possible to produce any concentration of hydrogen peroxide, up to 99.5%, on-site using a revolutionary passive process making it a safe solution while being scalable and portable [15]. This novel technology its application will make highly concentrated hydrogen peroxide very abundant and relatively cheap in the future. This opens up a lot of different use cases in which concentrated hydrogen peroxide can be used.

One of the applications that SolvGE envisions is combining their highly concentrated hydrogen peroxide with a bipropellant propulsion system to reduce the cost-per-flight of the Launch Vehicle upper stage “Prototype X” through green storable propellant implementation. The technology that SolvGE provides will drastically lower the operation cost of pre- and post-launch procedures. The main reason for this is the cost and time-effective way of producing concentrated hydrogen peroxide on site. Mitigating transportation and storage burdens. This cost impact will become even more pronounced when dealing with reusable launch vehicles in the future.

This thesis research will investigate the storable upper stage concepts that use concentrated hydrogen peroxide as the designated oxidiser. The research was conducted under the supervision and guidance of the SolvGE team. The work presented describes possible use cases of how concentrated hydrogen peroxide can be implemented in upper stage designs in the future. SolvGE’s findings and advances in concentrated hydrogen peroxide procurement were taken into consideration throughout this research.

2

Research Objectives and Questions

This chapter will describe the research goal, research objectives and research questions. The research goal is coming forth from the problem statement as mentioned in chapter 1. To reach the research goal, research objectives are presented to dissect the challenges and hurdles that have to be overcome to reach the goal. These objectives can be met by answering their associated research questions.

2.1. Research Goal

The research goal is the baseline of the thesis research work and drives the research effort. This goal comes forward from the problem statement that was presented in chapter 1. The research goal is formulated as:

Investigate the cost benefit, payload performance and technical feasibility of green storable upper stage design concepts, compared to a conventional cryogenic upper stage design

2.2. Research Objectives and Research Questions

From the research goal, three main research objects are formulated. These are split up to focus on the field of Propulsion Engineering, Systems Engineering and Cost Engineering respectively. For all the research objectives the corresponding research questions are given. These research questions are stated broadly and are subject to change.

Objective 1 – Propulsion Engineering:

Analyse the effect of storable green hydrocarbon fuels in combination with hydrogen peroxide (H_2O_2) on the dry mass breakdown and required propellant mass, while maintaining the same performance characteristics as the conventional cryogenic propulsion system present in the ULPM

- **Research Question 1.1:**
What specific impulse can be obtained by hydrocarbon fuel combinations with hydrogen peroxide (H_2O_2)
- **Research Question 1.2:**
Under what combustion chamber conditions are the hypergolic storable propellant combinations optimised in performance?
- **Research Question 1.3:**
What design alterations have to be incorporated to allow for the use of the new propellant combination in the existing (TRL 9) propulsion system?
- **Research Question 1.4:**
What innovation is required to make the new hydrocarbon fuel and hydrogen peroxide (H_2O_2)

combination surpass the cryogenic propulsive performance characteristics and reduce the wet mass as set by the conventional cryogenic design?

Objective 2 – Systems Engineering:

Investigate the change in complexity, reliability and subsystem design for green storable upper stage design concepts

- **Research Question 2.1:**
How do the materials in the feed, storage and propulsion system react when in contact with the hydrogen peroxide?
- **Research Question 2.2:**
What new materials and manufacturing techniques can be proposed for the existing subsystem designs of the upper stage module, when introducing storable propellants?
- **Research Question 2.3:**
What will be the total mass reduction of the updated subsystem designs?
- **Research Question 2.4:**
What will be the typical change in dry and wet mass of the storable upper stage module and how does this relate to the payload capability

Objective 3 – Cost Engineering:

Compare and analyse the cost breakdown for the storable green propellant upper stage design with the conventional cryogenic upper stage module

- **Research Question 3.1:**
What are the production, transportation and storage cost per kilogram for the propellants?
- **Research Question 3.2:**
How is the development, manufacturing and operational cost affected by introducing storable green propellants in the upper stage design?
- **Research Question 3.3:**
How does the payload cost per kilogram for the storable upper stage relate to the conventional upper stage module?
- **Research Question 3.3:**
What will be the cost-benefit of using storable green propellants when the optimised future novel hydrocarbon fuel (Research Question 1.5) will be used?
- **Research Question 3.4:**
How are the launch and ground operations (risk and cost) for the “Prototype X” launch vehicle affected by the use of the novel hydrogen peroxide propellant?
- **Research Question 3.5:**
How does the integrated green storable upper stage design fit in the current medium/heavy launch vehicle market?

3

Literature Study

To start with a good level of background knowledge on the current state of art and general practices a literature review was conducted. This will form the baseline for this research project and encompasses the important literature that describes and discuss the current types of upper stage design, upper stage propulsion systems and green hypergolic fuel and oxidizer combinations. In this chapter, the most important findings from the literature study will be summarised [16].

3.1. Hydrogen Peroxide

In conventional hypergolic bi-propellant propulsion systems numerous oxidizers have been used. For example, dinitrogen tetroxide (NTO), red fuming nitric acid (RFNA) and white fuming nitric acid (WFNA) have been used for many space applications over the years as they are fairly cheap to manufacture and are relatively save to store, apart from being carcinogenic, toxic and corrosive [17]. In recent years more emphasis is put on the use of hydrogen peroxide as the oxidiser in hypergolic systems as this oxidiser compound is not carcinogenic and is very little toxic.

A. Okninski et al. [18] compared the specific impulse and density specific impulse (relates to the amount of impulse you get from a propellant per unit volume) of NTO and hydrogen peroxide. From this research, it was concluded that the maximum achieved density specific impulse is achieved for fuel combinations with hydrogen peroxide. The curves achieve their optimum at relatively larger oxidiser-to-fuel ratios (O/F) compared to the fuel combinations with NTO. Furthermore, it was found that the density specific impulse of the fuel/hydrogen peroxide combinations is less sensitive to changing the oxidiser-to-fuel ratios compared to when dinitrogen tetroxide is used. A higher density specific impulse is preferred over low-density specific impulses as this results in more impulse per volume of propellant. This requires less volume to achieve the same specific impulse performance characteristics, hence a lower storage mass is achieved. Thus, it can be concluded that hydrogen peroxide can be a very promising oxidiser for bi-propellant hypergolic systems. Under the right circumstances it can even outperform conventional oxidisers [18].

3.1.1. Chemical Properties of Hydrogen Peroxide

The following chemical properties are related to hydrogen peroxide which is 100% concentrated. Some of the most characterising chemical properties are listed below in Table 3.1.

The critical temperature is the temperature at which the hydrogen peroxide cannot be further liquefied through pressure alone. From around 730 K and upwards it is therefore required to cool down the substance to keep it in its liquid phase.

The novel hydrogen peroxide concentration and production systems developed by SolvGE show a reduction in production cost, production time and energy consumption compared to the conventional anthraquinone production process. Furthermore, handling and storage procedures were documented such that notable hazards and risks could be reduced or mitigated. It was found that the upper stage design optimisations often involved novel material and manufacturing techniques such that mass, cost

Table 3.1: Chemical Properties of 100% Hydrogen Peroxide [19]

Property	Hydrogen Peroxide
Melting Point [K]	272.72
Boiling Point [K]	423.35
Heat of Vaporization (25°C) [$Jg^{-1}K^{-1}$]	1519
Specific Heat (Liquid, 25°C) [$Jg^{-1}K^{-1}$]	2.629
Specific Heat (Gas, 25°C) [$Jg^{-1}K^{-1}$]	1.352
Relative Density (25°C)[gcm^{-3}]	1.4425
Viscosity (0°C)[$mPas$]	1.819
Viscosity (20°C)[$mPas$]	1.249
Critical Temperature [K]	730.15

and production time could be reduced. To use novel (lighter) materials, a material compatibility analysis was performed for hydrogen peroxide. Although very compatible with most aerospace-grade materials, special care should be given when designing propellant tanks, valves and feed systems to prevent material degradation or oxidiser decomposition. In order to reduce the mass, manufacturing cost and production time a brief literature review was performed on conventional and novel manufacturing techniques, such as additive manufacturing.

3.2. Green Hypergolic Propellants

Hypergolic bi-propellant rocket propulsion with hydrogen peroxide is currently a hot topic in the research and development of propulsion systems. NASA Marshall Space Flight Center investigated the capability of hydrogen peroxide as an oxidiser to be used in an upper stage design together with a non-toxic fuel back in 2000, this was documented by R. Ross, et al. ([20]). In this experiment, a 10,000 *lbf* thrust chamber was developed as part of the Upper Stage Flight Experiment (USFE). This thrust chamber, capable of producing the equivalent of approximately 44500 Newton, operated on hydrogen peroxide in combination with JP-8. During the experiments conducted on the USFE, with a burn time of 200 seconds, a vacuum specific impulse of 275 seconds was delivered by mixing the oxidiser-to-fuel on a ratio of 4.7 ([20]).

More recently, at the University of Purdue most notable research was done on combustion and catalyst performance of hypergolic propulsion systems to enhance auto-ignition of the hydrogen peroxide/kerosene combination ([18], [21]). The researchers tried to optimise the auto-ignition of the propellant combination by changing the contraction ratio of the combustion chamber ([22]). Furthermore, B.L. Austin et al. ([23]) tried to develop a 150 *lbf* thrust class pintle injector engine operating on hydrogen peroxide and nontoxic hypergolic miscible fuels. It was found that the characteristic chamber length and the contraction ratio have an impact on the ignition delay times (IDT). In multiple scenarios, as described by B.L. Austin et al., high-performance operation has been achieved under steady-state and pulse mode operation ([23]).

In other studies, it has been investigated what the required design specifications are to implement a hydrogen peroxide/kerosene combination in an apogee kick motor ([24]). In this study Y. Moon et al. formulated the objective: "to derive optimum design specifications to emulate the performance achieved by the existing systems" [24]. In their study they try to find these design specifications for an apogee kick motor, operating on a 90% concentrated hydrogen peroxide and kerosene combination, to minimise the total mass of a spacecraft for a given mission scenario. Even though the H_2O_2 /hydrocarbon rocket system typically performs less in terms of specific impulse than the conventional rocket propellant combinations, the green propellant combination has a definite advantage of being environmentally friendly. This will bring down the development cost ([24]). Moreover, H. Kang et al. [10], found that green hypergolic combinations can provide distinct advantages to the performance of the propulsion system restricted by geometrically severe constraints such as an upper stage and lunar descent/ascent modules.

Y.Moon et al. modelled a mission scenario in which a satellite, weighing between 2 and 5 tons at

launch, was inserted into GEO using multiple manoeuvres. By using his model they found that the minimised mass of the simulated satellite was slightly heavier, an increase of 0.5% of the total mass, than the satellite using conventional thrusters. This increase in mass was attributed to the lower specific impulse performance that the green propellant combination produces. A sensitivity analysis showed that the chamber pressure and mixture ratio in the combustion chamber and injector plate, respectively, were having the largest effect on the total propellant mass required ([24]).

In other research work, A. Okninski, et al. ([18]) a small and simple bi-propellant combustion engine was used to demonstrate that the combination Jet-A fuel/ hydrogen peroxide (98%) can have a specific impulse efficiency (compared to theoretical values) of 94%. The performance of the propellant combination can be improved by increasing the oxygen-to-fuel ratio. Furthermore, it was seen that the initial fuel injection and the corresponding feeding pressures will have a significant effect on combustion (in)stability ([18]). To use hypergolic propellants for rocket propellant applications often a gelling agent should be added to the fuel to prevent the ignition agent (catalytic/reactive metal hydrides) from settling as sediment. This will improve the storability and hypergolic efficiency of the fuel ([25]). M.S. Naseem, et al. ([26]) investigated the nature of an organic thickening agent in terms of combustion efficiency when added to two types of ethanol-based fuels. It was found that increasing the amount of added gelling agent to the fuels would increase the viscoelastic properties of the fuel (e.g. surface tension), sometimes resulting in the prevention of hypergolic decomposition. This could result in longer ignition delay times ([26]).

The research and development in green propellants are not only coming out of environmental considerations but also to enable safer handling and procurement. A project funded by the European Union named GRASP (Green Advanced Space Propulsion) is investigating green propellants as possible candidates that substitute the non-green conventional propellants ([27]). One of the most obvious fuel partners for hydrogen peroxide are alcohols. Alcohols are cheap, storable, have a low freezing point, are non-toxic, and have good performance compared to hydrazines ([28],[29]). After research by [30]–[32] it was found that hypergolic ignition can only be achieved when relatively large amounts of metal catalyst compounds or reducing agents are added ([33]). These compounds make the performance diminish while also increasing the toxicity. Furthermore, homogeneity of the fuel mixture over a longer storage duration is not always ensured due to often insoluble catalyst compounds.

In the experiments performed by B.M. Melof and M.C. Grubelich ([28]), several catalysts, fuels and fuel/catalyst mixtures were tested on their reaction rate and reaction intensity via a simple drop test in 90% hydrogen peroxide. From the fuels tested, only the pyrrole, ethanolamine and triethyl aluminium/hexane ignited during the drop test. In conclusion, B.M. Melof et al. found ethanolamine the best fuel that was tested having a relatively high density, low toxicity, rapid ignition and respectable performance ([28]).

Small scale tests have been used to prove that a hypergolic bipropellant thruster can operate and work on a combination of sodium borohydride (with different compositions of the energetic solvents tetrahydrofuran and toluene) ([34]). As discussed by H. Kang et al. ([34]) the fuel used, sodium borohydride, was specifically chosen as it hypergolically reacts very strong with a strong oxidizer such as hydrogen peroxide ([35]), it is the least expensive metal hydride commercially available, safe in terms of storage, use and handling and it is easy to manufacture ([34],[36]). In later work from H. Kang et al. ([37]), it was investigated what the minimum required content of ignition source is for the nontoxic hypergolic propellant combination to ensure low ignition delay times and good hypergolic initiation.

In search of non-toxic, non-carcinogenic and non-corrosive rocket grade green propellants that can be used without compromising the overall rocket engine performance ([38]), more recently, intensive research and development have started to develop a green hypergolic propellant combination with hypergolic ionic liquids (HIL) ([39]). From previous studies ([40]–[44]) it can be concluded from the demonstration that; typical specific impulses obtained from the HILs fuel types often are higher than the conventional monomethylhydrazine (MMH) and unsymmetrical dimethylhydrazine (UDMH) fuels, the reactivity with common oxidisers is better and more responsive compared to conventional fuels and the ignition delay and combustion characteristics of HILs is easily controlled and modified by changing the chemical structures. However, HILs are typically very expensive to manufacture in large quantities.

Research performed by G. Rarate et al. found that fuels enriched with aluminium lithium hydrides, borohydrides, borohydride ionic liquids and borane compounds dissolved in ionic liquids will be the best candidates for rocket grade fuels that will hypergolically interact with HTP. These mixtures typically have low ignition delay times, have relatively low toxicity, volatility and corrosivity and score high on performance [33]. In total 6 fuel mixtures with catalytic additives and a total of 5 fuel candidates with a mixture of reactive additive metal hydrides were tested. All the tests were performed with 98% of hydrogen peroxide. From these tests, it could be concluded that the ignition delay times, in general, are much smaller for the energetically promoted fuels. Furthermore, G. Rarate et al. [45] calculated the theoretical specific impulse performance of the fuels under consideration. The theoretical results of the energetically promoted and catalytically promoted fuels are graphically depicted in Figure 3.1.

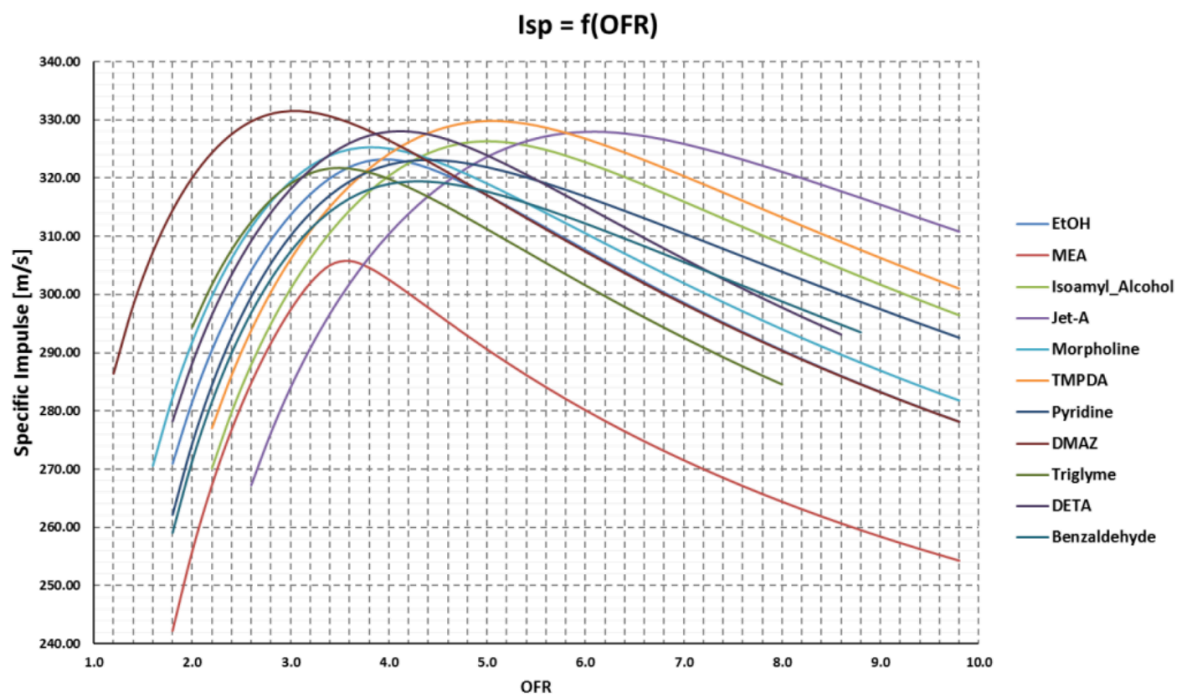


Figure 3.1: Theoretical Specific Impulse Performance for the Selected Fuels [45]

It is important to notice that the reference propellant combination, MMH/NTO has a specific impulse of about 320 seconds. Apart from the fuel option “MEA” all other fuel candidates will have a similar or even higher specific impulse than this reference case (theoretical specific impulse in the range of 305-330 seconds), under specific oxidiser-to-fuel ratio's [45].

The most promising fuels that react hypergolic with hydrogen peroxide (without energetically promoting additives) that were discussed in this section are summarised in Table 3.2. For these fuels, their respective type, availability, production price and storability are given.

Table 3.2: Promising Fuels that Hypergolically React with Hydrogen Peroxide. Compared on Type, Availability, Production Cost and Storability

Fuel Name	Type of Reaction with H2O2	Availability	Production Cost per kg	Storability
<i>Ethanolamine</i>	Reactive Hypergolic	Good [46]	€1.20 (2021) [46]	Good [28]
<i>Sodium Borohydride</i>	Reactive Hypergolic	Good [46]	€340.48 (2021) [46]	Medium [10]
<i>[EMIM][BH3CN]</i>	Hypergolic Ionic Liquid	Poor [46]	Unknown	Unkown
<i>Ethanol</i>	Catalytically Hypergolic	Excellent [46]	€0.40 (2021) [47]	Good [28]
<i>Pyridine</i>	Reactive Hypergolic	Medium [46]	€2.97 (2021) [48]	Poor [28]
<i>Diethylenetriamine (DETA)</i>	Reactive Hypergolic	Good [46]	€0.71 (2021) [49]	Good [45]
<i>Triglyme</i>	Reactive Hypergolic	Medium [46]	Unknown (2021) [46]	Medium [45]
<i>Isoamyl Alcohol</i>	Catalytically Hypergolic	Poor [46]	€1.78 (2021) [50]	Good [45]
<i>MMH (non-green)</i>	Reactive Hypergolic	Medium/Poor [46]	€322.83 (2018) [51]–[53]	Good [54]
<i>UDMH (non-green)</i>	Reactive Hypergolic	Medium/Poor [46]	€322.83 (2018) [51]–[53]	Good [54]

3.3. Upper Stage Designs

Traditionally storable hypergolic upper stages have been used for all sorts of missions and operations. These hypergolic systems often fly on UDMH or MMH in combination with the NTO oxidizer. Due to the increasing prices of these fuels, as a result of their toxicity and carcinogenic characteristics, currently, the upper stage designs are often designed around cryogenic propellants.

It was found that the upper stage modules often have very similar structures and subsystem components. Although these similarities, every upper stage module was specifically designed for its operating envelope which alters its overall dimensions, mass and launch cost (total launch vehicle cost). It is important to note that the launch cost values are corrected for inflation, this is especially important for older spacecraft. In Table 3.3 the differences between current operational upper stage designs is tabulated [16].

Table 3.3: Summary of the Upper Stage Designs [16]

Upper Stage Module	Manufacturer	Length [m]	Diameter [m]	Propulsion	Propellants	Engine	Dry Mass [kg]	Launch Cost
PS2 [55], [56]	ISRO	12.8	2.8	Hypergolic	UDMH/NTO	Vikas-4	Unknown	\$28M
EPS L10 [57], [58]	Astrium GmbH	4.711	5.8	Hypergolic	MMH/NTO	Aestus	1200	\$185M
GS2 [59], [60]	ISRO	11.56	2.8	Hypergolic	UH25/NTO	Vikas-4	5500	\$47M
Briz-M [60], [61]	Khrunichev	2.61	4.10	Hypergolic	UDMH/NTO	14D30	2500	\$65M
Fregat [60], [62], [63]	NPO Lavochkin	1.50	3.35	Hypergolic	UDMH/NTO	S5.92	902	\$80M
Falcon 9 Upper Stage [60], [64]	SpaceX	16	3.66	Cryogenic	LOX/Kerosene	Merlin 1D Vac	4500	\$61.2M
ESC-A [60], [65], [66]	ArianeGroup	4.7	5.4	Cryogenic	LOX/LH2	HM7B	4540	\$178M
H10-3 [67]	ArianeGroup	11.05	2.6	Cryogenic	LOX/LH2	HM7B	1240	65
DCSS (4 meter) [68]	Boeing	12.2	4.0	Cryogenic	LOX/LH2	RL10B2	2850	164
Centaur III [69]	ULA	12.68	3.05	Cryogenic	LOX/LH2	RL10C-1	2247	110
Delta II [70]	Delta K	5.89	2.40	Hypergolic	NTO/Aerozine 50	AJ10-118K	950	137

3.4. Upper Stage Propulsion Systems

In this section, the state-of-art bi-propellant propulsion systems will be discussed. The engines that have been used for upper stage propulsion vary a lot in performance and dimensions. In the literature review, the cryogenic and hypergolic engines that are currently under development or in production have been discussed in detail. As a quick reference, this data will be summarised in Table 3.4.

Table 3.4: Data Summary on the Upper Stage Propulsion Systems

Engine/ Parameter	<i>Vinci</i>	<i>RL10B2</i>	<i>HM7B</i>	<i>YF-75D</i>	<i>RD-0146</i>	<i>LE-5B</i>	<i>CE-20</i>	<i>Merlin 1D Vacuum</i>	<i>Vikas-4</i>
Propulsion Type [-]	Cryogenic	Cryogenic	Cryogenic	Cryogenic	Cryogenic	Cryogenic	Cryogenic	Cryogenic	Storable
Propellants [-]	LOX/ LH2	LOX/ LH2	LOX/ LH2	LOX/ LH2	LOX/ LH2	LOX/ LH2	LOX/ LH2	LOX/ RP-1	UDMH/ NTO
Mixture Ratio [-]	6.1	5.88	5.0	6.0	5.9	5.0	5.05	2.38	1.86
Nozzle Ratio [-]	240	280	83.1	80	30.8	110	100	165	Unknown
Vacuum Thrust [kN]	180	110.1	62.2	88.36	68.6	137	200	981	725
Chamber Pressure [MPa]	6.08	4.412	3.7	4.1	5.9	3.62	6	9.7	5.35
Vacuum Specific Impulse [s]	457	465.5	444.6	442	436	447	443	348	290
Dry Mass [kg]	280	301	156	550	261	285	588	Unknown	Unknown

3.5. Material Compatibility

An upper stage module of any launch vehicle consists of a multitude of materials. These materials can have are carefully selected for their properties and function in the system. The materials often have multiple functions at once (structural, thermal, etc.). The choice of what materials are used for the components in a rocket stage is typically also driven by mass and cost (both should be minimised). In this section, it will be discussed what kind of materials are typically used on a launch vehicle upper stage module and what their compatibility is with hydrogen peroxide. Furthermore, the conventional and novel manufacturing techniques will be investigated that can be used to lower the cost and mass of the individual components.

3.5.1. Type of Materials

Starting with the propulsion system, already a lot of different materials are in use. Mainly metallic alloys are used for the rocket engine components. The injector, that injects and diffuses the fuel and oxidiser at the beginning of the combustion chamber, is often comprised of alloy steel, copper alloys, stainless steel, aluminium alloys, titanium alloys, cobalt-base alloys or nickel based alloys [71]. Since the injector plate with its dedicated orifices is in direct contact with the propellants for a considerable period of time, it is important to carefully select a material that will not degrade upon contact with the propellants nor will it change the combustion reactivity or effectiveness of the propellant combination.

The combustion chambers and nozzles are constructed using multiple structural designs. Due to the wide temperature and pressure ranges that occur over the combustion chamber and nozzle these different design strategies are required to maintain good rigidity and thermal conductance during operation [54], [71].

Valves are very important for any propulsion system or feed system as flows of pressurant, fuel and oxidisers should be controlled during the operation of the systems. Valves are used to directly control the flow of propellants to the main engine, it helps to control regenerative cooling or other cooling methods, it assists the bleed flow and propellant on- and off-boarding [72]. When a valve closes a seal is required to make sure that the valve can be closed airtight. Sealing often is achieved by a hard surface that is pressed onto a softer surface. This softer material is often a polymeric or elastomeric material (like Teflon) or a soft metal (such as copper alloy) [72]. For the harder surface often a high-strength aluminium alloy, that was heat-treated, is used. In case of higher strength performance, nickel-base alloys or titanium alloys are used. Especially the reliability, strength and compatibility of the seal (softer material) should be investigated, as a failure of this component can result in catastrophic failure of the entire propulsion system [54], [72].

For ease of manufacturing, often austenitic stainless steel are used for their weldability and good corrosion resistance. More powerful propulsion systems, that operate on high combustion chamber pressures, require propellant lines with a high specific strength to limit engine weight. The high-strength

nickel-base 718 alloy is such a high specific strength material [72].

A propellant tank is comprised of different types of materials. You have materials that have specific functions, for example, structural materials, liners, sealing material and material for thermal insulation. Again, the specific strength of the material is an important parameter for the tank structure, to minimise weight and maintain performance. Typical materials that are used in hypergolic and cryogenic propellant tanks are [54];

- Aluminium Alloys
- Low-alloy Steel
- Titanium alloys
- Glass-epoxy
- Graphite-epoxy
- Kevlar/Aaramid

Looking at the reference case, the upper stage module of the Ariane 6 rocket, the tanks are made out of cylindrical segments that separate the fuel and oxidiser tanks by a common bulkhead. These propellant structures are built using a relatively new manufacturing technique, known as friction stir welding. This is done to reduce the weight while ensuring high strength and stress resistance [73].

The structure of the upper stage module has as function to provide for structural rigidity, strength, force load paths and prevent buckling. These structural components are built up out of skirts, that are stir welded out of aluminium alloys. These skirts are reinforced with ribs and stringers for strength considerations [73]. Carbon fibre, ceramic and polymeric composites will in the future have a more pronounced occurrence in the field of aerospace engineering due to their wide applicability and high specific strength performance characteristics [72]. As mentioned earlier, there are design optimisations that were proposed that involved manufacturing structural components and propellant tanks out of carbon fibre composites [74], [75].

3.5.2. Material Capability with Hydrogen Peroxide

Now that the important materials for upper stage designs have been identified it is necessary to look into the material compatibility with hydrogen peroxide. In particular, the materials that are in direct contact with hydrogen peroxide will have to be analysed on their ability to withstand degradation and prevent decomposition of hydrogen peroxide. The propellant tanks, the lines and ducts of the propellant feed system, the injector plate, and the combustion chamber are in direct contact with the highly concentrated hydrogen peroxide. These components consist primarily of aluminium alloys, stainless steel, titanium alloys, nickel-base alloys copper alloys. For future designs, it is important to consider also carbon-carbon, graphite epoxy and glass epoxy as possible materials that will be in contact with hydrogen peroxide.

In order to identify the compatibility of the different materials a class structure is formulated [76]:

- Class 1: Materials satisfactory for unrestricted use with H_2O_2
- Class 2: Materials satisfactory for repeated short-time contact with H_2O_2 . (Maximum of 4 hours at $71^\circ C$ or 1 week at $21^\circ C$)
- Class 3: Materials satisfactory for short-term contact only, single use only. (Less than 1 minute at $71^\circ C$ or 1 hour at $21^\circ C$ for unpressurized systems)
- Class 4: Not recommended for use with H_2O_2

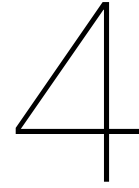
It is important to note that the surface finish or surface treatment can contribute to a large impact on the compatibility. For this reason, often metals are passivated before they are exposed to hydrogen peroxide [76]. A comprehensive material compatibility chart, for different types of polymeric, elastomeric, ceramic etc. materials is presented in Appendix B.

3.6. Executive Chapter Summary

Hydrogen peroxide is a widely used oxidising agent that has many applications. A concentration higher than 85% is called high-test peroxide. Environmental factors and the stability of hydrogen peroxide determine the decomposition rate of hydrogen peroxide. Hypergolic fuels (i.e. hypergolic with concentrated hydrogen peroxide) can be divided into three groups; catalytic hypergolic fuels, reactive hypergolic fuels and ionic liquids. The reactive hypergolic fuels are preferred as the metal compounds added

to the fuels increase the decomposition rate and improve the specific impulse compared to the catalytic hypergolic fuels and they are cheaper to manufacture than ionic liquids. A comprehensive state-of-art review was performed on the current conventional hypergolic and cryogenic upper stage designs and upper stage propulsion systems. From this state-of-art review it was found that, although the upper stage modules have very different performance and cost characteristics, they are comprised of similar subsystem designs. There are currently many different upper stage propulsion systems used to power the upper stage modules. They often work on the cryogenic liquid propellant combination LOX/LH₂. The data on the cryogenic and hypergolic propulsion systems are summarised in Table 3.4. Research on bipropellant engines that operate on hydrogen peroxide as an oxidiser show promising results. The specific impulse and produced thrust are encouraging for further research. It was found that green hypergolic bipropellant propulsion systems can be slightly heavier than the conventional propulsion systems. However, it was argued that the development cost of such engines could be lower due to the environmentally friendly propellants. The performance of the propulsion systems can be optimised by carefully selecting the mixture ratio, chamber pressure, nozzle contraction/expansion ratio and the characteristic chamber length. Gelling agents that were added to the fuels, to improve storability, could reduce the injection and ignition performance due to viscoelastic effects if not done carefully. The research on green propellant candidates is well underway. Research in promising reactive hypergolic fuels, catalytic hypergolic fuels and hypergolic ionic liquids (in combination with hydrogen peroxide) show exciting steps towards application in bipropellant systems. Furthermore, it was found that green hypergolic combinations can provide distinct advantages to performance of the propulsion system restricted by geometrically severe constraints such as an upper stage and lunar descent/ascent modules. The most promising fuels in terms of good ignition delay times, specific impulse are summarised in Table 3.2. It was shown that reactive fuels show beneficial specific impulse and ignition delay times compared to catalytic fuels when combusted with hydrogen peroxide. Hydrogen peroxide shows to be a very promising oxidiser compared to "non-green" oxidisers such as NTO. Hydrogen peroxide has a higher specific impulse and is less sensitive to oxygen-to-fuel ratio changes.

It was found that the upper stage design optimisations often involved novel material and manufacturing techniques such that mass, cost and production time could be reduced. In order to use novel (lighter) materials an material compatibility analysis was performed for hydrogen peroxide. Although very compatible with most aerospace grade materials, special care should be given when designing propellant tanks, valves and feed systems to prevent material degradation or oxidiser decomposition.



Research Methodologies

In this chapter, the research methodologies and verification and optimisation methods will be outlined. During this research, multiple models will be used that (in)directly depend on the input of each other. As discussed in the preceding chapters, there are multiple models developed to study the change in performance, mass and cost for various storable propellant combinations, compared with the conventional cryogenic hydrolox combination. To use these models it is important to set up a model architecture and framework according to the Model Based Systems Engineering (MBSE) philosophy. In this chapter, the architecture and framework of the models will be pointed out. Furthermore, the optimisation tools and strategies that will be used to find a converged solution to optimisation problems at hand will be discussed. Lastly, verification and validation methods will be described to verify models, tools and results.

4.1. Systems Engineering Framework

According to the International Council on Systems Engineering (INCOSE) systems engineering can be defined as “A trans-disciplinary and integrative approach to enable the successful realisation, use, and retirement of engineered systems, using systems principles and concepts, and scientific, technological, and management methods” [77].

The tools and methodologies often used in (space) systems engineering are constructed out of a mixture of qualitative and quantitative research methods. Systems engineering tries to quantify parameters and variables where possible. However, sometimes a qualitative assessment method has to be used to make a design choice or assessment. The quantitative methods vary from data collection to data production, data manipulation and the use of statistical (data) models to do an objective analysis. The data collected will sometimes also be used in qualitative research methods to offer interpretation or contextualisation. In this case, quantitative data will support qualitative research methods.

All these methods can be described in a more functional approach to the systems engineering process by model based systems engineering . Here models and tools are in place to assess the individual steps (e.g. stakeholder analysis, system optimisation, modelling and simulation etc.) in the design process [78].

MBSE is an architecture that allows systems engineering practices to move from the conventional document-centric approach to a model-centric approach. This enables the systems engineering efforts to be more efficient. The document-driven approach is often stand-alone and will provide tailored solutions. The MBSE approach is focusing on models that make it possible to do concurrent design iterations allowing for more modular/re-usable systems. Since the thesis research will be about the optimisation of the upper stage of a launch vehicle it is expected that multiple design iterations will be present. This asks for an adaptive model that allows for design iterations and changing requirements. It was chosen to use the MBSE approach throughout this thesis research as it allows for automation of the systems engineering design process [79], it makes the (often) complicated and complex interconnected structure of the project more insightful through the use of visual models and aids the understanding of

design change impacts.

The MBSE architecture is schematically illustrated in Figure 4.1.

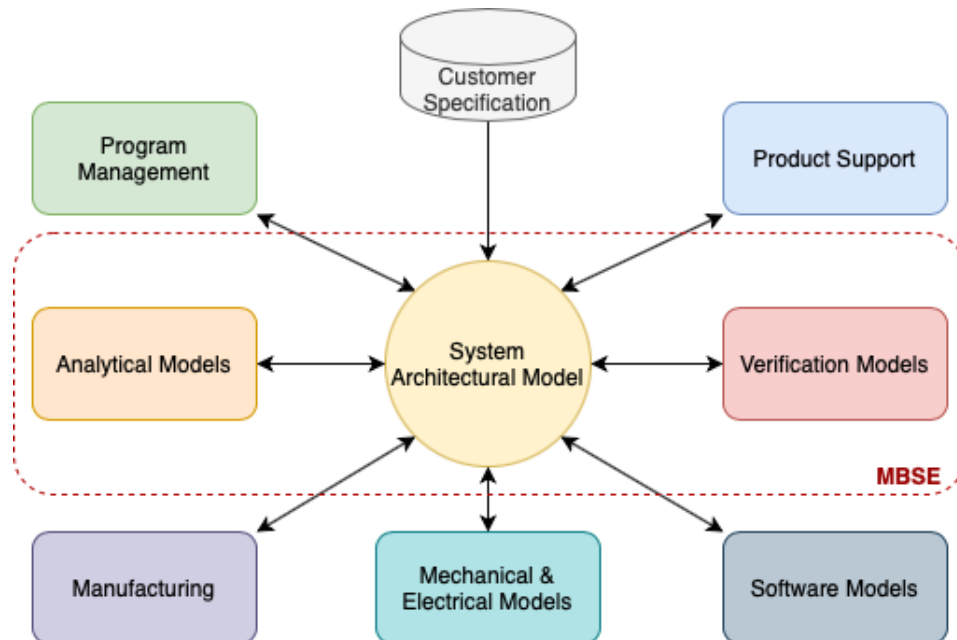


Figure 4.1: Model Based Systems Engineering Architecture

From Figure 4.1 it becomes clear that MBSE is part of an interconnected system [80]. The MBSE model consists of analytical and verification models that work together with the system architectural model. The analytical model helps to mathematically derive performance computations or simulations for a specific problem, whereas the system architecture model put emphasis on how computations and analyses fit together into a consistent whole. The system architecture model has a lot of interactions and behaves on and adapts to input scenarios [80], [81].

This thesis research work will be a combination of a so-called design thesis and an analytical thesis. Based on these two methodologies the research hypothesis and goal will be tested by systems engineering design models and analysis. Based on the results of this analysis a conclusion is drawn whether the hypothesis was rejected or not and whether the design is feasible and required.

In Figure 4.2 the research framework is presented for the research project. In this framework the individual engineering fields are present. The fields each have their specific focus to fulfil the research goal. With the use of arrows, it was tried to make it clear what the interconnections are between the fields and tasks.

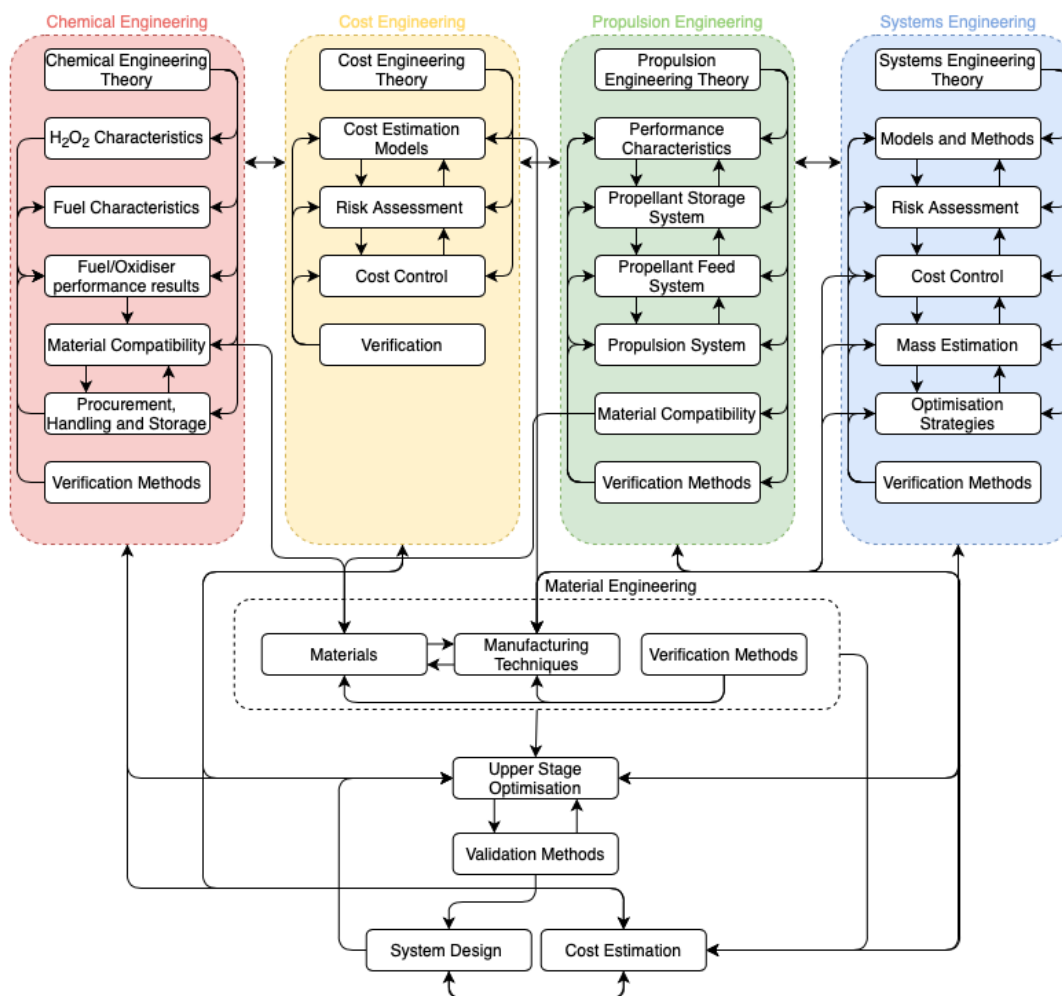


Figure 4.2: Thesis Research Framework

To manage the thesis research project it was chosen to use the MBSE approach through the use of the proprietary programming language and numeric computing environment MATLAB. MATLAB will be used to build the performance, mass and cost model. The analytical performance/mass model and cost model, described in chapter 5 and chapter 6 respectively, will be programmed in a designated MATLAB environment. This way, the large input and output data sets are structured and saved at every intermediate step, allowing for rapid error detection and root-cause analyses. The individual analytical models will be connected through MATLAB and the shared workspace will be used to allow communication between these analytical models. MATLAB will thus serve as the main programming language in which the models will be constructed. With the large engineering and optimisation database that comes with the MATLAB software it is possible to use the MATLAB interface to do Multidisciplinary Design Optimisation (MDO). MDO allows to incorporate important design variables of different problem disciplines simultaneously such that iterative optimisation strategies can be applied. This enables to analyse the effect, in this case, on performance, mass and cost by varying these variables. The system and the optimisation becomes interconnected and allows good insight into design drivers and variable specification. This multi-discipline analysis is called Multidisciplinary Design Analysis (MDA). MDO allows the optimisation of certain design variables that can be analysed in the MDA.

The analytical models that are being used are the combustion model, performance/mass model and cost model. The combustion model is ready to use model and will be further specified. The performance model and mass model, together comprise the vehicle model. These two models have to be developed for this research thesis. This vehicle model will provide data that will be an input to the fourth analytical cost model; the cost model. The analytical models are described in the section below.

4.1.1. Analytical Models

A validated combustion model will be used to analyse the combustion of several propellants. The combustion model software used is the RPA lite tool, which is using combustion analysis tools and databases from the validated NASA CEA tool to do the combustion calculations. For this thesis research the performance, mass and cost model will be developed. These models are all analytical models that will analyse the performance, mass and cost of upper stage design elements through the use of set design variables and assumptions.

In total four models will be used throughout this thesis research. These models are used iteratively. The performance model is built upon the combustion model RPA lite. This program will be further specified in chapter 5. The input for the performance model are:

- Propellant Combination
- Combustion Chamber Pressure P_c
- Oxidiser-to-fuel Ratio

With the use of these inputs the combustion model can start the analysis. Due to the optimisation loop there will be multiple iterations that will update these inputs accordingly. The output of the combustion model will be the input for the vehicle model (performance and mass model):

- Propellant Combination
- Combustion Chamber Pressure P_c
- Oxidiser-to-fuel Ratio
- Nozzle Exit Pressure P_e
- Nozzle Exit Diameter D_e
- Specific Heat Ratio γ
- Molar Mass (M)
- Combustion Chamber Temperature T_c

These input parameters will be used to run the performance and mass analysis. The performance and mass model together will describe the performance characteristics and mass breakdown of the Ariane 6 Cryogenic upper stage and the Prototype X storable upper stage concept. The vehicle model will use these parameters and variables to optimise for the mass and performance, again using an iterative loop architecture. This iterative loop can feedback design changes such as; propellant mass changes, subsystem mass changes, payload mass changes and material changes. In the case of dry mass calculations this is important. The propellant mass (and propellant density) determine the required tank volume and thus tank mass. Thus changing the propellant mass will directly influence the dry mass of the upper stage. This 'snowball' iteration effect will be further discussed in chapter 5.

From the performance and mass analysis that is done by the vehicle model, input parameters can be formulated that will be used to run the cost model. This cost model depends on the following inputs:

- Dry Mass of Components
- Type of Propellants
- Propellant Mass m_{prop}
- Oxidizer-to-Fuel Ratio
- Payload Mass (m_{pavl})
- Cryogenic/Storable System

These inputs will be used for the cost model. The cost model is a combination of cost estimating methods described by Koelle [82] in TRANSCOST 8.2 and the cost model described by Drenthe [83]. This cost model will be further specified in chapter 6.

4.1.2. Tool Architecture and Framework

The models and interconnections that have been discussed in the previous section are working together in an iterative loop to allow for optimisation strategies according to the MDO and MDA procedures. To understand how the individual models interact with each other and how optimisation loops are communicated, the tool architecture and framework are schematically depicted in Figure 4.3.

- $X_i(y_i, z_i)$: state variable computation functions. These functions yield the roots x_i of the equations [84].

Where the state equations and state variables depend on the design variables.

An MDO problem essentially is a standard constrained nonlinear programming problem[84]. The aim of the optimisation problem is to find the values for the design variables that minimise (or maximise) the objective function while not violating the objective constraints that have been set. The reason why MDO is so useful for this thesis research framework is the fact that it allows computer models to mutually interdependent work with each other to solve and analyse based on a given input. This interdependence also indicates the behaviour of the system to a great extent [84].

According to M. Balesdent [84], the MDO principles have historically shown to be especially useful for the design of launch vehicles. In these types of optimisation problems the main optimisation objective is to limit the Gross-Lift-Off-Weight (GLOW) of the launch vehicle or minimise the cost-per-flight, with constraints being; design constraints, mission-specific considerations and coupling constraints [84]. The main disciplines in the MDO as suggested by Balesdent for launch vehicle design optimisation are:

- Propulsion
- Structure
- Weight and Sizing
- Aerodynamics
- Cost Estimating
- Trajectory

Two types of MDO architectures can be used for solving launch vehicle type of optimisation problems. These are the monolithic architecture and the distributed architecture [16]. In a monolithic optimisation problem, one global optimiser objective is formulated that will be the same for all the aforementioned disciplines of the optimisation problem [16], [84]. In a distributed architecture separate optimiser objectives are formulated. For example, for the cost discipline the objective is formulated as: *“To find the lowest cost-per-flight upper stage concept”*, for the weight and sizing discipline the optimiser objective would focus on minimising the dry mass of the upper stage design. The most straightforward and less complicated architecture is the monolithic architecture for launch vehicle optimisation problems [84]. According to Balesdent, this monolithic architecture can provide good solutions for large scale problems in launch vehicle optimisation designs [84].

The optimisation algorithms that will be used are a combination of gradient-based algorithms and heuristic algorithms. The gradient-based algorithms provide optimisation solutions by using iterative methods. It is very important to make sure that the minimum found is not only a local minimum but also a global minimum [85]. This is the case when the objective function is convex. In this case it is important to give a sufficiently good first guess of the solution to find a proper solution to the problem. Such deterministic gradient-based algorithms are the Steepest Descent Method and Newton’s Method. Heuristic algorithms strive to find the minimum in a stochastic manner. In this case, a random probability distribution can still be optimised. Non-continuous, non-differentiable and non-smooth functions and constraints can be used as optimisation objective functions. Also, the heuristic algorithms do not need an initial guess for the solution. For heuristic optimisation, often genetic or evolutionary algorithms are used where evolutionary processes are mimicked to find optimised solutions.

The development of a heuristic optimisation algorithm is very time consuming. Furthermore, there is no specific optimisation algorithm that outperforms all other optimisation algorithms, according to the “no free lunch” theorem [85]. So there is no conclusive answer to what optimisation algorithm should be used. Therefore, it is chosen to use a combination of gradient-based and heuristic algorithms. The Tundat environment provides a platform that contains a large number of different optimisation algorithms. This platform is called PaGMO, Parallel Global Multiobjective Optimizer. PaGMO is developed and validated by ESA [86]. Furthermore, optimisation functions developed by MATLAB will be used together with optimisation algorithms suggested by PaGMO (as PaGMO works good in conjunction with MATLAB) [85]. This is done to verify results and test the best optimisation strategies.

4.3. Verification and Validation Methods

A schematic overview of the systems engineering process that will be conducted in the thesis research project is depicted by the “V-model”. This model describes the decomposition and requirement flow down and the integration and design synthesis through fundamental system engineering steps. Between the decomposition and integration of the design, the ongoing effort of verification and validation is present. This “V-model” is schematically depicted in Figure 4.4.

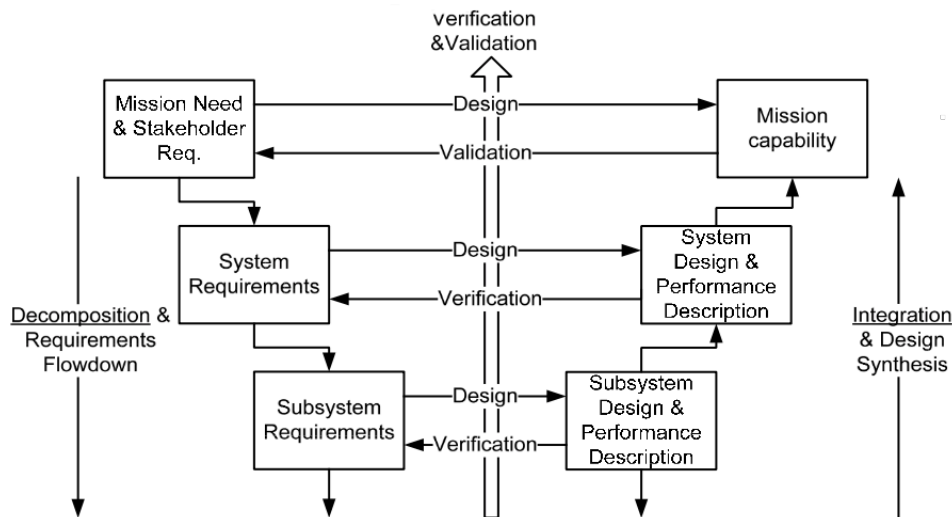


Figure 4.4: The Systems Engineering Process Described by the “V-Model” [81]

It is important to note that many elements of the systems engineering elements will be incorporated in the MBSE model to allow for concurrent design iterations.

To allow for proper (in)validation of the research work it is important to understand the pitfalls and challenges of validating results. Research in systems engineering and the corresponding designs can be validated through the use of application, comparison, statistical analysis or simulation [78]. For proper validation, it is key to select the right validation method. Unfortunately, it is sometimes hard to validate the outcome of a method or model. The outcome is not always a quantitative value that can be compared to reference data. For example, the life cycle cost of certain components or systems cannot always be directly measured and therefore becomes subject to human interpretation. The qualitative outcome of this reasoning is hard to be properly validated through quantitative models like statistical analysis or comparison [87]. The assessment or interpretation of qualitative data can result in inadequate decision-making.

The first step towards proper validation is the goal of acquiring and producing accurate and credible data. During the thesis research, the required methods and calculation procedures have to be verified. For example; to do proper cost engineering, it is required to have good verification methods to provide valuable data. Especially dealing with cost estimation analysis it is important that the methods used are verified. After verification, the outcome should be validated. This can be with the use of reference data/cases, simulation or application.

Next, the interpretation, argumentation and evaluation of results should strive for unbiasedness. The steps taken to go from the results to the interpretation should be documented and justified to avoid illogical reasoning [87].

Throughout the thesis research project the models, simulations and analytical calculations will be verified and the data will be validated, following the systems engineering process as described by Figure 4.4.

4.4. Executive Summary

In this chapter, the research methodologies and verification methods for the thesis research project were discussed. Systems engineering is a trans-disciplinary and integrative approach to the realisation of systems. Often qualitative and quantitative methods are combined to do analysis, make design choices, or give interpretation to results. It was chosen to use MBSE principles to construct the research framework for this thesis. Moving from a document-centric approach to a model-centric approach, aids in the automation of engineering design processes, understanding of design change impacts and improves communications between departments. To the system architectural model analysis, design, verification and validation tools are added to create a software model that monitors the systems engineering effort. Four analytical models are used to perform the systems engineering effort. These are the combustion model, performance model, mass and cost model. The combustion model will be described by the validated software RPA Lite. The performance and mass model together construct the vehicle model. The vehicle model, together with the cost model, will be developed specifically for this thesis research. They are further specified in chapter 5 and chapter 6.

For the development of these models, it was chosen to use the numeric computing environment MATLAB. This software will help to construct the models and enables to store large data sets at every intermediate step. This results in rapid error detection and root-cause analyses. Through the use of MATLAB, the design scenarios can be optimised through dedicated MDO and MDA. The upper stage design concept optimisation strategy and the internal communication between the models are schematically depicted in Figure 4.3.

To solve optimisation problems it is chosen to opt for the monolithic architecture as this has proven to be very useful for launch vehicle optimisation in the past [84]. A combination of gradient-based algorithms and heuristic algorithms will be used to tackle optimisation problems. This will be combined by the platform PaGMO. This platform was developed and validated by ESA and allows to use multiple optimisation algorithms to be used. To develop good knowledge it is important to do proper verification for the models, simulations and analytical calculations, and that the data is validated before this will be used in the design process. A schematic (preliminary) overview of the research framework is presented in Figure 4.2.

5

Prototype X Model

The “Prototype X” module is the name of the upper stage design concept that will be used for this research into the commercial feasibility and cost-effectiveness of the implementation of storable green propellants. The ‘Prototype X’ is based on the upper stage of the Ariane 6 launch vehicle, designed and manufactured by ArianeGroup. This way the Ariane 6 launch vehicle will serve as the conventional cryogenic reference case launch vehicle, such that changes in performance, cost and mass between the conventional and the hypergolic launcher can be compared.

In this chapter the “Prototype X” upper stage launch vehicle concept (Ariane 6 Upper Liquid Propulsion Module as reference case) will be described as discussed in the preceding literature review [16]. The dimensions, geometry and mass will be discussed along with the performance characteristics of the upper stage module. After discussing the subsystems of the upper stage launch vehicle a launch vehicle model will be set-up that allows for design optimisation analysis throughout this research. This model will be verified and validated based on reference case launch vehicles to ensure its accuracy and precision.

5.1. Ariane 6 Launch Vehicle

As described in the preceding literature review [16] the Ariane 6 Launcher is a medium-heavy launch vehicle that is able to put a wide array of payload types to Geostationary Transfer Orbit (GTO), Geostationary Orbit (GEO), Sun Synchronous Orbit (SSO) and Low Earth Orbit (LEO) [11], [16].

The Ariane 6 launch vehicle consists of two stages and is 63 meters in height and has an average diameter of 5.4 meters [11]. Depending on the mission profile the launcher can be equipped with either 2 or 4 boosters attached to the first stage resulting in a wet mass of 530 tons and 860 tons respectively. In the 2-booster configuration the Ariane 6 launcher is able deliver 5000 *kg* of payload to GTO, 6450 *kg* to SSO and 10350 *kg* to LEO [11]. For the launcher in the 4-booster configuration it is capable to deliver 11500 *kg* of payload to GTO, 5000 *kg* of payload to GEO, 14900 *kg* of payload to SSO and 21650 *kg* of payload to LEO [11].

The Ariane 6 launch vehicle is integrated and produced using some novel innovative techniques such as friction-stir-welding (FSW), 3D printed parts for the engine and a spray-on-insulation for the outer surfaces of the launcher [88]. The development of the Ariane 6 launch vehicle is expected to cost 3.8 *billion* Euro [89]. Once operational the cost per launch is expected to be 115 *million* Euro for the 4-booster configuration and 75 *million* Euro for the 2-booster configuration [90]. The Ariane 6 launcher has been schematically illustrated in Figure 5.1.

In Figure 5.1 the Upper Liquid Propulsion Module (ULPM) is graphically depicted. The information on and the performance characteristics of the ULPM will be investigated specifically in the next section.

A hydrolox (LOX-LH2) based launch vehicle is considered as the existing state-of-the-art reference case to enable comparison with the new green storable propellants. Cryogenic propellants produce the highest performance (Isp), but typically requires a large tank volume due to the low density of LH2. Furthermore, LOX-LH2 propulsion systems are costly in production and operation [9].

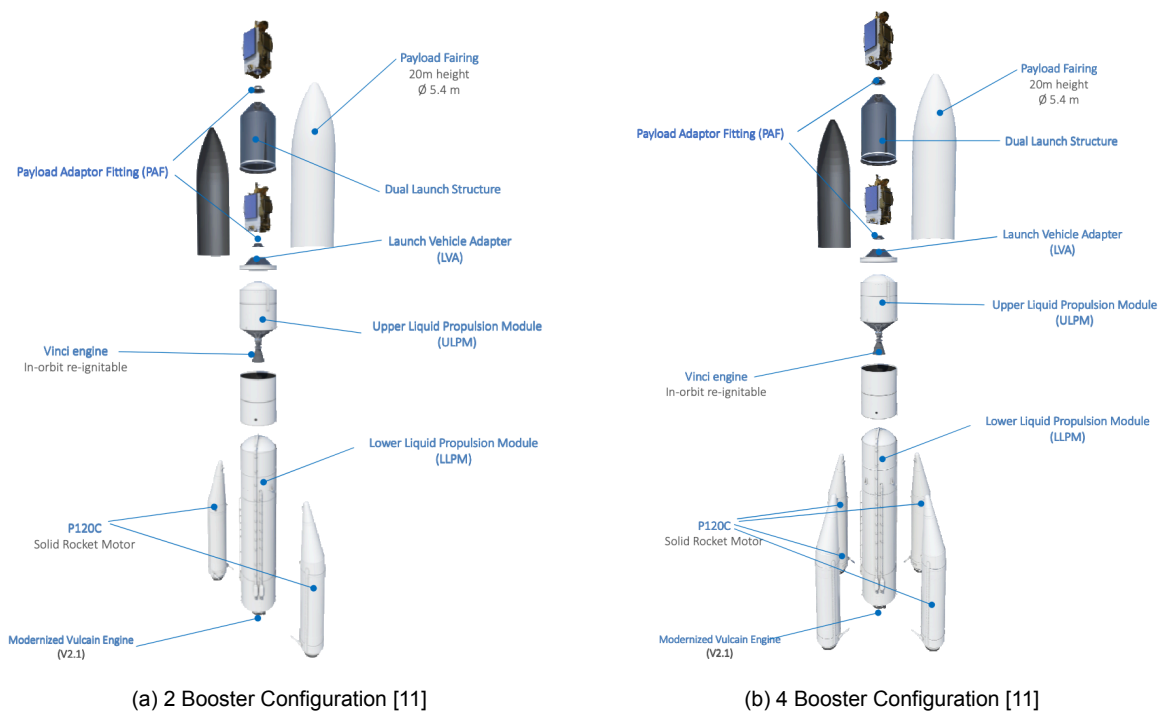


Figure 5.1: The Ariane 6 Launch Vehicle in Two Configurations [11]

5.2. The “Prototype X” Launcher Upper Liquid Propulsion Module (ULPM)

The last stage of the Ariane 6 launcher is the Upper Liquid Propulsion Module (ULPM). This stage is specifically designed to push the payload further towards the target orbit and provides the thrust required to allow for orbit insertion and inclination changes. The storable upper stage design concept is called the “Prototype X”. For this “Prototype X” upper stage module it is required that it operates on a bi-propellant liquid propulsion unit and has comparable performance characteristics. The engine has to be restartable to allow for a wide array of orbital insertion and inclination change profiles. The following data presented is relating to the conventional cryogenic ULPM and will provide the baseline for the “Prototype X” design optimisation, done at a later phase in the thesis research.

5.2.1. General Layout, Mass and Dimensions

The Upper Liquid Propulsion Module, schematically depicted in Figure 5.2, provides propulsion to the payload bay, that is mounted atop of the ULPM, through a designated Launch Vehicle Adapter (LVA). This LVA also serves as a connection to the fairing [88]. The design of the Ariane 6 ULPM will serve as a benchmark for the “Prototype X” concept. This design is dissected below.

The ULPM can be split up in 5 main structural components. These components are:

- **The main two tanks for liquid hydrogen (LH2) and liquid oxygen , (LOX)**
The LH2 tank is designed to allow for a maximum loading mass of about 5 tons of LH2, whereas the oxidizer tank can hold up to 26 tons of LOX [88].
- **The Intertank Structure (ITS)**
The ITS connects the fuel and oxidizer tanks with each other, provides for all the necessary connections and increases structural strength. [88].
- **The Vinci Thrust Frame (ViTF)**
The forces coming from the Vinci engines are introduced into the ULPM through the ViTF. The ViTF consists of fluid control equipment, electrical equipment and houses an Auxiliary Power Unit (APU) and two high pressure helium vessels (HPHV) for attitude control [88].

- **The re-ignitable Vinci engines**

The Vinci engines are connected to the ViTF and provide the thrust to the module and the attached payload bay. The Vinci engines are designed to be re-ignitable to allow for more flexibility and precise mission profiles [88].

- **The Avionics Support Structure (AvSS)**

The avionic main system and navigation computers are located in the AvSS. The AvSS is located between the aforementioned propellant tanks [88].

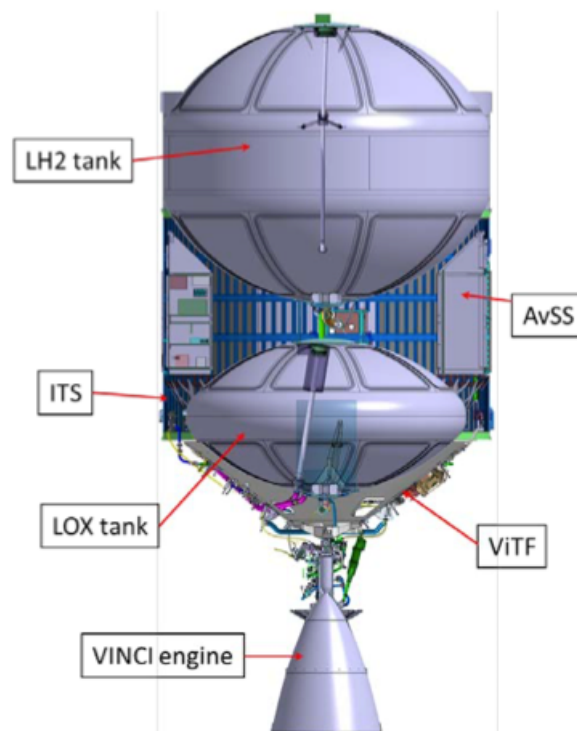


Figure 5.2: Schematic Depiction of the Upper Liquid Propulsion Module Configuration [88]

The ULPM measures 5.4 meters in diameter and is approximately 10 meters tall. The dry mass, accounting for the structure, (empty) tanks, feed systems, avionics and engine, weighs 7 tons. Considering the propellant mass of the fuel and oxidizer, 5 tons of LH2 and 26 tons of LOX respectively, the wet mass of the upper liquid propulsion module is approximately 38 tons [91].

5.2.2. Propulsion System

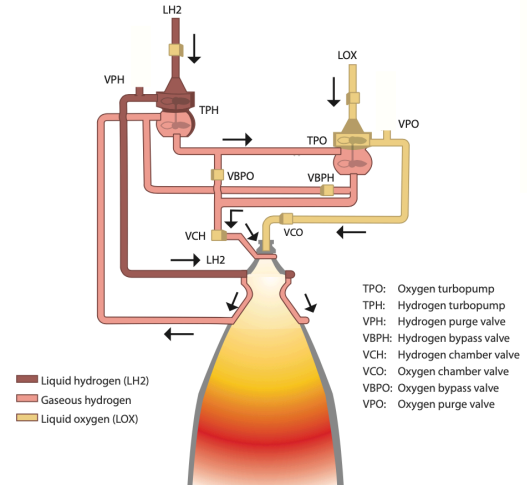
The Ariane 6 ULPM is powered by a cryogenic bipropellant propulsion system. The cryogenic reference case operates on vacuum-optimised Vinci engines, that operate on liquid hydrogen and liquid oxygen. The Vinci engine can generate variable thrust at two operating points and is reignitable. This is required to provide for the versatility in mission profiles. The Vinci engines can provide thrust levels of respectively 130 kilonewton and 180 kilonewton. For these two thrust levels the specific impulse, combustion pressure, mixing ratio and flow rates are different [92] [11]. The nominal operational data is summarised in Figure 5.3. It is important to note that all values are applicable to vacuum conditions [93]. In Figure 5.3 also the operating flowchart is presented. This gives a schematic idea of how the propellants are handled and fed towards the combustion chamber.

The “Prototype X” upper stage will have a great variety and flexibility in target orbits and required inclination. The ability to reignite the engine will provide this flexibility.

ENGINE FEATURES

Cycle	Expander
Vacuum thrust (kN)	180
Specific impulse (s)	465
Combustion pressure (bar)	60 (about 870 psi)
Expansion ratio	240
Propellants	LOX - LH2
Propellant flowrate (kg/s)	LOX: 33.70 - LH2: 5.80
Mixture ratio	5.80
Turbopump speed (rpm)	LOX: 18,000 - LH2: 90,000
Turbine power (kW)	LOX: 350 - LH2: 2,800
Height (m)	2.37 (stowed) - 4.20 (deployed)
Nozzle exit diameter (m)	2.20

(a) Vinci Cryogenic Upper Stage Engine specifications



(b) Vinci Operating Flowchart

Figure 5.3: Vinci Cryogenic Upper Stage Data [93]

5.2.3. System Requirements

It is important at this phase of the design to state important general requirements that apply to the overall launch vehicle and to the Prototype X respectively. The overall launch vehicle requirements that apply to the Ariane 6 reference case launch vehicle are tabulated below in Table 5.1. These apply to integrated system including the first and the second stage. Since the Prototype X design should still be able to be integrated with the first stage these requirements are very important to fulfill while designing and optimising the upper stage module.

Table 5.1: General System Requirements

ID	Requirement
SYS-REQ-01	The launch vehicle shall consist of two stages
SYS-REQ-02	The upper stage shall have a propulsion system that is reignitable
SYS-REQ-03	The upper stage shall operate on a bi-propellant propulsion system
SYS-REQ-04	The launch vehicle shall be able to reach LEO and GEO orbits
SYS-REQ-05	The system shall be able to be launched from existing launch sites
SYS-REQ-06	The launch vehicle shall be expendable
SYS-REQ-07	The system shall be operational for at least 20 years
SYS-REQ-08	The first stage shall operate on a bi-propellant cryogenic propulsion unit
SYS-REQ-09	The first and upper stages of the launch vehicle shall have a diameter of 5.4 meters

Since the conventional cryogenic upper stage module will be updated and optimised by using green hypergolic storable propellants it is important to also list the main requirements that relate to this design. The baseline requirements for the Prototype X design are tabulated in Table 5.2.

Table 5.2: Prototype X Vehicle Requirements

ID	Requirement
PX-REQ-01	The diameter of the upper stage shall be 5.4 meters
PX-REQ-02	The Prototype X vehicle shall have a bi-propellant engine operating on storable propellants
PX-REQ-03	The Prototype X vehicle shall use green hypergolic storable propellants
PX-REQ-04	The oxidiser of the Prototype X propulsion system shall be concentrated hydrogen peroxide (99 + %)
PX-REQ-05	The Prototype X shall be integrated into the conventional cryogenic first stage
PX-REQ-06	The Prototype X shall not change the performance of the first stage
PX-REQ-07	The Prototype X shall not impact the total mass of the first stage
PX-REQ-08	The Prototype X propulsion unit shall be able to re-ignite at least 3 times
PX-REQ-09	The Prototype X propulsion unit shall produce a nominal thrust of 180 kN
PX-REQ-10	The Prototype X shall produce the same level of performance, in terms of Delta-V, as the Ariane 6 upper stage
PX-REQ-11	The Prototype X shall be able to carry up to 21650 kg of payload to LEO in the 4-booster configuration
PX-REQ-12	The Prototype X shall use turbo-pumps as the designated propellant feed system
PX-REQ-13	The Prototype X shall use a single vacuum-optimised bi-propellant engine
PX-REQ-14	The Prototype X shall have a single fuel and single oxidiser tank
PX-REQ-15	The Prototype X shall have cylindrical tanks with semi-elliptical tanks

5.3. Launch Vehicle Model

Since this research work is focused on cost optimisation of the upper stage module while keeping performance the same, it is important to describe the considered launch vehicle in a designated model. This model will be used in combination with the combustion analysis model and the cost estimation model to do the green storable design analysis. By combining these models, Multidisciplinary Design Analysis (MDA) and Multidisciplinary Design Optimisation (MDO) tools can be applied such that the change in performance, cost and mass of the launch vehicle can be readily analysed. The launch vehicle model will be built following a similar approach described and validated by J. Vandamme [94]. The mass and performance model will be described below.

5.3.1. Performance Model Assumptions & Requirements

In order to model the performance of the launch vehicle, assumptions have to be made to allow for model simplifications. These assumptions influence the outcome, precision and accuracy of the model. Furthermore, for future research these assumptions need to be tabulated to investigate the validity of the model. The performance model assumptions are tabulated in Table 5.3.

Table 5.3: Performance Model Assumptions

ID	Assumption
PER-01	Ideal rocket theory describes performance of the engine
PER-02	Performance loss of the propulsion system will be modelled based on correction factors
PER-03	The ascent trajectory is not affected by the upper stage redesign
PER-04	No mass is lost during operation, apart from propellant mass
PER-05	Actual rocket performance can be modelled by quality factor corrections
PER-05	Vacuum conditions are assumed for the entire burn of the upper stage module
PER-06	Optimum expansion is assumed for the nozzle exhaust gasses
PER-07	The performance as result from the boosters will not be taken into account in the performance model
PER-08	The performance model analyses the steady-state conditions of the propulsion system

The requirements for the performance model are described below in Table 5.4.

Table 5.4: Performance Model Requirements

ID	Requirement
PERF-REQ-01	The model shall be able to estimate the performance of (semi-)cryogenic and storable engines
PERF-REQ-02	The model shall estimate the specific impulse with an absolute relative error of maximal 20%
PERF-REQ-03	The model shall estimate the vacuum thrust with an absolute relative error of maximal 20%
PERF-REQ-04	The model shall estimate the mass flow rate with an absolute relative error of maximal 20%

5.3.2. Performance Model

The performance model will provide valuable information on the mass flow, combustion chamber temperature and expansion ratio of the engine and nozzle. These parameters are required to estimate

the masses of various subsystem elements of the launch vehicle. The performance model that is used for the launch vehicle model is constructed by assumption of ideal rocket theory. This assumption is deemed valid at this stage of the design process as these preliminary performance parameters can characterise the nature of the system well enough such that design decisions can be made. As part of the ideal rocket theory some assumptions are made to simplify the problem whilst still producing valuable solutions for analysis. The following assumptions are taken [54].

- The exhaust gases are homogeneous and have a constant composition.
- The gas or gas mixture expelled obeys the ideal gas law.
- The heat capacity of the gas or mixture of gases expelled is constant.
- The flow through the nozzle is one-dimensional, steady and isentropic.

In order to initiate the performance model some parameters are required as input. These are:

- Fuel Type
- Oxidiser Type
- Oxidiser-to-Fuel Ratio
- Chamber Pressure
- Nozzle Exit Pressure
- Nozzle Exit Diameter

These parameters will be used in a dedicated combustion model. The combustion model will do the chemical and thermodynamic calculations that model the steady-state combustion in the rocket engine. To allow this combustion model to run, it is important to select a propellant combination and mixture ratio. Also, the expansion ratio of the throat-nozzle design is an important parameter for the combustion analysis. The combustion tool that will be used is the Rocket Propulsion Analysis (RPA) tool. This tool will provide the specific heat ratio (γ), molar mass (M) and the chamber temperature (T_c) as function of propellant combinations, chamber pressures and oxidiser-to-fuel ratio. These parameters will be provided by the RPA tool for the various propellant combinations that will be investigated. Based on these parameters the performance characteristics of the launch vehicle can be determined. Furthermore, the RPA tool uses the thermo-chemistry database of NASA's Combustion Equilibrium Analysis (CEA) tool. The RPA tool was validated by comparing it to NASA's CEA tool calculations [95].

The output of the combustion model allows doing the performance analysis. The performance of the engine is modelled by using equations that together describe the ideal rocket theory. First, the specific gas constant will be calculated:

$$R = \frac{R_A}{M} \quad (5.1)$$

Where:

- R_a = Universal Gas Constant [$8.3145 \text{ J} \cdot \text{K}^{-1} \cdot \text{mole}^{-1}$]
- M = Molecular Mass [g/mol]

With a specific heat ratio (γ) the Vandekerckhove function can be determined:

$$\Gamma = \sqrt{\gamma} \cdot \left(\frac{2}{\gamma + 1} \right)^{\left(\frac{\gamma + 1}{2(\gamma - 1)} \right)} \quad (5.2)$$

This Vandekerckhove function can help to describe the ideal characteristic velocity of the exhaust fumes. This is done through a combination of the specific gas constant R and the Chamber Temperature T_c that is provided by the RPA tool.

$$c_{id}^* = \frac{1}{\Gamma} \cdot \sqrt{R \cdot T_c} \quad (5.3)$$

To account for imperfections this ideal characteristic velocity c_{id}^* will be corrected with the use of the combustion efficiency factor (ϵ_b). With the use of quality factors the discrepancy between the ideal rocket theory and the actual performance of the rocket can be accounted for and corrected. These factors include the Nozzle Quality (ϵ_f) and the Combustion Quality (ϵ_b). The assumption of ideal rocket theory will result in theoretical performance parameters such as the characteristic velocity of the exhaust fumes and the ideal thrust coefficient. These ideal/theoretical parameters will give an overestimated approximation of reality. Ideal performance parameters result in higher specific impulse values than what you would find in reality. To account for this discrepancy the nozzle quality factor and the combustion quality factor will be used. These factors will take into account combustion losses such that the actual specific impulse can be more accurately approximated, resulting in more realistic results. The RPA tool has a designated nested analysis tool to approximate these correction factors based on the combustion chamber pressure and temperature and based on the combustion products that were formed after ignition [96].

This combustion quality factor varies between 0.85 and 0.98 according to [97]. For now, a value of 0.95 will be set, as described by Vandamme [94], for the "Prototype X" storable design concept this value will be estimated by the RPA Lite tool [96]. This correction factor will be subject to sensitivity analysis later in this chapter.

$$c_{real}^* = \epsilon_b \cdot c_{id}^* \quad (5.4)$$

To calculate for the exit pressure first the average chamber density has to be estimated. The average chamber density (ρ_c) can be calculated through:

$$\rho_c = \frac{P_c}{T_c \cdot R} \quad (5.5)$$

Where:

- P_c = Combustion Chamber Pressure [Pa]

Since the ideal rocket theory was assumed to be valid it is possible to use the Poisson relationships that apply for isentropic flow:

$$\frac{T_e}{T_c} = \left(\frac{P_e}{P_c}\right)^{\left(\frac{\gamma-1}{\gamma}\right)} = \left(\frac{\rho_e}{\rho_c}\right)^{(\gamma-1)} \quad (5.6)$$

Where:

- T_e = Nozzle Exit Temperature [K]
- P_e = Nozzle Exit Pressure [Pa]

From these relationships it is possible to deduce the exit density (ρ_e) of the mass flow:

$$\rho_e = \rho_c \cdot \left(\frac{P_e}{P_c}\right)^{\frac{1}{\gamma}} \quad (5.7)$$

Now that the exit and chamber pressures are known the area ratio can be determined:

$$\frac{A_e}{A_t} = \frac{\Gamma}{\sqrt{\left(\frac{2\gamma}{\gamma-1}\right) \cdot \left(\frac{P_e}{P_c}\right)^{\frac{2}{\gamma}} \cdot \left(1 - \frac{P_e}{P_c}\right)^{\frac{\gamma-1}{\gamma}}}} \quad (5.8)$$

Where:

- A_e = Nozzle Exit Area [m^2]
- A_t = Nozzle Throat Area [m^2]

This relationship allows to calculate the ideal thrust coefficient:

$$C_{F_{id}} = \Gamma \cdot \sqrt{\frac{2\gamma}{\gamma-1} \cdot \left(1 - \left(\frac{P_e}{P_c}\right)^{\frac{\gamma-1}{\gamma}}\right)} + \frac{P_e}{P_c} \cdot \frac{A_e}{A_t} \quad (5.9)$$

This thrust coefficient can be used to calculate the exhaust velocity and thrust of the propulsion system respectively. This thrust coefficient is describing the ideal case as per assumption of ideal rocket theory. To correct for this assumption the ideal thrust coefficient is multiplied by the earlier discussed nozzle quality factor (ϵ_F).

$$C_{F_{real}} = C_{F_{id}} \cdot \epsilon_F \quad (5.10)$$

The nozzle quality factor varies between 0.92 to 0.96 according to [97]. For now, the nozzle quality factor will be fixed at 0.97 as described by Vandamme [94] but will be subjected to sensitivity analysis. For the “Prototype X” storable concept the nozzle quality factor will be estimated by the RPA Lite tool. It is important to note that in the equations described above the ambient pressure effect on performance is omitted as the model will be used to describe the performance of the launch vehicle in vacuum conditions only. The thrust that will be described below counts as the maximum vacuum thrust in this case.

The exhaust velocity can be calculated using the following relationship:

$$V_e = c^* \cdot C_F \quad (5.11)$$

To calculate the thrust of the rocket the exhaust velocity (V_e) is multiplied with the mass flow rate (\dot{m}). The mass flow rate can be calculated by:

$$\dot{m} = \frac{P_c \cdot A_t}{\sqrt{R \cdot T_c}} \cdot \Gamma \quad (5.12)$$

The individual oxidizer and fuel mass flows can be determined using the oxidiser-to-fuel ratio. The mass flow rate will be used to find the maximum vacuum thrust force:

$$T_{vac} = \dot{m} \cdot V_e + A_e \cdot (P_e - P_a) \quad (5.13)$$

Where:

- P_a = Ambient Pressure [Pa]

Since higher mass flows are present in storable engines, compared to cryogenic engines, the mass flow rate will also be considered a variable that can be adjusted to tweak the engine performance such that nominal vacuum thrust conditions (180 kN) can be obtained, such as the values presented by the Vinci engine. Keeping the vacuum thrust the same for both the storable and cryogenic engines will ensure proper and meaningful comparison between the two designs. To do this, the mass flow rate can be adjusted directly through the propellant feed system or by adjusting the nozzle and throat dimensions. While building the performance model, flexibility with regards to adjusting the mass flow rate parameter was taken into account.

5.3.3. Mass Model Assumptions & Requirements

Now that the performance model is set up it is possible to use its input to construct the mass model of the "Prototype X" upper stage concept. Before this mass model can be developed it is important to construct a list of important assumptions and requirements. These are tabulated below in Table 5.5 and Table 5.6.

Table 5.5: Mass Model Assumptions

ID	Assumption
MASS-01	No mass, apart from propellants, is lost during normal operation
MASS-02	A propellant safety margin of 10% is assumed.
MASS-03	The expulsion efficiency of the storage system is set to 0.98
MASS-04	There is no propellant boil-off during pre-launch and launch operations
MASS-05	There is no propellant refuelling uncertainty with regards to propellant handling
MASS-06	The maximum payload mass is assumed to be 21650 kg, targeted for LEO orbit
MASS-07	The vacuum thrust produced is considered constant and stable
MASS-08	The vacuum thrust will be maintained at a thrust of 180 kN by adjusting the mass flow rate
MASS-09	The thickness of the fuel and oxidiser tanks is constant at every point on the tank
MASS-10	The length of the tanks is minimised by maximising the diameter of the tanks, with a max of 5.4 meters
MASS-11	The combustion chamber pressure is considered stable and constant
MASS-12	The thermal control mass for storable tanks is 15% of the cryogenic thermal control mass [98]
MASS-13	The engine mass includes the mass of the turbo-pump system
MASS-14	The tank pressurisation system for the pump-fed upper stage will not be considered for this preliminary analysis [99]
MASS-15	The boosters mass will not be taken into account for the mass model calculations
MASS-16	The propellant tanks will always be completely filled up, independent of the payload mass or mission.

The requirements for the mass model are described below in Table 5.6.

Table 5.6: Mass Model Requirements

ID	Requirement
MASS-REQ-01	The model shall be able to estimate the individual elements of (semi-)cryogenic and storable launch vehicle stages
MASS-REQ-02	The model shall estimate the length of the stage with an absolute relative error of maximal 20%
MASS-REQ-03	The model shall estimate the dry mass of the stage with an absolute relative error of maximal 20%
MASS-REQ-04	The mass model shall be able to estimate the mass of structural elements for various types of materials
MASS-REQ-05	The mass model shall allow for volumetric iterations of the propellant tank

5.3.4. Mass Model

In this section, the mass model will be discussed that will help to estimate the mass of key elements of the upper stage module. These mass estimates allow to calculate the dry mass of the upper stage and can point out important design optimisation possibilities in terms of mass reduction or elimination when new propellant combinations are introduced.

Propellant Mass

The required propellant mass is built up from multiple propellant factors. These are the total impulse or ΔV factor ($m_{\Delta V}$), the propellant mass margin (m_{margin}), the expulsion efficiency ($m_{expulsion}$), the boil-off factor ($m_{boil-off}$) and the loading uncertainty (m_{error}):

$$m_{prop} = m_{\Delta V} + m_{margin} + m_{expulsion} + m_{boil-off} + m_{error} \quad (5.14)$$

Where $m_{\Delta V}$ is the mass of the propellant (in kg) that is required to fulfil the total impulse requirement. The m_{margin} is the added mass that accounts for a safety margin (f_{margin}), this is set to 10% or 1.1 [54]. The $m_{expulsion}$ is the amount of mass that is not expelled/ left behind in the storage system. The factor of expulsion efficiency ($f_{expulsion}$) is set to 0.98 [54]. Since the boil-off ($m_{boil-off}$) and loading uncertainty (m_{error}) are typically very low this will be disregarded in this preliminary mass estimation [54].

The most important contribution to the propellant mass is the $m_{\Delta V}$ mass fraction. The $m_{\Delta V}$ mass fraction will be calculated in the following way: The propellant mass is an important input variable for the succeeding mass estimation relationships. Since the dry mass is dependent on the amount of propellant mass that has to be taken, the propellant mass will be determined via an iterative process that tries to obtain a convergent answer. As mentioned before, the goal is to maintain the performance characteristics of the Ariane 6 upper stage module (ULPM). This performance cannot be specified in specific

impulse (I_{sp}) as different propellant combinations (hypergolic) will be introduced into the design. It is expected that the propellant combinations at hand produce different specific impulse characteristics.

A better way is to calculate the required propellant mass to maintain the total velocity increment or “Delta-V” (ΔV) that is obtained for the different propellant combinations. The total Delta-V that can be achieved by introducing ‘green’ hypergolic propellants has to remain roughly the same as the total Delta-V that is produced by the conventional hydrolox design. The amount of Delta-V that can be achieved can be calculated using the Tsiolkovsky/rocket equation:

$$\Delta V = I_{sp} \cdot g_0 \cdot \ln \frac{M_0}{M_f} = I_{sp} \cdot g_0 \cdot \ln \frac{M_{dry} + M_{PL} + M_{prop}}{M_{dry} + M_{PL}} \quad (5.15)$$

It is important to note that this will be done for different mission scenarios, that were described earlier. This is done to simplify the analysis and to make it easier to compare the results. In this case it was chosen to choose two mission scenarios. These scenarios will be a targeted Low Earth Orbit (LEO) orbit with 10350 kg of payload and a targeted Low Earth Orbit (LEO) with a 21650 kg payload, for the 2-booster and 4-booster configuration respectively, as discussed by ArianeGroup [11].

For simplification of the model, it is assumed that the propellant tanks, both oxidiser and fuel tanks, are always completely filled for launch, independent of the payload mass or mission at hand. The required propellant mass calculation will therefore be dependent on the dry mass and efficiency of the propellants and not on the payload mass. This assumption is deemed valid for the following two reasons:

- Changing the propellant mass based on the actual payload mass would introduce a lot of dynamical uncertainties during the launch. For example, if this assumption is not made, launching a relatively low payload mass would result in the reduction of required propellant mass and thus wet mass of the upper stage (to meet the DeltaV requirement). As a result, the launch vehicle experiences a higher thrust-to-weight ratio during launch. This would yield different launch accelerations and dynamic behaviour of the rocket. For instance, the maximum dynamic pressure (the moment when the rocket experiences the largest number of stresses and pressures) would be higher. This could result in a (structural) redesign of the entire launch vehicle to make up for this new pressure and stress envelope. Hence, changing the amount of propellants for every payload mission scenario would be very costly and time-consuming.
- The propellant cost will make up less than 1 percent of the total cost-per-flight. Filling up the propellant tanks with more propellants than necessary will not impact the cost-per-flight significantly. Changing the propellant mass based on the payload would be more expensive in terms of structural redesigns and pre-flight performance optimisation than the accrued cost of unused propellants.

For the conventional (hydrolox) design of the Ariane 6 ULPM the propellant mass is known. Namely, it was stated by ArianeGroup that the propellant mass is a total of 31 tons, 5 tons of LH2 and 26 tons of LOX respectively, the wet mass of the upper liquid propulsion module is approximately 38 tons [11], [91]. This will be the starting point for the succeeding mass estimation relationships and will serve its purpose for comparison. For the green storable upper stage design an initial propellant mass will be estimated. Based on this propellant mass the succeeding mass estimation relationships can be used to determine the dry mass of the upper stage. This dry mass and propellant mass (together with the fixed payload mass) will be used to determine the total ΔV increment that is obtained. If this is too high or too low, the propellant mass will be decreased or increased respectively such that the total ΔV will converge in the range of the required mission ΔV . This iterative process helps to determine the actual wet and dry mass of the upper stage module every time a new type of propellant combination is introduced.

The total ΔV that has to be attained can be calculated using the data provided in Figure 5.3 for the engine parameters and the data presented in the ArianeGroup user manual [11]. Since the “Prototype X” is required to carry two types of payload (10350 kg and 21650 kg) at a thrust level of 180 kN a

range of ΔV 's can be calculated. However, the driving ΔV requirement comes forth from the maximum payload scenario. This ΔV will be the maximum that can be attained. If this requirement is met, it automatically follows that the smaller payloads can reach the desired orbit too. This ΔV requirement will be calculated below:

For 180 kN at an I_{sp} of 457.2 seconds and a payload of 21650 kg:

$$\Delta V = I_{sp} \cdot g_0 \cdot \ln \frac{M_{dry} + M_{PL} + M_{prop}}{M_{dry} + M_{PL}} = 457.2 \cdot 9.81 \cdot \ln \frac{7000 + 21650 + 31000}{7000 + 21650} = 3289.13 \text{ m/s} \quad (5.16)$$

This ΔV of $\approx 3.3 \text{ km/s}$ will be the target value and iterative analysis will find the dry mass and propellant mass associated with that. It is important to note that the propellant mass found using this analysis should be corrected for the propellant mass margin and expulsion efficiency using the following equation:

$$m_{prop} = m_{\Delta V} + f_{margin} \cdot m_{\Delta V} + f_{expulsion} \cdot m_{\Delta V} \quad (5.17)$$

Now that the main input (the propellant mass) is constructed, it is possible to calculate the mass contributions of other elements and subsystems of the upper stage design.

Tank Mass

In this section, the masses for the fuel and oxidizer tanks will be approximated. The mass estimating relationships presented here are coming from the works of Balesdent [84].

In order to size the tanks, the following inputs are required:

- Propellant Mass - m_{prop}
- Mixture Ratio - $(O/F)_{ratio}$
- Stage Diameter - D_{stage}
- Density of Oxidizer - ρ_{ox}
- Density of Fuel - ρ_{fuel}
- Ultimate Strength of Tank material - σ_t
- Density of Tank Material - ρ_{tank}

Furthermore, Balesdent [84] states the following parameters to be fixed for the dry mass estimation analysis:

- Safety Coefficient $SF_t = 1.25$
- Margin of Safety for the Tanks Thickness $f_t = 1.2$

In Figure 5.4 the schematic layout of the tank design is presented. Based on the design of the Ariane 6 propellant storage design [11] the tanks are cylindrical and have semi-elliptical caps. The depth of this type of cap is lower than the hemispherical head and higher than the torispherical cap. The most common design was chosen, where the semi-elliptical heads have a ratio of 2:1, meaning that the depth of the cap is one-quarter of the diameter of the container. This cap is the result of a trade-off between structural strength and volumetric efficiency. The 2:1 semi-elliptical cap allows putting the oxidizer and fuel tank relatively close to each other, minimising the intertank structure [100]. In Figure 5.4 the intertank between the oxidiser and fuel tanks is also presented along with the important parameters for the tank mass estimation relationships.

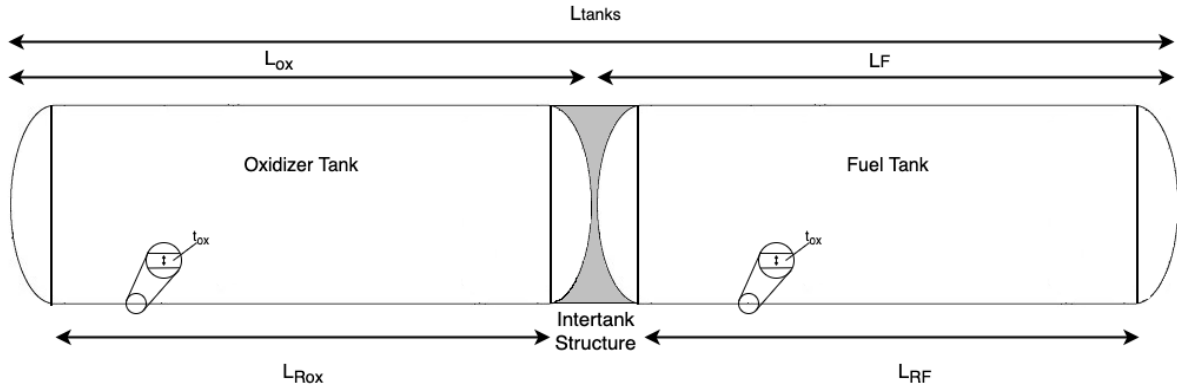


Figure 5.4: Schematic of the Cylindrical Tank Layout

The total volume of the caps (2 caps per tank) can be calculated by:

$$V_{caps} = 2 \cdot \frac{\pi D_{stage}^3}{24} \quad (5.18)$$

Where:

- D_{stage} = Diameter of the stage [m]

The volume of the caps will be useful to determine the required length of the propellant tanks at a later stage. Next, the required tank volume will be calculated. The required tank volume for the oxidizer and fuel tank, respectively, can be calculated by:

$$V_{ox} = \frac{1}{\rho_{ox}} \frac{m_{prop} \cdot (O/F)_{ratio}}{(O/F)_{ratio} + 1} \quad (5.19)$$

$$V_{fuel} = \frac{1}{\rho_{fuel}} \frac{m_{prop}}{(O/F)_{ratio} + 1} \quad (5.20)$$

Where:

- ρ_{ox} = Density of Oxidizer [kg/m^3]
- ρ_{fuel} = Density of Fuel [kg/m^3]

Now that the required tank volumes are known, the corresponding tank pressures will be estimated. There must be a distinction between cryogenic and hypergolic systems as these have different tank pressure behaviour as a result of their vapour pressure. For the (semi-)cryogenic, pump-fed, propellant combination the tank pressure can be calculated using a historical trend fitted curve developed by Humble et al. [101]:

$$P_{r_{ox}} = [10^{-0.1068(\log(V_{ox})-0.258810)}] \cdot 10^6 \quad (5.21)$$

$$P_{r_{fuel}} = [10^{-0.1068(\log(V_{fuel})-0.258810)}] \cdot 10^6 \quad (5.22)$$

For the storable propellant, Humble et al. developed another historical trend fitted curve to determine the tank pressures of a pump fed system based on the tank volumes. These pressure relationships are depicted below [101]:

$$P_{r_{ox}} = [10^{-0.2036(\log(V_{ox})+0.2538)}] \cdot 10^6 \quad (5.23)$$

$$P_{r_{fuel}} = [10^{-0.4281(\log(V_{fuel})+0.4498)}] \cdot 10^6 \quad (5.24)$$

- $P_{r_{ox}}$ = Pressure of Oxidiser Tank [Pa]
- $P_{r_{fuel}}$ = Pressure of Fuel Tank [Pa]

The tank pressures are required to determine the tank thickness of the tank. Higher tank pressures require a higher propellant tank strength to prevent catastrophic failure during operation. The required strength determines the thickness of the propellant tanks. The tank thickness can be calculated using the following equation:

$$t = SF_t \cdot \frac{P_r \cdot D_{stage}}{2\sigma_t} \quad (5.25)$$

Where:

- σ_t = Ultimate Strength [MPa]

It is assumed that the fuel and oxidizer tanks are cylindrical tanks with 2:1 semi-elliptical bulkheads. The volume of the tanks is calculated by:

$$V_R = \pi \cdot \left(\frac{D_{stage}}{2}\right)^2 \cdot L_R + V_{caps} \quad (5.26)$$

Where:

- L_R = Length of Cylindrical Part of Tank [m]

Since the required volume for the oxidizer and fuel tank is already known this formula can be used to find the length of the cylindrical part of the tank (L_R) by rewriting the formula into:

$$L_R = \frac{V_R - V_{caps}}{\pi \cdot \left(\frac{D_{stage}}{2}\right)^2} \quad (5.27)$$

Now that the dimensions of the tank are known it is possible to determine the surface area of the tanks. Together with the thickness the surface area allows to calculate the tank mass based on the tank material density characteristic. The surface area of the 2:1 semi-elliptical head (individual) can be calculated using:

$$S_{cap} = 1.084 \cdot D_{stage}^2 \quad (5.28)$$

The tank surface area follows from this by:

$$S_R = \pi \cdot D_{stage} \cdot L_R + 2 \cdot S_{cap} \quad (5.29)$$

And finally the mass of the tank:

$$m_{tanks} = t \cdot S_R \cdot f_t \cdot \rho_{tank} \quad (5.30)$$

Where:

- ρ_{tank} = Density of Tank Material [kg/m^3]

Furthermore, it is very useful to have the total length of the tank structure. This allows to calculate the length of the upper stage vehicle in a later phase. The length of the individual tanks can be calculated through:

$$L_{ox} = L_{R_{ox}} + D_{stage} \quad (5.31)$$

$$L_f = L_{Rf} + D_{stage} \quad (5.32)$$

Assuming that the tanks are configured next to each other, with the spherical heads of the individual tanks connected, the length of both tanks together can be determined through:

$$L_{tanks} = L_{ox} + L_f \quad (5.33)$$

The part that is in between the oxidizer and fuel tank, connecting the two and providing structural support, is called the intertank structure. This intertank structure mass is considered to be part of the total tank mass. In the mass model the intertank contributions will be distributed over the fuel and oxidiser tanks accordingly. In case of classical Al-alloy based structures the intertank mass can be estimated by the following relationships described by Castellini [99]:

$$M_{intertank} = \left\{ \begin{array}{ll} 5.4015 \cdot \pi \cdot D_{stage}^2 \cdot (3.2808 \cdot D_{stage})^{0.5169} & \text{for For Stage 1} \\ 3.8664 \cdot \pi \cdot D_{stage}^2 \cdot (3.2808 \cdot D_{stage})^{0.6025} & \text{for For Upper Stage} \end{array} \right\} \quad (5.34)$$

In case of advanced composite-based structures the intertank mass can be calculated for the first and upper stages using the following relationships [99]:

$$M_{intertank} = \left\{ \begin{array}{ll} 3.7811 \cdot \pi \cdot D_{stage}^2 \cdot (3.2808 \cdot D_{stage})^{0.5169} & \text{for For Stage 1} \\ 2.7065 \cdot \pi \cdot D_{stage}^2 \cdot (3.2808 \cdot D_{stage})^{0.6025} & \text{for For Upper Stage} \end{array} \right\} \quad (5.35)$$

The intertank mass contribution will be distributed over the fuel and oxidiser tank mass fractions. This is done because the cost model, discussed in chapter 6, considers the intertank mass as part of the fuel and oxidiser tanks respectively.

Stage Structure - Pressurisation System Mass

According to [99] the pressurisation system, in case of pump-fed scenarios, is not considered for preliminary estimates. For simplicity, it is assumed that the pressurisation system mass is incorporated into the propellant storage system mass and the engine mass. In this case the mass of the system will not be considered for this phase of the design.

Engine Mass

The engine is a significant part of the upper stage design. The mass of the engine is therefore important to take into account. Inputs required for the engine mass estimate are:

- Vacuum Thrust - T_{vac}

In order to make a good estimate of the engine mass, it is possible to dissect the engine into all the individual components and determine their masses. But this in-depth approach in this phase of the design development is considered out of scope and not very suitable for validation. The engine mass will be determined based on parametric relationships that have been developed for cryogenic and storable engines. In the work developed by Zandbergen [102] there was made a distinction between pressure-fed and pump-fed propulsion systems. In this research, only pump-fed propulsion systems are considered due to their required thrust performance. According to Zandbergen [102] the following mass estimation relationships of cryogenic and storable (hypergolic) pump-fed propulsion systems can be used to calculate the engine mass.

$$M_{eng} = \left\{ \begin{array}{ll} 1.866 \cdot 10^{-10} \cdot T_{vac}^2 + 0.00130 \cdot T_{vac} + 77.4 & \text{for Cryogenic} \\ 0.001104 \cdot T_{vac} + 27.702 & \text{for Storable, Semi-Cryogenic (Kerolox)} \end{array} \right\} \quad (5.36)$$

Where:

- T_{vac} = Vacuum Thrust [N]

The thrust range for the cryogenic propellant engines is between roughly 50 *kN* and 3.5 *MN* of vacuum thrust. For the storable/semi-cryogenic propulsion systems this range is between 20 *kN* and 8 *MN* of vacuum thrust [102]. According to Zandbergen [102] the Cryogenic mass estimation relationship has a coefficient of determination of 0.993 (R^2) and a relative standard error (RSE) of 13.6% at $N = 22$ (amount of data points). The Storable/Semi-cryogenic propulsion system mass has a R^2 of 0.987, RSE of 19.8% at $N = 21$. In order to check the validity of the engine mass estimation relationships the data on current upper stage propulsion units, obtained in the literature review [16], will be used to check the relative error between the calculated dry masses. This is summarised in the table below.

It is important to note that these mass estimation relationships include the weight of the turbo-pumps. In order to calculate the turbo-pump mass separately the following relationship can be used [54].

$$m_{pumps} = C_{propellant} \cdot C_{pumps} \cdot (T_{vac} \cdot p_c)^{0.71} \quad (5.37)$$

Where:

- $C_{propellant} = 0.19$ (for high energetic propellants)/ 0.11 (for low energetic propellants)
- $C_{pumps} = 0.5$ (for engines with pre-pumps)/ 1.0 (for engines without pre-pumps)

Engine Mass Validation

Based on the engine data mass on cryogenic (hydrolox), semi-cryogenic (kerolox) and storable (hypergolic) propulsion systems [16], [102]–[104], the dry mass could be estimated using the equations described above in Equation 5.36. The engine data is used to validate the engine mass estimation relationships. This validation is tabulated below in Table 5.7.

Table 5.7: Validation of Engine Mass Estimation Relationships [16], [102]–[104]

Engine	Propellant Type	Tvac [kN]	N [-]	Ae/At [-]	Pc [Mpa]	Mdry real [kg]	Mdry est [kg]	diff [%]
Vinci	Cryogenic	180	1	240	6.08	280	317.45	13.4
RL10B2	Cryogenic	110.1	1	280	4.412	301	222.79	-26.0
HM7B	Cryogenic	62.2	1	83.1	3.70	165	158.98	-3.6
YF-75D	Cryogenic	88.36	1	80	4.10	265	193.72	-26.9
Vulcain 2	Cryogenic	1150	1	45.1	10	1800	1819.18	1.1
LE-5B	Cryogenic	137	1	110	3.62	269	259.00	-3.7
CE-20	Cryogenic	220	1	100	6	588	372.43	-36.7
Vikas-4	Storable	725	1	30.8	5.35	900	828.10	-8.0
Viking 5C	Storable	758	1	10	5.50	826	864.53	4.7
RS-27	Semi-Cryogenic	1023	1	12	4.87	1146.6	1157.09	0.9
S-4	Semi-Cryogenic	364	1	25	4.60	470.4	429.56	-8.7

From the results in Table 5.7 it is found that the estimation relationships fit the dry mass described in literature relatively well. When the error percentage between the real dry mass value and the estimated dry mass value is within 20% the cell is coloured green, in accordance with the set mass model requirements. Apart from the YF-75D, RL10B2 and the CE-20 engines the dry mass estimates of the engines can be considered very accurate with an average absolute error percentage of 12.15%. The offset YF-75D, RL10B2 and the CE-20 engine mass estimates can be explained by contradicting data found in literature on thrust and dry mass [16]. Furthermore, the length of the engines can be approximated using the relationships [102]:

$$L_{eng} = \begin{cases} 0.1667 \cdot T_{vac}^{0.2238} & \text{for Cryogenic} \\ 0.1362 \cdot T_{vac}^{0.2279} & \text{for Storable, Semi-Cryogenic (Kerolox)} \end{cases} \quad (5.38)$$

These length estimation relationships have been validated by Zandbergen [102] and it was found that the cryogenic engine length estimation relationship has a coefficient of determination (R^2) of 0.890 and a (RSE) of 10.6% at $N = 18$ (amount of data points). The storable/semi-cryogenic engine length has a R^2 of 0.783, RSE of 17.6% at $N = 22$.

Stage Structure - Thrust Structure Mass

The forces and stresses from the propulsion subsystems are introduced into the upper stage structure using the thrust structure. Typically the thrust structure is, due to the required strength, a significant contribution to the upper stage dry mass. Inputs required for the thrust structure mass estimate are:

- Vacuum Thrust - T_{vac}

Rohrschneider [105] developed a variety of mass estimating relationships for upper stage elements and subsystems. These estimating relationships have been developed by parametric analysis [105]. In the following subsections, these mass estimating relationships are described. The following relationships are developed to determine the thrust structure or thrust cone mass of the upper stage module. This relationship is described by:

$$m_{TS} = 0.001949 \cdot T_{vac}^{1.0687} \quad (5.39)$$

Stage Structure - Skirt Mass

For the cost model, it is important to know the mass fraction of the skirt mass. The skirt mass is considered to be part of the upper stage design. Inputs required for the skirt mass estimate are:

- Stage Diameter - D_{stage}
- Skirt Surface Area - S_{skirt}

The skirt mass can be determined by estimating the width and surface area of the skirt. The mass can be obtained by the relationships set-up by Rohrschneider [105].

$$m_{skirt} = \begin{cases} S_{skirt} \cdot 38.70 \cdot D_{stage}^{0.6722} & \text{for For Stage 1} \\ S_{skirt} \cdot 15.46 \cdot D_{stage}^{0.5210} & \text{for For Upper Stage} \end{cases} \quad (5.40)$$

Where:

- S_{skirt} = The Surface Area of the Skirt [m^2]

The surface area of the skirt can be determined by:

$$S_{skirt} = 2 \cdot \pi \cdot \frac{D_{stage}}{2} \cdot L_{eng} \quad (5.41)$$

Stage Structure - Thermal Control Mass

Thermal control mass combines the contributions of multi-layer insulation (MLI), cryo-coolers, thermal paint, etc. Thermal control mass has a more pronounced contribution in (semi-)cryogenic upper stages compared to storable designs. Inputs required for the thermal control mass estimate are:

- Surface Area Tanks - S_R

The thermal control mass is primarily determined by the insulation mass that is added to the tank's external surface for cryogenic tanks (LO2 and LH2) to make sure that the tanks are thermally insulated from the rest of the upper stage design. A relationship described by Castellini [99] allows to calculate the mass of the thermal control insulation layer that is added to the cryogenic tanks:

$$M_{TPS} = \begin{cases} 0.9765 \cdot S_{OT} & \text{for LOX Tanks} \\ 1.2695 \cdot S_{FT} & \text{for LH2 Tanks} \end{cases} \quad (5.42)$$

Where:

- S_{OT} = The Surface Area of the Oxidiser Tank [m^2]
- S_{FT} = The Surface Area of the Fuel Tank [m^2]

It is important to note that for hypergolic or storable fuel and oxidizer tank little insulation is required as their required thermal insulation from other subsystems is limited. They are stored at non-cryogenic temperatures. In the work of Oglebay et al. it was estimated that the storable tanks require about 15% of the amount of Multi-Layer Insulation (MLI) that is required for the cryogenic thermal control mass budget [98]:

$$M_{TPS} = \left\{ \begin{array}{ll} 0.146475 \cdot S_{OT} & \text{for Storable Oxidiser Tanks} \\ 0.190425 \cdot S_{FT} & \text{for Storable Fuel Tanks} \end{array} \right\} \quad (5.43)$$

Thrust Vector Control Mass

The single, vacuum-optimised, bi-propellant engine is used to do trajectory and attitude control. To do this, there is a thrust vector control unit in place to move the propulsion system over a set number of degrees of freedom. Inputs required for the thrust vector control mass estimate are:

- Vacuum Thrust - T_{vac}
- Number of Engines with TVC - N_{eng}

The thrust vector control element, that allows for thrust direction changes can be determined by a relationship described by Rohrschneider [105].

$$M_{TVC} = 0.001185 \cdot T_{vac} \cdot N_{eng} \quad (5.44)$$

Where:

- N_{eng} = The Number of Engines with TVC [–]

Pipes & Valves Mass

For the propellant handling, feed and storage a complex architecture of pipes and valves is in place. Dependent on the engine characteristics a mass estimate of these elements can be determined. Inputs required for the pipes and valve mass estimate are:

- Vacuum Thrust - T_{vac}
- Combustion Chamber Pressure - P_c

In order to calculate for the piping and valve mass, the following relationship can be used [54]:

$$m_{valves} = 0.02 \cdot (T_{vac} \cdot P_c)^{0.71} \quad (5.45)$$

Interstage Structure Mass

The interstage is the structure that falls in between the first and upper stages of the launch vehicle. This section provides for a structural, protective and aerodynamic role during launch. The interstage encapsulates a large part of the vacuum-optimised upper stage engine. The interstage structure is considered in the mass model as this is required for cost estimates. Inputs required for the interstage mass estimate are:

- Lateral Surface Area of the Interstage - S_{IS}
- Stage Diameter - D_{stage}
- Length of the Engine - L_{eng}

The interstage structure mass can be estimated, according to Castellini [99], using the following parametric derived relationship:

$$m_{IS} = \left\{ \begin{array}{ll} k_{SM} \cdot 7.7165 \cdot S_{IS} \cdot (3.3208 \cdot D_{stage})^{0.4856} & \text{for Stage 1} \\ k_{SM} \cdot 5.5234 \cdot S_{IS} \cdot (3.3208 \cdot D_{stage})^{0.5210} & \text{for Upper Stage} \end{array} \right\} \quad (5.46)$$

Where:

- k_{SM} = Corrective Factor for the Structural Material
 $k_{SM} = 1$ for Al-alloy structures [105]
 $k_{SM} = 0.7$ for advanced composite-based structures[105]

- S_{IS} = Lateral Surface Area of the Interstage [m^2]

The lateral surface area can be obtained by:

$$S_{IS} = 2\pi \cdot \frac{D_{stage}}{2} \cdot L_{IS} \quad (5.47)$$

The length of the interstage can be calculated using the following relationship that was developed and validated by Castellini [99]:

$$L_{IS} = \begin{cases} L_{eng} + 0.2D_{stage} & \text{for Liquid Stage} \\ L_{eng} + 0.287D_{stage} & \text{for Liquid Upper Stage} \end{cases} \quad (5.48)$$

Payload Adapter Mass

Inputs required for the payload adapter mass estimate are:

- Mass of the Payload - M_{PL}

The structural mass of the elements that take care of the payload is often related to the payload mass it carries or protects. This is also the case for the payload adapter and the payload fairing mass. Since the Ariane 6 rocket is designed to take various payload masses to different orbital heights it is important to take the required payload mass into account. The payload adapter mass is a function of the payload mass following the relationship [99]:

$$M_{PLA} = 0.0477536 \cdot (M_{PL})^{1.01317} \quad (5.49)$$

Where:

- M_{PL} = Payload Mass [kg]

Payload Fairing Mass

Inputs required for the payload fairing mass estimate are:

- Diameter of the Stage - D_{stage}

The length of the fairing should first be approximated in order to estimate the fairing mass. This can be done by the approach discussed by Contant [104]. Contant made a fairing length estimation relationship as a function of the stage diameter (D_{stage}) using 23 existing launch vehicles:

$$L_{fairing} = 1.1035 \cdot (D_{stage})^{1.6385} + 2.3707 \quad (5.50)$$

This length estimation relationship has an R^2 of 0.8682 and a RSE of 16.1% [104]. This relationship can be used to determine the mass of the fairing [104]:

$$m_{fairing} = 49.3218 \cdot (L_{fairing} \cdot D_{stage})^{0.9054} \quad (5.51)$$

This mass estimation relationship has an R^2 of 0.8653 and a RSE of 32.0% [104].

Avionics Mass

Inputs required for the avionics mass estimate are:

- Diameter of the Stage - D_{stage}
- Length of Interstage - L_{IS}
- Length of Tanks - L_{tanks}
- Length of Fairing - $L_{fairing}$

The mass of the avionics can be estimated by a mass estimation relationship described by Castellini [99] and is based on data from the Ariane launch vehicle family specifically.

$$m_{avionics} = 0.25 \cdot (246.76 + 1.3183 \cdot D_s \cdot L_{vehicle}) \quad (5.52)$$

The length of the vehicle can be approximated by:

$$L_{vehicle} = L_{IS} + L_{tanks} + L_{fairing} \quad (5.53)$$

5.4. Sensitivity Analysis

During the set-up of the performance model, factors were proposed and assumptions were made. It is important to understand the effect of these set variables on the accuracy and precision of the model. First, to model the performance conditions of the propulsion system more accurately, the ideal characteristic velocity and thrust factor were corrected by the combustion and nozzle quality factors. Although these correction factors are modelled by the RPA program using a validated nested analysis, it is important to see the effect on the vacuum thrust (T_{vac}) and on the vacuum-specific impulse (I_{sp}). In Table 5.8 you see that varying the combustion efficiency factor from 0.95 (nominal value) to 0.92 and 0.98 results in a linear change in vacuum thrust of about 2.48 %. Changing the nozzle quality factor in the same way results in a relative change of 2.43 %. Changing these quality factors have similar results on the vacuum-specific impulse. In this case the impact of varying the factors results in a linear change of 3.16 % as seen in Table 5.8.

Table 5.8: Sensitivity Analysis Performance Quality Factors - Vacuum Thrust

Parameter	Lower Value	Nominal Value	Higher Value
Combustion Efficiency Factor ϵ_b [-]	0.92	0.95	0.98
Vacuum Thrust T_{vac} [kN]	189.244	194.051	198.859
Percentage Change [%]	-2.48	-	2.48
Nozzle Quality Factor ϵ_F [-]	0.94	0.97	1
Vacuum Thrust T_{vac} [kN]	189.342	194.051	198.760
Percentage Change [%]	-2.43	-	2.43

Table 5.9: Sensitivity Analysis Performance Quality Factors - Vacuum Isp

Parameter	Lower Value	Nominal Value	Higher Value
Combustion Efficiency Factor ϵ_b [-]	0.92	0.95	0.98
Isp Vacuum [s]	403.257	416.407	429.556
Percentage Change [%]	-3.16	-	3.16
Nozzle Quality Factor ϵ_F [-]	0.92	0.95	0.98
Isp Vacuum [s]	403.258	416.407	429.556
Percentage Change [%]	-3.16	-	3.16

Furthermore, the exit pressure is estimated based on the expansion ratio. The level of optimum expansion determines the exit pressure at the end of the nozzle. The exit pressure is an important parameter throughout the performance calculations. It is often used to determine the pressure ratio between the combustion chamber pressure and the exit pressure. Through the sensitivity analysis, it was found that the vacuum-specific impulse is non-linearly affected by changing the exit pressure parameter as seen in Table 5.10. Moreover, drastic effects were found by adjusting the isentropic coefficient. It was found that the vacuum-specific impulse changed 12.17 % and -9.11 % respectively, after changing the isentropic coefficient 9.5 %. This effect is tabulated below in Table 5.10.

Table 5.10: Sensitivity Analysis - Isentropic Coefficient and Exit Pressure

Parameter	Lower Value	Nominal Value	Higher Value
Exit Pressure P_e [MPa]	0.005	0.011	0.017
Isp Vacuum [s]	430.366	416.407	407.802
Percentage Change [%]	3.35	-	-2.07
Isentropic Coefficient γ [-]	1.05	1.15	1.25
Isp Vacuum [s]	463.492	413.216	375.561
Percentage Change [%]	12.17	-	-9.11

5.5. Verification and Validation

In this section, the verification and validation effort for the launch vehicle model is discussed. According to the International Council on Systems Engineering (INCOSE) verification can be described as:

Verification is the confirmation, through the provision of objective evidence, that the requirements for a specific intended use or application have been fulfilled [106]

This means that verification primarily checks if the system is in compliance with the design solution specifications. In case of the vehicle model verification will check whether the data produced by the model is indeed the required data that makes the model valuable for analysis. For validation, INCOSE gives the following definition:

Validation is the confirmation, through the provision of objective evidence, that specified requirements have been fulfilled [106]

Again, to translate this to the vehicle model described above, validation will test if the model accomplishes the intended purpose and accuracy as described by the stakeholder expectations. If a model is validated it will give an accurate representation of data. For the vehicle model, this means that the performance and mass model will accurately describe and estimates the performance of the engines and the mass of the individual components of the vehicle compared to data found in literature [106].

Since the vehicle model is designed such that its output can be used as an input for each consecutive model the data output of the model is exactly as expected. The performance model has as output; the vacuum-specific impulse, vacuum thrust and mass flow rate. The mass model has as output the length of the stage and the mass of all the individual components. This means that the models can be used as intended and are therefore verified.

The level of accuracy of the output data will determine the validity of the models. This will be done by inserting known parameters (from literature) into the models and comparing the outcome of the model calculations with the actual value found in literature. For example, for the mass model the propellant mass, thrust and launch vehicle dimensions will be used as input. The dry mass calculated by this model will be compared with the actual dry mass found in literature. The differences will be described using the statistical tools; relative mean error (μ), absolute relative error (E) and standard deviation (σ). The relative mean error describes the summed percentual difference (\pm) between the computed data from the model and the expected data from literature. This can be calculated using the following formula:

$$\mu = \frac{100\%}{n} \cdot \sum_{i=1}^n \frac{(y_i - \bar{y}_i)}{y_i} \quad (5.54)$$

Where y_i is the actual value found in literature and \bar{y}_i is the value obtained/ calculated by the model. The absolute relative error describes the summed percentual absolute difference between the value calculated using the model \bar{y}_i and the actual value found in literature y_i . The absolute relative error, therefore, describes the overall accuracy error. This is described by the following formula:

$$E = \frac{100\%}{n} \cdot \sum_{i=1}^n \frac{|y_i - \bar{y}_i|}{y_i} \quad (5.55)$$

The standard deviation describes the variation in the set of values between the calculated and actual values. This is described by the following formula:

$$\sigma = 100\% \cdot \sqrt{\frac{1}{n-1} \sum_{i=1}^n \left(\mu - \frac{(y_i - \bar{y}_i)}{y_i} \right)^2} \quad (5.56)$$

In all the formulas above the variable n describes the number of samples that are evaluated. These formulas will be used to analyse the accuracy and relative errors of the performance and mass models discussed above. It is important to note that the input and comparison data on performance and mass

are described in the preceding literature study [16]. For clarity, the required data for performance model validation is described in Table 3.4. To validate the mass model, data on the first and upper stages of several launch vehicles is summarised in Table 3.3 and Table 5.11.

Table 5.11: Data Summary of First Stage Designs used for Validation

First Stage Module	Manufacturer	Length [m]	Diameter [m]	Propulsion	Propellants	Type of Engine	Dry Mass [kg]
LLPM [107]	ArianeGroup	33.9	5.4	Cryogenic	LOX/LH2	Vulcain 2.1	15637
EPC H173 [108]	ArianeGroup	23.8	5.4	Cryogenic	LOX/LH2	Vulcain 2	14700
Falcon 9 v1.1 [109]	SpaceX	40.9	3.66	Cryogenic	LOX/RP-1	Merlin 1D	19000

5.5.1. Performance Model Validation

To validate the performance model data is used from Table 3.4. The data used in the validation process consists of a mixture of cryogenic, semi-cryogenic and storable engines. Important design parameters for the performance model are the combustion chamber pressure P_c , exit pressure P_e , nozzle exit diameter D_e and the oxidiser-to-fuel ratio OF . These design parameters will be the input for the performance model. From this, the difference between the actual performance characteristics will be compared with those described by the performance model. The performance characteristics are described by the vacuum-specific impulse I_{sp} , vacuum thrust T_{vac} and the mass flow rate \dot{m}_{tot} . These results are tabulated below in Table 5.12

Table 5.12: Validation of Performance Model

Engine	Propellants	Design Parameters				Actual Values			Model Values		
		P_c [Mpa]	P_e [Mpa]	D_e [m]	OF [-]	I_{sp} [s]	T_{vac} [kN]	\dot{m}_{tot} [kg/s]	I_{sp} [s]	T_{vac} [kN]	\dot{m}_{tot} [kg/s]
Vinci	Cryogenic (LOX/LH2)	6.08	0.0012	2.150	5.80	465.00	180.00	39.50	467.23	161.03	34.18
RL10B2	Cryogenic (LOX/LH2)	4.41	0.0007	2.150	5.88	465.50	110.10	24.10	473.65	97.20	20.37
HM7B	Cryogenic (LOX/LH2)	3.70	0.0026	0.995	5.00	446.00	62.20	14.80	454.71	62.60	13.58
Vulcain 2	Cryogenic (LOX/LH2)	10.00	0.0091	2.100	6.30	429.00	1150.00	320.00	439.87	919.96	205.89
LE-5B	Cryogenic (LOX/LH2)	3.62	0.0059	1.710	5.00	447.00	137.00	33.26	437.81	145.90	31.96
CE-20	Cryogenic (LOX/LH2)	6.00	0.0033	1.550	5.05	443.00	220.00	43.10	453.46	205.03	44.78
Vikas-4	Storable (NTO/UDMH)	5.35	0.0131	1.500	1.86	295.92	725.00	249.80	305.21	591.64	189.87
Viking 5C	Storable (NTO/UH25)	5.50	0.0629	0.990	1.71	277.78	758.00	244.00	280.83	894.94	307.27
RS-27	Semi-Cryogenic (LOX/RP1)	4.87	0.0496	1.500	2.25	302.00	1023.00	361.00	313.53	1312.21	398.14

The relative differences between the actual and modelled values for these performance characteristics are described in Table 5.13. If the difference between the actual and modelled value is smaller than $\pm 20\%$ the cell is coloured green. If the difference is larger or equal to $\pm 20\%$ the cell is highlighted in red, as set by the requirements.

Table 5.13: Performance Model Validation Results - Relative Differences

Relative Difference		
I_{sp} Diff [%]	T_{vac} Diff [%]	\dot{m}_{tot} Diff [%]
0.480	-10.538	-13.463
1.751	-11.714	-15.465
1.953	0.645	-8.236
2.533	-20.003	-35.659
-2.056	6.499	-3.906
2.361	-6.806	3.888
3.140	-18.394	-23.991
1.098	18.066	25.932
3.818	28.271	10.287

From Table 5.13 it is possible to determine the relative mean error, absolute relative error and the standard deviation. This is specified in Table 5.14.

Table 5.14: Performance Model Validation Results - Relative Error, Absolute Relative Error, Standard Deviation

	μ [%]	E [%]	σ [%]
I_{sp}	1.675	2.132	1.722
T_{vac}	-1.553	13.437	16.506
\dot{m}_{tot}	-6.735	15.648	18.493

From Table 5.13 and Table 5.14 it can be concluded that the specific impulse is accurately estimated with a small relative mean and absolute relative error. The spread of values is also very limited as the standard deviation is small at 1.722%. The relative mean error for the vacuum thrust is rather small with only -1.553%, however, the absolute relative error is larger with 13.437%. This indicates a widespread among the mean of the samples. This is confirmed by the relatively large standard deviation (16.506%). The same holds for the mass flow rate calculations. From Table 5.13 it can be concluded that some outliers will negatively influence these numbers. Because the absolute relative error is below 20% for all performance parameters it is deemed a valid model to be used for the research analysis to be conducted, as set by the requirements of the tool in Table 5.4.

5.5.2. Mass Model Validation

Using the launch vehicle data collected in the preceding literature study (Table 3.3 and Table 5.11) validation of the mass model can be conducted. It is important to note that the validation of the launch vehicle stages is done with their respective nominal payload. The dry mass is calculated by summing the mass of the individual components that comprise the stage module. A combination of upper stages and first stages is used to check the validity of the model in terms of dry mass and stage length. Since the model is required to calculate for both (semi-)cryogenic and storable propulsion units, a selection of both types is made for the validation process.

To calculate the dry mass the following input parameters are required:

- Propellant Mass
- Launch Vehicle Diameter
- Mixture Ratio
- Nominal Payload Capacity
- Vacuum Thrust
- Types of Propellants
- Number of Engines
- Combustion Chamber Pressure

Furthermore, the upper stage and first stage designs vary, in terms of components, quite a lot. To deal with this only the contributing mass elements have been summed for the specific stage design to find the modelled dry mass. The breakdown of elements in the upper stage designs was done in the preceding literature review [16].

The validation of the dry mass model is depicted in Table 5.15. For a selection of launch vehicles and stage sections the length and the dry mass of the stage are calculated by the model. These calculated values are compared with the actual values, as per the same procedure with the performance model validation. In the last two columns of Table 5.15 the difference (in percentages) is given between the calculated value and the actual value found in literature, both for the length and the dry mass of the stage. When the difference is equal to or larger than $\pm 20\%$ the cell turns red, otherwise it turns green.

Table 5.15: Validation of Mass Model

Launch Vehicle	Stage Name	Stage Section	Propellant Type	Actual Values		Model Values		Relative Difference	
				L_{stage} [m]	M_{dry} [kg]	L_{stage} [m]	M_{dry} [kg]	L_{stage} diff [%]	M_{dry} diff [%]
Ariane 6	ULPM	Upper Stage	Cryogenic	10.00	7000	9.25	6774	-7.50	-3.23
Ariane 5	EPS L10	Upper Stage	Storable	4.71	1200	4.21	1445	-10.63	20.42
GSLV	GS2	Upper Stage	Storable	11.56	5500	9.60	5506	-16.96	0.11
Falcon 9	Upper Stage	Upper Stage	Cryogenic	16.00	4500	15.96	5182	-0.25	15.16
Ariane 5	ESC-A	Upper Stage	Cryogenic	4.70	4540	5.38	3796	14.47	-16.39
Ariane 4	H10-3	Upper Stage	Cryogenic	11.05	1240	10.57	1408	-4.34	13.55
Delta IV	DCSS (4m)	Upper Stage	Cryogenic	12.20	2850	8.90	2876	-27.05	0.91
Atlas V	Centaur III	Upper Stage	Cryogenic	12.68	2247	12.15	2138	-4.18	-4.85
Delta II	Delta K	Upper Stage	Storable	5.89	950	4.62	891	-21.56	-6.21
Ariane 6	LLPM	First Stage	Cryogenic	33.90	15637	27.84	13349	-17.88	-14.63
Ariane 5	EPC H173	First Stage	Cryogenic	23.80	14700	27.29	13816	14.66	-6.01
Falcon 9	First Stage	First Stage	Cryogenic	41.20	25600	45.38	26542	10.15	3.68

The modelled stage length of the Delta IV DCSS (4m) upper stage is 27% below the actual value of 12.20 m. For the predecessor of this launch vehicle, the Delta II Delta K first stage, the stage length is underestimated too with about -22%. The dry mass calculation only has one instance that is above the set accuracy range. The Ariane 5 EPS L10 upper stage dry mass is overestimated with about 20%. The previously introduced statistical tools will be used to say something about the validity of the dry mass model. The relative mean error, absolute relative error and the standard deviation have been calculated from the samples present in Table 5.15. The result from these calculations are present in Table 5.16.

Table 5.16: Mass Model Validation Results - Relative Error, Absolute Relative Error, Standard Deviation

	μ [%]	E [%]	σ [%]
Stage Length	-5.923	12.469	13.869
Stage Dry Mass	0.208	8.762	11.423

From Table 5.16 it can be concluded that the stage length is on average underestimated by the model with 5.923%. The absolute relative error is around 12.5% and the variation in the samples, the standard deviation, is 13.869%. Since the absolute error for the stage length is only about 12.5% it fulfils the requirement set for the mass model in Table 5.6.

The dry mass is even more accurately approximated having a relative mean error of only 0.2%, an absolute relative error of 8.8% and a standard deviation of 11.423%. This gives reason to believe, based on the validation sample set, that the mass model can accurately approximate the dry mass of (semi-)cryogenic and storable first and upper stages.

Since both the stage length and dry mass absolute relative errors are below $\pm 20\%$, it agrees with the requirements set for the mass model in Table 5.6. This is considered to be proof that the mass model is valid to be used for the research analysis.

5.6. Executive Chapter Summary

In this chapter the "Prototype X" storable upper stage concept is introduced. The "Prototype X" will be based on the cryogenic upper stage of Ariane 6, called the ULPM. The chapter is focused on the development of a designated vehicle model that will describe the performance and mass distribution of the upper stage design. This model will be used throughout the thesis work to do optimisation and analysis on the various proposed concepts. The Ariane 6 upper stage module will serve as a reference case for these concepts. Ariane 6 is a medium/heavy launch vehicle that can deliver a wide variety of payloads to different orbits. The launch vehicle is a two-stage integrated system where both stages operate on cryogenic propellants (LOX/LH₂). The ULPM, the baseline design for "Prototype X", consists of two propellant tanks, an intertank structure, one Vinci vacuum-optimised engine, a thrust frame and an avionics support structure. The upper stage design is approximately 5.4 meters in diameter and 10 meters tall. The dry mass of the structure is 7 tons and the combined propellant mass is around 26 tons, bringing the total wet mass to ≈ 38 tons. The upper stage is operated by a vacuum-optimised Vinci engine that produces 180 kilonewton by combustion of liquid hydrogen and liquid oxygen. The engine is reignitable such that it can provide flexibility and variety in mission profiles.

To develop the vehicle model, consisting of the performance and mass model, general system and "Prototype X" specific requirements have been developed (Table 5.1 and Table 5.2). Furthermore, assumptions for the performance and mass models have been formulated in Table 5.3 and Table 5.5. The performance model describes the performance of the combustion engine in terms of mass flow rate, combustion chamber temperature and required expansion ratio. Furthermore, the thrust profile and the specific impulse can be determined. To do this the performance model requires input from a dedicated combustion model. The RPA Lite Combustion tool will be used to do the thermodynamic analysis of propellant combinations. This tool relies on the thermochemistry database developed in the NASA CEA tool. This combustion model provides the required oxidiser-to-fuel ratio for a specific propellant combination. It calculates the combustion chamber pressure and nozzle exit pressure. By

the assumption of using the ideal rocket theory it was possible to develop the performance tool. In the performance tool the ideal characteristic velocity and the ideal thrust coefficient are corrected using of quality factors to account for losses that occur during combustion making the values more realistic. The mass model is built around the propellant mass that is present in the vehicle. The propellant mass influences the dry mass of the launch vehicle significantly in an iterative manner. The required propellant mass is dictated by the "Delta-V" (ΔV) budget of the Ariane 6 under maximum payload conditions. From this Delta-V requirement the propellant mass, thus the dry mass, can iteratively be optimised. From the propellant mass the propellant tank mass can be determined together with other structural and non-structural elements that comprise the launch vehicle system.

To investigate the impact of the quality factors described above, a sensitivity analysis was performed. Here the impact of the quality factors on vacuum thrust and vacuum-specific impulse was investigated. It was found that these design parameters were limited sensitive with a relative impact of approximately $\pm 2.48\%$ and $\pm 3.16\%$ by changing the quality factors. More drastic effects were found by adjusting the isentropic coefficient (relative change of $-9.11 - 12.17\%$). The performance and mass models were verified and validated by data collected in the literature review. Data on propulsion systems and launch vehicle first and second stages was used to validate the corresponding models. The performance model produced absolute relative errors of 2.132%, 13.437% and 15.648% for the specific impulse, vacuum thrust and total mass flow rate respectively. The mass model produced an absolute relative error of 12.469% and 8.762% for the stage length and stage dry mass estimate respectively. It was concluded that both the performance and mass models fulfilled the requirements set for these models as their average absolute relative error in all cases was below $\pm 20\%$.

6

Cost Model

In this chapter, a cost model will be set up that will help to estimate the development, manufacturing and operation cost of the Prototype X launch vehicle. Furthermore, the cost model serves as a quick indicator of cost changes that correspond with certain design steps.

6.1. Cost Breakdown

Two decades ago information on launch vehicle cost was widely available in literature. The launch vehicles were designed and built primarily by governmental organisations such as the ESA and the NASA. These organisations provided detailed information on development cost, total manufacturing cost and launch cost-per-flight. Due to the privatisation and commercialisation of space flight in the last 20 years the openness in sharing cost details of space missions and launch vehicles has diminished. It is commercially strategic for privatised launch vehicle providers and manufacturers to not share their cost detail. The same is the case for the Ariane 6 Launch Vehicle. There is limited information on cost available for this reference launch vehicle. In order to proceed with the cost optimisation research for the “Prototype X” it is necessary to understand the cost breakdown of the reference launch vehicle. To do this, a cost estimation model will be used to understand where the cost is attributed to. The cost-per-flight of a launch vehicle is comprised out of several cost sectors. These cost sectors can be dissected into; non-recurring cost or development cost, manufacturing cost and operations cost. This is schematically depicted in Figure 6.1

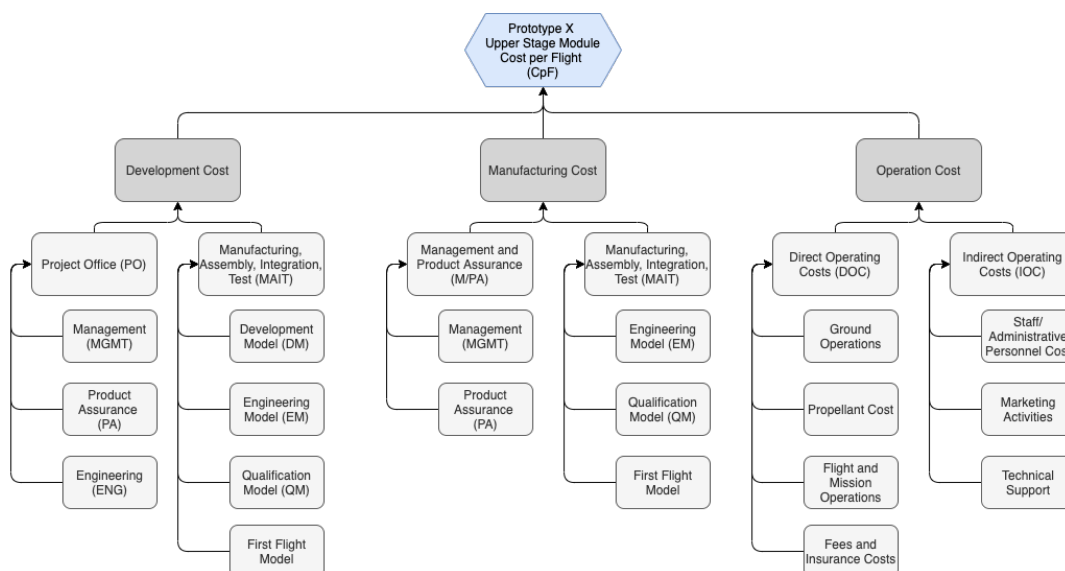


Figure 6.1: Cost Breakdown for Launch Vehicles

Traditionally, the space organisation that were responsible for launch vehicle design and manufacturing focused their efforts on optimising performance. The cost that came with these design choices were considered less important. This view on cost completely changed in the past few decades (due to the commercialisation of spaceflight). Cost has become a variable in the design process and drives important optimisation choices in all levels of systems engineering. To reduce the cost-per-flight and therefore the life-cycle cost of the launch vehicle, insight in factors that impact the cost is necessary in all phases of the design. Especially in early design phases important cost driving decisions are made. Having a good cost model at hand to do these cost estimates can result in cost, and risk, reductions later on in the process.

6.2. Cost Model Selection

Multiple cost models have been developed over the years. Especially due to the rising urge of reducing the cost-per-kg to allow access to space in a more cost effective way, these models have been tried to characterise all the important cost factors that ensures an accurate and precise model [83], [110]. From historical (publicly available) data multiple models were developed by academics [82], [111], [112]. The most used cost estimating tools are the *TRANSCOST* tool developed by Koelle [82], the Unmanned Space Vehicle Cost Model (USCM), Small Satellite Cost Model (SSCM), Price-H and *TruePlanner* by PRICE Systems Solutions, *ACES* by 4Cost, *SSER-H* by Galorath Incorporated and the NASA Air Force Cost Model (NAFCOM). Although often used, the majority of these models are not publicly available and are restricted to government use or are paid-for commercial tools. From the cost models described above, only the *TRANSCOST* 8.2 model from Koelle [82] is publicly available. However, the cost estimation accuracy is limited for newer and smaller launch vehicles, overestimating the cost by up to 140% [85], [113]. In responds to the aim of ESA/ESTEC (European Space Research and Technology Center) to develop a cost model capable of estimating the launch vehicle cost in an early phase of the design, N. Drenthe developed the hybrid parametric cost model; SOLSTICE. This model combines Koelle's *TRANSCOST* 8.2 model CERs as a basis to determine cost estimation relationships on sub-system level. These CERs help construct the first level cost estimation of the launch vehicle known as the Theoretical First Unit (T1 Equivalent Method, NASA/ESA) or Flight Unit (FU, NASA). This is often used for early phase parametric cost modelling, applied in models such as NAFCOM, *TruePlanning* and by organisations such as ESA and NASA [114]. From this Theoretical First Model estimations can be made on the development and manufacturing cost of the launch vehicle through proven parametric estimation techniques. The operating cost of the launch vehicle is estimated through the use of presented CERs by Koelle in his *TRANSCOST* 8.2 model. It was found that Drenthe's hybrid cost model (combining two cost model approaches) was able to increase the accuracy and precision of Koelle's *TRANSCOST* model. This model was made publicly available after a research cooperation between the Technical University of Delft and European Space Research and Technology Centre (ESTEC). To estimate the cost-per-flight of the "Prototype X" upper stage module it is opted to use Drenthe's hybrid cost estimation model throughout this research project.

6.2.1. Cost Model Justification

Drenthe's hybrid cost estimation model has proven to be able to accurately approximate the development cost, manufacturing cost and the cost/price-per-flight within 20% of the actual reported cost for three commercial rockets in its early validation phase [83]. Since then it has been successfully used at ESA's Concurrent Design Facility for numerous conceptual launch vehicles to estimate the early-phase program cost [113]. The model will be subject to change over time as more reference data on commercial launch vehicles becomes available.

The "Prototype X" upper stage module is based on the upper stage module of the Ariane 6 rocket, designed and built by ArianeGroup in cooperation with ESA. Which makes it a commercial launch vehicle. Moreover, the launch mass and mass distribution of the "Prototype X" spacecraft falls within the operational bounds of Drenthe's cost estimation model. Combining these factors together with the fact that the cost model has been validated for similar reference cases during its use at ESA's Concurrent Design Facility, it is considered a valid and useful model for the preliminary cost estimations that are required for this research project. During a discussion with Michel van Pelt - ESA/ESTEC Head of the Cost Engineering Section - Drenthe's model was recommended to be used in this case. Primarily because the cost model was developed around data that includes the Ariane 4 and Ariane 5

launch vehicles. These launch vehicles were developed by ArianeGroup too and have similar structures and equipment as the Ariane 6 launch vehicle. Furthermore, since this research will compare the conventional cryogenic upper stage design with the green storable upper stage design the accuracy of the cost model with regards to the actual cost of development, manufacturing and operation is not a key driver. The consistency and precision of the model is considered most important to allow for proper comparison between the "Prototype X" concept and conventional upper stage design. The absolute cost values that are produced by the cost model does not hold significant value. This is an estimation of the expected cost over the entire life span of a launch vehicle project. The relative percentile changes in cost between the two designs, in fact do give valuable insight cost benefits of design choices and the trade-off between the two designs.

Some of the variables presented by Drenthe in the model will be modified in order to ensure proper modelling of the described launch vehicle at hand. Variables subject to uncertainty will be tested in a sensitivity analysis.

6.3. Cost Model Assumptions & Requirements

During the set up and development of the cost model some important assumptions have been made. For clarity and overview the assumptions taken are tabulated below. Some of the most important assumptions will be subject to sensitivity analysis. The assumptions are depicted in Table 6.1.

Table 6.1: Cost Model Assumptions

ID	Assumption
CM-01	The development cost can be estimated with T1 equivalents described by NAFCOM
CM-02	The level-of-effort costs is associated with the experience and motivation of the team
CM-03	It is assumed that 20% of the production is contracted out to third party companies
CM-04	The average subcontractor profit is 8%
CM-05	Management and product assurance (M/PA) cost is assumed to be 5.25%
CM-06	Stage integration/testing (I&T) is set to be 3.2% of FU cost
CM-07	Payload, avionics and attitude control integration/testing (PAA I&T) is set to be 3.2% of FU cost
CM-08	The development learning factor is fixed and set to 0.9
CM-09	It is assumed that the launch vehicle will be produced in batches over multiple years
CM-10	A total of 50 launch vehicle units will be produced
CM-11	The hardware reusing factor is set to 1 for expendable rockets
CM-12	There will be 8 launches per year (LpA = 8)
CM-13	The cost model does have an estimating error of accuracy of approximately 20% [113]
CM-14	The cost model does not take alternative manufacturing techniques into account associated with novel materials

The requirements for the cost model are described below in Table 6.2.

Table 6.2: Cost Model Requirements

ID	Requirement
CM-REQ-01	The cost model shall provide cost estimates on development, manufacturing and operation
CM-REQ-02	The cost model shall give cost estimates per launch vehicle stage
CM-REQ-03	The cost model shall allow for design change cost comparison
CM-REQ-04	The cost model shall be integrated with the launch vehicle model
CM-REQ-05	The operation cost shall incorporate ground operation cost associated with different propellant types

6.4. Cost Estimating Relationships

In order to do the cost estimate for the development cost, manufacturing cost and operation cost it is necessary to define Cost Estimation Relationships (CERs). The SOLSTICE Cost Model developed by Drenthe [83] uses an innovative hybrid approach where subsystem CERs from the NAFCOM model are used to determine the cost of the subsystem elements based on its dry mass. This helps to develop the Theoretical First Unit (T1) cost of the launch vehicle. This is then used to determine the development and manufacturing cost. The more traditional *TRANSCOST* 8.2 Cost Model will be used to calculate the operation cost estimate. These three estimates together will be used to determine the cost-per-flight estimate. Including a profit margin this can give insight in the price-per-flight as well. The cost breakdown model that is depicted in Figure 6.1 helps to generate a workflow diagram of Drenthe's *SOLSTICE* Cost Model. This is depicted in Figure 6.2.

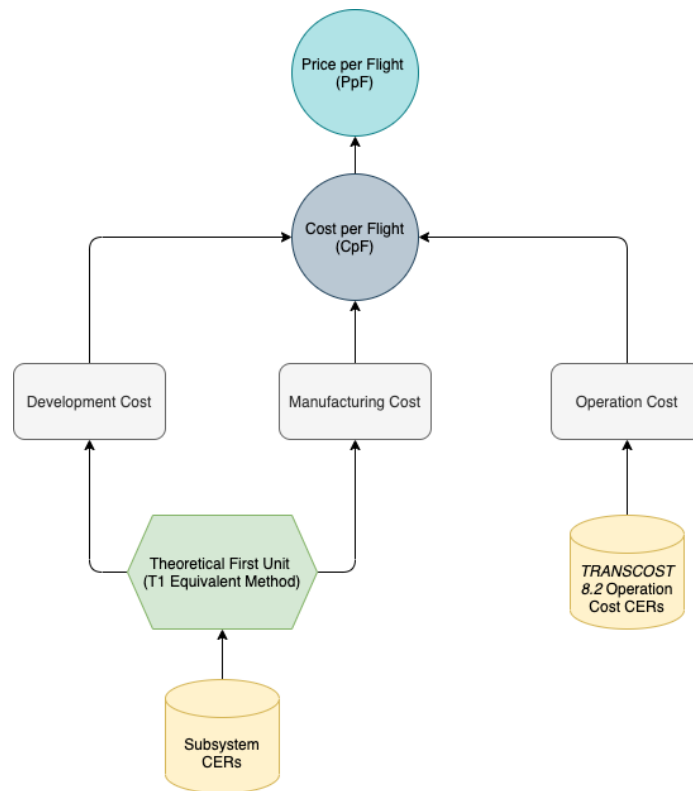


Figure 6.2: Drenthe's SOLSTICE Cost Model [83]

In mathematical terms the cost-per-flight can be estimated by the use of the following relationship:

$$CpF = C_{dev} + C_{man} + C_{ops} \quad (6.1)$$

To come up with the development and manufacturing cost, first the first Flight Unit Cost will be estimated. This will be discussed in the next section.

6.4.1. First Flight Unit Cost Estimate (T1)

In order to do make determine the First Flight Unit Cost it is important to breakdown the launch vehicle in subsystems. These elements can be further broken down into elements. This breakdown is done such that it points out the most important elements of the individual subsystems that make out the launch vehicle. A list of the subsystem elements is tabulated in Table 6.3.

The cost of these individual subsystem elements can be estimated using validated CERs. The CERs are either constructed by Drenthe or by NAFCOM. The regression fit for the cost of the equipment is of the form:

$$C = a \cdot M^b \quad (6.2)$$

Where C is the cost of the subsystem element, a is the initial value, M is the dry mass of the subsystem and b is the growth factor describing the cost-per-kg. By means of extensive regression fitting and normalisation of historical data Drenthe and NAFCOM came up with the relationships described in Table 6.4.

Table 6.3: Equipment Breakdown [83]

Unit	Equipment	Part	Part ID	
<i>Stage</i>	Pressurizant Tank		S-PT-	
	Fuel Tank		S-FT-	
	Oxidizer Tank		S-OT-	
	Stage Structure	Thrust Cone		S-SS-TRC
		Skirt		S-SS-SKI
		Thermal Control		S-SS-THM
	Engine(s)		S-EN-	
	Thrust Vector Control		S-TV-	
	Propellant	Fuel		S-PR-FUE
		Oxidizer		S-PR-OXI
		Pressurizant		S-PR-PRE
	Pressurization System		S-PS-	
	Pipes & Valves	Pipes		S-PV-PIP
		Valves		S-PV-VAL
Stage Harness		S-SH-		
<i>Interstage</i>	Interstage Structure		I-IS-	
<i>Payload</i>	Payload Adapter		P-PA-	
	Payload Fairing		P-PF-	
<i>Avionics</i>	Avionics	Comms	A-AV-COM	
		Power	A-AV-PWR	
		Data Handling	A-AV-DHL	
		GNC	A-AV-GNC	
		Avionics Harness	A-AV-HNS	
<i>Attitude Control</i>	Attitude Control Module		C-AC-	

Table 6.4: Cost Estimation Relationships for the Individual Subsystem Elements [83], [113]

Equipment Name	a Value	b Value	RSE [%]	SE(log)	Origin
Pressurizant Tank	19.99465	0.71253	27.6	0.2711	Drenthe
Fuel Tank	19.99465	0.71253	27.6	0.2711	Drenthe
Oxidizer Tank	19.99465	0.71253	27.6	0.2711	Drenthe
Thrust Cone	2.799300	0.91199	12.6	0.1253	Drenthe
Skirt	2.799300	0.91199	12.6	0.1253	Drenthe
Thermal Control	2.799300	0.91199	12.6	0.1253	Drenthe
Engine(s)	31.48271	0.78811	35.8	0.3469	Drenthe
Thrust Vector Control	33.90978	0.60977	13.7	0.1359	Drenthe
Pressurizant System	11.50618	1.06948	49.8	0.4708	Drenthe
Pipes	8.958770	0.68815	34.3	0.3333	Drenthe
Valves	8.958770	0.68815	34.3	0.3333	Drenthe
Stage Harness	27.45211	0.44623	34.9	0.3393	Drenthe
Payload Adapter	26.01794	0.44623	7.95	0.0794	NAFCOM
Payload Fairing	23.59239	0.70000	9.93	0.0991	NAFCOM
Comms	51.11253	0.80000	One data point	-	NAFCOM
Power	42.01174	0.80000	Two data points	-	NAFCOM
Data Handling	141.6820	0.80000	7.06	0.0705	NAFCOM
GNC	69.05491	0.82458	23.8	0.2346	Drenthe
Avionics Harness	27.45211	0.44623	34.9	0.3393	Drenthe
Attitude Control Module	257.8420	0.75000	29.1	0.2854	NAFCOM
Interstage Structure	6.70369	0.68041	19.3	0.1909	Drenthe

6.4.2. OECD Inflation Correction

It is important to note that the cost estimation relationships described by the SOLSTICE model are based around the fiscal year 2015 (FY2015) [83]. To make the cost estimation accurate for the current year (2021/2022) an inflation correction has to be applied. In Appendix A the inflation rates since 2015

are graphically depicted to determine the required inflation correction factor that has been applied to the First Flight Unit cost estimate to correct the cost estimate from 2015 to 2020/2021 value. The EU inflation rates are obtained from the Organisation for Economic Co-Operation and Development (OECD) and were also used to adjust figures for European manufacturing conditions [115].

6.4.3. Development Cost Estimate

In the early phases of launch vehicle design it is hard to define sufficient mission, configuration and environmental parameters. This makes it harder to come up with a reasonably accurate development cost estimate. Drenthe developed a heuristic approach to accurately estimate the development phase cost using modifiers of analogous systems coming from historical data [83]. This way the non-recurring/development cost can, already, accurately be estimated. The T1 equivalent method uses modifiers for *Design and Development* effort; the amount of engineering work performed, and *model philosophy*; the testing work performed on system and subsystem models. These modifiers are considered multiples of the first flight unit cost as defined in the previous section.

The modifiers that help to construct the development cost are coming from the ESA Costing Software (ECOS) support functions and are listed in Table 6.5 [116].

Table 6.5: ESA Costing Software (ECOS) Support Functions [116]

Cost Element	Sub-element	Meaning
PO		Project Office
	MGMT	Management
	PA	Product Assurance
	ENG	Engineering
MAIT		Manufacturing, Assembly, Integration, Test
	DM	Development Model
	EM	Engineering Model
	QM	Qualification Model
	FM1	First Flight Model
	FMR	Recurring Flight Models

The modifiers were constructed by assigning a value to the support functions defined in Table 6.5. This is done by adopting equivalents from conferences or proceedings of the Space Systems Cost Analysis Group (SSCAG) [83]. Following this method, Drenthe assumed the Engineering (ENG) support function to be equal to the Design and Development (DD) T1 equivalent. The following T1 Equivalents have been defined for development cost analysis, here the support functions are depicted as functions of the theoretical first unit:

- Design and Development (DD) = 3.0 T1
- Development Model (DM) = 0.3 T1
- Engineering Model (EM) = 1.3 T1
- Qualification Model (QM) = 1.3 T1
- Proto Flight Model (PFM) = 1.5 T1

It is important to note that the Design and Development factor can be adapted such that it is flexible in terms of the innovative character of the launch vehicle. For example, if the Technology Readiness Level (TRL) has to increase, being a fairly new concept that has to be made ready for flight, the DD factor can be approximated by:

$$DD' = DD + \Delta TRL \quad (6.3)$$

Before the other equivalents are quantified, it is important to list the most important assumptions that Drenthe made for the development cost estimate. First of all, it is assumed that the level-of-effort costs associated with the development phase cost is highly dependent on the experience and motivation of the team. In this case, the average expected value and effort is taken from historical data, centres around the Space Shuttle Management case. Furthermore, Drenthe investigated the level of subcontractorship that has to be taken into account. According to Koelle [82], a lower share of total work

contracted out results in reduced management effort. The percentage of production that is contracted out varies between 20% for commercial companies such as SpaceX to 60% for traditional launch vehicle development at a governmental agency at the prime contractor level [83]. Since the “Prototype X” upper stage module will be designed and manufactured by a commercial company (based on our reference case - ArianeGroup) a level of subcontractorship of 20% will be assumed. Drenthe showed that this assumption has a relative magnitude of less than 2.5% on the development cost, through dedicated sensitivity analysis. So although a rough estimate, the assumed relative level of work that is subcontracted out will be a valid way to estimate the development cost at this stage of the design process. Based on estimates presented by ESA [116] the average subcontractor profit is rated at 8%. The Management and Product Assurance (M/PA) cost is often described as a percentage of the theoretical first unit (T1). In this case, Drenthe assumed, based on historical project performance models described by Koelle [82], that the Management and Product Assurance percentage (M/PA%) is 5.25% of the theoretical first unit. Furthermore, Drenthe used data provided by Koelle [112] to estimate the profit retention cost reduction factor (c_p). This factor can be estimated using the following relationship:

$$C_p = \frac{s_{COM} \cdot q + 1}{s_{BAU} \cdot q + 1} \quad (6.4)$$

Where:

- s_{BAU} = Scope of subcontracted work under BAU (Business As Usual)
- s_{COM} = Scope of subcontracted work under commercial development
- q = Average subcontractor profit

This factor is a function of the number of subcontracts and is estimated to be 0.9695:

$$C_p = \frac{0.2 \cdot 0.08 + 1}{0.6 \cdot 0.08 + 1} = 0.9695 \quad (6.5)$$

Using these assumptions and factors defined it is now possible to determine the development cost. This is done through the multipliers defined above. First the First Flight Model (FM1) is determined from the theoretical first unit (T1):

$$FM1 = T1 - M/PA\% \quad (6.6)$$

Using this First Flight Model estimate it is possible to estimate the Project Office (PO) cost estimate. The project office consists of the Management, Product Assurance and Engineering (ENG) multiples and can be estimated through the following support functions:

$$PO = ENG + M/PA \quad (6.7)$$

Where:

$$ENG = DD \cdot FM1 \quad (6.8)$$

In order to estimate the M/PA support function first the multiplier for Manufacturing, Assembly, Integration and Test Cost (MAIT) has to be defined:

$$MAIT = FM1 \cdot STH \cdot L_d \cdot \#HW \quad (6.9)$$

Here it is important to note that STH is called the total system test hardware (STH) and can be calculated by the sum of the T1 equivalents:

$$STH = DM + EM + PFM = 3.1 \quad (6.10)$$

Furthermore, L_d is the development learning factor and is set to be 90% as a default in Drenthe's SOLSTICE cost estimating model [83]. In case of multiple engines, for example, the cumulative average development learning factor has to be taken into account. The factor $\#HW$ takes into account the

number of times a subsystem is re-used on the launch vehicle and is fixed at 1 for all hardware except for the engines.

Now M/PA can be estimated by:

$$M/PA = (MAIT + ENG) \cdot M/PA\% \quad (6.11)$$

The Project Office (PO) together with the Manufacturing, Assembly, Integration and Test Cost (MAIT) estimate makes up the total Development cost, either per subsystem or as a whole for the entire theoretical first unit. It is important to also take into account the profit retention reduction factor as the result of subcontracting work out. Mathematically this can be written as:

$$DEV = c_p \cdot (PO + MAIT) = c_p \cdot ([ENG + (MAIT + ENG) \cdot M/PA\%] + [FM1 \cdot STH \cdot L_d \cdot \#HW]) \quad (6.12)$$

6.4.4. Manufacturing Cost Estimate

Often the development cost of launch vehicles is advertised as one of the largest cost factors influencing the cost-per-flight. However, for expendable rockets, it is found that the total manufacturing cost grows well beyond the cost associated with the development of the rocket. The manufacturing cost can make up for 75% of the total Life Cycle Cost (LCC). In case of expendable rockets, the manufacturing cost have to be taken into account per launch vehicle built and is therefore also referred to as recurring costs.

Although some of the manufacturing effort is done during the development phase, it is considered a marginal contribution. During the manufacturing phase special care is given to setting up an efficient production line. The two major contributors to manufacturing cost are:

- Manufacturing, Assembly, Integration and Test of Hardware (MAIT)
- Management and Product Assurance (M/PA)

The way that the manufacturing cost is distributed depends a lot on the number of units that will be produced over the entirety of the project. It is assumed that multiple expendable rockets will be produced over a period of multiple years. This makes the manufacturing cost diminish over time due to time reductions in manufacturing as the result of the learning effect. This learning effect is described by a certain learning factor that indicates the reduction in time and effort that is obtained during the production of each subsequent unit.

This manufacturing learning factor (p) and cost relation can be described by the following formulas:

$$b = \frac{\ln(p)}{\ln(2)} \quad (6.13)$$

Where:

- b = learning exponent
- p = learning factor

This can be used to estimate the subsequent cost of the theoretical first unit (T1) through the relation:

$$U_n = T1 \cdot n^b \quad (6.14)$$

Where:

- U_n = Cost of the n-th unit
- $T1$ = Theoretical first unit cost
- n = n-th unit

Depending on the complexity of the mission, the number of units that will be produced and the lifetime of the project the learning factor p can be estimated. According to Fox et al. [117] a standard slope of 95% is often used and is also incorporated in the NASA Unmanned Space Vehicle Cost Model (USCM). Koelle [82] suggests a steeper learning factor curve of 85% to 90%. Based on historical

reference data and analysis in literature Drenthe tabulated a summary of the learning factor based on the total units that will be produced [83] (Table 6.6).

Table 6.6: Learning Factor Slopes based on the Total Manufactured Units [82], [83], [117]

Total Program Units	Cost Improvement Slope (%)
1 - 10	95
11 - 50	90
>50	85

In SOLSTICE the total number of units to be manufactured (n) is set to 50 [83]. The learning factor is therefore selected to be 0.90. It is important to note that selecting the learning factor has to be done with great care and precision. Drenthe showed in a dedicated sensitivity analysis that the learning factor was having a big impact on the estimated manufacturing cost accuracy. A discrepancy of 4% will result in approximately 22 to 28 percent cost estimation error on manufacturing level.

The manufacturing cost per unit can be described by the following relationship:

$$MAN = c_p \cdot (MAIT + M/PA\%) = c_p \cdot (FM1 \cdot L_m + M/PA\%) \quad (6.15)$$

6.4.5. Operating Cost Estimate

As mentioned before, the operating cost can be dissected into the Direct Operating Cost (DOC) and Indirect Operating Cost (IOC). Drenthe found that the *TRANSCOST* 8.2 model, developed by Koelle [82], was sufficiently accurate to estimate the operating cost of launch vehicles in early design stages [83], [113]. Drenthe applied the *TRANSCOST* model to his SOLSTICE cost model in a hybrid way, see Figure 6.2. In order to approximate the direct and indirect operating cost-per-flight (CpF) some general assumptions, variables and fixed values need to be defined. These are listed in Table 6.7.

Table 6.7: *TRANSCOST* Operations Cost Model with Variables, Assumptions and Fixed Values [82]

Parameter	Symbol	Units	Expendable Rocket	Justification
Launches per Year	LpA	-	<i>var</i>	Suggested by Koelle [82]
Assembly and Integration Factor	f_c	-	0.85	Vertical Assembly/Transportation, customer requirement [82]
Country Productivity Factor	f_B	-	1	Suggested by Koelle [82]
Launch Vehicle Type Factor	f_v	-	[0.8 - 1.0]	Storable Propellants = 0.8, Cryogenic Propellants = 1.0 [82]
Vehicle Complexity Factor	Q_N	-	0.8	Number of stages times 0.4 for ELV's [82]
Commercial Factor	f_{11}	-	0.55	Commercial operation multiple, Suggested by Koelle [82]
Average Learning Factor Operations	L_0	-	0.64	Constant over 50 launches at 90% learning curve, assumption CM-08
Work-Year Costs	W	k€	301200	Based on inflation, linearly extrapolated from Koelle [82]
Number of Stages	N	-	2-3	vehicle-specific
Fuel and Oxidizer Mass	M_p	kg	<i>var</i>	vehicle-specific
Gross Take-Off Weight (GTOW)	M_0	Mg	<i>var</i>	vehicle-specific
Pressurizant Mass	M_{press}	kg	<i>var</i>	vehicle-specific
Mass Mixture Ratio	r	-	<i>var</i>	vehicle-specific
Public Damage Insurance	I	M€	100	Typical range, from Koelle [82]
Payload Mass	P	kg	<i>var</i>	vehicle-specific
Payload Charge Site Fee	c_{payl}	€kg ⁻¹	5.51	Suggested by Koelle [82]
Launch Site Fee	F	k€	1220	Suggested by Koelle [82]
Specific Transportation Cost	T_s	€kg ⁻¹	5.365	ESA internal cost-per-kilogram reference [116]
Percent of Work Subcontracted Out	S	-	20%	Suggested by Drenthe [83]

It can be seen that some of the parameters need to be defined as they are launch vehicle-specific. Others are suggested, calculated or predicted by Koelle [82]. It is important to note that the learning factor that is applied in the operating cost estimate is the same as was defined for the manufacturing cost and development cost estimate (90%). This number is based on the total set of 50 manufactured units. Furthermore, the work-year cost is an estimate by Koelle and linearly extrapolated from his analysis. The number is converted to take into account Euro's and inflation.

The Direct Operations Cost (DOC) can be approximated using the following relationships:

Ground Operations [k€]:

$$C_{ground} = (W \cdot 8 \cdot M_0^{0.67} \cdot LpA^{-0.9} \cdot N^{0.7} \cdot f_c \cdot f_v \cdot L_0 \cdot f_B \cdot f_{11})/1000 \quad (6.16)$$

Propellant Cost [k€]:

$$C_{prop} = \left(\frac{M_p}{r+1} c_f + \left(M_p - \frac{M_p}{r+1} \right) c_{ox} + M_{press} c_{press} \right) / 1000 \quad (6.17)$$

Where:

- c_f = Fuel Specific Cost-per-Kilogram
- c_o = Oxidizer Specific Cost-per-Kilogram
- c_{press} = Pressurizant Specific Cost-per-Kilogram

Flight & Mission Cost [k€]:

$$C_{FM} = (W \cdot 20 \cdot Q_N \cdot LpA^{0.65}) \cdot L_0 \cdot f_8 / 1000 \quad (6.18)$$

Transportation Costs [k€]:

$$C_{Trans} = T_S \cdot M_0 \quad (6.19)$$

Fees & Insurance Costs [k€]:

$$C_{FI} = I + F + (c_{payl} \cdot P) / 1000 \quad (6.20)$$

The Indirect Operations Cost (IOC) [k€] can be approximated using the following relationship:

$$C_{IOC} = (40 \cdot S + 24) \cdot LpA^{-0.379} \cdot W / 1000 \quad (6.21)$$

Using the relationships above the total operating cost can be approximated by:

$$C_{ops} = C_{DOC} + C_{IOC} = C_{ground} + C_{prop} + C_{FM} + C_{Trans} + C_{FI} + C_{IOC} \quad (6.22)$$

6.4.6. Cost-per-Flight Estimate

Using the development, manufacturing and operations cost estimate it is possible to determine the cost-per-flight. This is a very important characteristic of the launch vehicles as it says a lot about the competitiveness of the launch vehicle in the market. In order to determine the cost-per-flight it is important to find the contribution of the development and manufacturing cost-per-flight. The operations cost is already calculated as cost-per-flight. The number of units that will be produced and flown determines this contribution. First, the contribution of development cost towards the cost-per-flight can be determined, this is called '*Development Cost Amortization*':

$$A = \frac{DEV}{N} \quad (6.23)$$

Where:

- DEV = Development Cost [k€]
- N = Number of Units Produced

Furthermore, the contribution of the manufacturing cost to the cost-per-flight can be determined by dividing the total manufacturing cost by the number of units that will be produced, this will be the Average Manufacturing Cost:

$$MAN_{avg} = \frac{MAN}{N} \quad (6.24)$$

Where:

- MAN_{avg} = Average Manufacturing Cost [k€]
- MAN = Total Manufacturing Cost [k€]
- N = Number of Units Produced

The average cost-per-flight (CpF_a) can now be calculated via:

$$CpF_a = MAN_a + OPS + A \quad (6.25)$$

6.5. Cost Modelling

The cost model discussed will be used to estimate the cost of the Ariane 6 rocket, the upper stage module and the “Prototype X” Upper Stage Module. Furthermore, the model will be used during the systems engineering design iteration phase of this research project to analyse the cost behaviour of various design choices. This asks for an adaptable system that is easy to use with the vehicle model, useful in cost analysis and portrays the total effect of mass changes in terms of development, manufacturing and operations cost.

The cost model parameters, variables, assumptions and relationships discussed, have been used to create a designated cost modelling tool in MATLAB. This programming software, specially designed for the engineering field, is easy to use and allows for intermediate calculations. MATLAB was chosen because this tool also allows for easy and smooth integration of optimising software.

Together with the performance model and the mass model, the cost model will be used to calculate the effects on cost-per-kg for different mission profiles carrying specific payloads. The models are dependent on inputs from each other to generate an iterative cycle that will find the most optimal design solution.

6.5.1. Sensitivity Analysis

The cost model is built upon some important assumptions that influence the outcome, precision and accuracy of the cost estimate. A sensitivity analysis will be used to investigate the impact these assumptions have on the cost estimates. Since the cost model is built up from the development, manufacturing and operation cost, this sensitivity analysis will be split up over these three contributors to the cost-per-flight (CpF) estimate. Once the effect of these assumptions on cost estimate is known it will give insight in the accuracy and precision of the estimate. The sensitivity analysis is based on actual cost estimates of the Ariane 6 Upper Liquid Propulsion Module, which will be described later on in this chapter.

Development Cost Sensitivity

The development cost is built up from different system test hardware pillars. These are also called T1 equivalents. These contributors are the Proto Flight Model (PFM), Qualification Model (QM), Engineering Model (EM) and the Development Model (DM). The PFM, QM and EM factors have their origin in the NAFCOM database for cost estimates [118]. The NAFCOM model, as discussed earlier, has been built upon a comprehensive historical database. However, the DM factor is not deeply rooted in historical data and is thus subject to sensitivity analysis. The nominal value is set to be 0.3 but variations ranging between 0.1 – 0.5 will be tested to see its effect on the total development cost.

Furthermore, the subcontractor profit is set to be 8%. This is identified by Koelle in his TRANSCOST 8.2 model [82]. This value was taken as the average subcontractor profit that was seen in commercial outsourcing contracts. Koelle identifies a subcontractor profit ranging between 4 – 14%. The effect of these profit ranges will be investigated in the sensitivity analysis too. Lastly, the percentage of subcontracted work is ranging in literature between 10 – 60% [82], [112]. The reference case launch vehicle is an ESA/ArianeGroup built venture. Historically the level of subcontractor-ship is around 20%. This is therefore set as default but in the sensitivity analysis the effect of other levels will be investigated.

In Table 6.8 the sensitivity analysis is carried out for the parameters discussed above.

The sensitivity analysis shows that varying the development T1 Equivalent (Development Model) has the biggest impact on the development cost ($\pm 5.2\%$). Both the subcontractor profit and percentage subcontracted do have some effect but it is limited. Based on these results it can be concluded that the impact of these assumptions will have a maximum effect of -5.2% and 5.2% on the total development cost.

Manufacturing Cost Sensitivity

As the manufacturing cost estimates are based on the development cost arithmetic some assumptions are carried over from the development cost estimate to the manufacturing cost estimate. The most important new assumption is the assumption of the learning curve factor. This factor illustrates the ability to become more efficient along the process of manufacturing. The learning curve factor is set at

Table 6.8: Sensitivity Analysis on Development Cost

Parameter	Cost Decreasing [k€]	Nominal [k€]	Cost Increasing [k€]
Development T1 Equivalent	0.1	0.3	0.5
Total Development Cost	213,617	225,344	237,071
Percentage Change	-5.20%	-	5.20%
Subcontractor Profit	14%	8%	4%
Total Development Cost	220,713	225,344	228,612
Percentage Change	-2.06%	-	1.45%
Percentage Subcontracted	10%	20%	40%
Total Development Cost	223,671	225,344	228,691
Percentage Change	-0.74%	-	1.49%

0.90 as default for the manufacturing and, indirectly, for the operation cost too. To investigate the effect of this learning curve factor a sensitivity analysis should be carried out. In this analysis, the learning curve factor will be varied between 0.82 – 0.97 resulting in a reduction and increase in manufacturing cost, respectively. In Table 6.9 the sensitivity analysis is carried out.

Table 6.9: Sensitivity Analysis on Manufacturing Cost

Learning Curve Factor [-]	Total Manufacturing Cost (50 Units) [k€]	Manufac. Avg Unit Cost [k€]	Increase/Reduction Cost [%]
0.82	353,100	7,062	-31.11%
0.86	426,294	8,526	-16.83%
<i>Assumption: p = 0.90</i>	512,529	10,251	-
0.94	613,582	12,272	19.72%
0.97	700,262	14,005	36.63%

From Table 6.9 it can be seen that the learning curve factor has a significant impact on the manufacturing cost of the upper stage module. The effect of the learning curve factor ranges between –31.1% to 36.6% in reduction or increase of manufacturing cost respectively. This emphasises the need to properly assess and determine the learning curve factor to ensure proper manufacturing cost estimates.

Operation Cost Sensitivity

The operation cost is determined by the cost model for operation cost developed by Koelle [82]. In this model, a lot of approximations and assumptions were taken to estimate the indirect and direct operation cost. The most important assumptions for the operation cost are; the number of launches per year (LpA), the commercial factor (f_{11}) and the assembly and integration factor (f_c). The latter was assumed by Koelle [82] and the number of launches per year is adjusted such that it corresponds to what is expected by the ESA for Ariane 6, ranging from 6 to 12 launches per year [11]. In Table 6.10 the sensitivity analysis was conducted.

Table 6.10: Sensitivity Analysis on Operation Cost

Parameter	Cost Decreasing [k€]	Nominal [k€]	Cost Increasing [k€]
Launches per Year	10	8	4
Total Operating Cost	7,672	8,435	11,629
Percentage Change	-9.05%	-	37.87%
Commercial Factor	0.35	0.55	0.85
Total Operating Cost	7,837	8,435	9,331
Percentage Change	-7.09%	-	10.62%
Assembly and Integration Factor	0.65	0.85	0.95
Total Operating Cost	8,048	8,435	8,628
Percentage Change	-4.59%	-	2.29%

From Table 6.10 it can be concluded that the assembly and integration factor have only a limited effect on the total operation cost, ranging from -4.59% to 2.29% . The biggest contributor to change is the LpA parameter. Reducing the number of launches will drastically increase the operation cost ($+37.87$). Also, the commercial factor has a significant impact on the operating cost, ranging from -7% to approximately 11% . The accuracy of the cost-per-flight (CpF) estimate, therefore, is strongly dependent on these parameters.

6.6. Verification and Validation

The SOLSTICE Cost Model and the *TRANSCOST* model as defined by Drenthe and Koelle respectively, have been slightly modified to take into account Dollar/Euro conversions and inflation. Also, some modifications have been pointed out to make the cost model suitable for the expendable launch vehicle under consideration. The cost model produces figures on the cost-per-flight (CpF) as a result of the development, manufacturing and operation cost. These cost parameters are fundamental to investigate the cost implications of certain design choices. It can thus be concluded that the cost model is verified to be used for cost estimation analysis.

Since the cost model will be used to compare the conventional cryogenic upper stage module with the new storable upper stage module, it is not necessary to validate the cost model. The cost implications of design choices can be expressed in the relative sense with respect to the standard design. This way the absolute cost figures will not be necessary to be validated. Validation of the cost model would introduce a lot of uncertainty. A large sample of accurate cost data for various launch vehicles is required to do meaningful validation. Since this extensive information on cost is hard to come by cost model validation would only be possible in a limited fashion. Furthermore, the accuracy on the cost figures presented by the cost model is limited too. These considerations led to the decision to not further validate the cost model. It is important to note that the cost model was validated by Drenthe using extensive cost analysis data provided by the ESA.

6.7. Ariane 6 Launch Vehicle Cost Estimate

The storable upper stage "Prototype X" will be compared to the conventional cryogenic Upper Liquid Propulsion Module (ULPM) of the Ariane 6 launch vehicle. Since this research investigates the cost-per-flight change between the two designs (by introducing different storable propellant combinations) it is useful to investigate the cost breakdown of the Ariane 6 launch vehicle. This cost breakdown will serve as a baseline to which potential cost changes will be compared.

To generate the cost breakdown, the launch vehicle was split into two parts; the first and upper stage. In this division, the boosters were not taken into account. As seen in Figure 5.1 the launch vehicle comes in two configurations; 2-booster or 4-booster configuration. Since the performance and mass model do not account for these boosters these will be neglected in the cost model estimate too. The research is focused on the upper stage and how their cryogenic and storable designs compare to each other. However, the first stage is also part of the analysis and will be estimated by the launch vehicle model and the cost model. This will help to understand better the cost breakdown of the entire launch vehicle and will give insight into the impact the design alterations can have on the cost-per-flight figure and payload performance. Having both stages analysed through the launch vehicle model and the cost model makes it possible to manage the entire launch vehicle mass and cost budgets. Furthermore, the impact of the upper stage design alterations on the first stage can be compared if there is a baseline cost budget for the first stage too.

In this section the cost breakdown for the first and upper stage of the Ariane 6 launch vehicle will be presented. To start, the First Unit Cost will be determined for both stages. This will be an input for the development cost estimate and the manufacturing cost estimate. The operation cost for both stages separately and the total launch vehicle will be calculated next. These cost estimates will be used to determine the Cost-per-Flight of the separate stages and the integrated launch vehicle.

6.7.1. First Unit Cost Estimate

From the basic stage characteristics the performance, and consequently, the mass breakdown of the stages could be calculated by the launch vehicle model. These mass fractions serve as inputs for the calculation of the First Unit estimate. This mass and cost breakdown is depicted in Table 6.11.

Table 6.11: First Unit Cost Estimate for Ariane 6 Stages (Excluding Boosters)

(a) Ariane 6 First Stage				(b) Ariane 6 Upper Stage				
Unit	Element	Mass [kg]	Flight Unit Cost [k€]	Unit	Element	Mass [kg]	Flight Unit Cost [k€]	
LLPM	Fuel Tank	3,270	7,169	ULPM	Fuel Tank	2,034	4,069	
	Oxidizer Tank	1,836	4,753		Oxidizer Tank	1,411	3,136	
	Thrust Structure	7,049	9,047		Thrust Structure	806	1,251	
	Skirt	3,254	13,401		Thermal Control	155	278	
	Thermal Control	464	757		Engines	317	2,949	
	Engines	2,209	13,602		Thrust Vector Control	213	892	
	Thrust Vector Control	1,623	3,076		Pipes & Valves	15	57	
	Pipes & Valves	89	196		Avionics	116	2,295	
	Avionics	143	2,718		Interstage	Interstage Structure	1,708	1,061
	Payload	Payload Adapter	558			2,178	Total UPLM	6,775
Payload Fairing		3,399	6,994	I&T	Stage I&T	-	404	
Total LLPM		23,894	63,891		PAA I&T	-	74	
I&T		3.2%		Total First Unit Cost [k€]			16,466	
	Stage I&T	-	1,664					
	PAA I&T	-	380					
Total First Unit Cost [k€]			65,935					

Looking at Table 6.11 there are some important things to note. First, the mass and cost contributions of the payload are added to the first stage module. Secondly, the interstage structure is added to the upper stage module. Both of which are in line with the procedure described by Drenthe [83]. Following Drenthe's arithmetic, the payload elements are part of the first stage design, although this physically is a separate section of the launch vehicle. The same holds for the interstage structure. This structure is "lumped" into the upper stage module as part of this arithmetic. This procedure will be kept fixed for the upcoming analysis.

The first unit cost of the first and upper stage section are approximately 66 M€ and 16.5 M€, respectively.

6.7.2. Development Cost Estimate

The first unit cost is the input for the development cost calculation. The development cost is calculated separately for the stage, payload section, interstage and for the integration/testing of the stage (Stage I&T) and integration/testing of the payload, avionics and attitude control (PAA I&T). To this development cost the cost that accounts for the Management and Product Assurance (M/PA) is added. The development cost breakdown for the first and upper stage of the Ariane 6 Launch Vehicle is depicted in Table 6.12.

Table 6.12: Development Cost Estimate for Ariane 6 Stages (Excluding Boosters)

(a) Ariane 6 First Stage				(b) Ariane 6 Upper Stage			
		Flight Unit Cost [k€]	Development Cost [k€]			Flight Unit Cost [k€]	Development Cost [k€]
		65,935	1,040,198			16,466	259,770
M&PA	Total		51,339	M&PA	Total		12,821
	5.3% M/PA		51,339		5.3% M/PA		12,821
LLPM	Total	65,935	988,859	ULPM	Total	16,466	246,949
	Stage	54,719	820,644		Stage	14,927	223,874
	Payload	9,172	137,553		Interstage	1,061	15,911
	3.2% Stage I&T	1,664	24,956		3.2% Stage I&T	404	6,062
	3.2% PAA I&T	380	5,706		3.2% PAA I&T	74	1,102

The development cost amounts to, approximately, 1 B€ and 260 M€, for the first and upper stage respectively. The total development cost of the Ariane 6 launch vehicle (excluding boosters) is the summation of the development cost for both stages; 1.26 B€.

6.7.3. Manufacturing Cost Estimate

The manufacturing cost is considered recurring cost. In the cost model, as discussed earlier, it was assumed that there will be 50 units produced in a batch. In this case, the manufacturing cost will be calculated based on these 50 units. The manufacturing cost is calculated based on the first unit cost and will be cumulative. The manufacturing cost of the first stage of the Ariane 6 Launch Vehicle (LV) is depicted in Table 6.13 and Table 6.14 respectively. Again, to the manufacturing cost per element the Management and Product Assurance (M/PA) is added.

Table 6.13: Manufacturing Cost Estimate for Ariane 6 First Stage (excluding boosters)

		Flight Unit Cost [k€]	Manufac. Avg Unit Cost [k€]	Total Manufac. Cost [k€]
		65,935	56,078	2,803,883
M&PA	Total		2,907	145,338
5.3%	M/PA		2,907	145,338
LLPM	Total	65,935	53,171	2,658,545
	Stage	54,719	44,126	2,206,297
	Payload	9,172	7,396	369,809
3.2%	Stage I&T	1,664	1,342	67,096
3.2%	PAA I&T	380	307	15,343

In Table 6.13 both the cumulative manufacturing cost as well as the average manufacturing cost per unit are depicted. The total manufacturing cost over 50 units is approximately 2.8 B€. This amounts to approximately 56 M€ per first stage.

Table 6.14: Manufacturing Cost Estimate for Ariane 6 Upper Stage (excluding boosters)

		Flight Unit Cost [k€]	Manufac. Avg Unit Cost [k€]	Total Manufac. Cost [k€]
		16,466	14,004	700,252
M&PA	Total		725	36,295
5.3%	M/PA		725	36,295
ULPM	Total	16,466	13,279	663,957
	Stage	14,927	12,038	601,916
	Interstage	1,061	856	42,777
3.2%	Stage I&T	404	326	16,300
3.2%	PAA I&T	74	59	2,964

In Table 6.14 this is done for the upper stage of the Ariane 6 LV. The total manufacturing cost over 50 units is approximately 700 M€. This amounts to approximately 14 M€ per upper stage.

6.7.4. Operation Cost Estimate

The operation cost is dependent on the payload capability and on the number of launches per year. It is assumed that there will be 8 launches per year (LpA). The operation cost per stage for the nominal payload is depicted in Table 6.15. The operating cost is dissected into direct and indirect cost. It is important to note that the contributions "Flight and Mission Operation" and "Fees and Insurance Cost" are the same for both stages. These contributions are considered fixed per launch and therefore do not depend on the type of stage. It is important to take this into account for the integration of both stages. In this case, these two contributions will only count once towards the operating cost. This holds for the "Commercialization Cost" too.

Table 6.15: Operation Cost Estimate for Ariane 6 Stages (Excluding Boosters) - Nominal Payload

(a) Ariane 6 First Stage		(b) Ariane 6 Upper Stage	
Segment	Cost [k€]	Segment	Cost [k€]
Direct Operating Cost	8,706	Direct Operating Cost	4,472
Ground Operations	5,512	Ground Operations	2,062
Propellant Cost	140	Propellant Cost	31
Flight and Mission Operations	798	Flight and Mission Operations	798
Transportation Cost	879	Transportation Cost	204
Fees and Insurance Cost	1,377	Fees and Insurance Cost	1,377
Indirect Operating Cost	4,383	Indirect Operating Cost	4,383
Commercialization cost	4,383	Commercialization cost	4,383
Total Operating Cost	13,089	Total Operating Cost	8,855

In Table 6.16 the operation cost for the first and upper stage are depicted in case of max payload capability. Primarily the “Fees and Insurance cost” is impacted by the change in operation cost.

Table 6.16: Operation Cost Estimate for Ariane 6 Stages (Excluding Boosters) - Maximum Payload

(a) Ariane 6 First Stage		(b) Ariane 6 Upper Stage	
Segment	Cost [k€]	Segment	Cost [k€]
Direct Operating Cost	8,745	Direct Operating Cost	4,535
Ground Operations	5,489	Ground Operations	2,062
Propellant Cost	140	Propellant Cost	31
Flight and Mission Operations	798	Flight and Mission Operations	798
Transportation Cost	879	Transportation Cost	204
Fees and Insurance Cost	1,439	Fees and Insurance Cost	1,439
Indirect Operating Cost	4,383	Indirect Operating Cost	4,383
Commercialization cost	4,383	Commercialization cost	4,383
Total Operating Cost	13,128	Total Operating Cost	8,917

To illustrate the fixed costs, as discussed above, for the integrated first and upper stage, the operation cost breakdown is depicted in Table 6.17 and Table 6.18, for nominal and maximum payload respectively. Here the contributions of “Flight and Mission Operation” and “Fees and Insurance Cost” are counted once towards the total operating cost.

For the first stage the total operating cost amount to approximately 13 M€ per launch. For the upper stage the operating cost is found to be 8.9 M€ per launch. The total launch vehicle operating cost, including the first and upper stage but excluding the boosters and depending on the payload capability, is around 15.4 M€ per launch, respectively.

Table 6.17: Operation Cost Estimate for total Ariane 6 Launch Vehicle (excluding boosters) - Nominal Payload

Segment	Cost [k€]
Direct Operating Cost	10,982
Ground Operations	7,553
Propellant Cost	171
Flight and Mission Operations	798
Transportation Cost	1,083
Fees and Insurance Cost	1,377
Indirect Operating Cost	4,383
Commercialization cost	4,383
Total Operating Cost	15,365

Table 6.18: Operation Cost Estimate for total Ariane 6 Launch Vehicle (excluding boosters) - Maximum Payload

Segment	Cost [k€]
Direct Operating Cost	11,044
Ground Operations	7,553
Propellant Cost	171
Flight and Mission Operations	798
Transportation Cost	1,083
Fees and Insurance Cost	1,439
Indirect Operating Cost	4,383
Commercialization cost	4,383
Total Operating Cost	15,427

It is important to note that the propellant cost, in this case liquid hydrogen and liquid oxygen, are calculated based on prices found in literature. Following this, it was found that the liquid hydrogen is approximately €6/kg and liquid oxygen is approximately €0.14/kg (2021 prices) [83].

6.7.5. Cost-per-Flight Estimate

From the contributions of development cost, manufacturing cost and operation cost, the Cost-per-Flight (CpF) can be determined. The development cost, being non-recurring, should be divided over the number of units that are allocated per batch/block. This amortization charge will be fixed per flight. The manufacturing charge per flight is simply the average manufacturing cost per unit. Although, this charge will diminish over time, the average will be used to determine a fixed average CpF. To these two contributions the operation cost will be added as depicted in Table 6.15 and Table 6.16. The total CpF can be determined for the first and upper stage separately. This is depicted in Table 6.19 and Table 6.20 for the nominal and maximum payload respectively.

Table 6.19: Cost-per-Flight Estimate for Ariane 6 Stages (Excluding Boosters) - Nominal Payload

(a) Ariane 6 First Stage		(b) Ariane 6 Upper Stage	
Contribution	Cost [k€]	Contribution	Cost [k€]
Amortization Charge per Flight	20,804	Amortization Charge per Flight	5,195
Manufacturing Cost per Flight	56,079	Manufacturing Cost per Flight	14,004
Operational Cost per Flight	13,089	Operational Cost per Flight	8,855
Total Cost per Flight	89,972	Total Cost per Flight	28,054

Looking at Table 6.19 the CpF for the first stage is approximately 90 M€. For the first stage the CpF is ≈ 28 M€. In Figure 6.3 a graphic representation of the Cost-per-Flight breakdown is given.

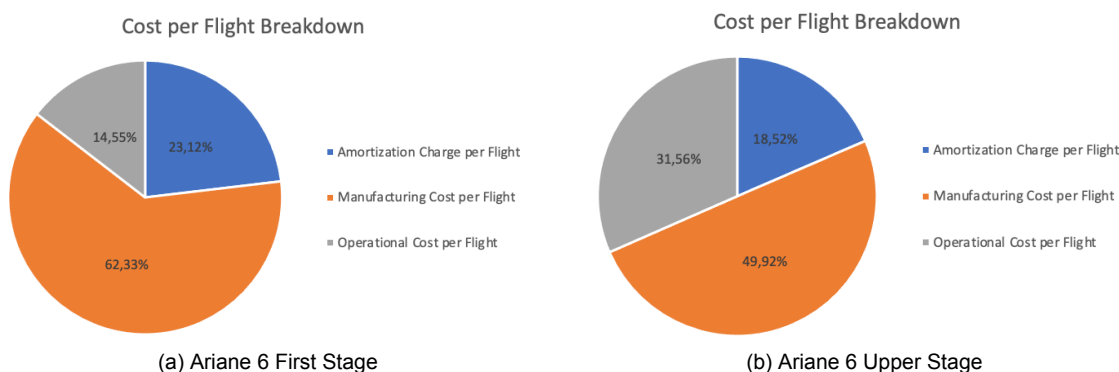


Figure 6.3: Cost-per-Flight Breakdown for Ariane 6 Stages (Excluding Boosters) - Nominal Payload

From Figure 6.3 it can be concluded that the manufacturing cost-per-flight is the biggest contributor to the CpF for the first and upper stage, being 62% and 50% respectively. Furthermore, the contribution

of operational cost is relatively large in the CpF for the upper stage. This is due to the fixed indirect cost of “Commercialization Cost”. The commercialization cost takes staff and administrative personnel costs, marketing activities and technical support like vehicle procurement into account [82].

Now the cost-per-flight can be determined in case of maximum payload capability. This is depicted in Table 6.20.

Table 6.20: Cost-per-Flight Estimate for Ariane 6 Stages (Excluding Boosters) - Maximum Payload

(a) Ariane 6 First Stage		(b) Ariane 6 Upper Stage	
Contribution	Cost [k€]	Contribution	Cost [k€]
Amortization Charge per Flight	20,804	Amortization Charge per Flight	5,195
Manufacturing Cost per Flight	56,079	Manufacturing Cost per Flight	14,004
Operational Cost per Flight	13,128	Operational Cost per Flight	8,917
Total Cost per Flight	90,011	Total Cost per Flight	28,116

Looking at Table 6.20 the CpF for the first stage is approximately 90 M€. For the first stage the CpF is ≈ 28 M€. In Figure 6.4 a graphic representation of the Cost-per-Flight breakdown is given.

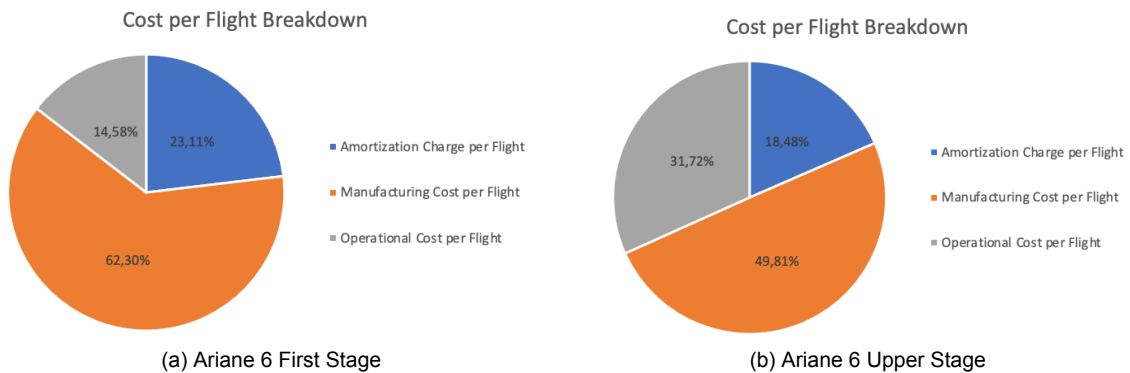


Figure 6.4: Cost-per-Flight Breakdown for Ariane 6 Stages (Excluding Boosters) - Maximum Payload

From Figure 6.4 it can be concluded that the CpF's for the two different payload configurations do not vary significantly. Next, the CpF of the integrated launch vehicle will be calculated.

Since it is not very realistic to account operating cost separately for the individual stages, it makes more sense to see this contribution in the integrated launch vehicle CpF budget. The CpF breakdown for the first and upper stages is depicted in Table 6.21 and Table 6.22, for the nominal and maximum payload capability respectively. Here the amortization charge and manufacturing cost per unit is the combined contribution of the first and upper stage.

Table 6.21: Cost-per-Flight Estimate for total Ariane 6 Launch Vehicle (excluding boosters) - Nominal Payload

Contribution	Cost [k€]
Amortization Charge per Flight	25,999
Manufacturing Cost per Flight	70,083
Operational Cost per Flight	15,365
Total Cost per Flight	111,447

In case of the maximum payload capability, the following CpF is found, as depicted in Table 6.22.

Table 6.22: Cost-per-Flight Estimate for total Ariane 6 Launch Vehicle (excluding boosters) - Maximum Payload

Contribution	Cost [k€]
Amortization Charge per Flight	25,999
Manufacturing Cost per Flight	70,083
Operational Cost per Flight	15,427
Total Cost per Flight	111,509

Looking at Table 6.21 and Table 6.22 the CpF for the first and upper stage is approximately 111.5M€. According to ESA the launch cost for the Ariane 6 is expected to be 115 M€ Euro for the 4-booster configuration and 75 M€ Euro for the 2-booster configuration [90]. It is important to note that the CpF found here is for the Ariane 6 without boosters. Although the calculated and projected launch cost have the same order of magnitude, it is very hard to compare these numbers, as per validation. The Ariane 6 launch vehicle is being developed with ESA financial support. This means that member-states of the European Space Agency are contributing financially to this project. These ESA fundings are not directly covered by the CpF. This means that the expected CpF, communicated by the ESA, is lower than the actual cost of the Ariane 6 launch vehicle [119].

In Figure 6.3 and Figure 6.4 a graphic representation of the Cost-per-Flight breakdown is given for the Ariane 6 LV (without external boosters).

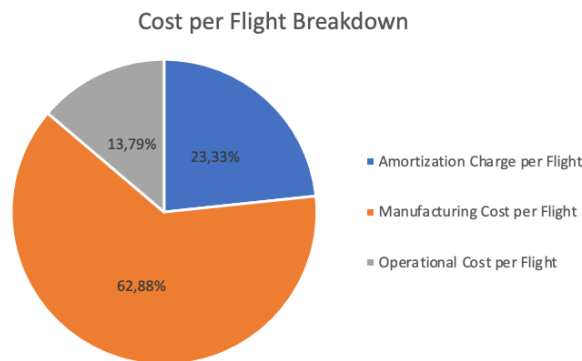


Figure 6.5: Cost-per-Flight Breakdown for total Ariane 6 Launch Vehicle (excluding boosters) - Nominal Payload

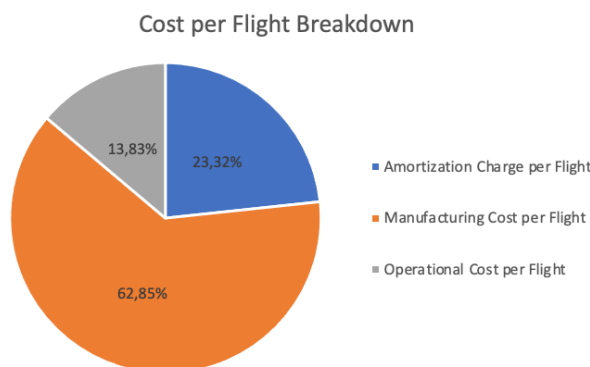


Figure 6.6: Cost-per-Flight Breakdown for total Ariane 6 Launch Vehicle (excluding boosters) - Maximum Payload

The cost figures found for the development cost, manufacturing cost, operation cost and the CpF are estimated by the cost model with an accuracy of ±20% compared to the actual reported cost [83], [113]. This means that the cost estimates, calculated by this cost model, in this research thesis have an accuracy of ±20% compared to the reported cost in literature. This error will be depicted in the subsequent chapters by designated error bars.

6.8. Executive Chapter Summary

In this chapter, the cost estimating model was developed. This cost model will be used to estimate the cost-per-flight of the Ariane 6 launch vehicle, ULPM and the “Prototype X” concept. The cost-per-flight is comprised of the development cost, manufacturing cost and operating cost. The individual contributions to these three cost fractions are schematically depicted in Figure 6.1. Because space flight is becoming more and more commercialised very little data on launch vehicle cost is found in literature. Therefore, it is required to have a good cost model in place that will estimate the cost of the launch vehicle stages, systems and subsystems based on their dry mass. For this thesis research it was chosen to use the SOLSTICE cost model developed by N. Drenthe in collaboration with ESA/ESTEC. This hybrid cost model combines parametric and heuristic estimation techniques. Also, SOLSTICE incorporates the TRANSCOST 8.2 model (designed and developed by Koelle) to do operation cost estimates. SOLSTICE was chosen as the dedicated cost model as this cost model was publicly available, is validated for European Launch Vehicles and is currently used by the ESA/ESTEC Cost Engineering Section as part of ESA’s Concurrent Design Facility for conceptual designs. Since the cost model will be primarily used to compare the cryogenic design with the storable concept, the absolute cost figures that are produced by this model do not carry much significance. SOLSTICE enables this comparative analysis while ensuring the cost estimate to be the right order of magnitude, with a maximum accuracy error of $\pm 20\%$.

Assumptions and requirements for the cost model have been tabulated in Table 6.1 and Table 6.2. These assumptions and requirements help to simplify the model and prescribe the verification effort respectively. Based on CERs developed for the NAFCOM model, the first unit cost can be determined. This is done by using the dry mass of the system, subsystem or element at hand. This first unit cost was corrected for currency and inflation (Appendix A). The first unit cost is an input for the development cost and manufacturing cost. To construct the development cost fraction, T1 equivalents are used. These are multiplied with modifiers that account for the Design and Development effort, Engineering effort, model philosophy and the testing work performed. These modifiers have been developed by ESA Costing Software (ECOS). Together with the level of subcontractorship, the development learning curve and profit retention cost reduction factor, these modifiers help to construct the total development cost figure. Using the same arithmetic the manufacturing cost estimate is developed. In this case, two modifiers were used; Manufacturing, Assembly, Integration and Test of Hardware (MAIT) and Management and Product Assurance (M/PA). For the manufacturing cost estimate it is very important to consider the manufacturing learning factor (p). This learning curve factor was set to 90% based on historical reference. The operating cost estimate is described by the TRANSCOST 8.2 model, developed by Koelle. Based on vehicle-specific parameters, assumptions and variables the direct and indirect operating costs can be approximated.

The amortisation charge, manufacturing charge per flight and the operation cost are summed together to construct the cost-per-flight estimate. This CpF figure describes how the launch vehicles fit in the current launch vehicle market. Furthermore, it allows proper comparison between the cryogenic design and storable concepts. The cost model was constructed in the MATLAB modelling tool to allow interconnection with the performance and mass model.

Since the cost model is built upon important assumptions, a sensitivity analysis was performed. In this analysis, it showed that the Development T1 Equivalent modifier has the biggest impact on the CpF. The level of work subcontracted out had a limited impact on the cost-per-flight estimate. Furthermore, the sensitivity analysis showed that the learning curve factor has such a significant impact on the cost estimates that it can greatly influence the accuracy of the model. Therefore it was chosen to keep the learning curve factor constant throughout this research work. The number of launches per year was the most pronounced parameter in the sensitivity analysis for the operation cost estimate. The cost model was verified to be used in combination with the vehicle model as it described all aspects of associated launch vehicle cost. Since the cost model will be used for comparative analysis only, it was decided that the cost model was not further validated. The SOLSTICE cost model was validated for Ariane type launches by ESA/ESTEC. When tried to validate the model for non-European launchers it was concluded that cost information in literature was too limited. This inability of validation was not deemed harmful due to the comparative nature of the analysis. To do this comparison, a launch vehicle cost

estimate was done for the Ariane 6. For both the first and upper stage designs the development cost, manufacturing cost and operation cost were determined. Both for the nominal and maximum payload configuration it was found that the ULPM was approximately 28.1 M€ Euro. The fully integrated Ariane 6 launch vehicle, comprised of the first and upper stage, was estimated to be approximately 111.5 M€ Euro. In all cost estimates provided in this thesis work, they can be assumed to be accurate by $\pm 20\%$ relative to the actual reported cost.

7

Propellant Selection

To investigate the cost impact storable propellants have when implemented in upper stage designs it is necessary to look at possible propellant combinations. In this chapter, the propellant selection will be done. To make it more specific, combinations of hydrogen peroxide with storable fuels will be investigated on their combustion efficiency. This, is to analyse possible propellant combinations that have the best possibility to compete with the conventional cryogenic upper stage. Highly concentrated hydrogen peroxide (99+%) is considered to be the fixed oxidiser for the bi-propellant combustion. In this propellant selection and trade-off strictly green storable fuels will be investigated.

7.1. Propellant Analysis Requirements & Assumptions

Before the propellant analysis can be done, requirements and assumptions have to be listed. This is important to quantify the possible fuel/oxidiser combinations on their relative score. The requirements and assumptions are listed in the tables below. The requirements for the performance model are described below in Table 5.4.

Table 7.1: Propellant Selection Requirements

ID	Requirement
PROP-REQ-01	The oxidiser component of the propellant combination shall be concentrated hydrogen peroxide (99+%)
PROP-REQ-02	The storable fuel shall be classified by the European Union as 'green'
PROP-REQ-03	The storable fuel shall be compatible with metals, plastics and elastomers
PROP-REQ-04	The storable fuel shall be storable for more than 7 days, necessary for pre-launch conditions
PROP-REQ-05	The storable propellant combination shall not be carcinogenic, toxic nor corrosive
PROP-REQ-06	The storable propellant combination shall have ignition delay times in the range of 1 to 25 milliseconds
PROP-REQ-07	The propellant combination shall produce a total thrust of 180 kN
PROP-REQ-08	The storable fuel shall be of a hydrocarbon kind
PROP-REQ-09	The storable fuel shall be liquid in the range of 273 - 313 K
PROP-REQ-10	The storable fuel shall be able to ignite with concentrated hydrogen peroxide
PROP-REQ-11	The storable fuel shall at least be in development
PROP-REQ-12	The combination of hydrocarbon fuel and concentrated hydrogen peroxide attains steady-state combustion

During the propellant selection and analysis assumptions are made. This is done to simplify the analysis but also to allow for meaningful and valuable comparison between the storable novel green propellant combinations and the conventional cryogenic combination. These assumptions are summarised in Table 7.2.

These requirements and assumptions will be important for further research and verification and validation of the obtained results. First the conventional cryogenic propellants will be discussed.

7.2. Conventional Cryogenic Propellants

Conventionally, liquid oxygen (LO₂ or LOX) is being used as the oxidiser in current bi-propellant rocket propulsion systems. Liquid oxygen is a pale blue substance that has a freezing point of 54.36 K and a boiling point of 90.19 K. These physical characteristics make liquid oxygen behave like a cryogenic substance. The low temperature at which the cryogenic LO₂ is stored makes the materials it touches

Table 7.2: Propulsion Analysis Assumptions

ID	Assumption
PROP-ANALYSIS-01	Combustion efficiency is corrected using combustion and nozzle quality factors
PROP-ANALYSIS-02	Vacuum atmospheric conditions are assumed
PROP-ANALYSIS-03	The optimum oxidiser-to-fuel ratio will be used to find the optimum vacuum specific impulse
PROP-ANALYSIS-04	Additives such as Sodium borohydrides can be added to reduce the IDT
PROP-ANALYSIS-05	The hydrogen peroxide oxidiser is 100% concentrated to investigate its best combustion performance
PROP-ANALYSIS-06	The density of the fuel is measured at a temperature of 20 deg C
PROP-ANALYSIS-07	The combustion performance of the propellant combination can be described by ideal rocket theory
PROP-ANALYSIS-08	The combustion efficiency analysis is calculated with a fixed combustion chamber pressure of 6 MPa
PROP-ANALYSIS-09	The nozzle flow analysis is based on a fixed expansion ratio of 240

become extremely brittle. The expansion ratio of liquid oxygen, the volume it takes going from a liquid to gas phase, is 1 to 861 [120].

Table 7.3: Chemical Characteristics Liquid Oxygen [120]

Liquid Oxygen	Value	Unit
<i>Molecular Formula</i>	LO ₂	-
<i>Molecular Weight</i>	31.999	<i>g/mole</i>
<i>Boiling Point (1 atm)</i>	90.19	<i>K</i>
<i>Freezing Point (1 atm)</i>	54.36	<i>K</i>
<i>Density Liquid (1 atm)</i>	1141	<i>kg/m³</i>
<i>Heat of formation</i>	-12.979	<i>kJ/mole</i>
<i>Specific Heat Capacity (1 atm, 273 K)</i>	0.9166	<i>kJ/kg – K</i>
<i>Expansion Ratio</i>	1:861	-

Typical fuels that are combined with liquid oxygen are liquid hydrogen (LH₂), Rocket Propellant-1 (RP1) or kerosene (T1). Liquid hydrogen (LH₂) is a cryogenic colourless liquid that is often used together with liquid oxygen to operate in a bi-propellant liquid propulsion system. The liquid hydrogen reacts very rapidly and powerful with liquid oxygen. Liquid hydrogen has to be cooled to 20.28 K to be in a fully liquid state at atmospheric pressure.

Table 7.4: Chemical Characteristics Liquid Hydrogen [120]

Liquid Hydrogen	Value	Unit
<i>Molecular Formula</i>	LH ₂	-
<i>Molecular Weight</i>	2.016	<i>g/mole</i>
<i>Boiling Point (1 atm)</i>	20.28	<i>K</i>
<i>Freezing Point (1 atm)</i>	14.01	<i>K</i>
<i>Density Liquid (1 atm)</i>	70.85	<i>kg/m³</i>
<i>Heat of formation</i>	-9.012	<i>kJ/mole</i>
<i>Specific Heat Capacity (1 atm, 273 K)</i>	14.304	<i>kJ/kg – K</i>
<i>Expansion Ratio</i>	1:848	-

Rocket Propellant-1 (RP-1) and kerosene (T-1) are chemically very similar products. RP-1 is a highly refined form of kerosene. RP-1 and T-1 both produce a lower specific impulse with liquid oxygen compared to liquid hydrogen. However, it is cheaper to produce and store as it is stable at room temperature. Due to this storable character of RP-1 and T-1 it presents a lower explosion hazard. Although the specific energy is lower for RP-1 and T-1, the higher density of RP-1 and T-1 results in a higher energy density when compared to liquid hydrogen. The chemical characteristics of Rocket Propellant-1 (RP-1) are tabulated in Table 7.5.

Table 7.5: Chemical Characteristics Rocket Propellant-1 (RP-1) [120]

Rocket Propellant-1 (RP-1)	Value	Unit
<i>Molecular Formula</i>	C _n H _{1.953n}	-
<i>Molecular Weight</i>	13.976	<i>g/mole</i>
<i>Boiling Point (1 atm)</i>	475.6	<i>K</i>
<i>Freezing Point (1 atm)</i>	213.15	<i>K</i>
<i>Density Liquid (1 atm)</i>	810	<i>kg/m³</i>
<i>Heat of formation</i>	-24.717	<i>kJ/mole</i>
<i>Specific Heat Capacity (1 atm, 273 K)</i>	1.8839	<i>kJ/kg – K</i>

The chemical characteristics of RP-1 are very similar to the characteristics of kerosene. To allow for comparison, the chemical characteristics of kerosene are tabulated below in Table 7.6.

Table 7.6: Chemical Characteristics Kerosene (T-1) [120]

Kerosene (T-1)	Value	Unit
<i>Molecular Formula</i>	C ₁₂ H ₂₆	-
<i>Molecular Weight</i>	13.982	<i>g/mole</i>
<i>Boiling Point (1 atm)</i>	448 - 598	<i>K</i>
<i>Freezing Point (1 atm)</i>	233	<i>K</i>
<i>Density Liquid (1 atm)</i>	806	<i>kg/m³</i>
<i>Heat of formation</i>	-27.377	<i>kJ/mole</i>
<i>Specific Heat Capacity (1 atm, 273 K)</i>	1.8495	<i>kJ/kg – K</i>

7.3. Propellant Selection for Analysis

As the requirements describe in Table 7.1, preferably a hypergolic storable fuel has to be selected that will operate in a bi-propellant propulsion system together with hydrogen peroxide. This section will discuss possible green storable fuels that combined with hydrogen peroxide will be tested on their performance. First their classification by the European Union's GRASP project will be discussed. Next, a brief summary of the chemical and physical characteristics of the propellants will be described.

7.3.1. Green Storable Propellant Classification

The European Union set up a consortium to find and investigate alternative propellants to the present highly toxic propellants in use. This project is called GReen Advanced Space Propulsion (GRASP). The GRASP consortium aims to identify possible alternatives to toxic (storable) propellants. This was deemed necessary to introduce better protection of the human operators and environment and to reduce the increasing cost of storage and handling of these toxic propellants. Apart from this, the GRASP team pointed showed that a large batch of these toxic propellants may become restricted or exceedingly expensive in the future due to their limitations in handling [121]. A variety of industries and research groups have been, and are currently, working on the development of novel green propellants. However, the GRASP consortium concluded that these industries and space agencies were reluctant in their efforts to share their advances with the academic and scientific community [121]. It was concluded that this contributes to the lack of information, biased information and significant delays.

GRASP put together 100 green propellant candidates that were investigated on their performance, compatibility, availability, stability and handling characteristics. The GRASP project concluded that the implementation of novel green propellants can “*significantly reduce associated handling cost, improve performance, ensure the competitiveness of the European industry and reduce human exposure to toxic and/or carcinogenic substances*” [121]. Furthermore, GRASP pointed out that the large upfront cost associated with the implementation of novel green propellants might become subservient to the total cost reduction in the long term. To summarise, the GRASP consortium considers the following potential advantages of using green storable propellants [121]:

- Similar or better performance than those propellants used currently
- System advantages
- Detailed investigation of the storage and handling properties

- Compatibility with existing hardware
- Likelihood of reduced costs in the long-term

The GRASP team assembled a large sample set of possible candidates to substitute, in the near future, toxic, carcinogenic and corrosive propellants such as hydrazine. This selection was done based on theoretical and experimental efforts [121]. In Table 7.7 the selected propellants that can be considered green alternative solutions for the future are tabulated.

Table 7.7: Possible Green Propellants that have been Investigated by Project GRASP [122]

Aniline	Heptane	Hydrogen peroxide
3-3'-Diaminopropylamine	Propyne	1,5-Hexadiyne
Ethylammonium nitrate	Triethylamine	Ionic liquids (ADN, HAN, HNF)
Ethylenoxide	Diethylenetriamine	Iso-octane
Ethyl nitrate	1,3-Diaminopropane	Isopropyl alcohol
Furfuryl alcohol	1,2-Diaminocyclohexane	Kerosene (Jet A-1, JP-4, JP-5, RP-1)
Monomethylamine	Ethane	Methane
Tetranitromethane	Cyclopropane	Methanol
Trimethylaluminium	Ethyl methyl ether	Methylammonium nitrate
2,4-Xylidine	Dibutyl ether	Nitrous oxide
Polynitrogens (e.g. N ₃)	Propadiene	N-propyl nitrate
2,5-Dimethyltetrazole	Ethanolamine	Octane
Allyl-dipropenylamine	Acetaldehyde	Oxygen (LOX)
JP-1	Ammonia	Pentane
JP-3	Ammonium nitrate	PMMA
RJ-5	Butane	Polyethylene
AFRL4	Diethylene glycol dimethyl ether	Propane
Tri-prop-2-ynyl-amine	Dimethylether	Propyl amine
Bicyclopropylidene	d-Limonene	Propyl ether
3-Prop-2-ynyloxy-propyne	DMAZ (and CINCH)	Propylene
Tris(azidomethyl)amine	Dimethylamine	Silanes
C-stoff	Ethanol	Tetrahydrofuran
Mixed oxides of nitrogen	Ethylene	Tetramethylethylenediamine
Nitromethane	Ethylenediamine	Toluene
Nitroglycerine	HTPB	Triethylaluminium
Propane	JP-10	Turpentine

7.3.2. Hydrocarbon Fuel Options

Some of these propellant options showed to be a promising candidates for combustion with hydrogen peroxide in experiments described in the preceding literature study [16]. These candidates have been tested on ignition delay times (IDT), hypergolic reactivity with hydrogen peroxide and storability by [28], [34], [35], [37].

In this section these promising fuels will be characterised by looking at their chemical and physical properties. But first, some information about the novel storable oxidiser; concentrated hydrogen peroxide will be given.

Hydrogen Peroxide

The designated oxidiser for the bi-propellant propulsion system of the "Prototype X" upper stage design is hydrogen peroxide. In section 3.1 this oxidiser is already discussed in detail. In Table 7.8 the chemical characteristics of the hydrogen peroxide are provided. These characteristics are very important for the propellant analysis. Different concentrations of hydrogen peroxide solution result in a wide variety of applications. From an oxidiser, bleaching agent to a propellant solution in rockets.

Table 7.8: Chemical Characteristics Hydrogen Peroxide [120]

Hydrogen Peroxide (100%)	Value	Unit
<i>Molecular Formula</i>	H ₂ O ₂	-
<i>Molecular Weight</i>	34.015	<i>g/mole</i>
<i>Boiling Point (1 atm)</i>	423.3	<i>K</i>
<i>Freezing Point (1 atm)</i>	272.72	<i>K</i>
<i>Density Liquid (1 atm)</i>	1442	<i>kg/m³</i>
<i>Heat of formation</i>	-187.80	<i>kJ/mole</i>
<i>Specific Heat Capacity (1 atm, 273 K)</i>	2.619	<i>kJ/kg – K</i>

Ethanol

Ethanol, also known as alcohol, is a hydrocarbon fuel that is very volatile and flammable. The liquid is colourless and can be obtained from a wide variety of production processes. For example, it can be produced from the fermentation of sugars, and yeast or it can be produced by ethylene hydration. A process often part of petrochemical industries. Ethanol is possible to dilute into different concentrations with water. The different concentrations will yield different application possibilities. In the light of this research ethanol will be considered a fuel that is not diluted, hence is at a concentration level of 100%. Ethanol has a very wide range of temperatures when it is in its liquid phase (159 – 351 K).

Table 7.9: Chemical Characteristics Ethanol [120]

Ethanol (100%)	Value	Unit
<i>Molecular Formula</i>	C ₂ H ₅ OH	-
<i>Molecular Weight</i>	46.068	<i>g/mole</i>
<i>Boiling Point (1 atm)</i>	351.5	<i>K</i>
<i>Freezing Point (1 atm)</i>	159.0	<i>K</i>
<i>Density Liquid (1 atm)</i>	789.29	<i>kg/m³</i>
<i>Heat of formation</i>	-276.9	<i>kJ/mole</i>
<i>Specific Heat Capacity (1 atm, 273 K)</i>	2.267	<i>kJ/kg – K</i>

DMAZ

DMAZ is novel fuel that is currently under development and under investigation to be used as a space-craft propellant. DMAZ, 2-dimethylaminoethylazide in full, has proven to be a very powerful and efficient fuel to be used in bi-propellant engines. DMAZ is a member of the Competitive Impulse Non-Carcinogenic Hypergol (CINCH) family. This makes it a candidate to replace the toxic, carcinogenic and corrosive hydrazine-based fuels that were used in the past while having a relatively good performance [123], [124]. Since DMAZ is currently under development by the Aviation and Missile Research Development, and Engineering Center (AMRDEC) and the NASA the fuel is relatively scarce in availability. It is expected however that the price will drop significantly when this fuel has been proven relevant in the aerospace industry [123]. The chemical characteristics of DMAZ are presented in Table 7.10.

Table 7.10: Chemical Characteristics DMAZ [123]

2-dimethylaminoethylazide (DMAZ)	Value	Unit
<i>Molecular Formula</i>	C ₄ H ₁₀ N ₄	-
<i>Molecular Weight</i>	114.152	<i>g/mole</i>
<i>Boiling Point (1 atm)</i>	408	<i>K</i>
<i>Freezing Point (1 atm)</i>	204.2	<i>K</i>
<i>Density Liquid (1 atm)</i>	993.0	<i>kg/m³</i>
<i>Heat of formation</i>	319.0	<i>kJ/mole</i>
<i>Specific Heat Capacity (1 atm, 273 K)</i>	1.150	<i>kJ/kg – K</i>

MEA

MEA or Ethanolamine is a combination of an ethanol/alcohol-group and an amino-group. Experimental research by Jyoti et al. shows that (gelled) ethanolamine fuel presents good hypergolicity with hydrogen peroxide and ignition delay times between 1 and 5 ms [125]. Ethanolamine has its freezing point at 283.4 K or at around 10.3 °C. This means that some thermal management is required to keep the

ethanolamine fuel from freezing during transport, storage and handling. Especially in space operations makes it hard to keep the ethanolamine in a liquid form. The density of the fuel is comparable to water and it has a relatively high heat of formation [125].

Table 7.11: Chemical Characteristics MEA [120], [125]

Ethanolamine (MEA)	Value	Unit
<i>Molecular Formula</i>	C_2H_7NO	-
<i>Molecular Weight</i>	61.084	<i>g/mole</i>
<i>Boiling Point (1 atm)</i>	443	<i>K</i>
<i>Freezing Point (1 atm)</i>	283.4	<i>K</i>
<i>Density Liquid (1 atm)</i>	1012.0	<i>kg/m³</i>
<i>Heat of formation</i>	-507.5	<i>kJ/mole</i>
<i>Specific Heat Capacity (1 atm, 273 K)</i>	2.080	<i>kJ/kg – K</i>

DETA

DETA or Diethylenetriamine is a colourless liquid that is easily soluble in water. DETA is found to be a by-product of the production of ethylenediamine and ethylene dichloride. Diethylenetriamine is in its liquid form for a wide range of temperatures (234 – 477 K) and has a relatively high density compared to other fuels discussed in this section. DETA was used in the past in a mixture with unsymmetrical dimethylhydrazine (UDMH) to produce 'Hydyne' fuel. This was used by Rocketdyne in bipropellant rockets. It was found by Kang et al. that the diethylenetriamine reacts hypergolically with hydrogen peroxide. However, a mixture with sodium borohydrides was suggested (Stock 3) to increase this hypergolic ignition and to improve the ignition delay times [10]. Furthermore, it was proven that this Stock 3 mixture was storable for four months during a lab-scale storability test [10]. The density specific impulse of the stock3/HTP combination suggested distinct advantages that can be used in upper stage designs.

Table 7.12: Chemical Characteristics DETA [10], [120]

Diethylenetriamine (DETA)	Value	Unit
<i>Molecular Formula</i>	$C_4H_{13}N_3$	-
<i>Molecular Weight</i>	103.169	<i>g/mole</i>
<i>Boiling Point (1 atm)</i>	477.2	<i>K</i>
<i>Freezing Point (1 atm)</i>	234.15	<i>K</i>
<i>Density Liquid (1 atm)</i>	955	<i>kg/m³</i>
<i>Heat of formation</i>	-65.7	<i>kJ/mole</i>
<i>Specific Heat Capacity (1 atm, 273 K)</i>	2.721	<i>kJ/kg – K</i>

Pyridine

Historically Pyridine was produced from coal tar. Currently, the colourless liquid is produced in large quantities (up to 20,000 tons per year) through synthesis [126]. Pyridine is structurally related to benzene and is highly flammable. The temperature range at which Pyridine is considered liquid lies between 232 – 388 K.

Table 7.13: Chemical Characteristics Pyridine [120], [126]

Pyridine	Value	Unit
<i>Molecular Formula</i>	C_5H_5N	-
<i>Molecular Weight</i>	79.102	<i>g/mole</i>
<i>Boiling Point (1 atm)</i>	388.3	<i>K</i>
<i>Freezing Point (1 atm)</i>	231.6	<i>K</i>
<i>Density Liquid (1 atm)</i>	982	<i>kg/m³</i>
<i>Heat of formation</i>	100.2	<i>kJ/mole</i>
<i>Specific Heat Capacity (1 atm, 273 K)</i>	2.445	<i>kJ/kg – K</i>

Isooctane

Isooctane, chemically 2,2,4-trimethylpentane, is a hydrocarbon fuel with isomers of octane. Looking at Table 7.14, Isooctane maintains liquid under a wide range of temperatures. It has a relatively high heat of formation and a relatively low density (690 kg/m^3). Like Pyridine, Isooctane is produced in large volumes by the petroleum industry. Isooctane is formed under the alkylation of isobutene with isobutane [127]. In previous research, isooctane showed that it could obtain high specific impulse properties with hydrogen peroxide [9]. Due to the relatively low density and high specific impulse characteristics of isooctane comparative research showed that this fuel in combination with highly concentrated hydrogen peroxide (HTP) can result in mass and cost savings for small propulsion systems [128].

Table 7.14: Chemical Characteristics Isooctane [9], [120], [127]

Isooctane	Value	Unit
<i>Molecular Formula</i>	C_8H_{18}	-
<i>Molecular Weight</i>	114.23	<i>g/mole</i>
<i>Boiling Point (1 atm)</i>	372.45	<i>K</i>
<i>Freezing Point (1 atm)</i>	165.77	<i>K</i>
<i>Density Liquid (1 atm)</i>	690	<i>kg/m³</i>
<i>Heat of formation</i>	-259.3	<i>kJ/mole</i>
<i>Specific Heat Capacity (1 atm, 273 K)</i>	2.122	<i>kJ/kg – K</i>

Dimethylamine

Dimethylamine is a colourless hydrocarbon liquid that often is available in a solution of water. It consists of an amine-group that gives dimethylamine its distinctive ammonia-like odour. Dimethylamine is a base product from which unsymmetrical dimethylhydrazine (UDMH) is produced. The fuel is produced in bulk for various applications. An estimated 300,000 tons is produced worldwide annually [129]. Dimethylamine has a relative low boiling point. At around $9\text{ }^\circ\text{C}$ the fuel starts to boil and transform to its gaseous form. The density is relatively low at around 670 kg/m^3 .

Table 7.15: Chemical Characteristics Dimethylamine [120], [129]

Dimethylamine	Value	Unit
<i>Molecular Formula</i>	$(\text{CH}_3)_2\text{NH}$	-
<i>Molecular Weight</i>	45.085	<i>g/mole</i>
<i>Boiling Point (1 atm)</i>	282	<i>K</i>
<i>Freezing Point (1 atm)</i>	180.15	<i>K</i>
<i>Density Liquid (1 atm)</i>	670	<i>kg/m³</i>
<i>Heat of formation</i>	-19.0	<i>kJ/mole</i>
<i>Specific Heat Capacity (1 atm, 273 K)</i>	3.033	<i>kJ/kg – K</i>

Methanol

Methanol consists of a methyl structure that contains an alcohol group. Methanol is a very light volatile molecule that has a wide variety of use cases. 20 million tons of Methanol is produced annually [130]. Although methanol is listed as a toxic constituent for consumer food and drugs it is considered 'green' by the European Union' GRASP project. Methanol has a relatively low density at 792 kg.m^3 and a wide range of temperatures at which the methanol is in its liquid phase. The heat of formation is relatively high at 238.91 KJ/mole .

Table 7.16: Chemical Characteristics Methanol [120]

Methanol	Value	Unit
<i>Molecular Formula</i>	CH_3OH	-
<i>Molecular Weight</i>	32.04	<i>g/mole</i>
<i>Boiling Point (1 atm)</i>	337.8	<i>K</i>
<i>Freezing Point (1 atm)</i>	175.6	<i>K</i>
<i>Density Liquid (1 atm)</i>	792	<i>kg/m³</i>
<i>Heat of formation</i>	238.91	<i>kJ/mole</i>
<i>Specific Heat Capacity (1 atm, 273 K)</i>	2.530	<i>kJ/kg – K</i>

Isopropyl Alcohol

Isopropyl alcohol is a colourless very flammable liquid that consists of an isopropyl group that is connected to a hydroxyl group. Isopropyl alcohol is used in a lot of different industrial and household chemicals. The fuel is produced by combining water and propene in a hydration reaction or by hydro-generation of acetone [131]. Isopropyl alcohol is produced in large quantities of millions of tons per year in this process. Isopropyl alcohol has a large liquid temperature range and a relatively low density.

Table 7.17: Chemical Characteristics Isopropyl Alcohol [120], [131]

Isopropyl Alcohol	Value	Unit
<i>Molecular Formula</i>	C_3H_8O	-
<i>Molecular Weight</i>	60.096	<i>g/mole</i>
<i>Boiling Point (1 atm)</i>	355.8	<i>K</i>
<i>Freezing Point (1 atm)</i>	184	<i>K</i>
<i>Density Liquid (1 atm)</i>	786	<i>kg/m³</i>
<i>Heat of formation</i>	-318.7	<i>kJ/mole</i>
<i>Specific Heat Capacity (1 atm, 273 K)</i>	1.54	<i>kJ/kg – K</i>

Isoamyl Alcohol

Another alcohol fuel species that is investigated for the propellant analysis is the isoamyl alcohol fuel. This is an isomer of pentanol with an amyl-group. Isoamyl alcohol is produced by ethanol fermentation. The use of isoamyl alcohol in rocketry is a recent development [131]. The fuel has a wide area of temperatures at which the fuel is liquid. The density is comparable with RP-1 and kerosene. The heat of formation is relatively high.

Table 7.18: Chemical Characteristics Isoamyl Alcohol [120], [131]

Isoamyl Alcohol	Value	Unit
<i>Molecular Formula</i>	$C_5H_{12}O$	-
<i>Molecular Weight</i>	88.148	<i>g/mole</i>
<i>Boiling Point (1 atm)</i>	404.2	<i>K</i>
<i>Freezing Point (1 atm)</i>	156	<i>K</i>
<i>Density Liquid (1 atm)</i>	810	<i>kg/m³</i>
<i>Heat of formation</i>	-356.4	<i>kJ/mole</i>
<i>Specific Heat Capacity (1 atm, 273 K)</i>	2.382	<i>kJ/kg – K</i>

Triglyme

Triglyme, or triethylene glycol dimethyl ether, is hypergolic with hydrogen peroxide. Triglyme was analysed by Kapusta et al. to investigate the effect of pressure and temperature on hypergolic ignition delay time [132]. It was found that it can become more reactive with HTP by the addition of sodium borohydrides into the triglyme fuel. Triglyme is relatively dense compared to other discussed fuels. The temperature is very useful for storable propellant systems as the temperature range is quite lenient.

Table 7.19: Chemical Characteristics Triglyme [120], [132]

Triglyme	Value	Unit
<i>Molecular Formula</i>	$C_8H_{18}O_4$	-
<i>Molecular Weight</i>	178.228	<i>g/mole</i>
<i>Boiling Point (1 atm)</i>	489	<i>K</i>
<i>Freezing Point (1 atm)</i>	228	<i>K</i>
<i>Density Liquid (1 atm)</i>	986	<i>kg/m³</i>
<i>Heat of formation</i>	379.560	<i>kJ/mole</i>
<i>Specific Heat Capacity (1 atm, 273 K)</i>	2.564	<i>kJ/kg – K</i>

7.4. Criteria Selection

The fuels mentioned in the previous section were identified as possible options for bipropellant combustion with hydrogen peroxide by the experiments and analysis described in the preceding literature

review [16]. This preliminary selection was primarily made on the chemical and physical properties and characteristics. During this selection special care was given to chemical characteristics such as reactivity with hydrogen peroxide, hypergolicity and stability. Furthermore, the fuels have been selected on their physical characteristics such as state change temperatures, specific heat, density and storability.

To do the trade-off analysis it is important to identify the best fuel options from the ones described above. To identify the best fuel options to be considered 'promising' for further research into the storable upper stage concepts, it is important to define criteria. These criteria will help to point out the advantages or disadvantages of the individual fuels with respect to the design goal. The selection criteria for the fuel will be based on the works of O.Frota, B. Mellor and M. Ford as described in their research paper "*Proposed Selection Criteria for Next Generation Liquid Propellants*" [8].

The following selection criteria have been chosen:

- **CR-1: Cost and Availability**

Due to the commercialisation and privatisation of space flight, cost are becoming increasingly important. In case of propellants the cost is determined by the cost of production, handling, transportation and storage. Cost and availability are important criteria that are dependent on each other. The availability and demand for a certain fuel will influence its cost. The availability is not only dependent on raw material but also on regulations and facilities that suppliers have "in-house". Furthermore, patents and licenses can influence the availability and cost of fuels. Since a lot of the fuels discussed are still under development or are in their early stage of production it is not always possible to accurately rate the current and future availability. Lastly, the cost of the fuels is greatly dependent on the handling and transportation hazards involved. In this case, the 'green' propellants discussed in this research thesis experience great advantages over conventional fuels. The reason why the European Union considers these fuels as 'green' under the GRASP project is because they are non-toxic, non-carcinogenic and not corrosive. This results in safer, easier and cheaper handling, storage and transportation. The ground support equipment and decontamination procedures can be simpler [8].

- **CR-2: Performance**

Performance of the propellants has always been an important criterion. The propellants that got selected as potential fuel options did have good performance characteristics in the first place. The main performance parameters of interest are; specific impulse and density specific impulse (the specific impulse multiplied with the density). Specific impulse describes the combustion efficiency and the density specific impulse describes the volumetric efficiency of the fuel respectively. It is argued by O. Frota et al. that any decrease in performance of these novel fuels can be overcome due to the "savings in other aspect such as infrastructure, health and safety requirements and operational procedures" that come to play when implementing these propellants into existing systems and ground facilities [8].

- **CR-3: Handling and Storage**

Potential risks that come to play when working with rocket propellants, such as explosions, fire and toxic contact, have to be minimised as much as possible. It is important to note, as discussed earlier for methanol, "non-toxic" refers to being 'less' toxic than the conventional hydrazine fuel options. The level of ease at which the fuels can be handled, stored and possibly off-loaded will rely on their relative toxicity and other characteristic hazards/risks. Furthermore, sufficient storability, in terms of time and temperature, is required for the fuels as this is often required during pre-launch operations and oceanic transportation.

- **CR-4: Materials Compatibility**

Since the fuels are inherently reactive, it is important to investigate and validate the material compatibility of the fuels. The rocket fuel will be transported, handled and stored by hoses, pipes, valves, tanks etc. manufactured with a variety of different materials. It is important to investigate the impact of the materials on the fuel and vice versa. This criterion is very important as it helps to prevent or early detect contamination or decomposition of the fuel, or corrosion/deterioration of the materials. Typical material types that will be in contact with the hydrogen peroxide have been identified in the preceding literature review [16].

- **CR-5: Impact on Existing Hardware**

To limit the added cost of implementing 'green' propellants into space systems it is beneficial to reduce the impact on existing hardware, being the launch vehicle systems and subsystems. By using existing tanks and propulsion systems the system complexity, time and cost are minimised. This criterion is therefore very useful to test the viability of the application of these fuels. It can be expressed by the dry and wet mass impact on the upper stage design concepts. Also, hypergolicity will introduce more reliability into the system and thus is a good measure of the impact on the existing hardware.

For the trade-off analysis, it is important to use these criteria to weigh the fuel options relative to each other. Before it is possible to score the fuel options on these criteria it is important to understand the relative importance of each criterion. This means that the criteria also need to be weighted with respect to each other. This is done using the Analytical Hierarchy Process (AHP) Trade-Off tool. This tool helps to analytically approach the trade-off process. First the relative score per criteria for each fuel option will be assessed by experts in the field. This (subjective) assessment is then the input for a mathematical model that will describe the relation between the characteristics of the options, the importance of the characteristics and the relative performance of the options. Furthermore, it performs consistency analysis to make sure the calculated scores per criterion are reliable.

To do this, the AHP tool constructed by Dutch Space B.V. will be used. This tool was constructed to find objective scores for criteria in trade-off analyses [133]. This tool can also be used to quantify the trade-off between the relative fuel options in a later phase of the trade-off analysis. The tool will first construct an analytical hierarchy that will form the basis for a pair-wise comparison analysis. In this pair-wise comparison a distinction is made between subjective and actual relative performance [133].

In Table 7.20 the subjective scoring system is described. This scoring system will help to do pair-wise analysis. The intensity score will be added to each pair-wise comparison between two criteria. This will then be the input for the AHP tool.

Table 7.20: Scoring System used in the AHP Tool to assess relative expert weights [133]

Intensity	Definition	Explanation
1	Equal	<i>Two items contribute equally to the objective</i>
3	Moderate	<i>Experience and judgement slightly favour one item over another</i>
5	Strong	<i>Experience and judgement strongly favour one item over another</i>
7	Very Strong	<i>An item is strongly favoured and its dominance demonstrated in practice</i>
9	Extreme	<i>The evidence favouring one activity over another is of the highest possible order of affirmation</i>
2,4,6,8	Intermediate Values	<i>When compromise is needed</i>

The combined assessment of multiple experts in the AHP analysis resulted in the relative weight distribution for the criteria described in Table 7.21.

Table 7.21: The AHP Relative Expert Weights per Criterion

ID	Criteria	Weight [-]
CR-1	<i>Cost and Availability</i>	0.203
CR-2	<i>Performance</i>	0.311
CR-3	<i>Handling and Storage</i>	0.151
CR-4	<i>Materials Compatibility</i>	0.130
CR-5	<i>Impact on Existing Hardware</i>	0.205

In Figure 7.1 the relative weight difference between the criteria is depicted. The average consistency ratio of the analysis was found to be 0.0675 and the Mean Absolute Error (MAE) is rated to be 0.0314. This MAE is added to the individual weights by means of error bars.

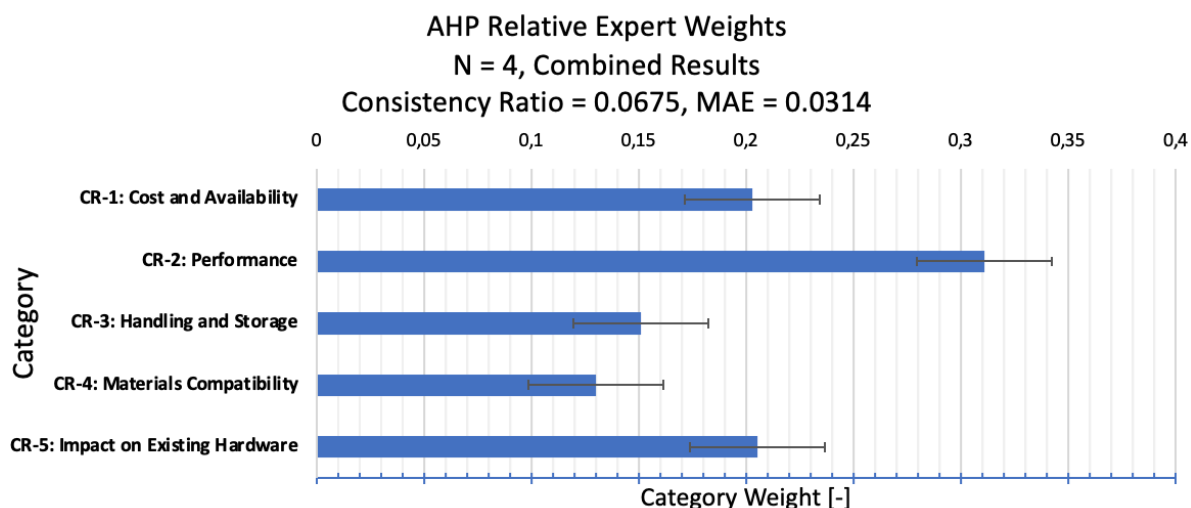


Figure 7.1: Relative Weight of Criteria, based on Combined AHP Relative Expert Analysis

7.5. Propellant Combustion Analysis

In order to weigh the presented fuel options on the criteria it is necessary to gather more information on the performance of the presented fuel options with concentrated hydrogen peroxide. In this section the individual performance characteristics of these propellant options will be discussed, through the use of a combustion analysis tool. The tool that is used to do this combustion analysis is RPA Lite and has been described in the set-up of the performance model. During this analysis the combustion chamber pressure was fixed at 6 MPa for all propellant combinations. This is the normal operating combustion chamber pressure for the VINCI engine that is part of the Ariane 6 upper stage design. Furthermore, the nozzle flow was simulated assuming a fixed expansion area ratio of 240 ($P_c = 6\text{ MPa}$, $A_e/A_t = 240$). These settings were used throughout the combustion analysis to simulate the combustion of the propellant combinations under the conventional VINCI engine settings. The combustion analysis calculates the thermodynamic properties of the combustion between the fuel and oxidiser in a pre-selected combustion pressure and expansion ratio. The analysis calculates the type of combustion products and their respective mass fractions. To do this, the thermodynamic database and calculation methods of the NASA CEA tool are used. These "ideal" combustion calculation results will then be adjusted by RPA lite to correct for the nozzle efficiency and combustion quality. These quality factors are modelled by the RPA tool itself. Based on the calculated value of divergence thrust loss as well as the friction thrust loss, the nozzle and combustion efficiency are approximated. This value will then be compared to a database of tabulated combustion and nozzle efficiencies (for various combustion chamber pressures) to verify and/or adjust these values [95], [96]. The nozzle and combustion quality factors help to better estimate the expected performance of the propellant combinations during actual operation in an engine. Therefore, a better trade-off and mass/cost estimate can be made for the fuel types. The combustion analysis of the various propellant combinations is discussed in Table 7.22.

In Table 7.22 the cryogenic and semi-cryogenic propellant combinations are highlighted in grey. These can be considered to be the conventional propellant combinations and are presented to allow for comparison with the novel storable fuel options. Also the effect of the addition of metal hydrides was investigated. To various (suitable) fuel options a concentration of sodium borohydride was added to investigate the impact on specific impulse, density and ignition delay time (IDT). The percentage of added sodium borohydride to the fuel mix is determined based on literature [16]. In these studies, the best mixture ratio of metal hydrides was determined based on criteria such as storability, specific impulse and ignition delay times. The percentage of added sodium borohydride is tabulated in Table 7.22.

The fuel and oxidiser combinations are specified by their name and chemical formula. The respective concentration for ethanol and hydrogen peroxide is described in the parentheses. Based on nested-analysis with the RPA tool the optimum oxidiser-to-fuel (O/F) ratio was determined, under the

Table 7.22: Combustion Analysis of Selected Propellant Combinations - $P_c = 6 \text{ MPa}$, $A_e/A_t = 240$

Type	Propellant Combination	Oxidizer	Fuel	Density Fuel (20°C) [kg/m ³]	Optimum O/F [-]	Isp [s] (vac)	Impulse Density [Kg-s/m ³]
Cryogenic	LO2/LH2	LO2	LH2	71.0	5.40	463.53	32910.63
Semi-Cryogenic	LO2/RP-1	LO2	CnH1.953n	810.0	3.00	369.96	299667.60
Semi-Cryogenic	LO2/T-1 (kerosene)	LO2	C12H26	806.0	3.00	369.37	297712.22
Storable (green)	H2O2/Ethanol	H2O2 (100%)	C2H5OH (100%)	789.0	4.40	328.13	258893.78
Storable (green)	H2O2/Ethanol + 2% NaBH4	H2O2 (100%)	C2H5OH (100%)	794.7	4.40	328.25	260862.26
Storable (green)	H2O2/Ethanol + 5% NaBH4	H2O2 (100%)	C2H5OH (100%)	803.3	4.40	328.22	263643.91
Storable (green)	H2O2/Ethanol + 10% NaBH4	H2O2 (100%)	C2H5OH (100%)	817.5	4.30	328.47	268524.23
Storable (green)	H2O2/Ethanol + 20% NaBH4	H2O2 (100%)	C2H5OH (100%)	846.0	4.20	328.57	277972.25
Storable (green)	H2O2/DMAZ	H2O2 (100%)	C4H10N4	993.0	3.40	341.06	338672.58
Storable (green)	H2O2/DMAZ + 10% NaBH4	H2O2 (100%)	C4H10N4	1001.1	3.40	339.93	340301.12
Storable (green)	H2O2/MEA	H2O2 (100%)	C2H7NO	1012.0	3.60	305.70	309372.85
Storable (green)	H2O2/MEA + 5% NaBH4	H2O2 (100%)	C2H7NO	1018.9	3.60	307.79	313609.07
Storable (green)	H2O2/MEA + 10% NaBH4	H2O2 (100%)	C2H7NO	1021.8	3.60	309.73	316484.36
Storable (green)	H2O2/MEA + 20% NaBH4	H2O2 (100%)	C2H7NO	1024.4	3.60	313.00	320634.23
Storable (green)	H2O2/DETA	H2O2 (100%)	C4H13N3	955.0	4.70	326.00	311287.88
Storable (green)	H2O2/DETA + 5% NaBH4	H2O2 (100%)	C4H13N3	961.0	4.70	334.60	321540.60
Storable (green)	H2O2/DETA + 10% NaBH4	H2O2 (100%)	C4H13N3	966.9	4.60	334.39	323321.50
Storable (green)	H2O2/Pyridine	H2O2 (100%)	C5H5N	982.0	5.30	333.66	327652.84
Storable (green)	H2O2/Pyridine + 8% NaBH4	H2O2 (100%)	C5H5N	989.4	5.20	333.12	329578.47
Storable (green)	H2O2/Isooctane	H2O2 (100%)	C8H18	690.0	7.20	336.31	232056.45
Storable (green)	H2O2/Isooctane + 10% NaBH4	H2O2 (100%)	C8H19	728.4	7.00	336.15	244851.00
Storable (green)	H2O2/Dimethylamine	H2O2 (100%)	C2H7N	670.0	5.60	340.18	227922.74
Storable (green)	H2O2/T-1 (kerosene)	H2O2 (100%)	C12H26-C15H32	806.0	7.20	335.53	270437.18
Storable (green)	H2O2/RP-1	H2O2 (100%)	C10H12N5O5PS	810.0	7.20	335.98	272141.13
Storable (green)	H2O2/Methanol	H2O2 (100%)	CH3OH	792.0	3.20	322.73	255604.77
Storable (green)	H2O2/Isopropyl Alcohol	H2O2 (100%)	C3H8O	786.0	5.10	329.80	259228.62
Storable (green)	H2O2/Isoamyl Alcohol	H2O2 (100%)	C5H12O	810.0	5.70	332.68	269468.30
Storable (green)	H2O2/Triglyme	H2O2 (100%)	C8H18O4	986.0	4.00	338.96	334214.56
Storable (green)	H2O2/Triglyme + 7% NaBH4	H2O2 (100%)	C8H18O4	992.2	3.90	338.02	335376.97

fixed combustion conditions as described above. From this optimum O/F ratio the vacuum specific impulse was obtained. The density specific impulse is determined by multiplying the specific impulse with the density of the fuel.

From the results of the combustion analysis it is found that the average specific impulse (329.81 seconds) of the green storable propellant combinations is approximately 29% less than the conventional hydrolox combination (463.53 seconds) and $\approx 11\%$ less than the semi-cryogenic combinations. The optimum O/F ratios that were found do vary between 3.4 – 7.2. Furthermore, the density specific impulse measures the specific impulse per volume. Denser propellants pack more propellant per volume. In essence, the density specific impulse is a measure of specific impulse per volume. In Table 7.22 it is found that the conventional fuel liquid hydrogen produces an density specific impulse of around $\approx 33000 \text{ Kg} \cdot \text{s}/\text{m}^3$. This is the lowest density specific impulse of all combinations analysed. The reason for this is the very low density of liquid hydrogen. The best storable propellant option that was identified by the combustion analysis is the combination of concentrated hydrogen peroxide and DMAZ (2-dimethylaminoethylazide). This combination obtained the highest specific impulse (341 seconds) and density specific impulse (340000 $\text{Kg} \cdot \text{s}/\text{m}^3$). Other options, such as dimethylamine, T-1, RP-1, triglyme and DETA are promising fuel options too.

At first glance, the added sodium borohydride does not necessarily result (on average) in a higher specific impulse. The density of the fuel mix, however, does increase and the O/F ratio reduces for higher concentrations of sodium borohydride. Also, the density specific impulse increases due to these higher densities. Although, it has been proven in literature [33], [45] that the ignition delay time reduces when the metal hydrides are added the effect of the changed density, specific impulse, O/F ratio and density specific impulse on the dry and wet system mass of the upper stage is not yet clear. To investigate the effect of these propellant combinations on the dry and wet mass of the “Prototype X” the found combustion characteristics, described in Table 7.22, will be used to run the mass model. The mass model allows to calculate the required propellant mass and the resulting system dry mass of the upper stage module, as discussed in chapter 5. Based on the Delta-V requirement, density, specific impulse and O/F ratio this mass analysis can be performed for all the propellant options described in Table 7.22. The result of this mass analysis is depicted in the figures below.

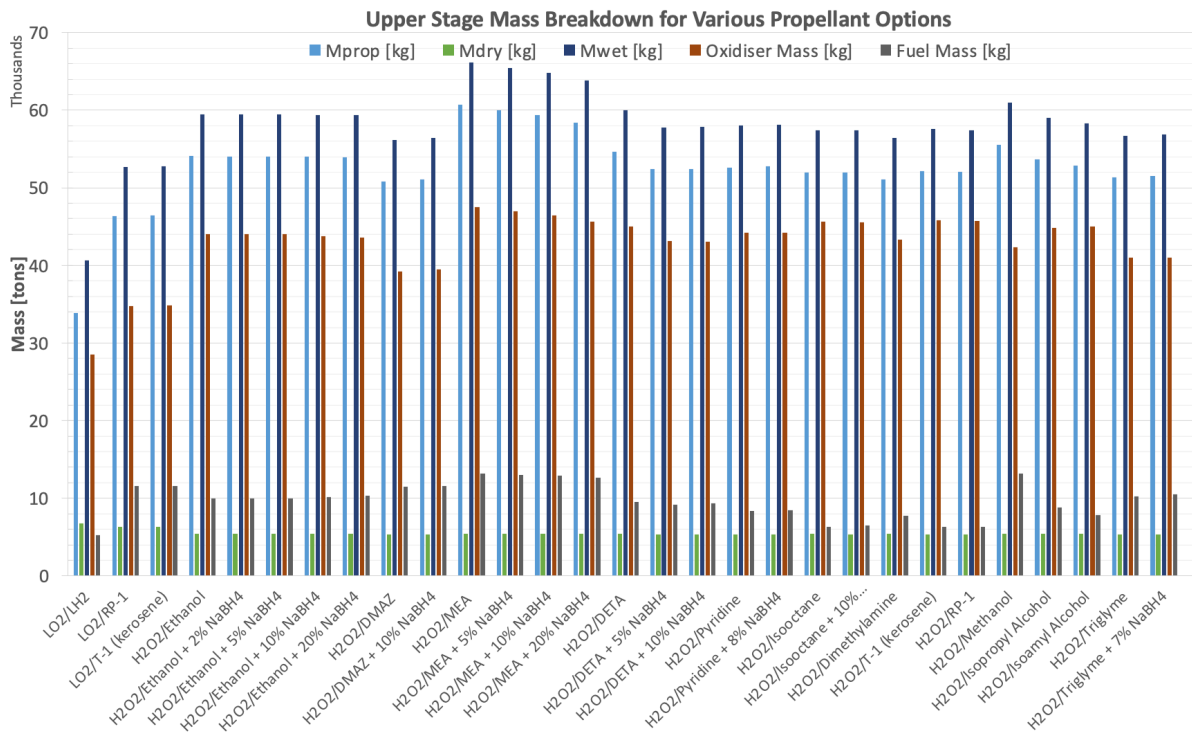


Figure 7.2: "Prototype X" Upper Stage Mass Breakdown per Propellant Combination

In Figure 7.2 the mass breakdown for the Prototype X upper stage per propellant combination is described. The conventional cryogenic and semi-cryogenic propellant combinations are also present in the graph and are there for reference. The propellant mass, dry mass, wet mass, oxidiser mass and fuel mass are represented in the figure per propellant combination. From Figure 7.2 it can be concluded that the oxidiser mass constitutes to the greatest extent to the propellant mass. Furthermore, it can be seen that the propellant mass on average is an order of magnitude larger than the dry mass of the upper stage module. Figure 7.3 and Figure 7.5 make the change in dry and wet mass more insightful.

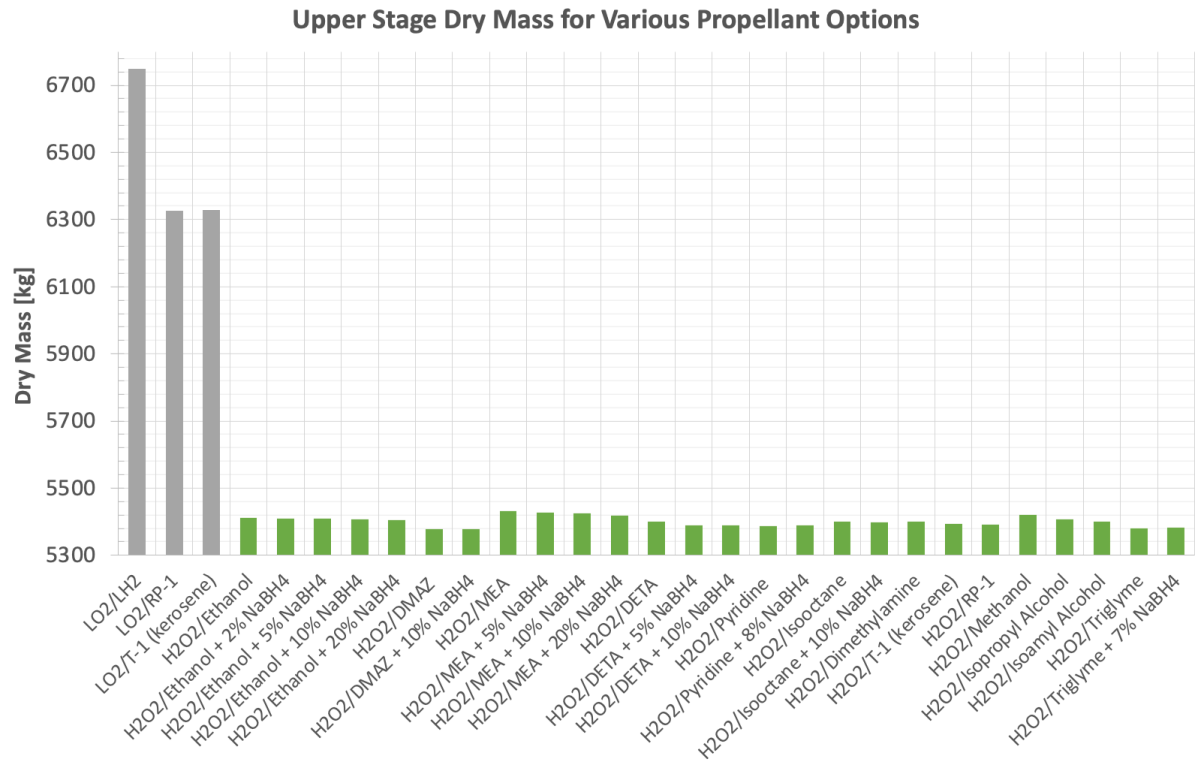


Figure 7.3: "Prototype X" Upper Stage Dry Mass per Propellant Combination

From Figure 7.3 it is clear that the dry mass of the conventional cryogenic and semi-cryogenic upper stages on average are more than 1000 kg heavier than the "Prototype X" concepts. The larger dry mass of the conventional cryogenic upper stage can be explained by the density specific impulse. The average propellant density of liquid oxygen and liquid hydrogen is far less than for the storable propellants. This results in a larger required tank volume, thus heavier storage systems. This difference in tank volume is graphically illustrated in Figure 7.4.

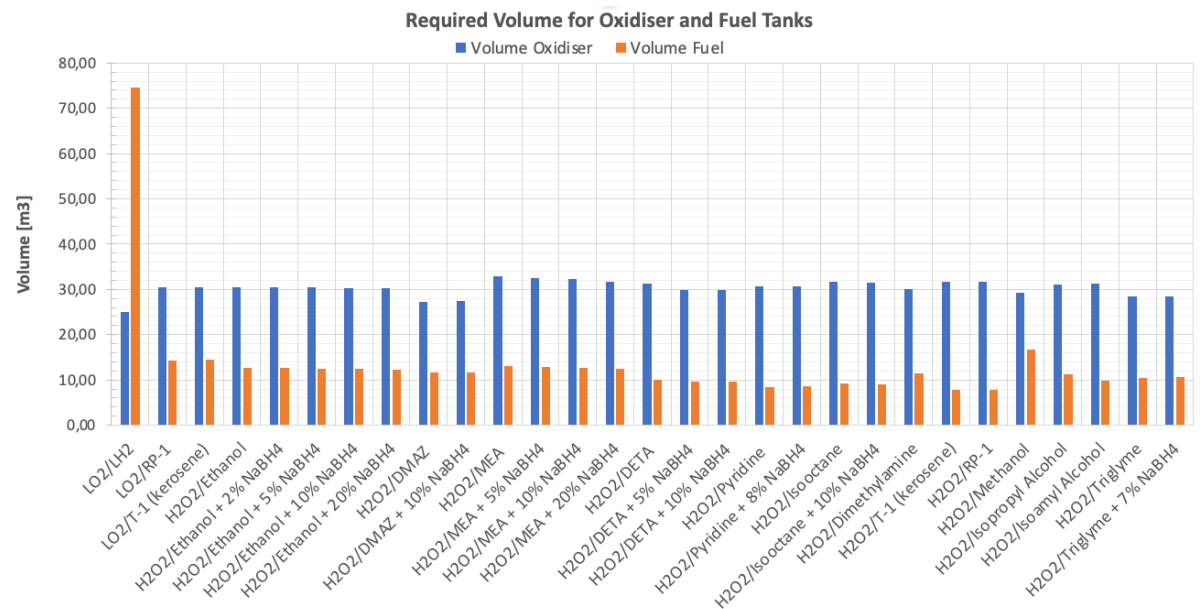


Figure 7.4: Required Volume for Oxidiser and Fuel

Looking at Figure 7.4 it can be concluded that the difference in required oxidiser volume between

the cryogenic and storable designs is little compared to what is seen for the required fuel volume. Due to the low density of liquid hydrogen the fuel volume required to store this cryogenic is on average 6.75 times higher than the fuel volume required for storable fuels. This increase in volume results in larger tanks, heavier propellant feed systems (including pressurants) and heavy and bulky thermal insulation equipment. The impact of larger tanks also translates to the stage structure design. The larger tanks increase the lateral dimensions of the stage, introducing a heavier and more vulnerable stage structure.

The lower stage dry mass of the storable upper stage design shows an immediate benefit compared to the conventional design. The lower dry mass results in lower development and manufacturing cost. Especially for expendable rockets such as the Ariane 6, the lower dry mass is directly coupled to lower cost-per-flight. It is, however, relevant to take into account the other mass budgets as well. From Figure 7.2 it could be deduced that the wet mass (dry mass including the propellant mass) of the storable design is increased compared to the conventional cryogenic design. This increase in wet mass will impact the payload capability of the upper stage design and the launch vehicle as a whole.

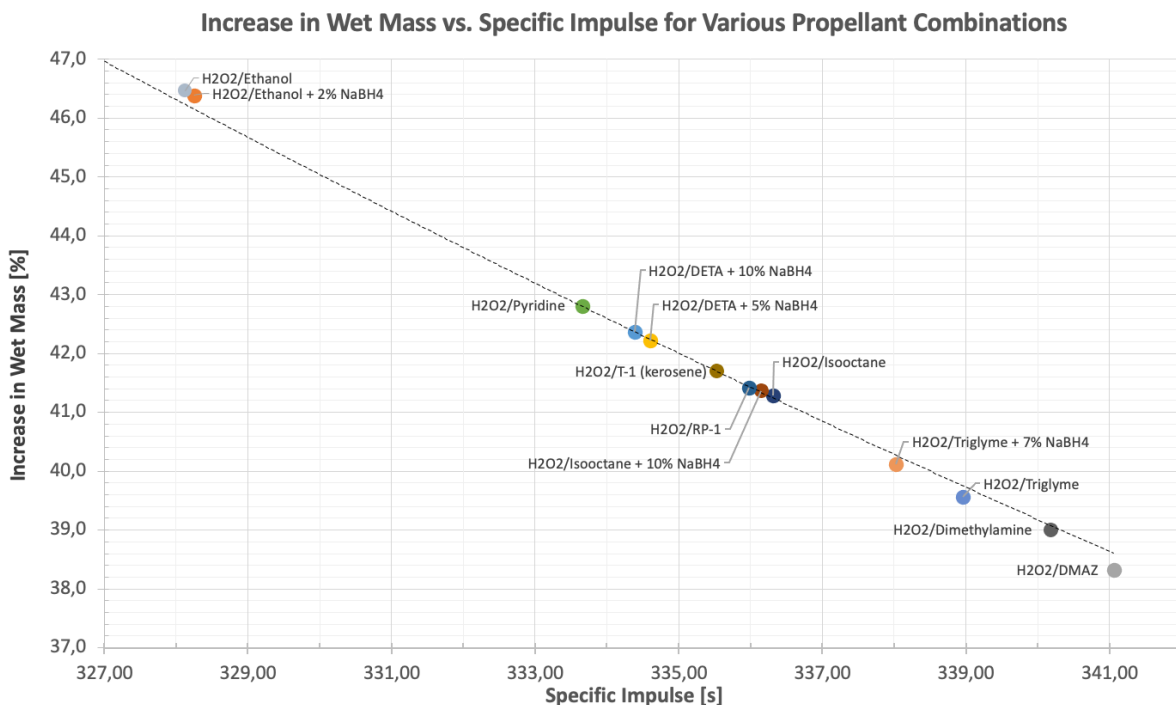


Figure 7.5: Relative Wet Mass Impact per Propellant Combination

Figure 7.5 describes the increase in wet mass in percentages compared to the conventional hydrolox design. For clarity, only a selection of the best performing propellant combinations is depicted in the graph. The relative increase in wet mass is significant as it ranges between 46.5% – 38.3%. It is clear that the relative increase in wet mass is proportional to the specific impulse of the combinations. The best option, in terms of relative wet mass increase, is H2O2/DMAZ. Still, this option results in an upper stage design that is 38.3% larger than the wet mass of the hydrolox design. This is a significant increase and will affect the payload capability. The amount of payload mass the upper stage can deliver is reduced if the wet mass (dry mass including the propellant mass) is increased. To investigate this reduced payload capability, the absolute increase in wet mass will be compared to the nominal and maximum payload capability of the conventional Ariane 6 upper stage design. This is illustrated in Figure 7.6.

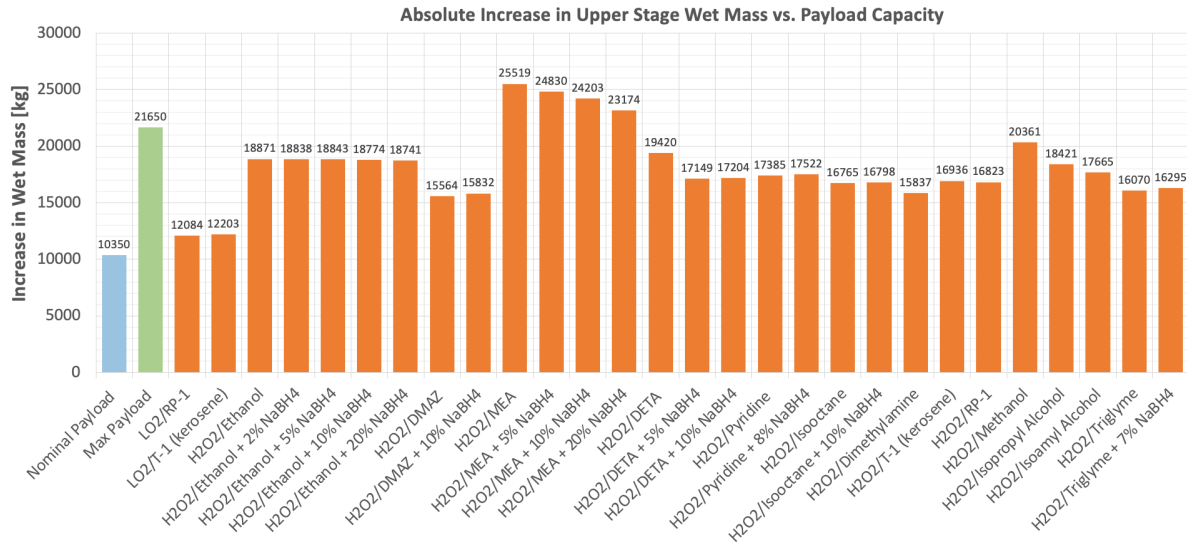


Figure 7.6: “Prototype X” Upper Stage Absolute Wet Mass Increase per Propellant Combination vs. Payload Capability

In Figure 7.6 the absolute increase of the wet mass for the propellant combinations is compared to the nominal and maximum payload capabilities as described by the Ariane 6 User Manual [11]. The nominal and maximum payload is illustrated as blue and green bars in Figure 7.6, respectively. It is clear that the storable propellant combination options all will hurt the payload capacity of the upper stage design. Due to the higher propellant mass (although it has a smaller volume) the wet mass increases and grows above the dry mass saving that was obtained. To make the effect on the payload capability clear, an analysis was done to investigate the available payload capability of the storable propellant combinations if implemented in the storable upper stage design of Prototype X. The results from this analysis are depicted in Figure 7.7 and Figure 7.8.

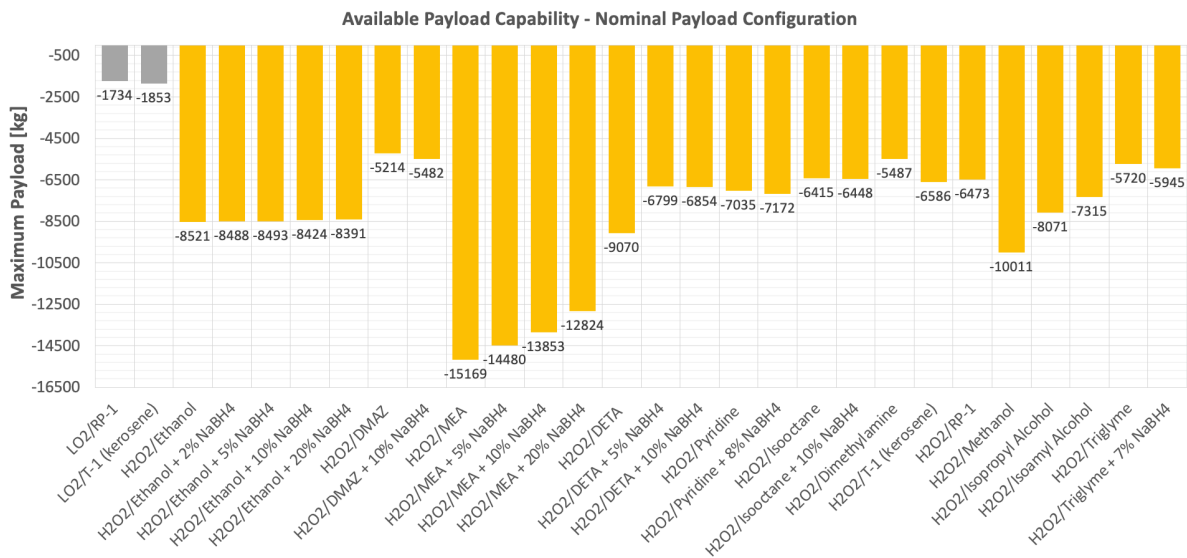


Figure 7.7: “Prototype X” Upper Stage Available Payload per Propellant Combination - Nominal Payload Configuration

From Figure 7.7 it can be concluded that none of the storable propellant options can be used for nominal payload configuration missions. The increased wet mass of the storable upper stage consumed more mass than was allocated for the nominal payload of 10352 kg. From Figure 7.6 it was found that some storable propellant combinations, however, do fall within the nominal and maximum payload capability. The available payload capability for the maximum payload configuration is graphically illustrated in Figure 7.8.

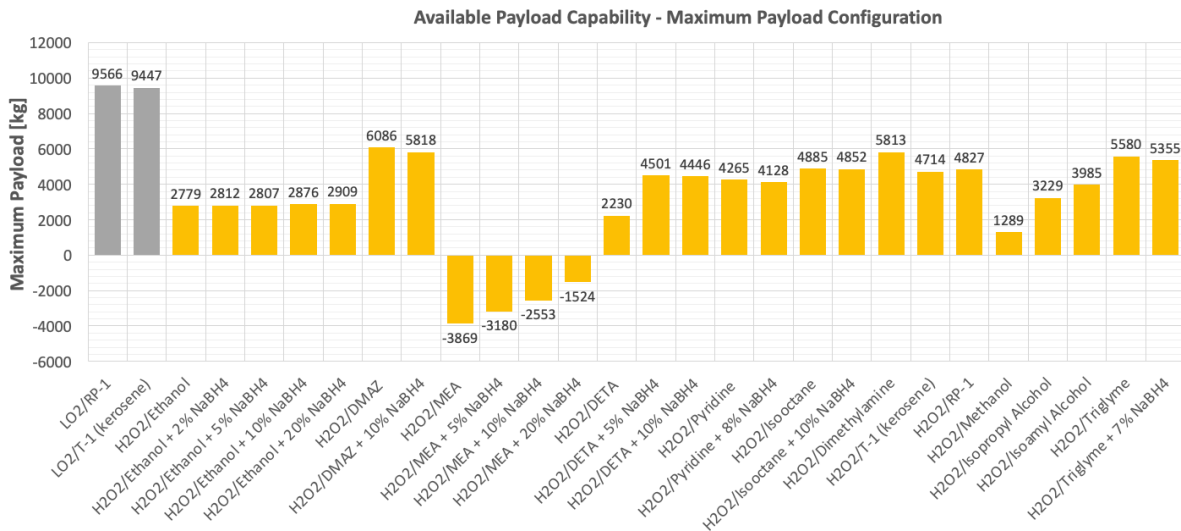


Figure 7.8: "Prototype X" Upper Stage Available Payload per Propellant Combination - Maximum Payload Configuration

The maximum payload configuration opens up the possibility of implementing the storable upper stage design, as can be seen in Figure 7.8. The increase in wet mass for the storable designs is within the range of the maximum payload of 21650 kg of the Ariane 6. This means that some of the storable designs can still carry payload even though the wet mass of the upper stage module has been increased. The positive numbers of payload capability indicate the availability of payload mass, where the negative numbers in Figure 7.8 show the inability to carry any payload mass at all.

The data obtained from the mass analysis is useful to do the propellant trade-off analysis. In this propellant trade-off analysis the best fuel options, based on the criteria, will be selected for the detailed mass and cost analysis for the Prototype X. For the trade-off the mixtures with sodium borohydride will not be considered candidates, only the pure fuel/hydrogen peroxide combination will be subject to the trade-off analysis. The effect of added sodium borohydride to the fuel mixture will be investigated at a later stage in the detailed mass/cost analysis. The level of added sodium borohydride will be considered a design parameter in the propellant optimisation.

During the detailed analysis, that will be discussed in chapter 8, the cost-per-flight for the storable upper stage designs will be approximated. Since it was already found that storable propellants have a reduced payload capability it is also very interesting to see what the cost-per-kg will be for these selected fuel options. This cost-per-kg figure is also called the 'payload performance'.

7.6. Propellant Trade-Off

The data obtained from the combustion analysis will help to give scores to some of the identified criteria, such as CR-2 and CR-5. Furthermore, data found in literature was used to assign scores to CR-1, CR-3 and CR-4. These relative scores for all the propellant options discussed are tabulated below in Table 7.23.

Table 7.23: Trade-Off Table as input for the AHP Analysis

Fuel Option/ Criteria	CR-1: Cost and Availability (0,223)	CR-2: Performance (with H ₂ O ₂) (0,311)	CR-3: Handling and Storage (0,191)	CR-4: Materials and Compatibility (0,135)	CR-5: Impact on Existing Hardware (0,140)
Ethanol	Cost: 0.40 €/kg (2022) [47] Annual Production: 111,400 tons (2021) [134]	Isp (vac): 328.13 s Density Specific Impulse: 259 Mg-s/m ³	Handling: Safe Storage: Shelf-life 36 months in dry and cool conditions [120]	Metals: Good/Excellent Plastics: Excellent Elastomers: Excellent [135]	Pseudo-hypergolic with Hydrogen Peroxide Dry Mass Impact: -19.84% Wet Mass Impact: +46.47%
DMAZ	Cost: NA €/kg (2022) Annual Production: NA	Isp (vac): 341.06 s Density Specific Impulse: 339 Mg-s/m ³	Handling: Safe/Moderate Danger Storage: Shelf-life 7.73 years at 25 degrees Celsius [136]	Metals: Excellent Plastics: Excellent Elastomers: Excellent [123]	Hypergolic with Hydrogen Peroxide Dry Mass Impact: -20.34% Wet Mass Impact: +38.32%
MEA	Cost: 1.20 €/kg (2022) [137] Annual Production: 2,500 tons (2018) [138]	Isp (vac): 305.70 s Density Specific Impulse: 309 Mg-s/m ³	Handling: Safe/Moderate Danger Storage: Shelf-life 24 months in sealed packaging [139]	Metals: Good/Excellent Plastics: Good to Fair Elastomers: Fair to Poor [135]	Hypergolic with Hydrogen Peroxide Dry Mass Impact: -19.53% Wet Mass Impact: +62.84%
DETA	Cost: 0.71 €/kg (2022) [49] Annual Production: 4,540 tons (2021)[140]	Isp (vac): 326.00 s Density Specific Impulse: 311 Mg-s/m ³	Handling: Danger Storage: 24 months [120]	Metals: Excellent Plastics: Poor Elastomers: Not Recommended [135]	Hypergolic with Hydrogen Peroxide Dry Mass Impact: -19.96% Wet Mass Impact: +47.82%
Pyridine	Cost: 2.97 €/kg (2022) [126] Annual Production: 20,000 tons (2021)[126]	Isp (vac): 333.66 s Density Specific Impulse: 328 Mg-s/m ³	Handling: Moderate Danger Storage: 24 months [120]	Metals: Good Plastics: Poor/ Not Recommended Elastomers: Poor [135]	Hypergolic with Hydrogen Peroxide Dry Mass Impact: -20.18% Wet Mass Impact: +42.81%
Isocetane	Cost: 3.09 €/kg (2022) [128] Annual Production: 1,180 tons (2010) [141]	Isp (vac): 336.31 s Density Specific Impulse: 232 Mg-s/m ³	Handling: Safe/Moderate Danger Storage: 120 months in cool and dark conditions [142]	Metals: Excellent Plastics: Excellent Elastomers: Excellent [135]	Hypergolic with Hydrogen Peroxide Dry Mass Impact: -20.00% Wet Mass Impact: +41.28%
Dimethylamine	Cost: 0.49 €/kg (2022) [143] Annual Production: 300,000 tons (2021) [129]	Isp (vac): 340.18 s Density Specific Impulse: 228 Mg-s/m ³	Handling: Safe/Moderate Danger Storage: 24 months [120]	Metals: Good/Excellent Plastics: Good/ Fair [135] Elastomers: Good/ Fair [135]	Hypergolic with Hydrogen Peroxide Dry Mass Impact: -20.00% Wet Mass Impact: +39.00%
Methanol	Cost: 0.38 €/kg (2022) [144] Annual Production: 200 million tons (2021) [130]	Isp (vac): 322.73 s Density Specific Impulse: 256 Mg-s/m ³	Handling: Safe/Moderate Danger Storage: 3 months [120]	Metals: Excellent Plastics: Good/ Excellent Elastomers: Fair/ Poor [135]	Not hypergolic with Hydrogen Peroxide Dry Mass Impact: -19.68% Wet Mass Impact: +50.13%
Isopropyl Alcohol	Cost: 1.16 €/kg (2022) [145] Annual Production: 2,170 tons (2020)[146]	Isp (vac): 329.80 s Density Specific Impulse: 259 Mg-s/m ³	Handling: Safe/Moderate Danger Storage: 24- 36 months [120]	Metals: Good/Poor Plastics: Excellent Elastomers: Not Recommended [135]	Not hypergolic with Hydrogen Peroxide Dry Mass Impact: -19.90% Wet Mass Impact: +45.36%
Isoamyl Alcohol	Cost: 1.78 €/kg (2022) [50] Annual Production: NA	Isp (vac):332.68 s Density Specific Impulse: 269 Mg-s/m ³	Handling: Safe/Moderate Danger Storage: 24 months [147]	Metals: Good/ Fair Plastics: Good Elastomers: Excellent/ Good [135]	Not hypergolic with Hydrogen Peroxide Dry Mass Impact: -20.01% Wet Mass Impact: +43.50%
Triglyme	Cost: NA €/kg (2022) Annual Production: 227 tons (2006) [148]	Isp (vac): 338.96 s Density Specific Impulse: 334 Mg-s/m ³	Handling: Safe Storage: 18 months for closed container, 12 months for opened container [132]	Metals: Good/Excellent Plastics: Excellent Elastomers: Good/ Fair [135]	No Data Available on Hypergolicity Dry Mass Impact: -20.28% Wet Mass Impact: +39.57%

The data collected in Table 7.23 will be used as an input to the AHP trade-off analysis. The relative options will be attributed to a score by the use of pair-wise analysis. The Analytical Hierarchy Process (AHP) trade-off tool will be used to combine the qualitative and quantitative data in Table 7.23 to generate a quantifiable trade-off decision on the best propellant options at hand. The AHP trade-off tool, as described earlier, makes a distinction between objective and subjective pair-wise analysis [133]. The combined effort of this subjective and objective distribution of scores is summarised in Table 7.24.

Table 7.24: Propellant Analytical Hierarchy Process Trade-Off Analysis Results

Criteria / Fuel Options	CR-1 Cost & Availability	CR-2 Performance	CR-3 Handling & Storage	CR-4 Materials Compatibility	CR-5 Impact on Existing Hardware	Total Weight
Weights	0.203	0.311	0.151	0.130	0.205	1.000
<i>Ethanol</i>	0.168	0.082	0.208	0.185	0.074	0.130
<i>DMAZ</i>	0.056	0.128	0.213	0.185	0.142	0.136
<i>MEA</i>	0.061	0.036	0.051	0.057	0.045	0.048
<i>DETA</i>	0.083	0.070	0.026	0.020	0.065	0.058
<i>Pyridine</i>	0.070	0.098	0.041	0.027	0.098	0.074
<i>Isooctane</i>	0.061	0.113	0.105	0.165	0.103	0.106
<i>Dimethylamine</i>	0.118	0.117	0.065	0.100	0.133	0.110
<i>Methanol</i>	0.180	0.059	0.031	0.062	0.052	0.078
<i>Isopropyl Alcohol</i>	0.071	0.085	0.066	0.032	0.086	0.073
<i>Isoamyl Alcohol</i>	0.056	0.096	0.056	0.055	0.092	0.076
<i>Triglyme</i>	0.076	0.116	0.138	0.112	0.110	0.109
Total Score per Criterion	1.000	1.000	1.000	1.000	1.000	1.000

From the trade-off analysis results, depicted in Table 7.24, it can be concluded that there are two clear winners. DMAZ (relative score: 0.136) and ethanol (relative score: 0.130). A third fuel option that is selected for the detailed mass and cost analysis is Dimethylamine. These three 'green' fuel options in combination with hydrogen peroxide are deemed the best options based on the selected criteria.

The best-identified option is DMAZ. This fuel has great performance characteristics (Isp = 341.06 seconds, Density Specific Impulse = $339 \text{ Mg} \cdot \text{s}/\text{m}^3$). These performance characteristics resulted in the largest dry mass reduction (-20.34%) and the smallest wet mass increase ($+38.32\%$). DMAZ has a shelf-life of almost 8 years and is able to be handled with moderate safety. Furthermore, the fuel is compatible with almost all kinds of materials. Although less information is available on the annual production and cost-per-kg of DMAZ, it is expected by literature that the development of DMAZ will yield a lot of demand in the future [123], [124]. It is expected that this will result in large production quantities and cost reductions in the future.

The second fuel that got selected is ethanol. The specific impulse is found to be 328.13 seconds, resulting in a dry mass reduction of roughly -19.48% and a wet mass increase of $+46.47\%$. These performance characteristics do not favour ethanol compared to other propellant options discussed. The reason why ethanol was selected comes from the fact that it is a very accessible fuel as it is very cheap (0.40 €/kg (2022) [47]) and is produced in large quantities annually. Furthermore, it is vastly compatible with a wide range of materials. Also, ethanol is easy to store and safe to handle.

The last fuel that got selected for detailed analysis is dimethylamine. This fuel is comparable to ethanol in terms of cost and availability. It is possible to acquire dimethylamine for 0.49 €/kg (2022) [143] and annually 300.000 tons of dimethylamine are produced. Furthermore, it has very good performance characteristics (Isp of 340.18 seconds) and results in good dry mass savings. The wet mass impact is roughly 39.00%. Dimethylamine is, however, (moderately) dangerous to be handled but has good storability of two years. The fuel is compatible with metals and elastomers but is not very good with plastics.

From the propellant options described in this chapter the best options are found to be DMAZ (2-dimethylaminoethylazide), ethanol and dimethylamine.

7.7. Executive Chapter Summary

In this chapter, a variety of 'green' fuels were investigated as potential candidates for a propellant combination with highly concentrated hydrogen peroxide. Since hydrogen peroxide will be the selected storable oxidiser, this selection was focused on storable fuels that can combust with HTP. Apart from this prerequisite, other requirements have been formulated that help to select propellants for further analysis. Moreover, assumptions for this selection analysis have been summarised in Table 7.2. For sake of comparison, the conventional cryogenic propellants liquid oxygen, liquid hydrogen, kerosene and RP-1 have been discussed too. Their physical and chemical characteristics are provided to aid the comparison with the storable oxidiser and fuel candidates. For this propellant selection, it was required that the fuels had a classification of being 'green'. This classification is provided by the GRASP consortium that was put together by the European Union. The GRASP consortium set out to identify possible alternatives to toxic (storable) propellants. They expect the potential advantages of reduced handling costs, improved performance and reduced human exposure to toxic substances outweigh the large upfront cost associated with the implementation of these novel 'green' propellants. The GRASP consortium put together a comprehensive list of (semi-)storable fuels that are considered 'green' as per their classification. From this list, the most promising fuels got selected, which were identified in the preceding literature review, for further analysis. These candidates are:

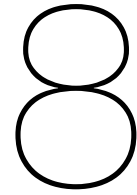
- Ethanol
- 2-dimethylaminoethylazide (DMAZ)
- Ethanolamine (MEA)
- Diethylenetriamine (DETA)
- Pyridine
- Isooctane
- Dimethylamine
- Methanol
- Isopropyl Alcohol
- Isoamyl Alcohol
- Triglyme

To do the selection of the best candidates it is important to have functional criteria. Criteria for 'green' propellant selection were determined by the works of O. Frota, B. Mellor and M. Ford [8]. The selection criteria are: **CR-1**: Cost and Availability, **CR-2**: Performance, **CR-3**: Handling and Performance, **CR-4**: Materials Compatibility, **CR-5**: Impact on Existing Hardware. These criteria have been weighed relative to each other. This process of weighing the criteria was done using an Analytical Hierarchy Process (AHP) Trade-Off tool. This tool helps to analytically approach the trade-off process by using subjective assessment of experts and objective reasoning in a combined mathematical pair-wise comparison analysis. This tool helped to come up with the AHP relative expert weights per criterion.

Before the trade-off analysis is performed, more data on combustion and the potential design impact of the fuels was required. This was done by an extensive propellant combustion analysis. In this combustion analysis, with hydrogen peroxide, the optimum mixture ratio, vacuum specific impulse and density specific impulse was calculated for the fuel candidates. These characteristics were used as input to the mass model. The mass model helped to describe the dry and wet mass impacts on the design. Through this propellant analysis, it could be concluded that the dry mass for storable designs was reduced by approximately 20%. However, it was found that the wet mass increase significantly due to the higher density of the fuels and their reduced specific impulse. This wet mass burden translates to the payload capability of the storable concepts. It was found that the "Prototype X" is unable to carry any propellant in the nominal payload configuration. However, if the launch vehicle is configured for the maximum payload configuration it was found that some storable propellant combinations enable to bring a reduced payload mass. These payload capabilities are summarised in Figure 7.7 and Figure 7.8. The data obtained from this mass analysis enabled to do the propellant trade-off analysis.

Through the use of a Trade-Off table, depicted in Table 7.23, and the AHP tool, a selection of the fuel candidates could be made. The quantitative scoring system of the combined tools pointed out that DMAZ is the best candidate for a storable combination with hydrogen peroxide. The fuel has great performance characteristics ($I_{sp} = 341.06$ seconds, Density Specific Impulse = $339 \text{ Mg} \cdot \text{s}/\text{m}^3$), has a relatively small wet mass burden, can be stored and handled safely, and is compatible with most materials. The other two candidates that got selected for detailed mass and cost analysis were ethanol

and dimethylamine. Both fuels scored relatively high on availability, storability and low cost. Ethanol was, in terms of performance, the least performing fuel of the three selected candidates.



Detailed Mass and Cost Analysis

In chapter 7 the propellant analysis and selection were done under combustion chamber conditions comparable to the Vinci engine of the Ariane 6 upper stage module. That is, a combustion chamber pressure of 6 MPa and a nozzle expansion ratio of 240. In this chapter the selected propellants; DMAZ, Ethanol and Dimethylamine, will be optimised in terms of reactive additive mixture ratio, oxidiser-to-fuel ratio, combustion chamber pressure and combustion chamber temperatures. This optimisation is gravitates the optimum (minimal) wet mass of the Prototype X upper stage module. After the propellants have been optimised in terms of combustion conditions, a detailed mass and cost analysis will be performed. The results from this analysis will give valuable insight into payload capability for different mission characteristics. The potential commercial value of the payload capability for the storable upper stage design will be discussed, and compared to the conventional cryogenic upper stage, in a market outlook analysis.

8.1. Propellant Optimisation

In this section, the selected propellants will be optimised in terms of combustion conditions and additive material mixture ratio's. The optimisation will be focused on minimising the dry and wet mass of the upper stage design while making sure feasible combustion conditions are ensured and propellant storability is met. First, the impact of reactive additives on the overall design is investigated.

8.1.1. Design Impact of Reactive Additives

During the propellant selection analysis various fuels were investigated with different mixture ratio's of reactive additives, measured in weight percentage ($wt.\%$). In this section, the effect of these reactive additives on specific impulse and wet mass of the storable upper stage design will be investigated.

For simplicity, sodium borohydride will be the selected reactive additive. In rocket fuels, metal hydrides with a low molecular weight are preferred. As discussed by H. Kang et al. [34], sodium borohydride was specifically chosen as it hypergolically reacts very strong with a strong oxidizer such as hydrogen peroxide [35], it is the least expensive metal hydride commercially available, safe in terms of storage, use and handling and it is easy to manufacture [16], [34], [36].

After experiments, H. Kang et al. concluded that if $5\text{ wt}\%$ content of the ignition source was added to the stock 3 fuel mixture the hypergolic initiation was repeatedly and reliably achieved in all cases [37]. Therefore this quantity was to be the optimum amount of ignition source that should be added to the fuel to maximise performance and hypergolicity of the fuel while maintaining a storability of over 4 months [16], [37].

To understand the effect of sodium borohydride on the specific impulse, density specific impulse and the wet mass of the upper stage design, the selected fuels will be analysed with a variety of additive weight contents. This combustion analysis was performed on different fuel/reactive additive mixture ratio's, as depicted in Table 8.1. It is important to note that here the baseline combustion chamber pressure of 6 MPa and expansion ratio of 240 is assumed.

Table 8.1: Combustion Analysis for Different Fuel Mixtures with Sodium Borohydride - $P_c = 6 \text{ MPa}$

Type	Prop Comb	Oxidizer	Fuel	Density Fuel (20°C) [kg/m ³]	Optimum O/F [-]	Isp (vac) [s]
Storable (green)	H2O2/DMAZ	H2O2 (100%)	C4H10N5	993.0	3.85	341.45
Storable (green)	H2O2/DMAZ + 0.5% NaBH4	H2O2 (100%)	C4H10N5	993.4	3.84	341.36
Storable (green)	H2O2/DMAZ + 1% NaBH4	H2O2 (100%)	C4H10N5	993.8	3.84	341.28
Storable (green)	H2O2/DMAZ + 2% NaBH4	H2O2 (100%)	C4H10N5	994.5	3.84	341.14
Storable (green)	H2O2/DMAZ + 5% NaBH4	H2O2 (100%)	C4H10N5	996.9	3.82	340.72
Storable (green)	H2O2/DMAZ + 7.5% NaBH4	H2O2 (100%)	C4H10N5	998.8	3.81	340.37
Storable (green)	H2O2/DMAZ + 10% NaBH4	H2O2 (100%)	C4H10N5	1000.7	3.80	340.00
Storable (green)	H2O2/DMAZ + 20% NaBH4	H2O2 (100%)	C4H10N5	1008.4	3.63	338.25
Storable (green)	H2O2/Ethanol	H2O2 (100%)	C2H5OH (100%)	789.0	4.43	328.22
Storable (green)	H2O2/Ethanol + 0.5% NaBH4	H2O2 (100%)	C2H5OH (100%)	790.4	4.42	328.21
Storable (green)	H2O2/Ethanol + 1% NaBH4	H2O2 (100%)	C2H5OH (100%)	791.8	4.42	328.24
Storable (green)	H2O2/Ethanol + 2% NaBH4	H2O2 (100%)	C2H5OH (100%)	794.6	4.41	328.28
Storable (green)	H2O2/Ethanol + 5% NaBH4	H2O2 (100%)	C2H5OH (100%)	803.1	4.38	328.40
Storable (green)	H2O2/Ethanol + 7.5% NaBH4	H2O2 (100%)	C2H5OH (100%)	810.1	4.36	328.49
Storable (green)	H2O2/Ethanol + 10% NaBH4	H2O2 (100%)	C2H5OH (100%)	817.1	4.34	328.57
Storable (green)	H2O2/Ethanol + 20% NaBH4	H2O2 (100%)	C2H5OH (100%)	845.2	4.25	328.67
Storable (green)	H2O2/Dimethylamine	H2O2 (100%)	C2H7N	670.0	5.64	340.21
Storable (green)	H2O2/Dimethylamine + 0.5% NaBH4	H2O2 (100%)	C2H7N	672.0	5.63	340.16
Storable (green)	H2O2/Dimethylamine + 1% NaBH4	H2O2 (100%)	C2H7N	674.0	5.62	340.12
Storable (green)	H2O2/Dimethylamine + 2% NaBH4	H2O2 (100%)	C2H7N	678.0	5.60	340.04
Storable (green)	H2O2/Dimethylamine + 5% NaBH4	H2O2 (100%)	C2H7N	690.0	5.53	339.82
Storable (green)	H2O2/Dimethylamine + 7.5% NaBH4	H2O2 (100%)	C2H7N	700.0	5.47	339.64
Storable (green)	H2O2/Dimethylamine + 10% NaBH4	H2O2 (100%)	C2H7N	710.0	5.42	339.44
Storable (green)	H2O2/Dimethylamine + 20% NaBH4	H2O2 (100%)	C2H7N	750.0	5.20	338.50

The three selected propellants are analysed on their density, optimum O/F ratio and vacuum-specific impulse. The mixture ratio in weight percentage (*wt.%*) ranges between 0.5% – 20%. From Table 8.1 it can be concluded that, as expected, the density increases if more sodium borohydride is added. Sodium borohydride is a relatively dense material (1070 kg/m^3) compared to the density of the selected fuels. Furthermore, it is found that the optimum O/F ratio drops lower when more reactive additives are added. This can be explained by the fact that decomposition of hydrogen peroxide is obtained faster as a result of sodium borohydride. This results in a slightly more fuel-rich combustion condition. The O/F ratio is also affected by the amount of sodium borohydride that is consumed during combustion.

From Table 8.1 it can be concluded that the vacuum-specific impulse does slightly increase for higher weight percentages of sodium borohydride in the mix for ethanol. For both DMAZ and Dimethylamine the vacuum-specific impulse is not positively impacted by the added sodium borohydride. The effect of the reactive additives on the specific impulse and on the wet mass of the storable upper stage concept is graphically depicted in Figure 8.1, Figure 8.2 and Figure 8.3

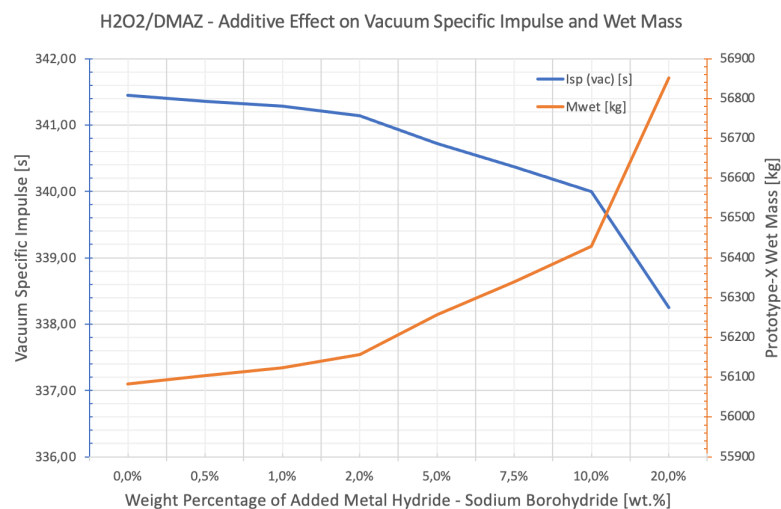


Figure 8.1: Impact of DMAZ/Sodium Borohydride Fuel Mixtures on Specific Impulse and Wet Mass

From Figure 8.1 it can be concluded that none of the DMAZ/sodium borohydride fuel mixtures will contribute to a higher Isp or a lower wet mass. It can thus be concluded that sodium borohydride cannot be used to optimise the combustion of the H₂O₂/DMAZ combination.

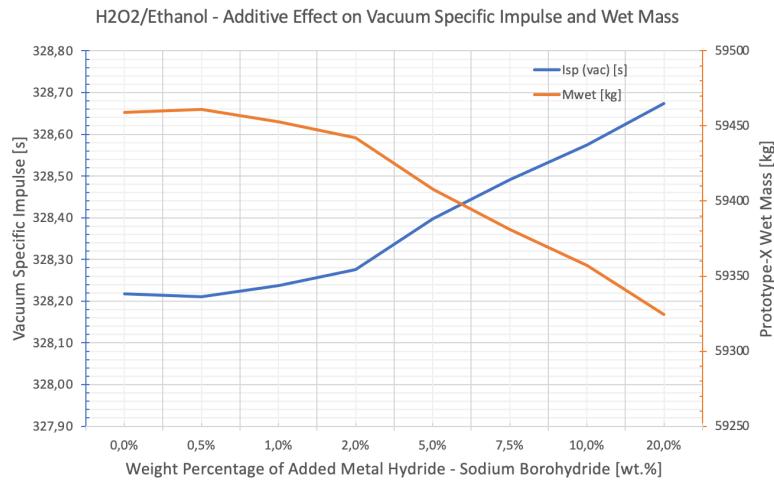


Figure 8.2: Impact of Ethanol/Sodium Borohydride Fuel Mixtures on Specific Impulse and Wet Mass

Adding sodium borohydride to the ethanol fuel mixture will positively increase the specific impulse. A higher wt.% of sodium borohydride will result in a lower O/F ratio and a higher specific impulse. This will directly influence the required propellant mass, hence the wet mass of the storable upper stage concept. This is graphically depicted in Figure 8.2. According to H. Kang et al. the maximum added sodium borohydride, to allow for good combustion performance and storability, is 5% [37]. Setting this constraint will result in a maximum 0.05% increase in vacuum-specific impulse. This relates to a wet mass reduction of 0.086%. It can be concluded that the sodium borohydride additives do not yield a significant effect on upper stage mass reduction. Comparing this to the added complexity and cost of introducing reactive additives to fuel mixtures it is decided that no sodium borohydride additives are added to the ethanol.

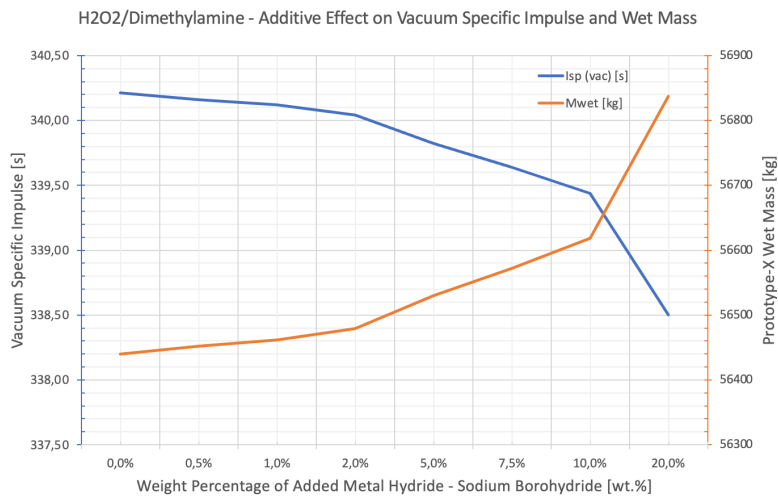


Figure 8.3: Impact of Dimethylamine/Sodium Borohydride Fuel Mixtures on Specific Impulse and Wet Mass

Looking at Figure 8.3 it can be concluded that dimethylamine does react, in a comparable manner as DMAZ, to the additives. The specific impulse of dimethylamine is not increased by the addition of sodium borohydride. It can, thus, be concluded that no additives will be mixed into the H₂O₂/dimethylamine mixture to optimise the combustion process.

8.1.2. Combustion Condition Optimisation

Now that the best propellants are selected for detailed mass and cost analysis it is important to further optimise their performance by finding the best oxidiser-to-fuel ratio (O/F) and combustion chamber pressure (P_c). In the previous analyses a fixed combustion chamber pressure of 6 MPa (typical for the Vinci engine) was maintained.

DMAZ Optimisation Analysis

As discussed earlier, the previous combustion analyses were conducted under standard chamber pressure conditions as found in the Vinci engine. To do sound propellant optimisation it is helpful to analyse the behaviour of the wet mass, combustion chamber temperature and specific impulse as a function of the O/F ratio. It is important to note that in reality the selected O/F ratio is not the stoichiometric mixture ratio. In the case of stoichiometric mixture ratio's full combustion occurs (all fuel and oxidizer are consumed). Engines typically run fuel-rich. This to limit the combustion chamber temperature. Oxygen rich is also possible, depends on the type of engine cycle. Oxygen rich mixture ratio's can result in very high temperatures if not well managed. This will be discussed in detail in chapter 10. Throughout this chapter an expansion ratio of 240 is assumed. For the HTP/DMAZ propellant combination this is depicted in Figure 8.4 and Figure 8.5.

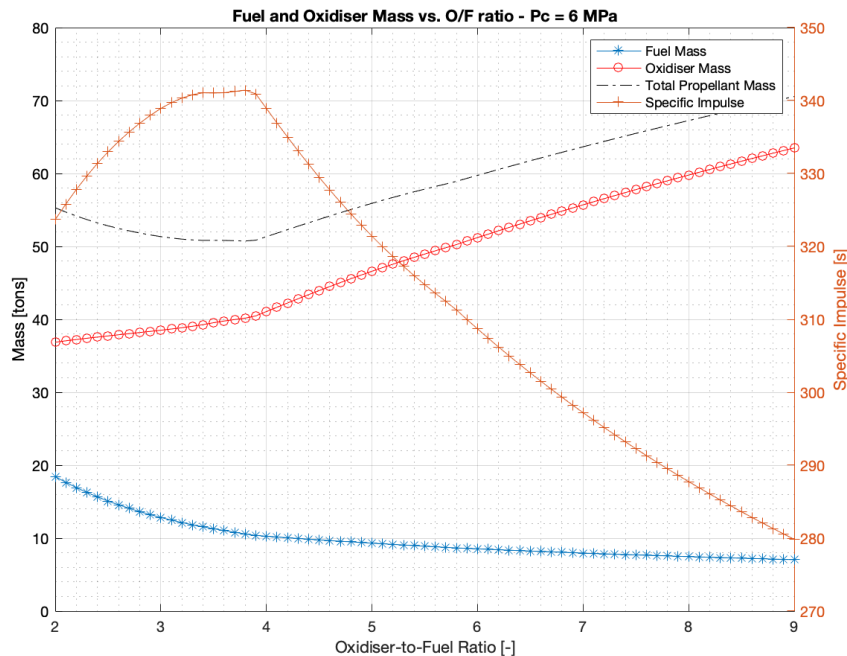


Figure 8.4: DMAZ and H₂O₂ Mass vs. O/F ratio under Fixed Combustion Chamber Pressure - $P_c = 6 \text{ MPa}$

From Figure 8.4 it can be concluded that there clearly is an optimal oxidiser-to-fuel ratio that will minimise the total propellant mass. This local optimum is found at an O/F ratio between 3 and 4. This optimum is directly related to the specific impulse, illustrated in orange. It can be deduced that the oxidiser mass is affected more by the specific impulse than the fuel mass. To understand the effect of this change in O/F ratio and specific impulse the wet and dry mass of the Prototype X should be analysed. This is depicted in Figure 8.5.

From Figure 8.5 it is clear that the dry mass of the upper stage concept is directly related to the wet mass of the system. The dry mass follows the same behaviour of the wet mass with respect to the specific impulse and O/F ratio. This is the direct result of the propellant volume required in the upper stage module. Most notable in Figure 8.5 is the combustion chamber temperature. It can be concluded that for a combustion chamber pressure of 6 MPa the combustion temperature is above 3000 K around the optimum O/F ratio. The combustion chamber temperature is a very important parameter for propellant optimisation. This temperature should be limited as much as possible to prevent significant mass

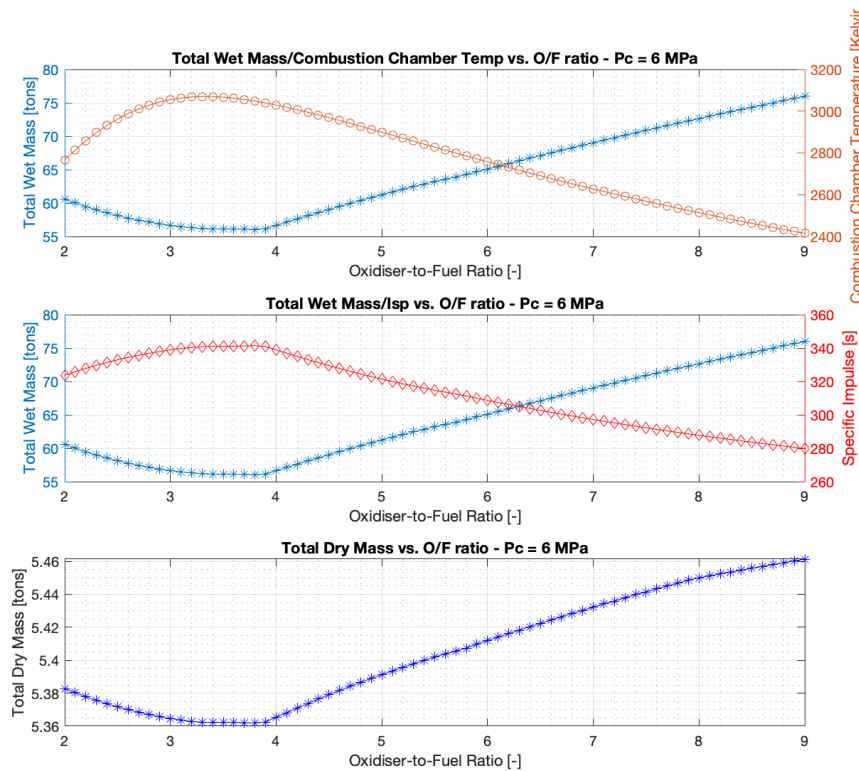


Figure 8.5: Specific Impulse, Combustion Chamber Temperature and Mass Behaviour vs. O/F ratio - DMAZ/H₂O₂

and cost growth as the result of exotic materials being used in the combustion chamber. The chamber temperature is a function of the chamber pressure and O/F ratio's. This is graphically depicted in Figure 8.6.

In Figure 8.6 the specific impulse and combustion chamber temperature is described as a function of the combustion chamber pressure. This is done for a range of O/F ratio's, ranging between 3 and 9 with an interval of 0.5. From these graphs, it can be concluded that the combustion chamber temperature rises for higher combustion chamber pressures and optimal O/F ratio's. This is to be expected as at the optimum O/F ratio ideal combustion occurs. That is, most energy is released during the reaction. This energy results in higher thermal output. Furthermore, it can be seen that a higher specific impulse is obtained under higher combustion chamber pressures, as expected.

To find the optimum combustion conditions for the propellants, however, one cannot simply keep increasing the combustion chamber pressure or combustion chamber temperature. Typical combustion chamber pressures ranges between 10 and 20 bar, or 1 – 20 MPa [149]. Current cryogenic and hypergolic propulsion systems available on the market limit the pressure to a maximum of 9 MPa [16]. Due to the high pressures during steady-state operation, the combustion chamber experiences significant hoop stresses. Due to the elevated chamber temperatures that go along with that, the materials used often in the combustion chamber tend to lose some tensile strength performance. To prevent the combustion chamber from failing, it can be equipped with thicker walls. This will add a significant mass and cost burden. To limit this, the maximum combustion chamber pressure is set to 9 MPa .

In addition, significant temperature gradients are set up in the walls of the chamber and nozzle. These combustion chamber temperatures should be limited to reduce the internal stresses of the chamber. Typical maximum combustion chamber temperatures that can be seen in rocket engines go up to 3500 K. At these high temperatures radicals are formed; partially broken up compounds that form electrically neutral fractions. Above temperatures of 4000 K dissociation occurs. This dissociation is an endothermic reaction that will cause the flame temperature to go drop, resulting in less efficiency.

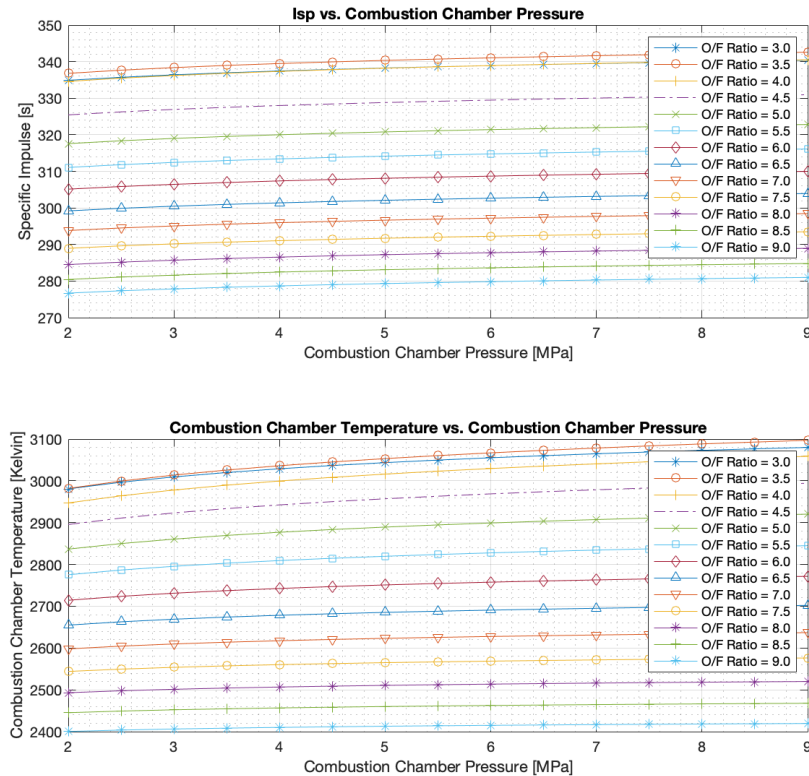


Figure 8.6: Specific Impulse and Combustion Chamber Temperature vs. Combustion Chamber Pressure for various O/F ratio's - DMAZ/H₂O₂

Moreover, it is very hard to find combustion chamber material that can withstand these temperature levels. Exotic/heavy materials should be introduced at temperatures above 3500 K to prevent melting [54]. For the propellant analysis, it is assumed that the combustion chamber temperature will be limited to below 3500 K. For the Vinci engine, operating on a LO₂/LH₂ propellant combination, the combustion chamber temperatures were found to be around 3440 K during steady-state operations, per comparison.

To find the best mixture ratio and combustion chamber pressure (while limiting the combustion chamber temperature) an extensive propellant optimisation analysis was conducted. The objective of this optimisation is to minimise the wet mass of the "Prototype X" upper stage. The result is graphically depicted in Figure 8.7.

The performance model was used to produce a large data set of performance characteristics for the combination of DMAZ and hydrogen peroxide. These performance characteristics entail; vacuum-specific impulse and combustion chamber temperature for various combustion chamber pressures (2 - 10 MPa) and O/F ratio's (2 - 9). This data set with 5700 data points was the input for the mass analysis. For each data point the specific impulse, O/F ratio and combustion chamber pressure were used to calculate the dry and wet mass of the "Prototype X" upper stage module. This mass analysis produced a 3x3 matrix containing the wet mass per O/F ratio and combustion chamber pressure. This is put into a contour plot, depicted in Figure 8.7. The resulting contour plot shows that the best wet mass region is skewed around a mixture ratio between 3 and 4 (dark area). To find the best combustion chamber pressure, taking into account the constraints in combustion chamber pressure and temperature the optimisation was conducted using MATLAB.

To solve for the most optimal combustion conditions the `fmincon` non-linear optimisation function of MATLAB was used. This function helps to find the minimum in nonlinear multi-variable functions and

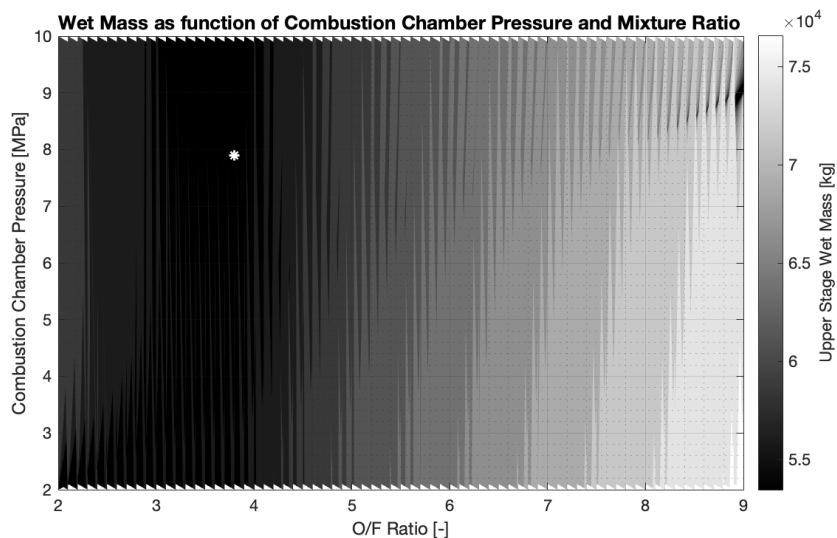


Figure 8.7: Propellant Optimisation Analysis - DMAZ/H₂O₂

has been proven to be functional in similar problems [14]. To run this function lower and upper bounds have been provided in the form of the constraints in combustion chamber temperature and pressure. Furthermore, the 3x3 matrix was used as the input matrix that return the scalar $f(x)$, being wet mass. This optimisation tool was used to find the optimum combustion conditions while minimising the combustion chamber pressure and temperature. From the optimisation the following optimum conditions, indicated in Figure 8.7 with a white asterisk, were found:

Optimum Conditions:

- $O/F = 3.85$
- $P_c = 7.9 \text{ MPa}$
- $I_{sp} = 342.54 \text{ s}$ (overall efficiency of combustion = 0.9562)

It is important to note that the ideal (vacuum) specific impulse that corresponds with these optimum conditions is corrected for combustion quality and efficiency, to obtain the corrected specific impulse of 342.54 s. The overall efficiency of combustion was rated to be 0.9562. The method that is applied to obtain these corrected performance characteristics is discussed in chapter 5.

Ethanol Optimisation Analysis

The same optimisation procedure has been done for the other two fuels under investigation; ethanol and dimethylamine. In this section, the optimisation of ethanol in combination with hydrogen peroxide will be discussed. The wet and dry mass response of the ethanol/H₂O₂ combination is graphically depicted in Figure 8.8. This gives a baseline for the optimum O/F ratio and the relative contribution of the fuel and oxidiser mass.

From Figure 8.8 there is a clear optimum in mixture ratio between 4 and 4.5. The effect of the mixture ratio on the dry/wet mass and the combustion chamber temperature is graphically depicted in Figure 8.9.

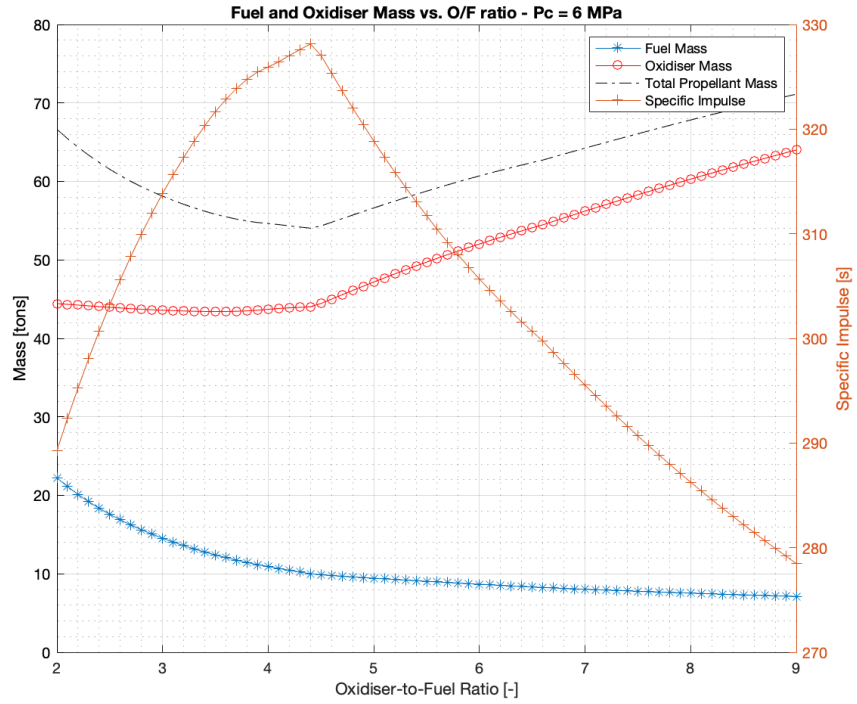


Figure 8.8: Ethanol and H2O2 Mass vs. O/F ratio under Fixed Combustion Chamber Pressure - Pc = 6 MPa

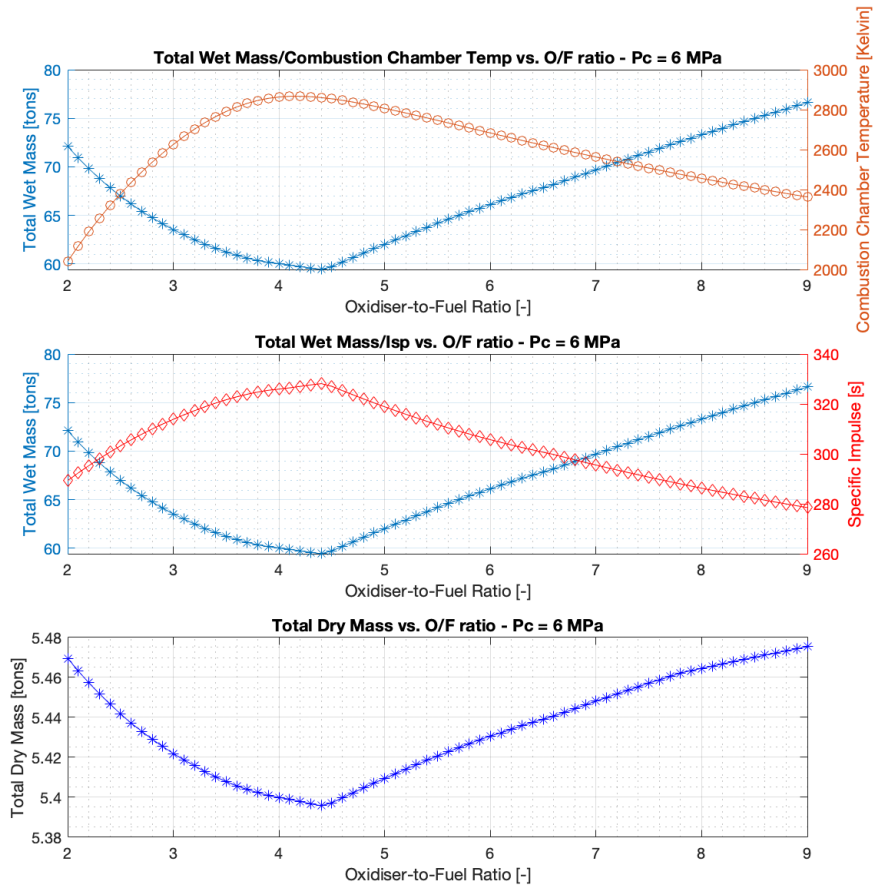


Figure 8.9: Specific Impulse, Combustion Chamber Temperature and Mass Behaviour vs. O/F ratio - Ethanol/H2O2

To optimise the ethanol/H₂O₂ combination the specific impulse and combustion chamber temperature will be plotted as a function of the combustion chamber pressure and the mixture ratio. This is graphically depicted in Figure 8.10. From these graphs, it can be concluded that the specific impulse and combustion temperature increase for larger combustion chamber pressures. This is comparable to what was found for the DMAZ/H₂O₂ combination.

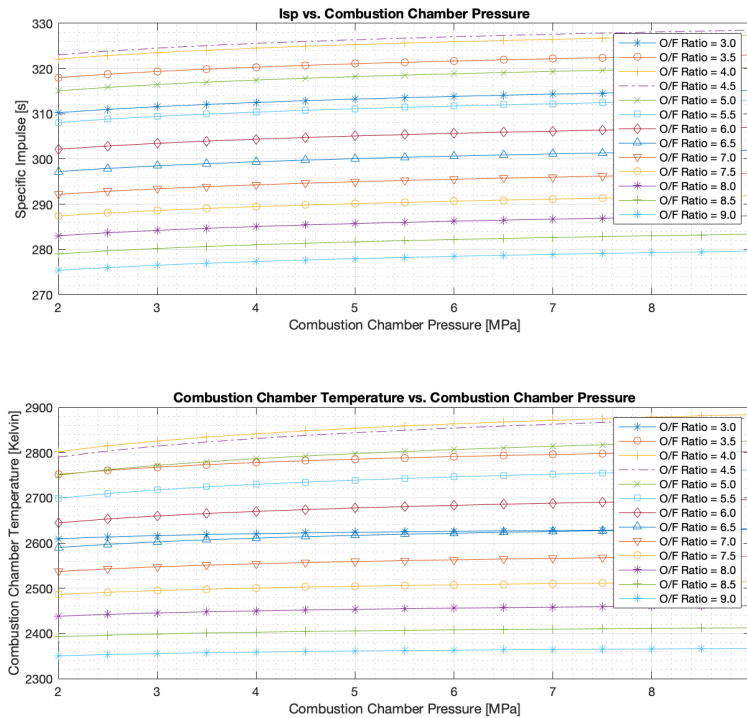


Figure 8.10: Specific Impulse and Combustion Chamber Temperature vs. Combustion Chamber Pressure for various O/F ratio's - Ethanol/H₂O₂

To find the most optimum combination of mixture ratio and combustion pressure the propellant optimisation analysis will be performed. This was done using the same method that was used for the DMAZ/H₂O₂ combination. The result of this optimisation is graphically depicted in Figure 8.11.

From Figure 8.11 it is clear that the most optimum combustion conditions (in terms of minimised wet mass) is found around a mixture ratio that lies between 4 and 5. Furthermore, the optimum wet mass location (darker areas) is skewed towards higher combustion chamber pressures. To find the best conditions while limiting the combustion chamber pressure and temperature as much as possible, as per the design constraints, the same optimisation tool (fmincon) will be applied. The most optimum combustion conditions for the ethanol/hydrogen peroxide mixture are indicated by the white asterisk in Figure 8.11. This point corresponds to the following conditions:

Optimum Conditions:

- O/F = 4.4
- $P_c = 8.3 \text{ MPa}$
- $I_{sp} = 329.30 \text{ s}$ (overall efficiency of combustion = 0.9567)

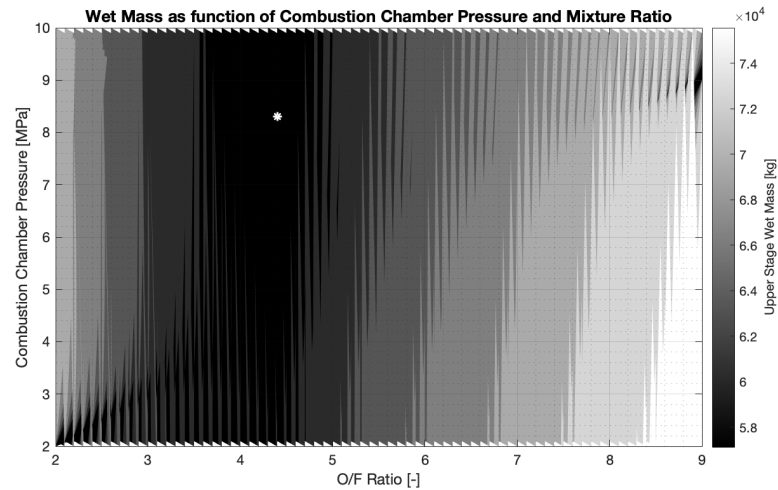
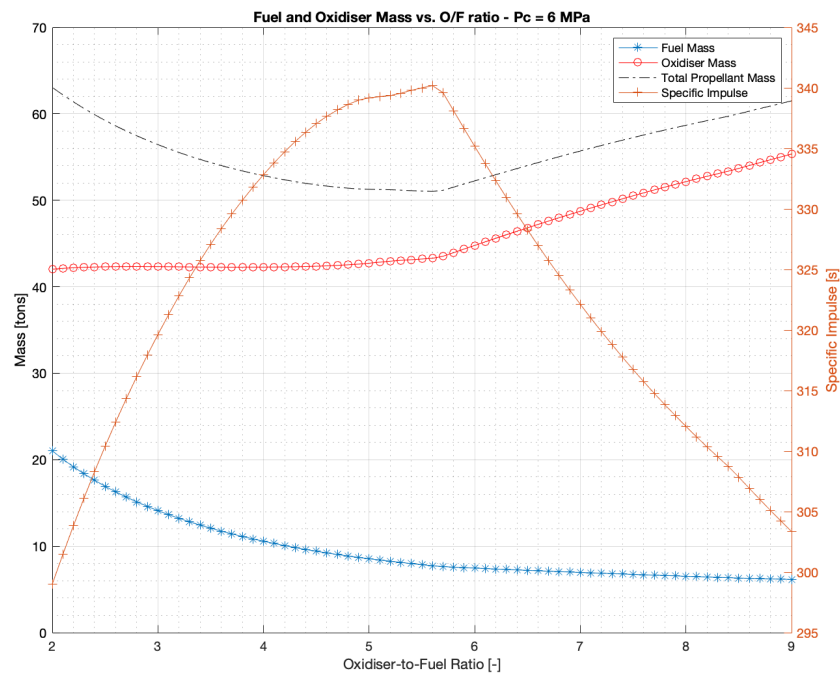


Figure 8.11: Propellant Optimisation Analysis - Ethanol/H2O2

Dimethylamine Optimisation Analysis

Again, to optimise the combustion conditions for dimethylamine first behaviour of the dimethylamine/H₂O₂ combination in terms of wet and dry mass will be investigated. This behaviour is graphically depicted in Figure 8.12. This gives a baseline for the optimum O/F ratio and the relative contribution of the fuel and oxidiser mass.

Figure 8.12: Dimethylamine and H₂O₂ Mass vs. O/F ratio under Fixed Combustion Chamber Pressure - $P_c = 6$ MPa

From Figure 8.12 there is a clear optimum in mixture ratio between 4.5 and 6. The effect of the mixture ratio on the dry/wet mass and the combustion chamber temperature is graphically depicted in Figure 8.13.

To optimise the dimethylamine/H₂O₂ combination the specific impulse and combustion chamber temperature will be plotted as a function of the combustion chamber pressure and the mixture ratio.

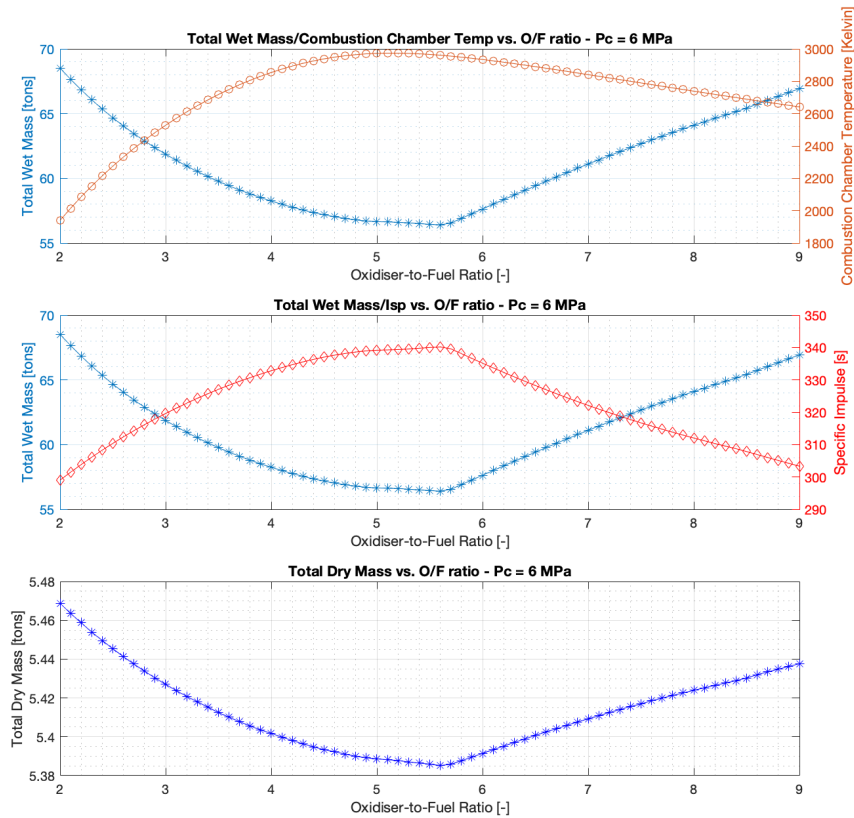


Figure 8.13: Specific Impulse, Combustion Chamber Temperature and Mass Behaviour vs. O/F ratio - Dimethylamine/H₂O₂

This is graphically depicted in Figure 8.14. From these graphs, it can be concluded that the specific impulse and combustion temperature increase for larger combustion chamber pressures.

To find the most optimum combination of mixture ratio and combustion pressure the propellant optimisation analysis will be performed. This was done using the same method that was used for the other two fuel types. The result of this optimisation is graphically depicted in Figure 8.15.

From Figure 8.15 it is clear that the most optimum combustion conditions (in terms of minimised wet mass) are found around a mixture ratio that lies between 4.5 and 6. Furthermore, the optimum wet mass location (darker areas) is skewed towards mid/higher combustion chamber pressures. To find the best conditions while limiting the combustion chamber pressure and temperature as much as possible the same optimisation tool (fmincon) will be applied. The most optimum combustion conditions for the dimethylamine/hydrogen peroxide mixture are indicated by the white asterisk in Figure 8.15. This point corresponds to the following conditions:

Optimum Conditions:

- $O/F = 5.6$
- $P_c = 8\text{ MPa}$
- $I_{sp} = 341.28$ (overall efficiency of combustion = 0.9564)

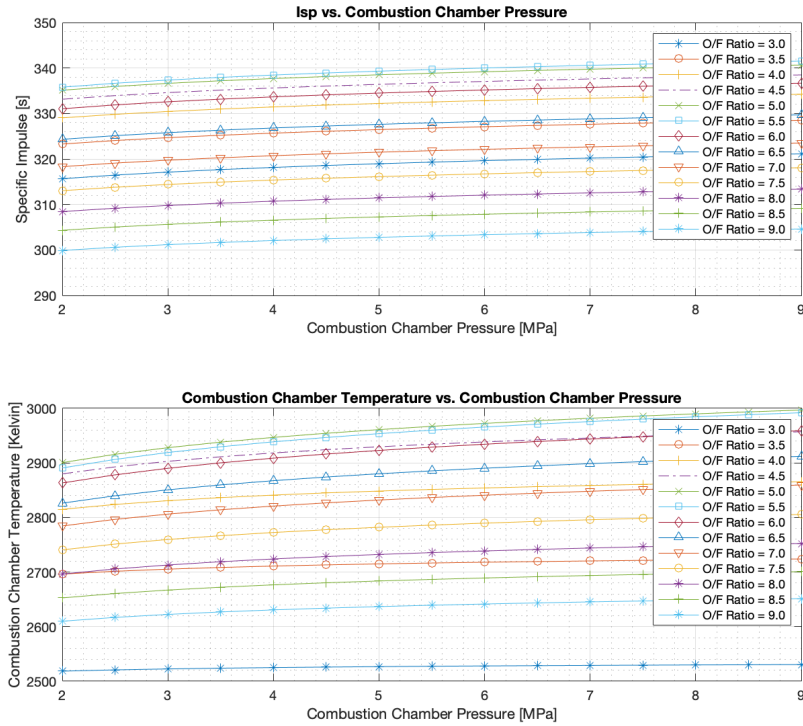


Figure 8.14: Specific Impulse and Combustion Chamber Temperature vs. Combustion Chamber Pressure for various O/F ratio's - Dimethylamine/H2O2

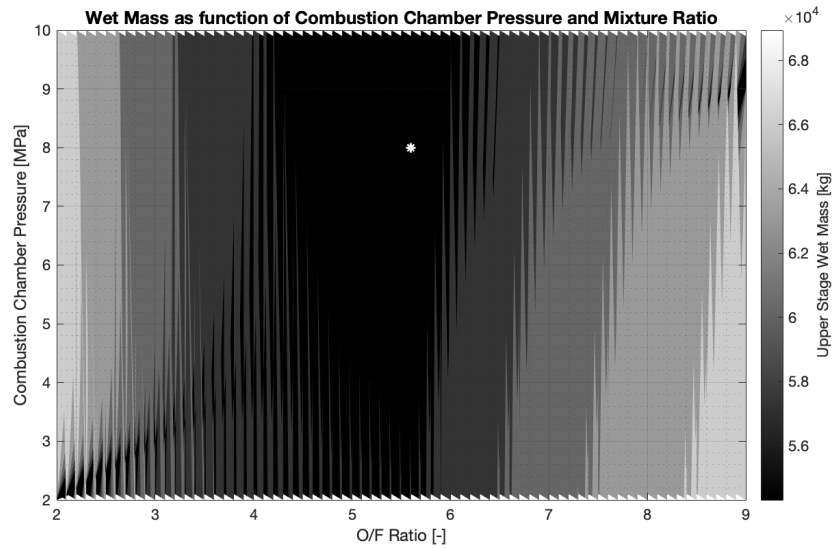


Figure 8.15: Propellant Optimisation Analysis - Dimethylamine/H2O2

8.2. Prototype X - Mass & Cost Analysis

The optimum combustion conditions that were found in the previous section will now be input to find the mass and cost estimates of the various components that "Prototype X" is comprised of. Since it was found that storable propellant implementation results in a significant wet mass increment, the cost and mass estimation are calculated for the maximum payload scenario. In chapter 7 it was found that

this is the only possible scenario in which storable propellants can be used, while maintaining payload capability. It is important to note that in this chapter the only significant design change for the “Prototype X” concepts is the type of propellants. Nothing in terms of the type of material, number of elements or dimensions is changed throughout the upcoming mass and cost analysis. This allows for one-to-one comparison with the conventional cryogenic Ariane 6 upper stage design. These design variables will be further investigated in chapter 9.

The mass and cost analysis will be done for the three selected fuels. First, the mass of the upper stage elements will be estimated. This is done by running the vehicle model iteratively, as discussed in chapter 5 and chapter 4. This process will give converged solutions that yield the mass breakdown of the separate elements. These mass fractions will be the input to the cost model to obtain cost estimates on the development, manufacturing and operation cost. Eventually, the cost-per-flight is obtained. It is important to note that these cost figures are estimates and do not model the actual cost of such a project with great accuracy. The individual broken-down cost contributions are given to serve as a comparison with the Ariane 6 upper stage design. Therefore the relative cost change (in percentage) with regards to the conventional cryogenic design is more insightful. In the cost analyses tabulated in the sections below, both the absolute cost estimate and the relative cost change, compared to the cryogenic design, are given.

8.2.1. Prototype X Cost Estimation - H2O2/DMAZ

The optimum mixture ratio for the H2O2 combination with DMAZ was identified to be 3.85. Together with a combustion chamber pressure of 7.9 MPa the optimal vacuum-specific impulse was found at 342.54 s . These combustion conditions will be put into the mass and cost model to obtain the corresponding mass breakdown of the elements. The propellant mass required is obtained through iteratively updating the dry mass of the upper stage. The mass breakdown of the upper stage elements, the corresponding first unit cost per element and the development cost are tabulated in Table 8.2. It is clear from the mass breakdown in Table 8.2a that the oxidizer tank has the biggest contribution to the total dry mass. Due to the oxidiser-rich mixture ratio of 3.85, this is as expected. Next are the interstage structure, thrust structure and fuel tank, respectively. Each with relatively large individual contributions to the total dry mass. The thermal control mass is relatively small, both in mass and estimated cost. This is due to the beneficial storage characteristics of the storable propellants. The thermal control mass is determined by the size of the tanks and the type of propellants. It is expected that in reality this element will have more mass than what is determined using the described vehicle model. Due to redundancy, and detailed design the mass of the actual thermal control subsystem is expected to be larger. Moreover, the fuel and oxidiser tank together amount to the biggest contribution in terms of the first unit estimated cost. In total, including 3.2% integration and testing cost for the stage, payload, avionics and attitude control (Stage I&T and PAA I&T), the total first unit has an estimated cost of approximately 14.2 M€ . This is approximately $\approx 13.8\%$ cost reduction compared to the conventional cryogenic design for the upper stage of the Ariane 6.

Table 8.2: First Unit Cost and Development Cost - H2O2/DMAZ

(a) “Prototype X” First Unit Cost					(b) “Prototype X” Development Cost				
Unit	Element	Mass [kg]	Flight Unit Cost [k€]	Cost Change [%]	Flight Unit Cost [k€]		Development Cost [k€]	Cost Change [%]	
ULPM	Fuel Tank	480	1,628	-60.0%	M&PA	Total	11,053	-13.8%	
	Oxidizer Tank	1,951	4,419	+40.9%		5.3%	M/PA	11,053	-13.8%
	Thrust Structure	806	1,252	+0.1%	ULPM	Total	14,196	212,896	-13.8%
	Thermal Control	12	27	-90.3%		Stage	12,790	191,806	-14.3%
	Engines	226	2,259	-23.4%		Interstage	997	14,952	-6.0%
	Thrust Vector Control	213	892	0.0%		3.2% Stage I&T	337	5,059	-16.5%
	Pipes & Valves	18	65	+14.0%		3.2% PAA I&T	72	1,079	-2.1%
	Avionics	113	2,248	-2.0%					
	Interstage	Interstage Structure	1559	997					
	Total UPLM	5,378	13,787	-13.8%					
I&T	3.2%								
	Stage I&T	-	337	-16.6%					
	PAA I&T	-	72	-2.7%					
	Total First Unit Cost [k€]		14,196	-13.8%					

Based on the first unit cost estimate the development cost are calculated, this is tabulated above in Table 8.2b. To obtain this development cost estimate the same parameters, that describe the development cost as a function of the first unit, are used. This was also done to calculate the development cost of the Ariane 6 upper stage design. These parameters include the design and development equivalent, the development effort, the level of subcontracted work and the development learning profit. These parameters are kept the same to allow for valid comparison. It is assumed that the implementation of green propellants will not yield a significant change in the development process nor in the amount of work that will be subcontracted out. The same goes for the learning curve. The materials and technologies used in the development effort for a storable design are not very new or different from the cryogenic design. Following these assumptions the development cost is determined. Including the 5.3% management and product assurance (M/PA) the total development cost is approximately 224M€, the ULPM stage (including integration and testing) having the largest contribution. Compared to the cryogenic upper stage design of the Ariane 6, this is a relative cost reduction of $\approx 13.8\%$.

The biggest contribution to the cost-per-flight is coming from the manufacturing cost. The manufacturing cost is estimated based on the first unit cost too. Again, the same parameters have been used for the storable upper stage concept as for the cryogenic upper stage. These parameters include the number of units that will be manufactured during the entire project. This is fixed at 50 units. The same learning curve factor of 0.97 as was used for the Ariane 6 manufacturing cost estimation is used to take into account the learning effect. The manufacturing breakdown is depicted in Table 8.3.

Table 8.3: "Prototype X" Manufacturing Cost - H2O2/DMAZ

		Flight Unit Cost [k€]	Manufac. Avg Unit Cost [k€]	Total Manufac. Cost [k€]	Cost Change [%]
		14,196	12,074	603,701	-13.8%
M&PA	Total		626	31,290	-13.8%
5.3%	M/PA		626	31,290	-13.8%
ULPM	Total	14,196	11,448	572,411	-13.8%
	Stage	12,790	10,314	515,706	-14.3%
	Interstage	997	804	40,199	-6.0%
3.2%	Stage I&T	337	272	13,604	-16.5%
3.2%	PAA I&T	72	58	2,902	-2.1%

In Table 8.3 the total manufacturing cost and the average manufacturing cost per unit is depicted. The total manufacturing cost of 50 upper stage units for the prototype x, with the H2O2/DMAZ combination, is estimated to be roughly 604M€. Again, the manufacturing cost is reduced for the storable design with regards to the cryogenic design. A cost reduction of $\approx 13.8\%$ is estimated.

The operation cost is very dependent on the design specification and the propellant selection. The operation cost is calculated by the set variables described in Table 6.7. Although most of these variables remained unchanged, like the launches per year, assembly and integration factor etc., some variables have been changed to model for the new propellant combination. For the H2O2/DMAZ combination the operation cost is determined by changing the following variables compared those described in Table 6.7:

- Vehicle Type Factor (f_v) = 0.8 (for storable propellants)
- Propellant Mass (M_p) = 50456.75 kg
- Gross Lift-Off Weight (GLOW) (M_0) = 55.84 Mg
- Mixture Ratio (r) = 3.85
- Payload Capacity (P) = 6426.48 kg

Furthermore, the price per kg for the fuel and oxidiser is required to calculate the propellant cost. As described in Table 7.23 the cost for hydrogen peroxide is $\text{€}0.80/\text{kg}$ [16]. For DMAZ it is currently not possible to formulate an accurate cost-per-kg figure. Because the fuel is currently still in development. The sparked interest in this fuel [123], [124] will most certainly result in stable demand in the future. In order to calculate the propellant cost a price-per-kg will be assumed for now. This assumption will probably be quite off from the actual price-per-kg in the future. This uncertainty is manageable as the

propellant cost per launch is often in the range of a few percentile points of the total cost-per-flight (0.5% – 1.5%). For now, a price-per-kg of €15/kg is assumed. This price-per-kg is significantly larger than for ethanol and dimethylamine, €0.40/kg and €0.49/kg respectively. This price is estimated by taking into account the current low availability, the chemical complexity and production process compared to other experimental fuels and by looking at the price of the required feed-stock [123], [124], [132]. Moreover, this relatively high cost-per-kg allows formulating a worst-case scenario in terms of the propellant cost. The operation cost breakdown is tabulated in Table 8.4.

Table 8.4: “Prototype X” Operating Cost - H2O2/DMAZ

Segment	Cost [k€]	Cost Change [%]
Direct Operating Cost	4,776	+5.3%
Ground Operations	2,135	+3.5%
Propellant Cost	188	+506.5%
Flight and Mission Operations	798	0.0%
Transportation Cost	300	+47.1%
Fees and Insurance Cost	1,355	-5.8%
Indirect Operating Cost	4,383	0.0%
Commercialization cost	4,383	0.0%
Total Operating Cost	9,159	+2.7%

It is found that the operation cost is increased by 2.7% compared to the conventional cryogenic upper stage design. The main reason for this operation cost increment is the larger wet mass (excluding payload) of the upper stage design. Due to the fact that the propellant combination is less efficient than the hydrolox combination more propellant mass is required. This added wet mass influences the ground operation cost, although the Vehicle Type Factor (f_v) is more cost-efficient for the storable propellants. The added propellant cost, although small in final contribution to the operation cost, is increased by $\approx 507\%$. The transportation cost is increased, again due to the larger wet mass of the upper stage. The fees and insurance cost fraction is reduced by 5.8%. This is directly the result of the smaller payload. Due to the larger wet mass, the storable upper stage is only capable to carry 6426 kg of payload, compared to the maximum payload of 21650 kg for the hydrolox design.

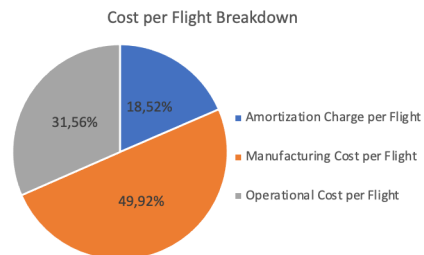
The cost-per-flight (CpF) is constructed from the individual contributions of the development cost, manufacturing cost and operation cost. This breakdown is depicted in Table 8.5.

Table 8.5: Cost-per-Flight Estimate for the Prototype X - H2O2/DMAZ

(a) Cost-per-Flight Breakdown

Contribution	Cost [k€]	Cost Change [%]
Amortization Charge per Flight	4,479	-13.8%
Manufacturing Cost per Flight	12,075	-13.8%
Operating Cost per Flight	9,159	+2.7%
Total Cost per Flight	25,713	-8.5%

(b) Cost-per-Flight Distribution



The development cost-per-flight is specified as “Amortization Charge per Flight” and amounts to 4.48M€ per flight or 18.52% of the CpF. The largest contribution to the CpF is the manufacturing cost-per-flight ($\approx 50\%$) which is approximately 12.1M€. The total Cost-per-Flight is approximately 25.7M€. This is a reduction in CpF of about 8.5% compared to the cryogenic upper stage design.

8.2.2. Prototype X Cost Estimation - H2O2/Ethanol

The second propellant combination that will be analysed is H2O2/Ethanol. The optimum specific impulse of 329.30 s is found at a combustion chamber pressure of 8.3 MPa and a mixture ratio of 4.4. The mass analysis was done with these optimum combustion condition parameters. The mass breakdown of the upper stage elements and the corresponding first unit cost of the storable upper stage with the

H₂O₂/Ethanol combination is tabulated in Table 8.6a. It is found that again large mass reductions are obtained for the fuel tank and the thermal control subsystem. Including the I&T for the stage and PAA the dry mass of the H₂O₂/ethanol storable upper stage design is 5412 kg. This amounts to a first unit cost of 14.3M€. This is approximately a reduction of 13.3% compared to the conventional hydrolox design. The development cost, depicted in Table 8.7b, has the same cost reduction. The total development cost is ≈ 225.3M€. Although the specific impulse of H₂O₂/DMAZ is significantly higher specific impulse (+4%) this only results in a relative cost-benefit of 0.2% compared to the H₂O₂/ethanol combination.

Table 8.6: First Unit Cost and Development Cost - H₂O₂/Ethanol

(a) "Prototype X" First Unit Cost					(b) "Prototype X" Development Cost						
Unit	Element	Mass [kg]	Flight Unit Cost [k€]	Cost Change [%]	Flight Unit Cost [k€]			Development Cost [k€]		Cost Change [%]	
ULPM	Fuel Tank	512	1,704	-58.1%	14,279			225,267		-13.3%	
	Oxidizer Tank	1,952	4,420	+40.9%							
	Thrust Structure	806	1,251	0.0%							
	Thermal Control	13	29	-89.6%							
	Engines	226	2,26	-23.4%							
	Thrust Vector Control	213	892	0.0%							
	Pipes & Valves	18	66	+15.8%							
	Avionics	113	2,248	-2.0%							
	Interstage	Interstage Structure	1559	997							
		Total UPLM	5,412	13,866	-13.3%						
I&T			3.2%								
	Stage I&T	-	340	-15.8%							
	PAA I&T	-	72	-2.7%							
	Total First Unit Cost [k€]		14,279	-13.3%							
					M&PA Total			11,118		-13.3%	
					5.3% M/PA			11,118		-13.3%	
					ULPM Total			14,279		-13.3%	
					Stage			12,870		-13.8%	
					Interstage			997		-6.0%	
					3.2% Stage I&T			340		-15.9%	
					3.2% PAA I&T			72		-2.1%	

The manufacturing cost is calculated using the same approach as was applied for the hydrolox and H₂O₂/DMAZ combination, as discussed above. The manufacturing cost estimate is depicted in Table 8.7. The manufacturing cost for 50 units of H₂O₂/ethanol optimised upper stage design is expected to cost approximately 607.3M€, or 12.15M€ per unit produced. This is a cost reduction of 13.3% compared to the conventional hydrolox upper stage design.

Table 8.7: "Prototype X" Manufacturing Cost - H₂O₂/Ethanol

		Flight Unit Cost [k€]	Manufac. Avg Unit Cost [k€]	Total Manufac. Cost [k€]	Cost Change [%]
		14,279	12,145	607,255	-13.3%
M&PA	Total		630	31,475	-13.3%
5.3%	M/PA		630	31,475	-13.3%
ULPM	Total	14,279	11,516	575,780	-13.3%
	Stage	12,870	10,379	518,970	-13.8%
	Interstage	997	804	40,199	-6.0%
3.2%	Stage I&T	340	274	13,708	-15.9%
3.2%	PAA I&T	72	58	2,903	-2.1%

The operation cost is largely dependent on the vehicle design and propellant selection. The variables discussed in Table 6.7 will be used to determine the individual cost contributions that make up the operation cost. Following a similar procedure as explained in the previous subsection, the following variables are specified for the H₂O₂/ethanol combination:

- Vehicle Type Factor (f_v) = 0.8 (for storable propellants)
- Propellant Mass (M_p) = 53768.86 kg
- Gross Lift-Off Weight (GLOW) (M_0) = 59.181 Mg
- Mixture Ratio (r) = 4.4
- Payload Capacity (P) = 3080.83 kg

Furthermore, the price per kg for the fuel and oxidiser is required to calculate the propellant cost. As described in Table 7.23 the cost for hydrogen peroxide is €0.80/kg [16] and the cost for ethanol is €0.40/kg [47]. The operation cost breakdown is tabulated in Table 8.8.

Table 8.8: "Prototype X" Operating Cost - H₂O₂/Ethanol

Segment	Cost [k€]	Cost Change [%]
Direct Operating Cost	4,712	+3.9%
Ground Operations	2,220	+7.7%
Propellant Cost	39	+25.8%
Flight and Mission Operations	798	0.0%
Transportation Cost	318	+55.9%
Fees and Insurance Cost	1,337	-7.1%
Indirect Operating Cost	4,383	0.0%
Commercialization cost	4,383	0.0%
Total Operating Cost	9,095	+2.0%

The operating cost is 2% larger compared to the conventional hydrolox upper stage design. The reason for this is the higher ground operations and transportation cost of the upper stage section. Due to the implementation of the storable propellants the wet mass of the upper stage increased. The lower payload capability of 3079.39 kg results in a reduction of cost for "fees and insurance". The relative increase in propellant cost for the H₂O₂/Ethanol combination is far less than what was found for the H₂O₂/DMAZ combination. In total the operating cost amount to approximately 9.1M€ per launch.

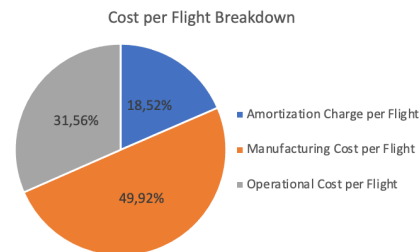
The contributions of the development, manufacturing and operation cost determine the final Cost-per-Flight of the upper stage module. This is depicted in Table 8.9.

Table 8.9: Cost-per-Flight Estimate for the Prototype X - H₂O₂/Ethanol

(a) Cost-per-Flight Breakdown

Contribution	Cost [k€]	Cost Change [%]
Amortization Charge per Flight	4,505	-13.3%
Manufacturing Cost per Flight	12,146	-13.3%
Operating Cost per Flight	9,095	+2.0%
Total Cost per Flight	25,746	-8.4%

(b) Cost-per-Flight Distribution



The amortization charge per flight is approximately 4.51M€, the manufacturing cost-per-flight is 12.15M€ and operation cost is 9.16M€ per flight. These charges combined result in a total Cost-per-Flight of 25.7M€. This is a cost change of -8.5% compared to the CpF of the hydrolox system. The amortization charge is approximately 18.5% of the total CpF. The manufacturing and operation cost-per-flight are approximately 49.9% and 31.6% of the total CpF.

8.2.3. Prototype X Cost Estimation - H₂O₂/Dimethylamine

The third propellant combination that will be analysed is H₂O₂/Dimethylamine. The optimum combustion conditions have been identified. At a combustion chamber pressure of 8.0 MPa and a mixture ratio of 5.6 the specific impulse is 341.28 s. The mass analysis was done at the optimum combustion condition. The mass breakdown of the upper stage elements and the corresponding first unit cost of the storable upper stage with the H₂O₂/Ethanol combination is tabulated in Table 8.10a. Including the I&T for the stage and PAA the dry mass of the H₂O₂/Dimethylamine storable upper stage design is 5403 kg. This amounts to a first unit cost of 14.2M€. This is approximately a reduction of 13.5% compared to the conventional hydrolox design. The development cost, depicted in Table 8.10b, has the same cost reduction. The total development cost is ≈ 224.7M€.

Table 8.12: "Prototype X" Operating Cost - H2O2/Dimethylamine

Segment	Cost [k€]	Cost Change [%]
Direct Operating Cost	4,635	+2.2%
Ground Operations	2,144	+4.0%
Propellant Cost	38	+22.6%
Flight and Mission Operations	798	0.0%
Transportation Cost	301	+47.5%
Fees and Insurance Cost	1,353	-6.0%
Indirect Operating Cost	4,383	0.0%
Commercialization cost	4,383	0.0%
Total Operating Cost	9,017	+1.1%

The operating cost is 1.1% larger compared to the conventional hydrolox upper stage design. The reason for this is the increased wet mass due to the implementation of the storable propellants. The lower payload capability of 6066.78 kg results in a reduction of cost for "fees and insurance". In total the operating cost amount to approximately 9.0M€ per launch.

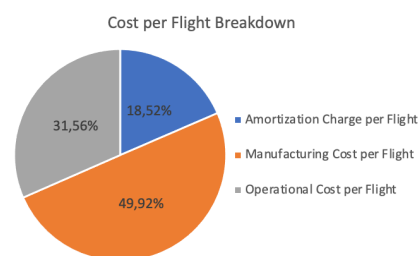
The contributions of the development, manufacturing and operation cost determine the final Cost-per-Flight of the upper stage module. This is depicted in Table 8.13.

Table 8.13: Cost-per-Flight Estimate for the Prototype X - H2O2/Dimethylamine

(a) Cost-per-Flight Breakdown

Contribution	Cost [k€]	Cost Change [%]
Amortization Charge per Flight	4,494	-13.5%
Manufacturing Cost per Flight	12,116	-13.5%
Operating Cost per Flight	9,017	+1.1%
Total Cost per Flight	25,627	-8.9%

(b) Cost-per-Flight Distribution



The amortization charge per flight is approximately 4.49M€, the manufacturing cost-per-flight is 12.11M€ and operation cost is 9.0M€ per flight. These charges combined result in a total Cost-per-Flight of 25.6M€. This is a cost change of -8.9% compared to the CpF of the hydrolox system. The amortization charge is approximately 18.5% of the total CpF. The manufacturing and operation cost-per-flight are approximately 49.9% and 31.6% of the total CpF.

It is important to note that the cost analysis performed in this section was done using the cost model described in chapter 6. This model was developed by N. Drenthe [83] and was validated to estimate the development cost, manufacturing cost and operating cost within $\pm 20\%$ of the reported cost [83], [113]. The cost figures presented in this chapter are therefore subjected to this error of $\pm 20\%$ and are visualised in the graphs using error bars.

8.2.4. Sensitivity Analysis

The three most prominent design variables; specific impulse, density of the fuel and the mixture ratio, that have been determined during the propellant selection all have an impact on the mass and cost analysis. To investigate the sensitivity of the obtained results to these design parameters a sensitivity analysis was done. In this section, the sensitivity of the dry mass, wet mass and the cost-per-flight on these design variables are analysed. The sensitivity analysis is done using the first propellant combination discussed; H2O2/DMAZ. The outcome of the sensitivity analysis for the combination of H2O2/DMAZ will be insightful and representable for the other propellant combinations too.

First, the impact of these prominent design variables on the dry mass is tabulated in Table 8.14.

Table 8.14: Sensitivity Analysis on Storable Upper Stage Dry Mass

Parameter	Dry Mass Decreasing	Nominal	Dry Mass Increasing
Vacuum Specific Impulse [s]	370.00	342.54	310.00
Dry Mass [kg]	5,344.27	5,378.30	5,428.66
Percentage Change	-0.63%	-	+0.94%
Density Fuel [kg/m ³]	1300	993	600
Dry Mass [kg]	5,363.41	5,378.30	5,414.63
Percentage Change	-0.28%	-	+0.67%
Mixture Ratio [-]	5.00	3.85	3.00
Dry Mass [kg]	(Increasing) 5,407.81	5,378.30	5,381.10
Percentage Change	+0.06%	-	+0.05%

From Table 8.14 it can be deduced that the dry mass is only mildly affected by changing the design variables. The impact on the dry mass observed ranges between -0.63% – 0.94% . The (vacuum) specific impulse has the largest contribution to this sensitivity. The dry mass of the storable upper stage design is least sensitive to changes in the mixture ratio. The density of the fuel has a moderate effect on the dry mass sensitivity. These findings can be explained by looking at the propellant tanks. The specific impulse is a measure of propellant efficiency. A higher specific impulse yields less required propellants, thus a smaller tank mass. Higher density fuels amount to a smaller required volume for storage, again this result in a smaller dry mass due to the smaller tanks. The mixture ratio affects both the specific impulse and the relative volumetric ratio between the oxidiser and the fuel tank. Since the payload capability is dependent on the dry mass and total required propellant mass, the wet mass will be subject to sensitivity analysis in Table 8.15.

Table 8.15: Sensitivity Analysis on Storable Upper Stage Wet Mass

Parameter	Wet Mass Decreasing	Nominal	Wet Mass Increasing
Vacuum Specific Impulse [s]	370.00	342.54	310.00
Wet Mass [kg]	50,079.67	55,835.05	64,744.45
Percentage Change	-10.31%	-	+15.96%
Density Fuel [kg/m ³]	1300	993	600
Wet Mass [kg]	55,792.42	55,835.05	55,938.86
Percentage Change	-0.08%	-	+0.19%
Mixture Ratio [-]	5.00	3.85	3.00
Wet Mass [kg]	(Increasing) 61,031.20	55,835.05	56,457.91
Percentage Change	+9.31%	-	+1.12%

The effect of propellant efficiency, measured by specific impulse, on the wet mass is visible in Table 8.15. Changing the specific impulse by -9.5% and $+8\%$ results in a significant wet mass change of -10.31% and $+15.96\%$ respectively. The density of the fuel does not significantly impact the wet mass of the storable upper stage design. The density of the fuel does only affect the required volume for the propellants. Furthermore, changing the mixture ratio results in a significant response on wet mass. Changing the mixture ratio by $+30\%$ and -22% results in a wet mass change of $+9.31\%$ and $+1.12\%$ respectively. The mixture ratio both affects the specific impulse of the propellant combination and the ratio of oxidiser and fuel. To investigate how these changes affect the cost-per-flight, a sensitivity analysis on CpF is conducted. This is tabulated in Table 8.16.

Table 8.16: Sensitivity Analysis on Storable Upper Stage Cost-per-Flight

Parameter	Cost Decreasing	Nominal	Cost Increasing
Vacuum Specific Impulse [s]	370.00	342.54	310.00
Cost-per-Flight [k€]	25,438	25,713	26,124
Percentage Change	-1.07%	-	+1.60%
Density Fuel [kg/m ³]	1300	993	600
Cost-per-Flight [k€]	25,612	25,713	25,914
Percentage Change	-0.39%	-	+0.78%
Mixture Ratio [-]	5.00	3.85	3.00
Cost-per-Flight [k€]	(Increasing) 25,857	25,713	25,814
Percentage Change	+0.56%	-	+0.39%

The Cost-per-Flight (CpF) is mostly dependent on the dry mass. The first unit cost, development

cost and manufacturing cost are all dependent on the dry mass of the upper stage elements. This effect is clearly shown in Table 8.16. The relative sensitivity of the CpF is comparable to what was found for the dry mass sensitivity analysis of Table 8.14. The CpF is most sensitive to the operation cost. This is dependent on the propellant mass and wet mass of the upper stage vehicle.

Combining the sensitivity analysis on wet mass and the CpF it can be concluded that the CpF is not much affected by the change in wet mass. Although not significantly represented in the CpF (due to the small contribution of propellant cost) the wet mass is however a very important parameter to take into account for the design. The wet mass of the upper stage design determines the remaining payload capability. The remaining payload capability and the corresponding cost-per-kg of these payload scenarios will be discussed in the next section.

8.3. Payload Capability and Mission Characteristics

In this section, the payload capability and the corresponding payload cost-per-kg, or payload performance, for the various upper stage designs will be discussed. First, the cost breakdown for the selected upper stage designs will be compared. This helps to trace back the cost distribution for the storable concepts when compared to the conventional cryogenic upper stage design. The cost contributions per flight from the development, manufacturing and operation cost are summarised in Table 8.17. The amortization charge, manufacturing cost-per-flight and operation cost-per-flight are tabulated for both the Ariane 6 upper stage design as well for the "Prototype X" upper stage with the selected propellant combinations.

Table 8.17: Cost Breakdown for Selected Upper Stage Designs

Vehicle Design - Propellant Combination	Amortization Charge [k€]	Manufacturing Cost per Flight [k€]	Operation Cost [k€]
Ariane 6 Upper Stage - LO2/LH2	5,195	14,004	8,917
Prototype X - H2O2/DMAZ	4,479	12,075	9,159
Prototype X - H2O2/Ethanol	4,505	12,146	9,095
Prototype X - H2O2/Dimethylamine	4,494	12,116	9,017

From Table 8.17 it is clear that the amortization charge and manufacturing cost-per-flight is in all cases lower for the "Prototype X" design compared to the Ariane 6 upper stage. The operation cost-per-flight, however, is lower in all cases for the Ariane 6 upper stage, compared to the "Prototype X" concepts. The total cost-per-flight is constructed from this cost breakdown and is tabulated below in Table 8.18.

Table 8.18: CpF Comparison Between Selected Upper Stage Designs

Vehicle Design - Propellant Combination	Cost-per-Flight [k€]
Ariane 6 Upper Stage - LO2/LH2	28,116
Prototype X - H2O2/DMAZ	25,713
Prototype X - H2O2/Ethanol	25,746
Prototype X - H2O2/Dimethylamine	25,627

The cost-per-Flight is, as discussed in the previous section, lower in all cases for the "Prototype X" concept with the various propellant combinations. To graphically show the comparison between the concept designs and the Ariane 6 upper stage design, the cost breakdown of the various cost contributions is graphically depicted in Figure 8.16. Here the error bars of $\pm 20\%$, as discussed earlier, are illustrated too.

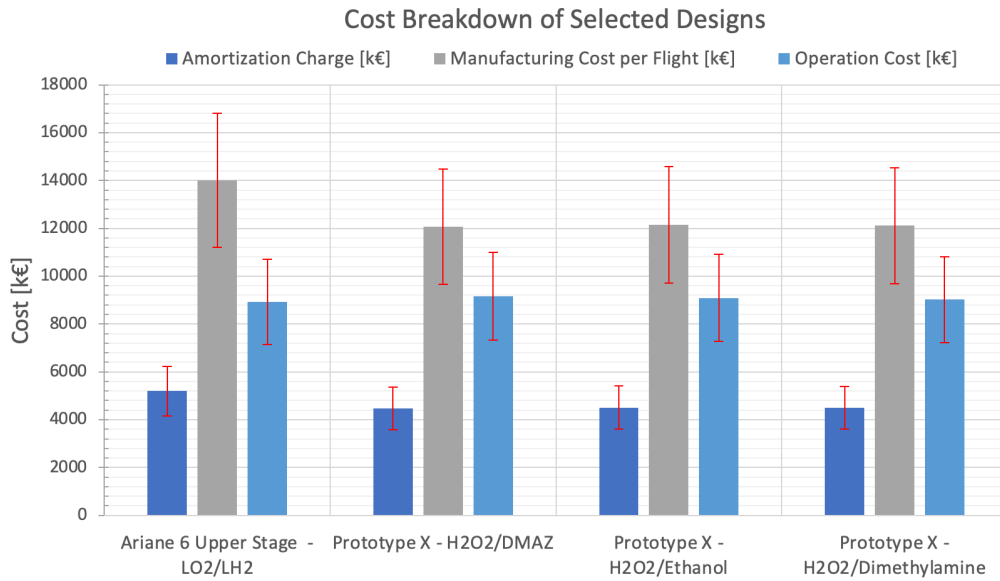


Figure 8.16: Cost Breakdown Comparison for Selected Upper Stage Designs

The cost-per-flight (CpF) is graphically depicted in Figure 8.17. This graph shows how the CpF of the storable design concepts for the “Prototype X” compare with the conventional cryogenic Ariane 6 upper stage design.

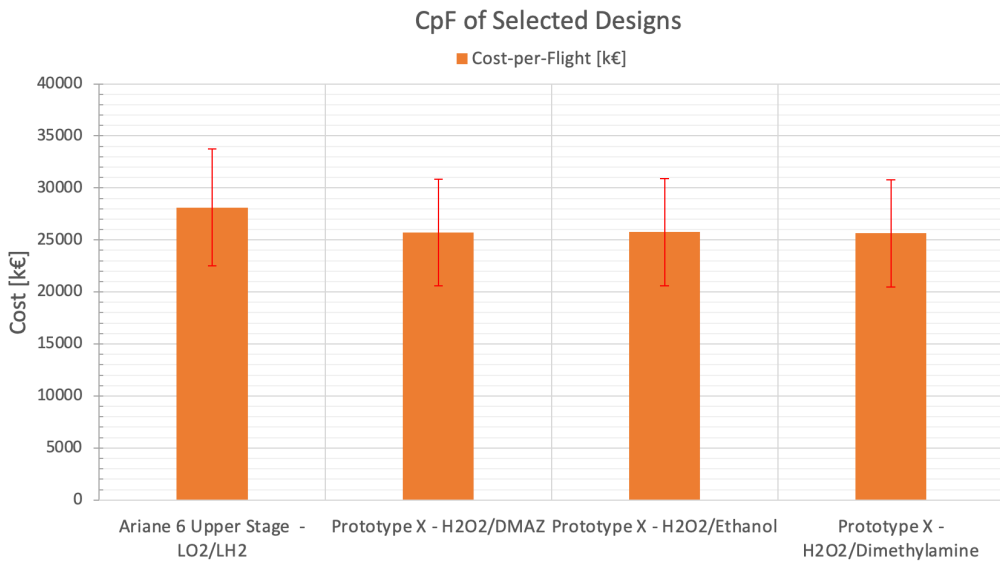


Figure 8.17: CpF Graphical Comparison Between Selected Upper Stage Designs

A very important design parameter is the wet mass of the upper stage vehicle. Since the propellant cost is only a small contribution to the CpF, the CpF does not fully paint the picture of the impact storable propellants have on the wet mass. The wet mass determines the amount of payload mass that still can be brought to space assuming that the first stage will be unaltered in terms of thrust to weight performance. To understand how the CpF of the various “Prototype X” concepts compare, it is useful to determine the payload capability. Although the CpF for the storable designs is lower than that of the cryogenic design, it is found in chapter 7 that the wet mass is significantly increased by the implementation of the new propellants. This is the direct result of the lower specific impulse that is achieved by the storable propellant combinations. This increase in wet mass will thus affect the amount of payload mass still available to be carried. This is called the payload capability. To correctly compare the cryogenic design with the storable designs it is, therefore, necessary to compare both the payload

capability and the CpF. This can be done by analyse the cost-per-kg of payload for each of the design options.

First, the available payload capability should be determined for all design concepts. This is done by comparing the increased wet mass for the “Prototype X” with the maximum payload that the Ariane 6 upper stage is designed to carry. The Ariane 6 wet mass will be the baseline for this comparison. The remaining mass above this wet mass increment is the available payload capability. This is graphically depicted in Figure 8.18.

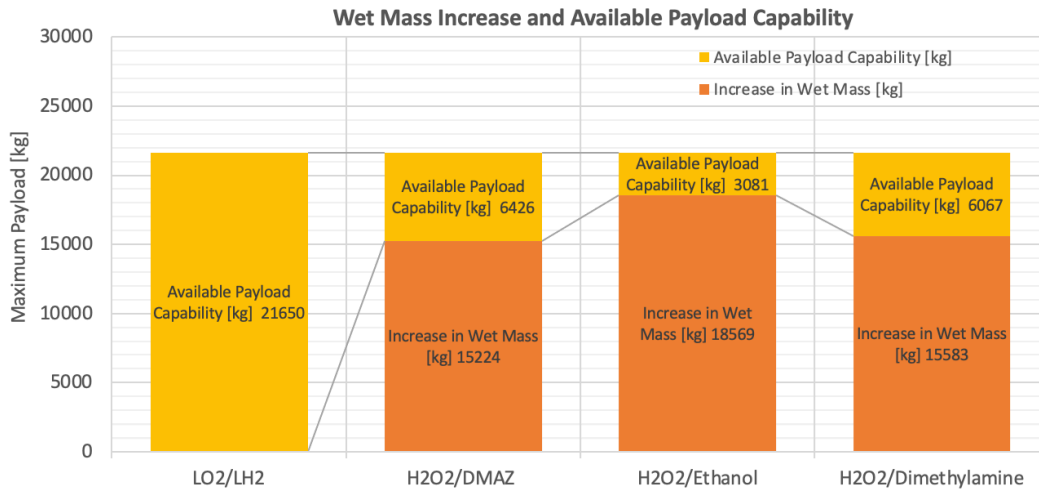


Figure 8.18: Wet Mass Increase and Available Payload Capability for Selected Propellant Combinations

From Figure 8.18 it is clear how the available payload capabilities of the “Prototype X” concept vehicle relate with the maximum payload capability of the Ariane 6 upper stage. The following payload capabilities for the storable fuels are found:

- DMAZ = 6426.48 kg
- Ethanol = 3080.83 kg
- Dimethylamine = 6066.77 kg

The individual payload mass each of the “Prototype X” designs can carry is graphically depicted in Figure 8.19. Here the payload capabilities are compared to the payload capability of the Ariane 6 upper stage design, which can carry 21650 kg of payload into LEO orbit.

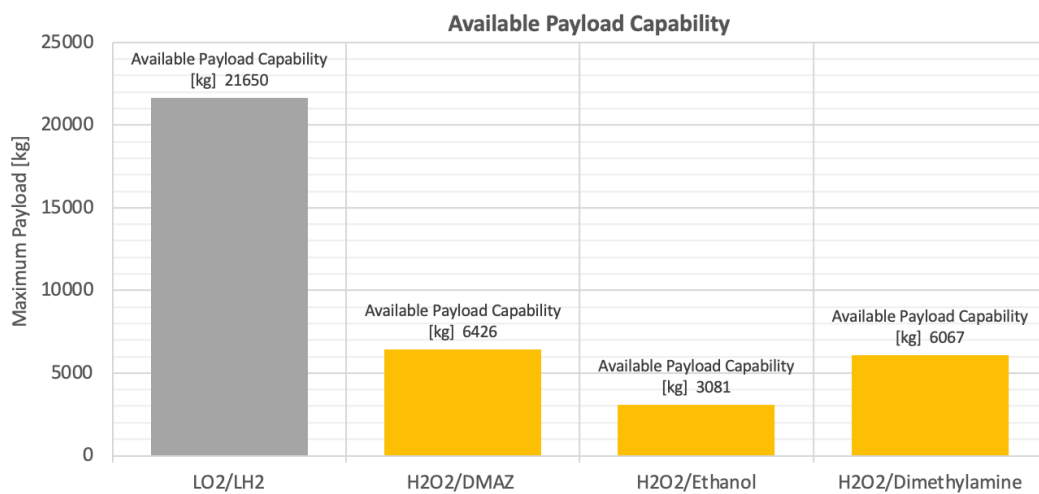


Figure 8.19: Available Payload Capability for Selected Propellant Combinations, Compared to Conventional Hydrolox Combination

Sensitivity Analysis

The payload capability is primarily affected by the specific impulse, density and the mixture ratio of the propellants. To investigate the sensitivity of the payload capability to these parameters, a sensitivity analysis is performed. Similar to the sensitivity analysis of Table 8.14, Table 8.15 and Table 8.16 the sensitivity analysis will give insight into the most efficient ways of optimising the payload capability. The sensitivity analysis is tabulated below in Table 8.19.

Table 8.19: Sensitivity Analysis for Payload Capability

Parameter	Payload Decreasing	Nominal	Payload Increasing
Vacuum Specific Impulse [s]	310.00	342.54	370.00
Payload Capability [kg]	-2,482.92	6,426.48	12,181.86
Percentage Change	-138.64%	-	+89.56%
Density Fuel [kg/m ³]	600	993	1300
Payload Capability [kg]	6,086.01	6,426.48	6,469.11
Percentage Change	-5.30%	-	+0.66%
Mixture Ratio [-]	5.00	3.85	3.00
Payload Capability [kg]	1,230.33	6,426.48 (Decreasing)	5,803.62
Percentage Change	-80.85%	-	-9.69%

Changing the specific impulse of the propellant combination has a significant impact on the payload capability. Changing the specific impulse by -9.5% and $+8.0\%$ results in a -138.64% and $+89.56\%$ respectively. Furthermore, changing the density of the fuel has a limited effect on the dry mass of the upper stage module. The impact of reducing the density of the fuel is larger than increasing the density, -5.30% and $+0.66\%$ respectively. Changing the mixture ratio affects both the relative mass and volume distribution of the propellants as well as the vacuum-specific impulse that can be attained. Changing the mixture ratio by $+29.9\%$ and -22.1% results in a payload decrease of -80.9% and 9.70% respectively.

Now that the payload capabilities are known the mission characteristics can be investigated. This is done by looking at the mission characteristics that have been determined for the Ariane 6 launch vehicle [11]. The mission characteristics describe the amount of payload that can be carried to the type of orbit, specified by altitude and inclination. These payload capabilities and mission characteristics are calculated using the same method as described above. The following mission characteristics per propellant combination have been found:

Mission Characteristics “Prototype X” - H₂O₂/DMAZ Combination

- Low Earth Orbit (LEO) = 6426 kg at 300 km ($i = 5^\circ$) [11]
- Sun Synchronous Orbit (SSO) = 276 kg at 900 km ($i = 97.4^\circ$) [11]
- Polar Orbit = 176 kg at 900 km ($i = 90^\circ$) [11]
- ISS Servicing = 4776 kg at 250 km ($i = 51.6^\circ$) [11]

Mission Characteristics “Prototype X” - H₂O₂/Ethanol Combination

- Low Earth Orbit (LEO) = 6426 kg at 300 km ($i = 5^\circ$) [11]
- ISS Servicing = 1431 kg at 250 km ($i = 51.6^\circ$) [11]

Mission Characteristics “Prototype X” - H₂O₂/Dimethylamine Combination

- Low Earth Orbit (LEO) = 6067 kg at 300 km ($i = 5^\circ$) [11]
- ISS Servicing = 4417 kg at 250 km ($i = 51.6^\circ$) [11]

Now that the CpF and payload capabilities have been determined for each of the storable design concepts, it is possible to construct the payload cost-per-kg for each of the design. For this analysis the maximum payload capability will be used. This corresponds to the Low Earth Orbit (LEO) mission characteristics, as described above. Again, this is compared to the Ariane 6 upper stage. The CpF, payload capability and cost-per-kg is tabulated in Table 8.20. In the furthest right column the relative change of the cost-per-kg is calculated, compared to the Ariane 6 upper stage cost-per-kg.

Table 8.20: Cost-per-Kg per Upper Stage Design

Vehicle Design - Propellant Combination	Cost-per-Flight [k€]	Payload Capability [kg]	Cost-per-kg [€/kg]	Relative Change [%]
Ariane 6 Upper Stage - LO2/LH2	28,116	21,650	1298.66	-
Prototype X - H2O2/DMAZ	25,713	6,426	4001.10	+308.09%
Prototype X - H2O2/Ethanol	25,746	3,080	8356.85	+643.50%
Prototype X - H2O2/Dimethylamine	25,627	6,066	4224.16	+325.27%

To graphically compare the results of the cost-per-kg characteristics of each design, the findings are schematically shown in Figure 8.20.

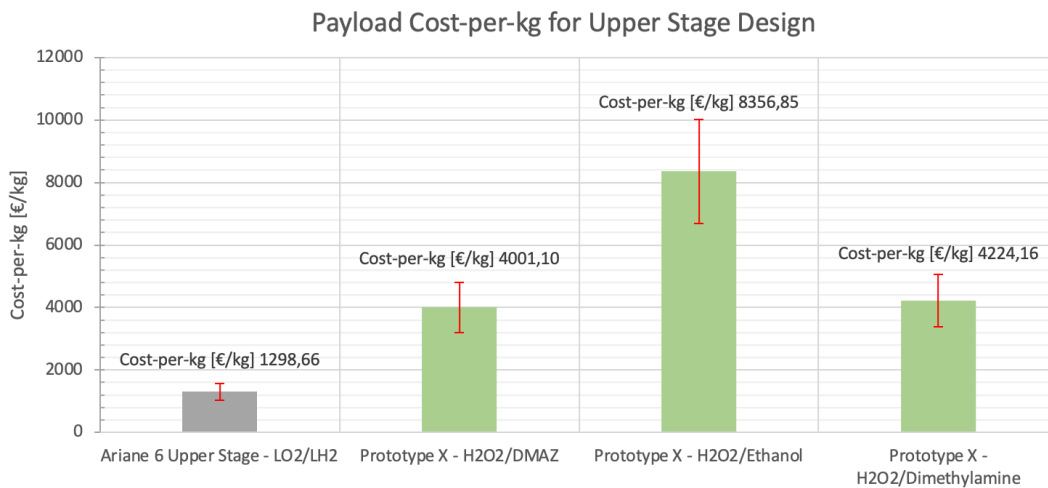


Figure 8.20: Graphical Comparison between the Cost-per-Kg of Upper Stage Designs

From both Table 8.20 and Figure 8.20 it can be concluded that the cost-per-kg is in all cases significantly increased for the “Prototype X” storable upper stage design concepts. The cost-per-kg for the H2O2/DMAZ propellant combination is +308% of the conventional cryogenic cost-per-kg. This is the best payload performance found among the storable propellant combinations. The worst payload performance can be attributed to H2O2/Ethanol. This combination sees a +644% rise in cost-per-kg. The H2O2/Dimethylamine combination lies somewhere in between these figures with a relative cost-per-kg increment of +325%.

8.4. Current Market Outlook Analysis

To understand the fitness of the “Prototype X” design in the current market of medium to heavy-sized launch vehicles it is necessary to do a market outlook analysis. In this analysis the calculated payload performance for “Prototype X” concepts will be compared to currently available launch vehicles on the market. This market outlook research gives insight into the competitiveness of other launch systems.

In the previous section, the cost-per-kg was determined for the “Prototype X” conceptual upper stage designs. The launch capability and the cost-per-flight were calculated for the three selected fuels; DMAZ, Ethanol and Dimethylamine. This allowed to calculate the cost-per-kg for these propellant combinations. These payload performance figures were compared to the Ariane 6 upper stage cost-per-kg characteristic. It was found that the cost-per-kg figure of the storable upper stage concepts experiences a relative cost increment of at least +308% compared to the Ariane 6 upper stage. This result clearly shows that the storable upper stage design (for integration with Ariane 6), currently, is not preferred from a financial point of view.

To understand how the payload performance characteristic of storable upper stage designs compare to current launchers it is important to first integrate the “Prototype X” upper stage with the cryogenic first stage of Ariane 6. This allows for proper cost-per-kg comparison between the integrated Ariane 6

launch vehicle and the hybrid launch vehicle constructed out of the first stage of the Ariane 6 and the “Prototype X” storable upper stage. This comparison is tabulated in Table 8.21.

Table 8.21: Cost-per-Kg Analysis of Integrated Prototype X Designs

Modelled Launch Vehicles (Excluding Boosters)	Upper Stage Propellants	Payload to LEO [kg]	Cost-per-Flight [M€]	k€/kg (2021)
Ariane 6 LLPM + Ariane 6 ULPM	LO2/LH2	21650	111.51 (2021)	5.15
Ariane 6 LLPM + Prototype X	H2O2/DMAZ	6426	109.21 (2021)	16.99
Ariane 6 LLPM + Prototype X	H2O2/Ethanol	3080	109.26 (2021)	35.47
Ariane 6 LLPM + Prototype X	H2O2/Dimethylamine	6066	109.12 (2021)	17.99

In the analysis, described in Table 8.21 above, the integrated launch vehicle, comprised of the cryogenic first stage with the storable “Prototype X” upper stage, is compared with the integrated Ariane 6 first and upper stage. It is important to note that these cost-per-flight figures correspond to what was found in chapter 6 and thus do not accurately reflect the actual cost-per-flight. Primarily because this cost-per-flight figure does not include the cost of the boosters nor does it take into account the extensive funding capital provided by European Union member states. Even though this makes it harder to compare the conceptual designs one-to-one with the current launch vehicle market, it does allow to compare the payload performance in terms of the “order of magnitude” scale. However, from Table 8.21 the modelled cost-per-kg characteristics of the conventional Ariane 6 launch vehicle and the hybrid launch vehicle can one-to-one be compared. It is clear that the hybrid launch vehicle will increase the cost-per-kg in the best case scenario by +329.90%. This is comparable to what was found for the payload performance of the upper stage designs.

To see if these designs compare to the current medium to heavy launch vehicle market a market outlook analysis has been done. This is tabulated in Table 8.22.

Table 8.22: Current Medium/Heavy Launch Vehicle Market

Launch Vehicle	Type	Payload to LEO [kg]	Cost-per-Flight (2021) [M€]	k€/kg (2021)	Reference
Ariane 5G	Expendable	21,000	167.69	7.99	[150]
Falcon 9	Partially Reusable	22,800	56.60	2.48	[150]
Falcon Heavy	Partially Reusable	63,800	82.10	1.29	[150]
Ariane 6	Expendable	21,650	115.00	5.31	[11], [90]
Atlas V 551	Expendable	18,850	176.66	9.37	[151]
Delta IV Heavy	Expendable	28,790	319.45	11.00	[152]
Long March 3B	Expendable	11,500	66.12	5.75	[150]
Proton-M	Expendable	23,000	65.00	2.39	[153]
Soyuz-2	Expendable	9,000	68.40	7.60	[150]
Angara A5	Expendable	24,500	88.56	3.61	[154]
GSLV Mk III	Expendable	10,000	43.92	4.39	[155]

In Table 8.22 the current medium to heavy launch vehicles have been documented. Their type is specified. In most cases, it concerns an expendable rocket, whereas the Falcon 9 and Falcon Heavy are partially reusable (only the first stage). The payload capability to LEO and their cost-per-flight were used to construct the cost-per-kg per launch vehicle. It is important to note that the cost-per-flight figures are converted to Euro’s and have been corrected for inflation, using the inflation charts provided in Appendix A. The cost-per-kg characteristics of each launch vehicle are graphically depicted in Figure 8.21.

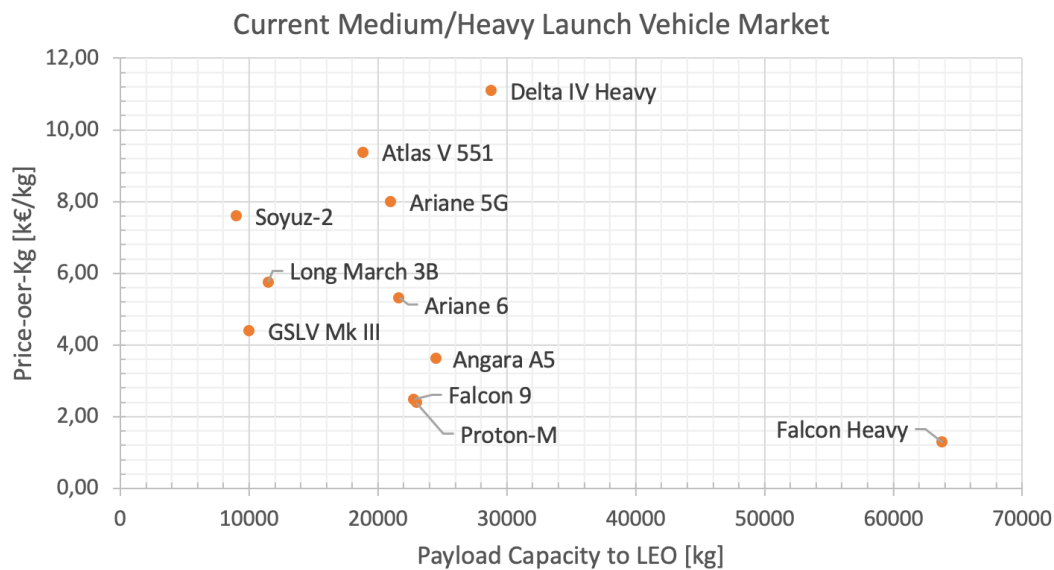


Figure 8.21: Current Medium/Heavy Launch Vehicle Market - Cost-per-Kg vs. Payload Capacity

Looking at Table 8.22 and Figure 8.21 it is clear that the hybrid launch vehicle design, combining the “Prototype X” storable upper stage design with the cryogenic Ariane 6 first stage, is played out against the current launch vehicle market. The payload performance of the hybrid launch vehicle is an order of magnitude larger compared to the average launch vehicle competitors. Therefore, it can be concluded that the storable “Prototype X” upper stage will not be commercially attractive in the current launch vehicle market.

8.5. Executive Summary

In this chapter, the propellant combinations that got selected in chapter 7 were subjected to detailed mass and cost analysis. This analysis was done by only changing the propellant combinations for each storable design concept. The effects of changing materials, dimensions and manufacturing methods will be investigated in the next chapter.

First, the selected propellant combinations were optimised in terms of their combustion conditions. A preliminary combustion and mass sensitivity study showed that reactive additives do improve the specific impulse and ignition delay times for the H₂O₂/ethanol combination. For H₂O₂/DMAZ and H₂O₂/dimethylamine, this effect is reversed. The specific impulse is reduced for larger quantities of reactive additives. Even though the H₂O₂/ethanol combination showed some performance improvements it was concluded that these effects are insignificant. It was decided to use reactive additives for the propellant optimisation.

A comprehensive optimisation analysis was performed to tweak the propellants in terms of their combustion chamber pressure, mixture ratio and specific impulse. The main optimisation objective was to reduce the wet mass of the storable concept. This optimisation was done using the dedicated combustion model to acquire specific impulse performance ratings for various mixture ratio and combustion chamber pressure levels. The combustion chamber pressure and combustion chamber temperature were the main optimisation constraints. The chamber pressure and temperature were limited to 9 MPa and 3500 K. Through the use of non-linear multi-variable optimisation functions the optimum combustion conditions were determined for all three propellant combinations. DMAZ obtained the (corrected) vacuum-specific impulse of 342.54 seconds, followed by dimethylamine and ethanol having a (corrected) vacuum-specific impulse of 341.28 and 329.3 seconds, respectively.

The optimum specific impulse characteristic for each combination, together with their respective combustion conditions, were used as input to the detailed mass and cost analysis. The mass and

cost analysis showed significant cost reductions in development and manufacturing, in the range of 13.8 – 13.3%. The operating cost was increased by approximately 2.0 to 2.7%. This can be explained by the larger transportation cost as the result of the larger wet mass of the vehicle. On average the cost-per-flight was reduced by 8.4 – 8.9% for the “Prototype X” storable concepts. Through a sensitivity analysis it was found that the vacuum-specific impulse effectuates the largest sensitivity in dry mass, wet mass and cost-per-flight. It can be concluded that the specific impulse has the largest contribution to the cost performance of the various storable concepts.

Apart from the cost-per-flight it is important to take into account the corresponding payload capability and payload performance. The reduced cost-per-flight that was found for storable designs does not correct for the payload mass that can be carried. The payload capability is used to construct the cost-per-kg or payload performance for each storable design. This can be compared one-to-one with the conventional Ariane 6 cryogenic upper stage. To do this, the payload capability of each design was analysed. Here it was found that DMAZ, ethanol and dimethylamine had a payload capability of; 6.4 tons, 3.1 tons and 6.1 tons, respectively. A sensitivity analysis pointed out that the vacuum-specific impulse and mixture ratio both had a significant effect on the payload capability of the storable designs, effectuating changes of –138.54% – 89.56% and –80.85% – 9.69% respectively. The payload capability calculations showed that the H₂O₂/DMAZ enabled the largest variety in mission characteristics. H₂O₂/DMAZ was able to have missions to LEO, SSO, Polar Orbit and can do ISS servicing missions. Combining the payload capability with the CpF for the various storable designs showed that all “Prototype X” concepts were subject to a significant payload performance reduction. The minimum cost-per-kg increment was found for the H₂O₂/DMAZ combination and was estimated to be +308.09%.

To compare the “Prototype X” concept with current medium/heavy launch vehicles, a market outlook analysis was done. To do this, the “Prototype X” upper stage module was integrated with the cryogenic first stage. This way both the cryogenic design and the storable concepts could be compared one-to-one. Furthermore, the construction of this ‘hybrid’ launch vehicle allowed comparison with other launch vehicles on the market. From Table 8.22 and Figure 8.21 it could be concluded that none of the storable “Prototype X” concepts were deemed commercially attractive to be used in the current launch vehicle. The wet mass burden, as a result of lower propellant efficiency, resulted in a smaller payload capability. The reduced payload capability diminished the advantage of a lower CpF and a simpler system design.

9

Cross-Over Analysis

In chapter 8 a detailed mass and cost analyses was done on the selected propellant combinations. It is important to note that during this detailed mass and cost analysis only the type of propellants and their respective combustion conditions were considered to be design variables. The “Prototype X” upper stage design was not changed in terms of materials used, type/number of elements present nor the engine and stage dimensions were altered. This was done such that the impact of storable propellants on the design could be compared one-to-one to the conventional cryogenic design. The analysis yielded the conclusion that current storable propellant combinations do not yet provide sufficient specific impulse performance to be commercially attractive, looking at the current launch vehicle market. Due to the relatively low I_{sp} , compared to the hydrolox propellant combination, the wet mass increment was significant enough to limit the payload capability, driving up the cost-per-kg to $18 \text{ k€}/\text{kg}$. Considering the fact that the average cost-per-kg in the medium/ heavy launch vehicle market is approximately $5.56 \text{ k€}/\text{kg}$ this outcompeted the storable propellant concepts.

In this chapter, a cross-over analysis will be conducted. This will help to formulate requirements for storable propellants performance to make the “Prototype X” design commercially attractive for future customers. The cross-over analysis is primarily focused from a propellant efficiency point of view, as the specific impulse showed most prominence during sensitivity analysis conducted in chapter 8. Propellant and design iterations will be investigated on their ability to enhance the payload performance. These propellant and design requirements will then be analysed on mass and cost. This is done to formulate a CpF range for the hypothetical propellant combination and design specification. Together with the payload capability this allows to determine the payload performance characteristic. Following this, a future market outlook analysis will be conducted to evaluate the suggested designs.

9.1. Propellant and Design Iterations

In this chapter the default fuel will be DMAZ. In chapter 8 this fuel was evaluated as being the most promising fuel for combustion with hydrogen peroxide. From the combustion characteristics and performance efficiency of DMAZ further iterations will be done to find the cross-over point. This cross-over point is defined as the point where the wet mass of the storable “Prototype X” design intersects with the wet mass of the conventional cryogenic Ariane 6 upper stage design. At this point the wet mass of both the cryogenic and storable designs is the same, meaning that the same payload capability is achieved.

There are three main ways to reduce the propellant mass. These are; the specific impulse of the propellant combination, the density of the propellants and the mixture ratio of the propellants. The latter being directly related to the specific impulse itself. The mixture ratio determines the attainable specific impulse. In this thesis research the stoichiometric mixture ratio is chosen. At this mixture ratio the most ideal combustion occurs; all the oxidiser and fuel are used for combustion. In reality this will not be the best option. Often a fuel rich (sometimes oxygen rich) mixture ratio is chosen for thermal control considerations for the propulsion system. From Table 8.19 it is clear that adjusting the density of the fuel

has little effect on the payload capability (directly related to the wet mass of the design), impacted only between -5.30% and $+0.66\%$. The payload capability and wet mass are mostly sensitive to changing the specific impulse (between -138.64% and $+89.56\%$). Since the mixture ratio is dependent on the propellant combination and is driven partly by the specific impulse obtained, it is chosen to keep the mixture ratio constant at 3.8 (as default for DMAZ) for the cross-over analysis. Furthermore it is chosen to keep the combustion chamber pressure constant at a pressure of 7.9 MPa . The sensitivity analysis (chapter 8) showed that the mixture ratio and combustion chamber pressure have limited effect on reducing the wet mass and will therefore not be driving variables that can yield sufficient propellant efficiency improvement. Lastly, the density of the hypothetical fuel will be kept constant to the density found for DMAZ (993 kg/m^3). The most effective way to improve the propellant efficiency, (consequently reducing the wet mass and increasing the payload capability) is to increase the specific impulse (as described in Table 8.15). During the cross-over analysis it is attempted to find the specific impulse that yields a cross-over point, where the wet mass of the cryogenic design is identical to that of the storable design.

In the cross-over analysis the mass model will be used to perform iteratively calculate dry mass and propellant mass estimates. The specific impulse will be the variable in the process and will be increased in a step-wise manner. Increasing the specific impulse will affect the required propellant mass. This propellant mass on its turn will influence the required tank volume and tank mass, resulting in a first order dry mass estimate. This dry mass impacts the achieved Delta V budget, again adjusting the required propellant mass. Hence, the iterative character.

The propellant combination that is discussed in this chapter will be a combination of hydrogen peroxide, acting as oxidiser, and a fuel (DMAZ will function as a baseline fuel). The cross-over analysis is focused on finding the required specific impulse such that the wet mass of the storable design will be identical to the wet mass of the cryogenic design. The fuel that produces this required specific impulse with HTP is therefore a hypothetical fuel. This hypothetical fuel will be referred to in this chapter by the name of "Fuel X", for clarity. This hypothetical fuel is currently not available on the market but will serve as an example to what is necessary for future propellant innovation. The H₂O₂/Fuel X propellant combination is therefore a performance measure to show when the storable design is having the same payload capability performance as the cryogenic design. As mentioned earlier, during the cross-over analysis the density and mixture ratio of the hypothetical fuel will be kept constant and mimics the density and mixture ratio of DMAZ. Furthermore, the combustion chamber pressure will be fixed at 7.9 MPa . These assumptions are deemed valid by looking at Table 8.15. The wet mass and payload capability are not significantly effectuated by changes in the density and combustion chamber pressure.

9.1.1. Cross-Over Analysis for Conventional Propellant Tank Material

In this subsection the cross-over analysis will be performed while keeping the materials and dimensions of the upper stage design the same as the upper stage of the Ariane 6. This means that the conventional Aluminium alloy will be used for the propellant tanks, intertank and interstage section. This means that the analysis is solely focused on changing the type and performance of the propellants, like the analysis done in chapter 8. The iterative cross-over process, as described above, is graphically depicted in Figure 9.1.

The cryogenic threshold line corresponds to the wet mass of the conventional cryogenic upper stage of the Ariane 6. The blue line dictates the wet mass of the storable upper stage design concept and the red line the corresponding dry mass. The point at which the wet mass of the storable upper stage intersects with the cryogenic threshold line describes the cross-over point. This point is highlighted by the line in magenta. From Figure 9.1 it can be concluded that the wet mass of the upper stage is decreasing exponentially for increasing specific impulse. The y-axis on the left corresponds to the wet mass of the upper stage, while the y-axis on the right describes the dry mass.

It is found that the cross-over point occurs at a specific impulse of 433.5 seconds. This required I_{sp} makes the H₂O₂/Fuel X propellant combination efficient enough to limit the wet mass to the level of the Ariane 6 upper stage. The reduction of wet mass is driven by two effects. The most obvious is the specific impulse. A higher specific relates to a more efficient propellant combination. Having a

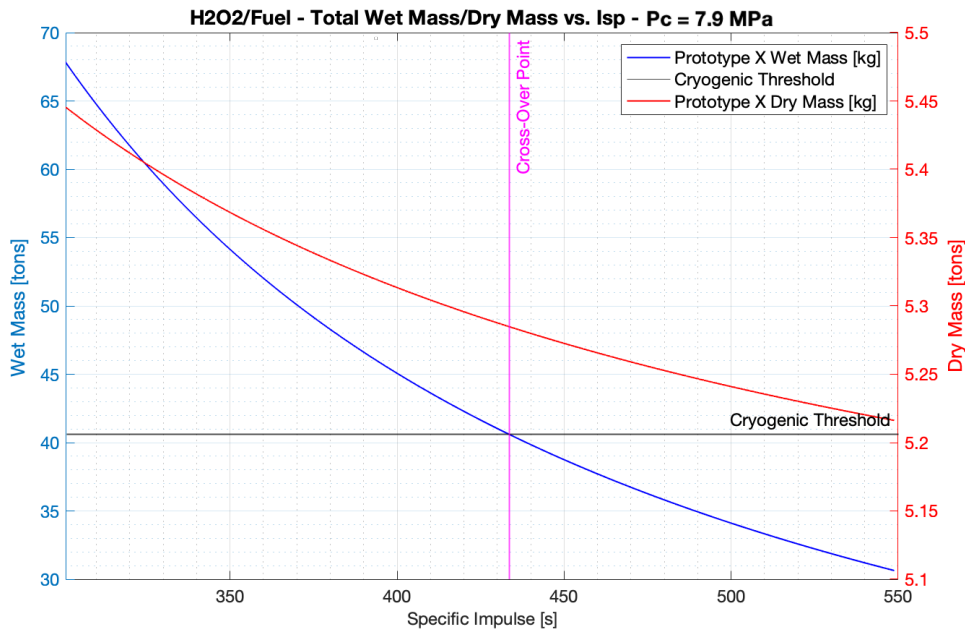


Figure 9.1: Wet Mass and Dry Mass Cross-Over Analysis (H2O2/Fuel) - Conventional Aluminium Propellant Tanks

more efficient propellant combination results in a lower propellant mass. Furthermore, the dry mass is also affected by the specific impulse. Less propellant means smaller and lighter tanks. The mass differences between the hydrolox and storable systems is tabulated in Table 9.1.

Table 9.1: Required Isp for Storable Propellants to Eliminate Wet Mass Growth - Conventional Storage System Material (Aluminium Alloy)

Parameters	LH2/LO2	H2O2/Fuel
Storage System Material	Aluminium Alloy	Aluminium Alloy
Specific Impulse [s]	463.53	433.5
Mixture Ratio [-]	5.40	3.85
Dry Mass [kg]	6749.69	5284.84
Fuel Mass [kg]	5290.91	7283.85
Oxidiser Mass [kg]	28,570.93	28,042.83
Propellant Mass [kg]	33,861.84	35,326.69
Wet Mass [kg]	40,611.52	40,611.53

From Figure 9.1 it can be concluded that due to the lower dry mass, more propellant mass can be carried. This reduces the required efficiency of the propellant combination. In this case, a required Isp of 433.5 seconds is necessary to end up with the same wet mass as the cryogenic design. The storable design is approximately 1.5 tons lighter. It has 2 tons more fuel on board and due to the fuel richer mixture ratio there is 530 kg less oxidiser mass present. Combining the fuel and oxidiser, there is approximately 1.5 tons more propellant mass present in the storable design.

9.1.2. Cross-Over Analysis for Advanced Propellant Tank Material

Since the storable propellants are easier to handle/store under normal conditions the use of storable propellants in launch vehicle designs opens up a lot of mass reducing options. Cryogenic storage system designs are driven by the cryogenic nature of the propellants; the propellant tanks should be able to cope with large thermal stresses [16], [74]. The vapour pressure and boil-off that comes with cryogenic propellants requires a higher strength/ thickness of the tanks [16]. To mitigate this, ArianeGroup and MT Aerospace are working together on an upper stage design iteration focused on constructing the propellant tanks of the upper stage out of carbon fiber composite material [74], [75], [156]. The development project PHOEBUS (Prototype Highly OptimizEd Black Upper Stage) is focused on de-

signing a cryogenic carbon fiber composite upper stage called ICARUS (Innovative Carbon ARiane Upper Stage) [157]. Although there are promising test results for the cryogenic tank pressure tests it is a challenge to make the tanks withstand the extremely cold temperatures and high cryogenic pressures while maintaining leak free. To prevent the tank from leaking and catastrophic failure the development team came up a metal liner that was added to the carbon fiber composite (CFC) tanks, reducing the net benefit of the lighter composite material [75].

The development on carbon fiber structures for cryogenic upper stage design are very promising, however, the hydrolox system still introduces a lot of challenges that must be overcome in the future to allow these designs to be used. To solve these issues, more safety and peripheral equipment should be added. Potentially making the PHOEBUS and ICARUS design complex and less reliable. Storable propellants, on the contrary, are easy to store under normal room temperatures, while having a limited boil-off and advantageous low vapour pressure. Furthermore it is found in Table 7.23 that most fuels under consideration are compatible with plastics and reinforced plastic composites. Highly concentrated hydrogen peroxide is compatible with aluminium (Appendix B [16]) and can be made compatible with carbon fiber composite as well. To make HTP compatible with carbon fiber, however, some modifications have to be made. These modifications are comparable to the ones used to store cryogenic liquids described above [74], [75]. However they are fabricated with a different procedure as these tanks do not have to incorporate insulation to prevent boil-off or to deal with the high cryogenic thermal stresses [158]. Hydrogen peroxide is not suitable for storage by pure carbon fiber composite structures as rapid decomposition could occur. To prevent this, a liner material (fluorinated ethylene/propylene (FEP)) is incorporated in the tanks and fittings. This liner material protects the carbon fiber composite, that carries the crucial hoop-stresses, from the highly concentrated hydrogen peroxide [158]. Both Aluminium and FEP showed to be the best materials for storage of hydrogen peroxide during experimental tests. Other thermoplastic liner materials that are suitable for some applications include nylon 6 and polyethylene [158].

To conclude, introducing storable propellants into the upper stage design opens up the possibility to conveniently use carbon fiber composite structures for the propellant tank, intertank and interstage. In this section the effect of this lighter and stronger material on the upper stage design and performance will be investigated. It is important to note that in this case the upper stage elements and materials normally used in the Ariane 6 upper stage will now be optimised for the use of storable propellants. The use of this carbon fiber composite material will further reduce the dry mass of the upper stage, bringing down the specific impulse requirement of the H₂O₂/Fuel X propellant combination. The cross-over analysis is described below in Figure 9.2.

From Figure 9.2 it is clear to see that the cross-over point is found for a lower required specific impulse. In this case the wet mass of the cryogenic and storable upper stage designs is equal to each other at a specific impulse of 407.1 seconds. This is a significant drop compared to the aluminium upper stage design. Due to the use of carbon fiber composite material the dry mass is further reduced. CFC material is very strong, limiting the required thickness of the propellant tanks. Furthermore, the CFC material has a very low density compared to aluminium alloys. Combining this the propellant tank, intertank and interstage structure mass is reduced, resulting in a lower dry mass for the upper stage design. This can be seen on the y-axis on the right of the graph, portraying the dry mass of the upper stage design. The mass breakdown of the carbon fiber composite storable upper stage design is tabulated below in Table 9.2.

Table 9.2: Required Isp for Storable Propellants to Eliminate Wet Mass Growth - Advanced Storage System Material (Carbon Fiber Composite)

Parameters	LH2/LO2	H2O2/Fuel
Storage System Material	Aluminium Alloy	Carbon Fiber Composite
Specific Impulse [s]	463.53	407.1
Mixture Ratio [-]	5.40	3.85
Dry Mass [kg]	6749.69	3903.01
Fuel Mass [kg]	5290.91	7568.78
Oxidiser Mass [kg]	28,570.93	29,139.80
Propellant Mass [kg]	33,861.84	36,708.58
Wet Mass [kg]	40,611.52	40,611.59

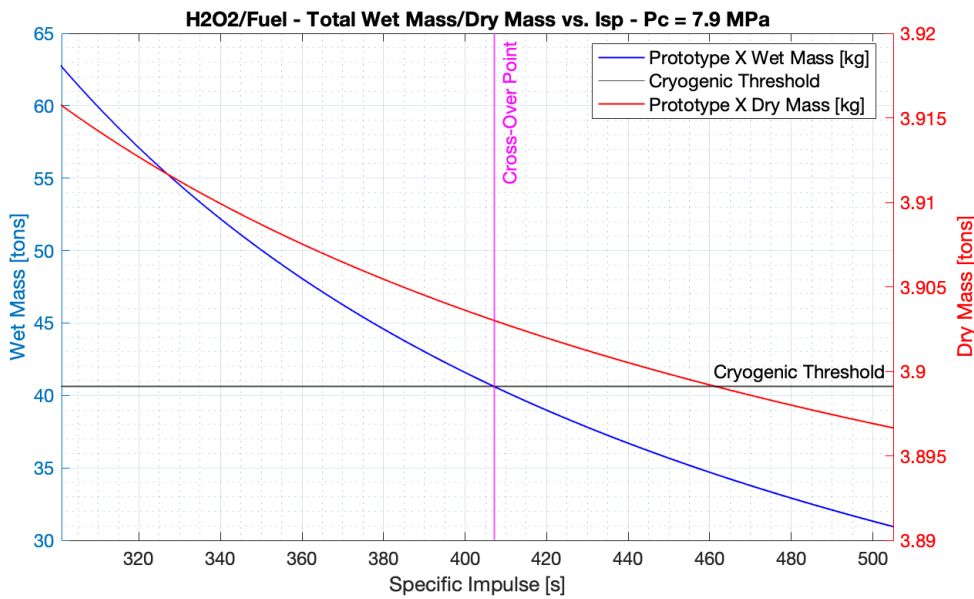


Figure 9.2: Wet Mass and Dry Mass Cross-Over Analysis (H2O2/Fuel) - Advance Carbon Fiber Composite Propellant Tanks

The dry mass reduces approximately 2850 kg, this allows to have a lower specific impulse as more propellant mass can be used due to this reduced dry mass.

Compared to the hydrolox system the specific impulse for the aluminium storable upper stage is 6.47% lower. For the carbon fiber composite structure this reduction is more significant. With a required specific impulse of 407.1 seconds it is a reduction of 12.17% compared to the hydrolox system. Although quite challenging, looking at the upwards trend in specific impulse in the past, it is not unachievable to find a propellant combination that will produce a specific impulse of 407.1 seconds in the future [7].

9.2. Mass & Cost Analysis

The cross-over analysis of both structural designs give important information that describe the effect of Isp on the mass breakdown of the upper stage module. The associated development, manufacturing and operation cost will be investigated in this section. The specific impulse, fixed mixture ratio and fixed density of the propellants will be used as input for the mass and cost analysis. From this cost analysis it is possible to find the cost-per-flight of each hypothetical design with the illustrative Fuel X. From this CpF characteristics the payload performance (cost-per-kg) can be determined for the upper stage designs. This will be useful to compare the storable designs with the current launch vehicle market.

9.2.1. Mass & Cost Analysis for Conventional Propellant Tank Material

The mass breakdown of the upper stage elements and the first unit cost is depicted in Table 9.3a. The development cost for the Prototype X (aluminium structure) is depicted in Table 9.3b. The fuel tank is reduced in mass and cost by 61.15%. This is the largest contributor to the reduction of first unit cost. The cumulative average reduction in first unit cost is approximately 14.8%. This is directly translated to the development cost of the Prototype X upper stage.

Table 9.3: First Unit Cost and Development Cost - H2O2/ Hypothetical Fuel - Conventional Aluminium Structure

(a) "Prototype X" First Unit Cost					(b) "Prototype X" Development Cost			
Unit	Element	Mass [kg]	Flight Unit Cost [k€]	Cost Change [%]	Flight Unit Cost [k€]	Development Cost [k€]	Cost Change [%]	
ULPM	Fuel Tank	462	1,584	-61.15%	14,023	221,226	-14.8%	
	Oxidizer Tank	1,878	4,301	+37.1%				
	Thrust Structure	806	1,251	0.0%				
	Thermal Control	9	22	-92.1%				
	Engines	226	2,259	-23.4%				
	Thrust Vector Control	213	892	0.0%				
	Pipes & Valves	18	65	+14.0%				
	Avionics	113	2,248	-2.0%				
	Interstage							
	Interstage Structure	1559	997					
Total UPLM		5,284	13,619	-14.8%				
I&T	3.2%							
	Stage I&T	-	332	-17.8%				
	PAA I&T	-	72	-2.7%				
Total First Unit Cost [k€]			14,023	-14.8%				

From the first unit cost, also the manufacturing cost can be determined. The manufacturing cost is calculated for the total life cycle of 50 units that are planned to be built by ArianeGroup. The manufacturing cost is depicted in Table 9.4. It is seen that the manufacturing cost is reduced by 14.8%.

Table 9.4: "Prototype X" Manufacturing Cost - H2O2/ Hypothetical Fuel - Conventional Aluminium Structure

		Flight Unit Cost [k€]	Manufac. Avg Unit Cost [k€]	Total Manufac. Cost [k€]	Cost Change [%]
		14,023	11,927	596,359	-14.8%
M&PA	Total		618	30,910	-14.8%
	5.3% M/PA		618	30,910	-14.8%
ULPM	Total	14,023	11,309	565,449	-14.8%
	Stage	12,622	10,179	508,96	-15.4%
	Interstage	997	804	40,199	-6.0%
	3.2% Stage I&T	332	268	13,388	-17.9%
	3.2% PAA I&T	72	58	2,902	-2.1%

The manufacturing cost will be the largest contribution to the CpF. The average manufacturing cost of the aluminium storable upper stage module is approximately 11,927 k€. The integration and testing cost for the stage and payload, avionics and attitude control is reduced by 17.9% and -2.1% respectively.

The operating cost for the storable aluminium upper stage is depicted in Table 9.5. Due to the higher required Isp for Fuel X compared to the fuel DMAZ (433.5 s compared to 342.54) it is assumed that the cost-per-kg for the Fuel X is 30 euro. This is an assumption that will take into account the added R&D required to develop a propellant combination to produce this specific impulse. This assumption of 30 euro per kg of Fuel X is determined by looking at comparable fuel innovation that is currently conducted [123], [124], [132]. It is quite challenging to present accurate approximations of propellant cost. As mentioned earlier, this assumption will only have a limited effect on the accuracy of the CpF estimate. This is due to the relatively small contribution that the propellant cost have to the CpF, as discussed earlier.

Table 9.5: "Prototype X" Operating Cost - H2O2/ Hypothetical Fuel - Conventional Aluminium Structure

Segment	Cost [k€]	Cost Change [%]
Direct Operating Cost	4,407	-2.5%
Ground Operations	1,725	-16.3%
Propellant Cost	241	+677.4%
Flight and Mission Operations	798	0.0%
Transportation Cost	204	0.0%
Fees and Insurance Cost	1,439	0.0%
Indirect Operating Cost	4,383	0.0%
Commercialization cost	4,383	0.0%
Total Operating Cost	8,790	-1.4%

The operating cost is reduced by approximately 1.4% compared to the conventional cryogenic upper stage. This cost reduction is primarily achieved by the reduction of ground operation cost. Although the propellant cost is increased by +677.4%. The transportation cost is unchanged as the wet mass of the storable upper stage is identical to the cryogenic upper stage.

From the development cost, manufacturing cost and operating cost the cost-per-flight can be determined. This is tabulated below in Table 9.6.

Table 9.6: Cost-per-Flight Estimate for the Prototype X - H₂O₂/ Hypothetical Fuel - Conventional Aluminium Structure

(a) Cost-per-Flight Breakdown			(b) Cost-per-Flight Distribution		
Contribution	Cost [k€]	Cost Change [%]	Cost per Flight Breakdown		
Amortization Charge per Flight	4,425	-14.8%		Amortization Charge per Flight	18,52%
Manufacturing Cost per Flight	11,929	-14.8%		Manufacturing Cost per Flight	49,92%
Operating Cost per Flight	8,790	-1.4%		Operational Cost per Flight	31,56%
Total Cost per Flight	25,144	-10.6%			

From Table 9.6 it is clear that the cost-per-flight is reduced by 10.6%. The total cost-per-flight is estimated to be approximately 25 M€. In this case it can be concluded that the aluminium storable upper stage design, with a propellant combination that produces an Isp of 433.5 seconds, can result in a cost reduction of 10.6% while keeping the materials, elements and dimensions similar to the conventional cryogenic upper stage. To understand the relative impact of this cost reduction on the payload performance, the cost-per-kg will be investigated later in this chapter.

9.2.2. Mass & Cost Analysis for Advanced Propellant Tank Material

In this scenario the cost-per-flight will be determined in case the upper stage module will be optimised with carbon fiber composite (CFC) material. The propellant tanks, intertank and interstage structures will be produced using carbon fiber composite material instead of the conventional aluminium structure. This analysis, thus, also takes into account system optimisation next to changing the propellants.

The mass breakdown for the CFC upper stage elements and their respective first unit cost is depicted in Table 9.7a. The associated development cost is tabulated in Table 9.7b.

Table 9.7: First Unit Cost and Development Cost - H₂O₂/ Hypothetical Fuel - Advanced Carbon Fiber Composite Structure

(a) "Prototype X" First Unit Cost					(b) "Prototype X" Development Cost						
Unit	Element	Mass [kg]	Flight Unit Cost [k€]	Cost Change [%]	Flight Unit Cost [k€]			Development Cost [k€]	Cost Change [%]		
ULPM	Fuel Tank	282	1,113	-72.6%	12,001	5.3%	M&PA	Total	189,344	-27.1%	
	Oxidizer Tank	1,144	3,021	-3.7%							
	Thrust Structure	806	1,251	0.0%							
	Thermal Control	10	22	-92.1%							
	Engines	226	2,259	-23.4%							
	Thrust Vector Control	213	892	0.0%							
	Pipes & Valves	18	65	+14.0%							
	Pipes & Valves	18	65	+14.0%							
	Avionics	113	2,248	-2.0%							
Interstage	Interstage Structure	1091	782		12,001	3.2%	ULPM	Total	179,999	-27.1%	
	Total UPLM	3,903	11,653	-27.1%							
I&T	Stage I&T	-	276	-31.7%	12,001	3.2%	ULPM	Stage	10,871	163,051	-27.1%
	PAA I&T	-	72	-2.7%				Interstage	782	11,730	-26.3%
	Total First Unit Cost [k€]		12,001	-27.1%				Stage I&T	276	4,139	-31.7%
							PAA I&T	72	1,079	-2.1%	

From Table 9.7 it is clear that there are significant mass reductions achieved for the fuel and oxidiser tanks. Furthermore, the thermal control is reduced, as expected, due to the storable characteristics of the propellants. The total first unit cost reduction is approximately 27.1%. This cost reduction is directly translated to the development cost of the storable CFC upper stage module. The development cost is

reduced by an equal 27.1%.

The first unit cost, as depicted in Table 9.7, is used to determine the manufacturing cost. The manufacturing cost is tabulated below in Table 9.8.

Table 9.8: "Prototype X" Manufacturing Cost - H2O2/ Hypothetical Fuel - Advanced Carbon Fiber Composite Structure

		Flight Unit Cost [k€]	Manufac. Avg Unit Cost [k€]	Total Manufac. Cost [k€]	Cost Change [%]
		12,001	10,209	510,425	-27.1%
M&PA	Total		529	26,455	-27.1%
5.3%	M/PA		529	26,455	-21.7%
ULPM	Total	12,001	9,679	483,970	-27.1%
	Stage	10,871	8,768	438,400	-27.2%
	Interstage	782	631	31,538	-26.3%
3.2%	Stage I&T	276	223	11,130	-31.7%
3.2%	PAA I&T	72	58	2,902	-2.1%

From Table 9.8 it is clear that the manufacturing cost is reduced by 27.1%. Since this cost analysis is for an iterated and optimised design for the upper stage module it can be argued that the manufacturing cost estimation process should be changed. Indeed, a mass reduction is not always directly related to a cost reduction. Especially when new materials and manufacturing methods are introduced at the manufacturing and assembly line. In this case the propellant tanks, intertank and interstage structure have been optimised from a conventional aluminium to an advance carbon fiber composite structural design. This means that new materials and manufacturing techniques have to be applied. The manufacturing cost estimate takes into account a learning curve. This learning curve will help to properly estimate the reduced effort per unit built. It is argued that the same learning curve can be applied to the use of CFC material. If the carbon fiber composite structure design is introduced at the beginning of the life cycle of the project the same manufacturing cost and effort distribution is expected as what would be seen for manufacturing the conventional aluminium structure. The same reasoning applies to the materials and manufacturing techniques used. If the CFC upper stage concepts are developed the manufacturing phase will not significantly change, taking into account that 50 units will be produced over the course of many years. Hence, it is assumed that for the carbon fiber composite optimised storable upper stage, the same manufacturing cost estimating parameters can be used. The effect of introducing advanced materials such as CFC in the design of launch vehicles, should however, be investigated in future work.

The associated cost estimating error that was identified to be 20% for the current cost model might change due to this assumption. Since relatively little validation data is present to estimate this new error it is not taken into account for this research. It is however recommended to investigate this effect in future research.

Table 9.9: "Prototype X" Operating Cost - H2O2/ Hypothetical Fuel - Advanced Carbon Fiber Composite Structure

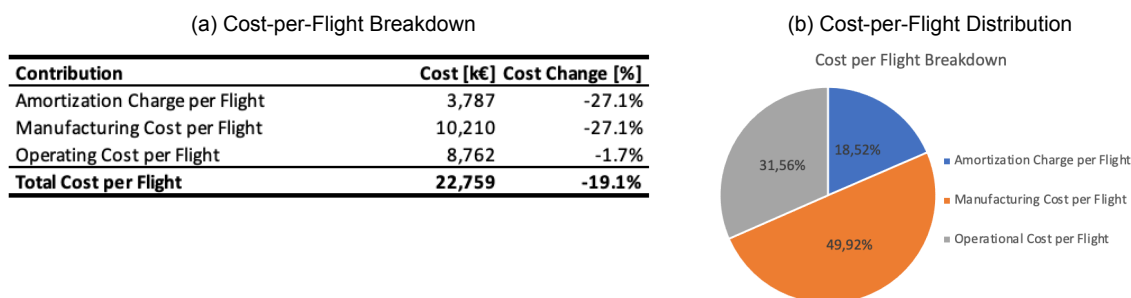
Segment	Cost [k€]	Cost Change [%]
Direct Operating Cost	4,379	-3.1%
Ground Operations	1,725	-16.3%
Propellant Cost	213	+587.1%
Flight and Mission Operations	798	0.0%
Transportation Cost	204	0.0%
Fees and Insurance Cost	1,439	0.0%
Indirect Operating Cost	4,383	0.0%
Commercialization cost	4,383	0.0%
Total Operating Cost	8,762	-1.7%

The operating cost of the CFC storable upper stage is depicted in Table 9.9. For the propellant cost estimate, a cost-per-kg of 25 euro for Fuel X is assumed. Following the same reasoning as for DMAZ this estimate is based on other experimental fuels in development at the moment. The cost estimate also takes into account the relative specific impulse change the propellant combination should attain.

This results in a propellant cost increase of approximately +587%. Even though this is a significant increase in cost. The total operating cost is reduced by 1.7% compared to the conventional cryogenic upper stage design.

Now that the development cost, manufacturing cost and operating cost are known, it is possible to estimate the cost-per-flight for the storable CFC upper stage design. This is tabulated below in Table 9.10.

Table 9.10: Cost-per-Flight Estimate for the Prototype X - H₂O₂/ Hypothetical Fuel - Advanced Carbon Fiber Composite Structure



The cost-per-flight for the storable CFC upper stage design is reduced by approximately 19.1% compared to the conventional cryogenic upper stage with aluminium structures. This is a significant improvement. The carbon fiber composite material used for the propellant tanks, intertank and inter-stage structure help to lower the mass and cost of the upper stage further. This reduction in dry mass is accountable in the CpF figure.

9.3. Cryogenic Performance Level Comparison

In this section the cross-over analysis is taken a bit further. In the cross-over analysis described above the focus was on finding the required specific impulse to limit the wet mass of the storable upper stage to the level found for the cryogenic upper stage. In this section the mass and cost for the aluminium and carbon fiber composite storable upper stage designs will be investigated in case the performance of the propellants is comparable to the hydrolox combination. This means that it is assumed that a storable propellant combination exists that achieves a propellant efficiency of 463.53 seconds, the specific impulse of liquid oxygen with liquid hydrogen. For this analysis two scenarios will be investigated; the storable aluminium upper stage design and the storable carbon fiber composite upper stage design. In both cases, it is assumed that the specific impulse of the hypothetical hydrogen peroxide/Fuel X combination achieves an Isp of 463.53 seconds.

In Table 9.11 the mass breakdown and first unit cost estimate are tabulated for the aluminium "Prototype X" design.

Table 9.11: Prototype X with Aluminium Structure, First Unit Cost for Cryogenic Performance Level - Isp = 463.53 seconds

Unit	Element	Mass [kg]	Flight Unit Cost [k€]	Cost Change [%]
ULPM				
	Fuel Tank	458	1,574	-61.3%
	Oxidizer Tank	1,861	4,273	+36.3%
	Thrust Structure	806	1,251	0.0%
	Thermal Control	9	22	-92.1%
	Engines	226	2,259	-23.4%
	Thrust Vector Control	213	892	0.0%
	Pipes & Valves	18	65	+14.0%
	Avionics	113	2,248	-2.0%
Interstage				
	Interstage Structure	1559	997	
	Total UPLM	5263	13,581	-15.1%
I&T				
	Stage I&T	-	331	-18.1%
	PAA I&T	-	72	-2.7%
	Total First Unit Cost [k€]		13,984	-15.1%

From Table 9.11 it is clear that large mass savings and cost savings are achieved. The relatively large specific impulse and average density of the propellants bring down the dimensions and mass of the upper stage elements. An approximate 15.1% cost reduction is achieved for the first unit. The first unit cost serves as input for the development cost and manufacturing cost. Together with the operating cost this allows to calculate for the cost-per-flight estimate. The cost-per-flight estimate is tabulated below in Table 9.12.

Table 9.12: Prototype X with Aluminium Structure, Cost-per-Flight for Cryogenic Performance Level - Isp = 463.53 seconds

Contribution	Cost [k€]	Cost Change [%]
Amortization Charge per Flight	4,412	-15.1%
Manufacturing Cost per Flight	11,894	-15.1%
Operating Cost per Flight	8,670	-2.8%
Total Cost per Flight	24,976	-11.2%

If the specific impulse can be boosted up to the level seen for hydrolox systems, a cost-per-flight reduction of -11.2% can be achieved. This is a significant reduction and primarily comes from the development cost and manufacturing cost reductions. In the next section, it will be investigated how this CpF relates to the payload performance of the design. The carbon fiber composite "Prototype X" design with a specific impulse of 463.53 seconds will be investigated next. In Table 9.13 the mass and cost breakdown of the upper stage elements is depicted.

Table 9.13: Prototype X with Carbon Fiber Composite Structure, First Unit Cost for Cryogenic Performance Level - Isp = 463.53 seconds

Unit	Element	Mass [kg]	Flight Unit Cost [k€]	Cost Change [%]
ULPM				
	Fuel Tank	281	1,111	-72.7%
	Oxidizer Tank	1,142	3,017	-3.8%
	Thrust Structure	806	1,251	0.0%
	Thermal Control	9	20	-92.8%
	Engines	213	2,259	-23.4%
	Thrust Vector Control	226	892	0.0%
	Pipes & Valves	18	65	+14.0%
	Avionics	113	2,248	-2.0%
Interstage				
	Interstage Structure	1091	782	
	Total UPLM	3,886	11,645	-27.2%
I&T				
	Stage I&T	-	276	-31.7%
	PAA I&T	-	72	-2.7%
	Total First Unit Cost [k€]		11,993	-27.2%

From Table 9.13 it can be concluded that large cost reductions are achieved for both the fuel and oxidiser tank. In the previous design suggestions it was found that the oxidiser tank was heavier. This

comes from the fact that hydrogen peroxide has a relatively large density. Using CFC material for the fuel tank changes this. The oxidiser and fuel tank have a reduced first unit cost of -3.8% and -72.7% respectively. Together with mass reductions for the thermal control and engine subsystems the total first unit cost reduction is approximately -27.2% compared to the conventional cryogenic upper stage design with aluminium structures.

The first unit cost is used to determine the development cost and manufacturing cost of the design. Together with the operating cost the cost-per-flight can be estimated. This estimate is tabulated below in Table 9.14.

Table 9.14: Prototype X with Carbon Fiber Composite Structure, Cost-per-Flight for Cryogenic Performance Level - Isp = 463.53 seconds

Contribution	Cost [k€]	Cost Change [%]
Amortization Charge per Flight	3,784	-27.2%
Manufacturing Cost per Flight	10,202	-27.1%
Operating Cost per Flight	8,554	-4.1%
Total Cost per Flight	22,541	-19.8%

From Table 9.14 it can be concluded that the largest cost reductions are found for this particular design. The storable CFC "Prototype X" design with a specific impulse of 463.53 seconds results in a cost reduction of -19.8% compared to the conventional cryogenic design with aluminium structures. Both the development cost and manufacturing cost is reduced by -27.1% . The operating cost is reduced by approximately -4.1% . In the next section, it is investigated how the reduction in CpF relates to the payload performance characteristic of the design concepts.

9.4. Payload Capability and Mission Characteristics

The different "Prototype X" design iterations (aluminium or CFC structures) together with the various performance levels of the hypothetical propellant combination H₂O₂/Fuel X can now be investigated in terms of their payload capability and mission characteristics. The various suggested performance levels of the hypothetical "Fuel X" combination with hydrogen peroxide will be compared to the conventional hydrolox system and to the H₂O₂/DMAZ propellant combination analysed in the previous chapter. To do this, the cost breakdown will be compared. From this the cost-per-flight can be constructed. Together with the resulting payload capability a conclusion can be drawn on the payload performance of the designs.

In Table 9.15 the cost breakdown is tabulated for the various "Prototype X" design concepts discussed. In this table the propellant combination is specified together with its relative specific impulse performance. Furthermore, the type of material used for the structure of the propellant tanks, intertank and interstage of the upper stage is specified.

Table 9.15: Cost Breakdown for Selected Upper Stage Designs

Vehicle Design - Propellant Combination	Type of Structure Material	Amortization Charge [k€]	Manufacturing Cost per Flight [k€]	Operation Cost [k€]
Ariane 6 Upper Stage - LO ₂ /LH ₂ - Isp = 463.53 s	Aluminium Structure	5,195	14,004	8,917
Prototype X - H ₂ O ₂ /DMAZ - Isp = 342.54 s	Aluminium Structure	4,479	12,075	9,159
Prototype X - H ₂ O ₂ /Fuel X - Isp = 433.5 s	Aluminium Structure	4,425	11,929	8,790
Prototype X - H ₂ O ₂ /Fuel X - Isp = 407.1 s	Carbon Fibre Composite Structure	3,787	10,210	8,762
Prototype X - H ₂ O ₂ /Fuel X - Isp = 463.53 s	Aluminium Structure	4,412	11,894	8,670
Prototype X - H ₂ O ₂ /Fuel X - Isp = 463.53 s	Carbon Fibre Composite Structure	3,784	10,202	8,554

From Table 9.15 it is clear that both the amortization and manufacturing cost for the carbon composite material is smaller than for the conventional aluminium structure. It is important to take note here that this comes forth from a very strict assumption that all 50 units built during the project lifetime are constructed using these carbon fiber composites (CFC). In this case the learning curve seen for the conventional manufacturing of aluminium can be applied to the carbon fiber composite. It is also important to understand that the manufacturing process will be quite different for CFC material compared to aluminium structures. For aluminium structures drilling, milling, forming and welding are the

most prominent techniques used to produce the complex shapes required. For carbon fiber composites this is different. In this case fiber and resin lay-up, wrapping and curing techniques are required. It is assumed that these manufacturing techniques are all in place before the start of the development and production of the storable CFC upper stage design. The cost model is based upon cost estimating relationships that use the mass of the individual elements as input. It is recommended for future research to investigate how these cost estimating relationships are impacted by using CFC material. For the analysis of the H₂O₂/Fuel X combination with an aluminium structure these cost estimation relationships are already verified and validated.

The combination of development cost, manufacturing cost and operating cost is detailed in the cost-per-flight figure. These are tabulated for the various discussed designs in Table 9.16.

Table 9.16: CpF Comparison Between Selected Upper Stage Designs

Vehicle Design - Propellant Combination	Type of Structure Material	Cost-per-Flight [k€]
Ariane 6 Upper Stage - LO ₂ /LH ₂ - Isp = 463.53 s	Aluminium Structure	28,116
Prototype X - H ₂ O ₂ /DMAZ - Isp = 342.54 s	Aluminium Structure	25,713
Prototype X - H ₂ O ₂ /Fuel X - Isp = 433.5 s	Aluminium Structure	25,144
Prototype X - H ₂ O ₂ /Fuel X - Isp = 407.1 s	Carbon Fibre Composite Structure	22,759
Prototype X - H ₂ O ₂ /Fuel X - Isp = 463.53 s	Aluminium Structure	24,976
Prototype X - H ₂ O ₂ /Fuel X - Isp = 463.53 s	Carbon Fibre Composite Structure	22,541

In all cases the “Prototype X” concept describes cost reductions for all vehicle design iterations compared to the hydrolox and the H₂O₂/DMAZ system. The relative cost-per-flight for all the design iterations are graphically depicted in Figure 9.3. In Figure 9.3 error bars are present. These error bars correspond to an expected cost estimation uncertainty of $\pm 20\%$, as described by N. Drenthe [83], [113]. The propellant combination and the structural material used are specified under their corresponding bar plot.

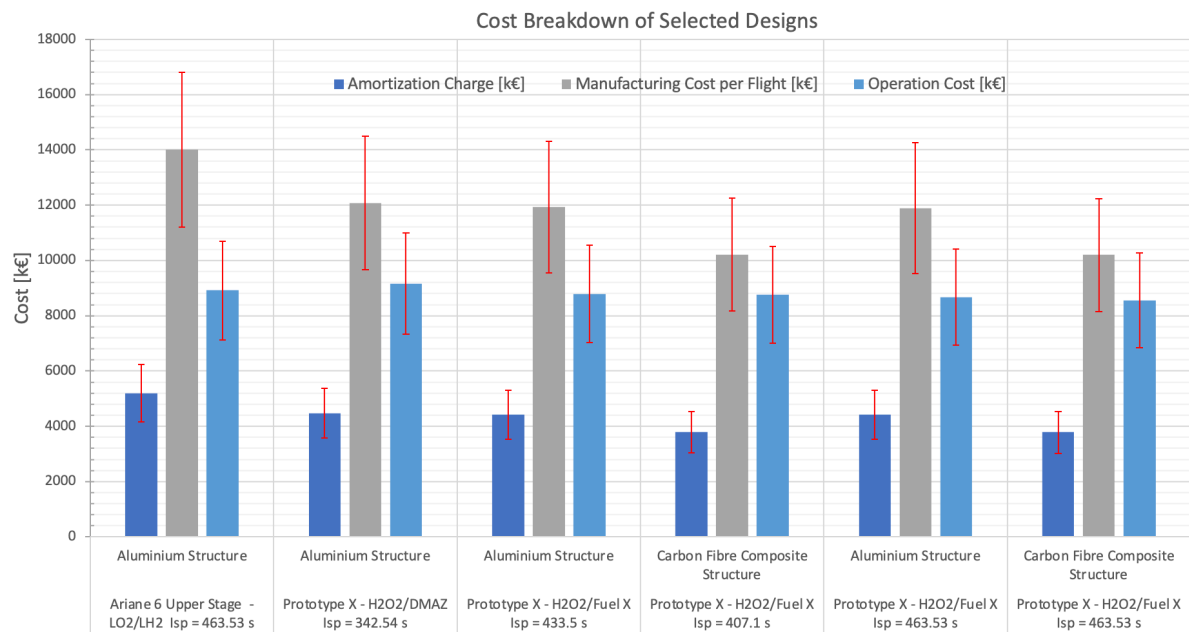


Figure 9.3: Cost Breakdown Comparison for Selected Upper Stage Designs

The resulting cost-per-flight for the various design options discussed is graphically depicted in Figure 9.4. The cost-per-flight figure presented in the graph is related to the upper stage module only. Again, error bars are present that indicate a cost estimating uncertainty of $\pm 20\%$.

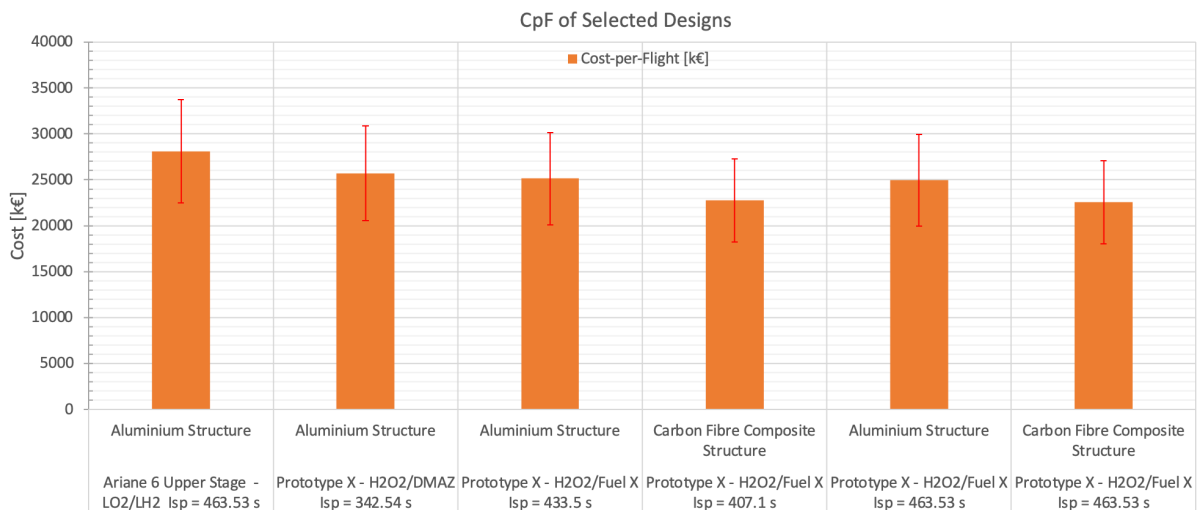


Figure 9.4: CpF Graphical Comparison Between Selected Upper Stage Designs

As discussed earlier, to usefully compare the cost of each design with respect to the conventional cryogenic upper stage one should look at the payload capability and the payload performance of each design. In the previous chapter, it was found that a cost-per-flight saving does not necessarily yield a useful design if the payload capability was changed. The cost-per-kg for every design is tabulated below in Table 9.17.

Table 9.17: Cost-per-Kg per Upper Stage Design

Vehicle Design - Propellant Combination	Type of Structure Material	Cost-per-Flight [k€]	Payload Capability [kg]	Cost-per-kg [k€/kg]	Relative Change [%]
Ariane 6 Upper Stage - LO2/LH2 Isp = 463.53 s	Aluminium Structure	28116	21650	1298,66	-
Prototype X - H2O2/DMAZ Isp = 342.54 s	Aluminium Structure	25713	6426	4001,10	+308.09%
Prototype X - H2O2/Fuel X Isp = 433.5 s	Aluminium Structure	25144	21650	1161,39	-10.52%
Prototype X - H2O2/Fuel X Isp = 407.1 s	Carbon Fibre Composite Structure	22759	21650	1051,22	-19.01%
Prototype X - H2O2/Fuel X Isp = 463.53 s	Aluminium Structure	24976	24906	1002,81	-22.78%
Prototype X - H2O2/Fuel X Isp = 463.53 s	Carbon Fibre Composite Structure	22541	27899	807,95	-37.79%

The cost-per-kg is compared to the conventional cryogenic upper stage design. Also, the best propellant combination described in the previous chapter serves for comparison (H2O2/DMAZ). Moreover, in Table 9.17 the 4 cross-over scenarios discussed in this chapter are tabulated. The first two scenarios are: the cross-over performance characteristic of the hypothetical storable propellant combination for both aluminium structures as well as a carbon fiber composite structures, respectively. The third and fourth scenario describe the payload performance in case a storable propellant combination exists that describes comparable performance characteristics to the hydrolox system, both for aluminium and carbon fiber composite structures.

Looking at Table 9.17 it can be seen that the payload capability is an important factor to consider. For the propellant analysis done in the previous chapter it was found that the combination of H2O2/DMAZ resulted in a significant wet mass increase. This reduced the available payload to LEO to a fraction of the nominal rated payload. For the first two cross-over scenarios the required specific impulse was calculated that limits the wet mass to the level seen for cryogenic upper stage designs. This means that the available payload capability is remained unchanged compared to the conventional hydrolox system. For the last two scenarios described, it is investigated what the resulting wet mass will be in case a storable propellant combination exists that is having similar performance characteristics as the hydrolox system. Since storable propellants have more favourable volumetric properties this results in a lower dry mass. As a consequence, it can be seen in Table 9.17 that the available payload is increased compared to the conventional cryogenic design. A lower dry mass impacts the payload performance positively.

The reduced dry mass corresponds to lower cost-per-flight figures. Resulting in a lower payload

performance. At the wet-mass cross-over point the aluminium storable upper stage design proves to be -10.52% cheaper compared to the conventional cryogenic upper stage. In case performance characteristics can be obtained for storable propellants that are similar to the level of hydrolox systems, the aluminium storable upper stage design proves to be -22.78% cheaper than the conventional upper stage design.

Taking into structural design iterations, by introducing carbon fiber composite (CFC) materials, the payload performance can be further improved. At the wet-mass cross-over point the CFC storable upper stage design proves to be -19.01% cheaper than the conventional design. Combining the structural design iteration with a performance characteristic that is comparable to hydrolox systems this is improved to a reduction in payload performance of -37.79% . The main reason for these improvements points toward the relatively low dry mass when CFC material is introduced. This improves the payload capability and lowers the cost-per-kg. The results, including the estimated errors, are graphically depicted in Figure 9.5.

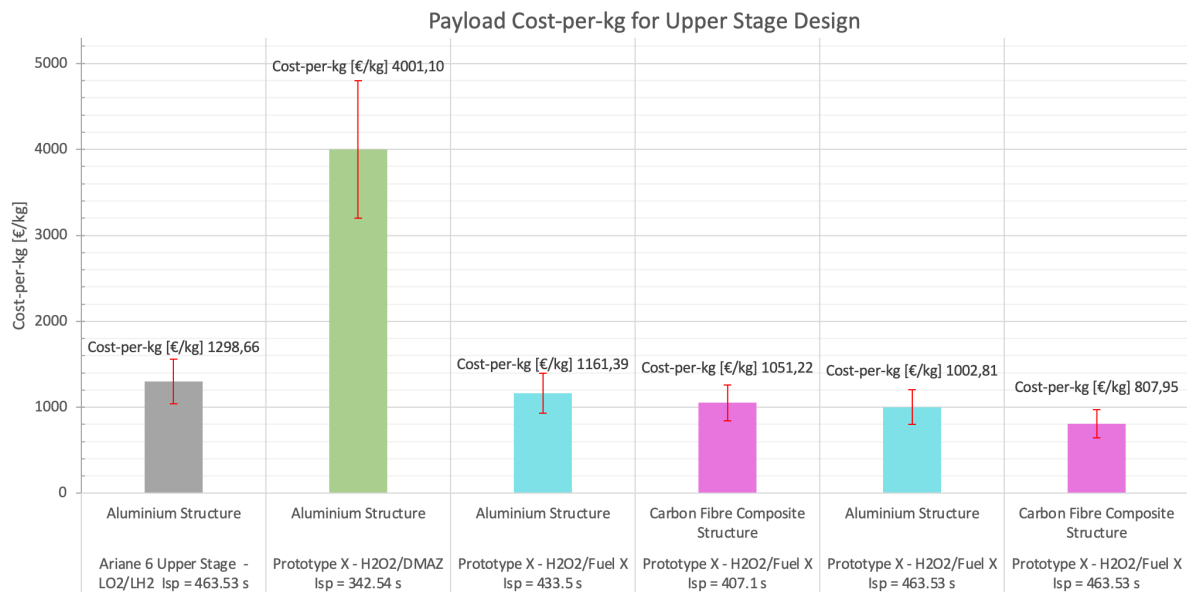


Figure 9.5: Graphical Comparison between the Cost-per-Kg of Upper Stage Designs

In Figure 9.5 the conventional cryogenic upper stage design is depicted in gray. The “Prototype X” design with the H2O2/DMAZ propellant combination is depicted in green. The cross-over design iterations are depicted in blue for aluminium structures and in magenta in case CFC material was used for the upper stage structure.

It can be concluded from Table 9.17 and Figure 9.5 that already at the cross-over point the storable upper stage designs have a significant advantage over cryogenic upper stages. Although a storable propellant combination with a specific impulse ranging between 407 – 434 seconds has yet to be found, it looks promising for application in the future.

To understand the effect of storable propellants on the physical design of the upper stage, a geometrical comparison will be conducted between the conventional cryogenic upper stage design and the “Prototype X” design concept in the next section.

9.5. Geometrical Comparison

As was discussed in chapter 5 and chapter 7, the storable propellants have distinct advantages in propellant tank design. The volumetric specifications of storable propellants are favourable over the less dense liquid hydrogen. To understand this in more detail, a geometrical comparison analysis was performed.

For this analysis the best case scenario of the proposed “Prototype X” concept was used. As indicated in Figure 9.5, this is the “Prototype X” concept that was constructed out of carbon fibre composite material and operates on the propellant combination H₂O₂/Fuel X. This hypothetical Fuel X produces an Isp of 463.53 seconds. The same physical and chemical characteristics have been applied to Fuel X as was found for DMAZ. This best case scenario was then compared to the conventional cryogenic Ariane 6 upper stage design that operates on LO₂/LH₂.

The geometrical comparison is schematically shown in Figure 9.6

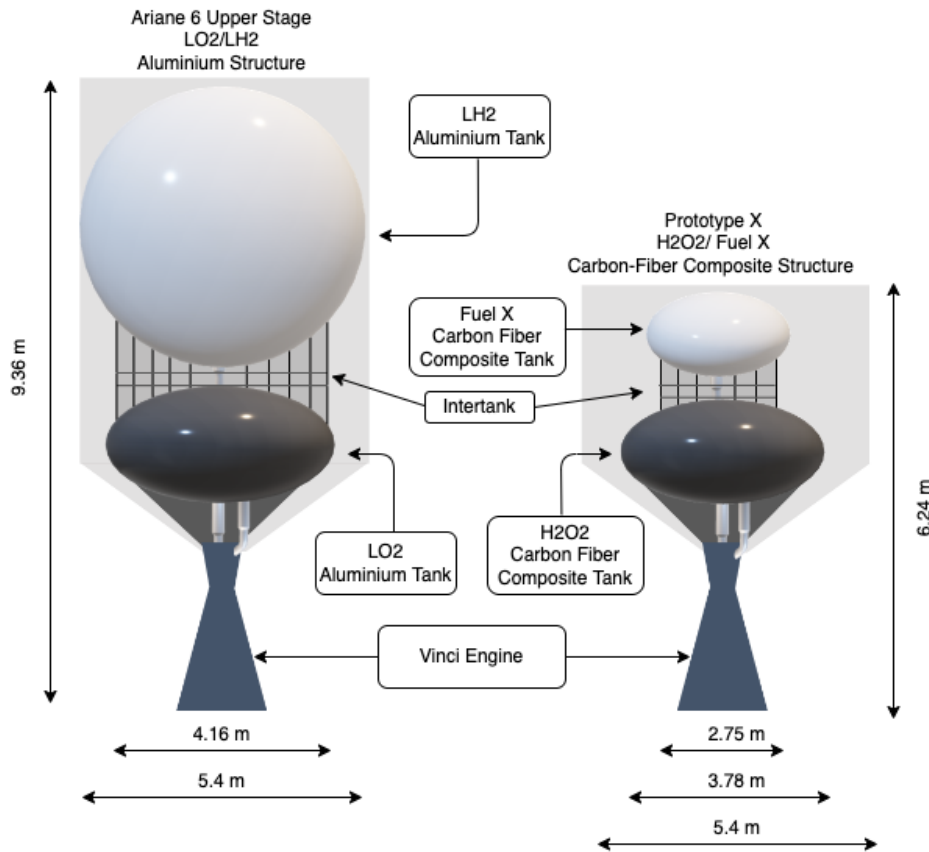


Figure 9.6: Geometrical Comparison Analysis between the Cryogenic Upper Stage and Best Case “Prototype X” Concept - To Scale

From Figure 9.6 it is clear that the storable design concept is superior to the conventional cryogenic upper stage design. Due to the higher density propellants the propellant tank dimensions are drastically reduced. The entire stage is condensed in a smaller lateral size, compared to the Ariane 6 upper stage. The main contributor to the geometrical reduction is the fuel tank. The physical properties of the storable fuel brings the diameter of the fuel tank back from 5.4 m to only 2.75 m. The oxidiser tank for hydrogen peroxide experiences a limited reduction in diameter; 3.78 m compared to 4.16 m for the LO₂ tank. The length of the storable concept is reduced by approximately 33%. Due to the reduced propellant tanks, the intertank can also be reduced in size and volume. It is important to understand that in this analysis the diameter was constraint at 5.4 m. This to make the “Prototype X” integration with the first stage possible. As seen in Figure 9.6 it can be concluded that this diameter, ideally, can be optimised too.

To understand how the estimated payload performance compares to the current market of launch vehicles, the “Prototype X” should be integrated with the cryogenic first stage. This will give insight into the total cost-per-kg for the entire launch vehicle. This cost-per-kg figure allows to compare with the payload performance of competitive medium/heavy launch vehicles. This is done in the next section.

9.6. Market Outlook Analysis

Again it is important to note that the cost-per-flight estimate can't be used to compare one-to-one with the launch vehicle cost found in literature. The reason for this has been explained in the "Current Market Analysis" of the previous chapter. The estimate, however, gives the expected order of magnitude of the cost-per-flight estimate. This can be used to compare with other launch vehicles.

First, the various "Prototype X" design iterations have to be integrated with the cryogenic first stage. This is done to obtain the total cost-per-flight of the modelled launch vehicle. This together with the payload capability allows to determine the cost-per-kg or payload performance of the launch vehicle concepts. This is tabulated in Table 9.18.

Table 9.18: Cost-per-Kg Performance of Integrated Prototype X Designs - Excluding Boosters

Modelled Launch Vehicles (Excl. Boosters)	Upper Stage Propellants	Type of Material	Cost-per-Flight [M€]	Payload to LEO [kg]	Cost-per-kg [k€/kg]	Relative Change [%]
Ariane 6 LLPM + Ariane 6 ULPM	LO2/LH2 - Isp = 463.53 s	Al Structure	111.51 (2021)	21650	5.15	-
Ariane 6 LLPM + Prototype X	H2O2/DMAZ - Isp = 342.54 s	Al Structure	109.21 (2021)	6426	16.99	+329.94%
Ariane 6 LLPM + Prototype X	H2O2/Fuel X - Isp = 433.5 s	Al Structure	108.57 (2021)	21650	5.01	-2.64%
Ariane 6 LLPM + Prototype X	H2O2/Fuel X - Isp = 407.1 s	CFC Structure	106.18 (2021)	21650	4.90	-4.78%
Ariane 6 LLPM + Prototype X	H2O2/Fuel X - Isp = 463.53 s	Al Structure	108.39 (2021)	24906	4.35	-15.51%
Ariane 6 LLPM + Prototype X	H2O2/Fuel X - Isp = 463.53 s	CFC Structure	105.95 (2021)	27899	3.80	-26.27%

From Table 9.18 it is clear that all design concepts that use a propellant combination of hydrogen peroxide with "Fuel X" result in a cost-per-flight reduction. At the cross-over point, the cost-per-kg reduction is in the range of 2.64% – 4.78%, for the aluminium upper stage and CFC upper stage respectively. If the specific impulse of the storable propellants is boosted to the level of hydrolox systems, the cost-per-kg reduction is even more pronounced. In this case the payload performance is improved with 15.51% – 26.27% for the aluminium and CFC upper stage respectively.

To understand how this compares to other medium/heavy launch vehicles that currently are operational, a market analysis has been performed. Due to the inaccuracies and assumptions taken in this research analysis, it is important to emphasise the illustrative character of this comparison. The market analysis will give only an estimated performance in terms of order of magnitude compared to other launch vehicles. The market analysis is graphically depicted in Figure 9.7.

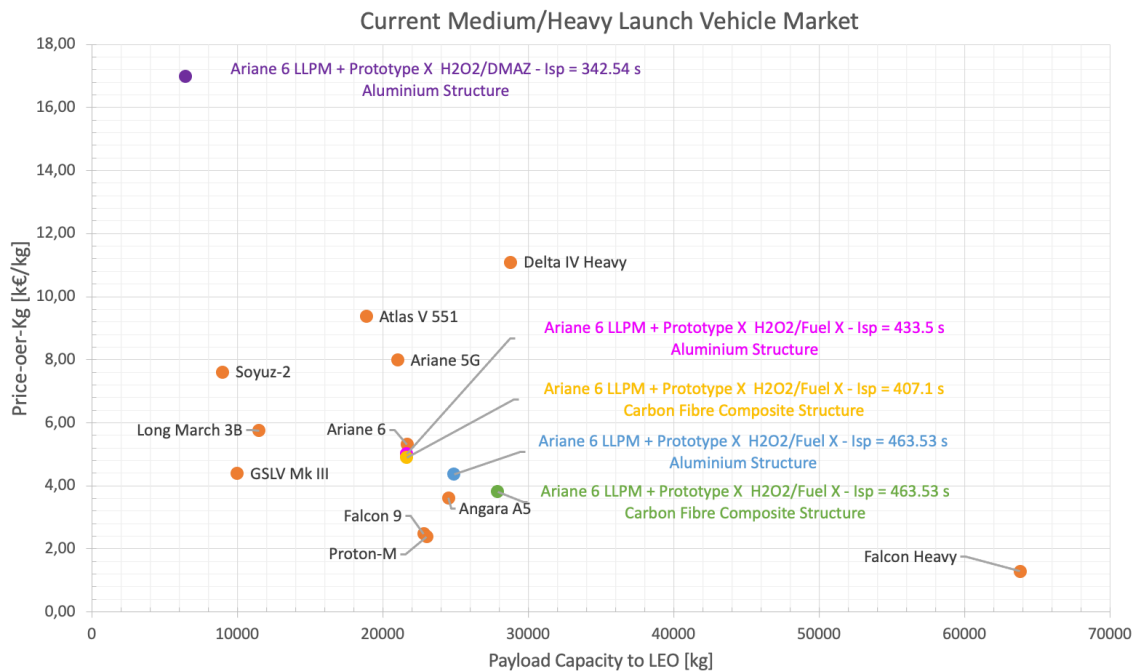


Figure 9.7: Current Medium/Heavy Launch Vehicle Market - Cost-per-Kg vs. Payload Capacity

As illustrated in Figure 9.7 it is clear that the “Prototype X” concepts that have been developed during the cross-over analysis all seem to be competitive in the medium/heavy launch vehicle market. All concepts prove to be economically more attractive than the conventional Ariane 6 launch vehicle. The “Prototype X” concepts that have cryogenic level performance can be among the most cost-efficient designs on the current market. The Angara A5 and Proton-M are the only expendable launch vehicles that are more cost-effective. It argued that these Russian launch vehicles can bring down their prices so low due to their high (full) production rate. Furthermore, the Angara A5 and Proton-M vehicles are massively subsidised by the Russian Space Federation ROSCOSMOS [159].

From Figure 9.7 it can be concluded that future storable propellants can be used in upper stage designs while maintaining the performance of their conventional cryogenic counterpart. This can be done by keeping the material used for the propellant tanks, intertank and interstage the same. By changing the material used for these upper stage sections to carbon fiber composite material, further cost-per-kg reductions can be obtained. Comparing the hybrid launch vehicle (cryogenic and storable stages) with the current launch vehicle market, it can be concluded that the hybrid launch vehicle can become one of the most competitive expendable launch vehicles on the market.

Although a storable propellant combination with a specific impulse ranging between 407 – 434 seconds has yet to be found, it looks promising for application in the future. Apart from the reduced complexity of the propulsion and storage systems, the added reliability and the safer handling, storable propellants also allow the use of the typical lighter and stronger carbon fiber composite material. Together with the reduced thermal insulation requirements, this results in further reduction of the dry mass. Adding to the improvement of the payload performance. Introducing carbon fiber composite material lowers the research and development gap in terms of specific impulse that currently exists. As predicted by Silverman and Greene [7] in the past, storable propellants showed significant improvements in combustion efficiency over the recent years [124], [160]. Although a lot of *R&D* is required, the performance gap in terms of specific impulse is deemed manageable looking at the trend-line of innovation in storable propellants. Furthermore, the implementation of storable propellants in reusable systems can greatly benefit from this safer handling, added reliability and reduced system complexity. The CpF of reusable systems is primarily based on the cost involved with operation and refurbishment. Safer handling, storing and procurement of the inherently stable storable propellants can significantly reduce the operation cost while lowering the cost involved with ground equipment and staff. The refurbishment cost will reduce due to the inherently simple systems and high reliability of the storable designs. All this combined will result in a significant reduction of the cost that is involved with future storable reusable systems, potentially outperforming all current cryogenic systems on the launch vehicle market.

It can thus be concluded that future storable upper stage designs can result in significant cost and complexity reductions while improving payload performance, safety and reliability. The proposed hybrid launch vehicle, composed of a cryogenic first stage and the storable “Prototype X” concept is prospected to be one of the most competitive expendable launch vehicles on the market. Storable reusable launch vehicles will potentially outperform all expendable and reusable launch vehicle systems in the future due to the added benefit of lower complexity, higher reliability and safer systems.

9.7. Executive Chapter Summary

In this chapter a cross-over analysis was conducted for the “Prototype X” storable design concept. Here the focus was on finding the required performance of a hypothetical “Fuel X” that would make the storable concept more economically attractive. This analysis investigates the research and development gap in propellant engineering. It helps to point out what is necessary for storable propellants to make them competitive with the conventional cryogenic propellants. DMAZ served as a benchmark for the hypothetical “Fuel X”. The density, optimum mixture ratio and combustion chamber pressure were kept fixed at the values that were found for DMAZ.

First, the cross-over analysis focused on finding the specific impulse where the wet mass of the storable design concept was limited to what was found for the ULPM. Limiting the wet mass by increasing the propellant efficiency maintains the payload capability to the level of cryogenic designs. The lower CpF associated with the reduced dry mass would positively impact the payload performance

of the storable concepts. This analysis was performed for the aluminium storable concept, where only the propellant combination was considered the design variable, and for a carbon fiber composite storable concept. In the latter, the interstage, intertank and propellant tanks of the "Prototype X" were constructed from carbon fiber composite material, essentially adding a structural design variable. The carbon fiber composite material is suitable for use with storable propellants. Because there is limited thermal stress and boil-off involved with storable propellants, the "Prototype X" concept is a good candidate for such a design iteration. To make the carbon fiber composite compatible with HTP it was discussed to add a FEP liner to the internal contours of the propellant tank and fittings. Storable propellants inherently have significant advantages over cryogenic propellants in terms of handling and storage. A carbon fiber composite upper stage design thus can have significant mass and cost saving advantages.

In the cross-over analysis it was found that the aluminium "Prototype X" concept had a cross-over point at a specific impulse of $I_{sp} = 433.5 \text{ s}$. Here, the wet mass of the storable concept was in the same range as the cryogenic design. The dry mass, however, was 1.5 tons less for the aluminium ULPM. The carbon fiber composite "Prototype X" got to this cross-over point when "Fuel X" reaches a specific impulse of $I_{sp} = 407.1 \text{ s}$. This comes from the fact that the dry mass is further reduced. Mainly because of the favourable density of carbon fiber composite. Furthermore, the carbon fiber composite propellant tanks can be thinner due to the inherently higher strength of the material. The dry mass was reduced by approximately 2.85 tons. These performance characteristics for "Fuel X" were used to put into the mass and cost models to investigate the conceptual design in detail. Here it was found that the CpF for the aluminium "Prototype X" was reduced by 10.6% compared to the conventional Ariane 6 ULPM. Here all three cost contributors experienced a cost reduction. For the composite "Prototype X" concept an even larger cost reduction was obtained. Compared to the conventional cryogenic design the composite "Prototype X" vehicle was 19.1% cheaper in CpF. The payload capability in this cross-over analysis was maintained to be 21650 kg.

A second analysis was performed to investigate the design concepts in case the "Fuel X" could produce cryogenic levels of performance with hydrogen peroxide. This means that it was assumed that the combination H₂O₂/Fuel X could produce a specific impulse of 463.53 s. Again, two scenarios were investigated; the aluminium and composite "Prototype X". For both design concepts, the corresponding mass distribution and cost were calculated. Due to the relatively high specific impulse the storable combination essentially became more efficient. This efficiency together with the inherently lower dry mass, reduced the wet mass of the concepts to well below the cryogenic design. This means that the payload capacity was significantly increased. It was found that the CpF was reduced by 11.2% and 19.8% for the aluminium and composite concept, respectively.

To understand the impact of the reduced CpF, found for these four concepts, the payload performance was calculated. All storable design concepts experienced a lower CpF. The two composite design concepts achieved the best CpF. The cross-over designs maintained the payload capability of 21650 kg, whereas the designs with cryogenic level performance had an improved payload capability of 24906 kg and 27899 kg for the aluminium and composite concept, respectively. This improved the payload performance significantly. The aluminium conceptual designs experienced an improved payload performance of 10.52% and 22.78% respectively. The composite concepts improved the payload performance by 19.01% and 37.79% respectively. The results are summarised in Table 9.17. It was found that the storable propellants can reduce the geometrical dimensions of the upper stage concept by roughly 33%. The smaller propellant tanks make the upper stage structure more condensed. It is important to note that the specific impulse characteristics assumed here are currently not achieved yet for storable combinations. It was, however, argued that the relative performance gap, in terms of specific impulse, can be overcome in the future.

To understand how these design concepts fit in the current market of medium/heavy launch vehicles, the "Prototype X" concepts first were integrated on top of the cryogenic first stage. This followed the same procedure as was described in chapter 8. The hybrid launch vehicle (comprised of the cryogenic first stage and the storable "Prototype X" design concepts) was used for comparison with other launch vehicles on the market. First, the payload performance was calculated for the launch vehicle

as a whole. An increase in payload performance was found for all proposed "Prototype X" concepts. These improvements range from 2.64% to 26.27% of payload performance increase. Compared to other medium/heavy launch vehicles the hybrid design promised to be one of the most cost-effective expendable launch vehicles on the market.

10

Subsystem Considerations and Re-design

In this chapter, possible redesigns and considerations are discussed that come to play when introducing storable propellants in the upper stage design concepts. These are considerations that will partly serve as recommendations for research. Introducing storable propellants will influence other subsystems too. These required redesigns are outside the scope of the current research thesis but the subsystems that most prominently are affected will be briefly discussed in the sections below. Future research into these individual subsystems is recommended to investigate the in-depth optimisation of storable upper stage concepts. These research topics will also allow to develop a detailed design concept.

10.1. Subsystems under Consideration

Storable propellants directly impact the size and thickness of the propellant tanks. Furthermore, the limited boil-off and low thermal footprint of storable propellants make the tanks less complex in terms of pressure maintenance and thermal control. These are clear direct implications coming forth from the introduction of storable propellants. However, more subsystems are impacted by the implementation of storable propellants. A selection of the subsystems that will be discussed is listed below:

- Propulsion Subsystem
- Propellant Storage and Feed Subsystem
- Thermal Control Subsystem
- Structural Subsystem
- Ground Operations and Handling

In the subsequent sections, the considerations and possible redesigns of these subsystems will be discussed in more detail.

10.2. Propulsion Subsystem Considerations

Under propulsion subsystem the following subsystems are considered:

- Injector Plate Design
- Combustion Chamber Design
- Thermal Control of Combustion Chamber and Nozzle
- Propellant Pump Design

Currently, the majority of current research and development in propulsion systems is focused on improving cryogenic engines. The primary reason is the excellent performance level at which the hydrolox (LH2/LO2) system operates. The combination of liquid hydrogen and liquid oxygen show very efficient combustion characteristics in terms of specific impulse. This high performance of hydrolox systems comes at a cost. The hydrolox system is typically very complex, bulky and costly to develop.

Storable propulsion systems are inherently less complex and costly due to the beneficial hypergolic behaviour of the propellants.

To ensure hypergolicity of the selected storable propellants, it is required to look into injector designs for hypergolic combustion. Research by T. Borsboom [161] investigates the effect of vaporisation and initiation of hypergolicity for different types of injector designs. As mentioned earlier, storable propellants sometimes are improved on their performance and shelf-life by adding constituents to the propellant mix [16]. One popular solution to improve the performance of propellants is to apply “gelling”. A gel fuel combines solid and liquid fuels to improve the performance [26]. It is important to investigate the injection behaviour of these gelled fuels as their viscosity and viscoelastic properties play a vital role in injection and mixing, eventually leading up to the required hypergolic combustion reaction [26], [161].

The propellant injection is also influenced by the ignition delay time (IDT). It is important to investigate the IDT of the storable propellants at hand. The ignition delay time describes the time between contact (of the oxidiser and fuel) and combustion. According to G. Rarata et al. [162] appropriate additives can be used to tweak the ignition delay time. These findings are promising it can help to fine-tune the IDT for particular combustion chambers. Too small IDT can have the effect of melting the injector plate as combustion occurs too close to these orifices. Longer IDT times result in a longer combustion chamber length which consequently adds to the mass of the propulsion system. The combustion chamber is typically very sturdy to cope with the high operating pressures of steady-state combustion. To withstand the high heat fluxes and to reduce the mass of the combustion chamber often exotic materials are used. Optimising the combustion chamber length of the propulsion system therefore is a very important design consideration.

According to the analysis conducted in chapter 8, and specifically in Figure 8.6, Figure 8.10, Figure 8.14, it was found that the steady-state combustion chamber temperatures for the selected storable propellants all fall below the maximum of 3000 K. Although this is a bit higher than the combustion chamber temperatures seen for hydrolox systems it is not necessarily hard to design a combustion chamber for these kinds of heat fluxes. In order to do this various active cooling techniques can be proposed. Film cooling and regenerative cooling are often used on current hydrolox and methalox systems. To use film cooling the propellant mixture ratio can be optimised to run fuel rich. In this way more fuel is consumed. This extra fuel is not directed into the combustion chamber for combustion but for cooling the chamber and nozzle walls. When hydrocarbon fuels are used this can result in sooting. Soot is material that is the product of incomplete combustion. Sooting happens when this soot material is deposited on the chamber walls or injector plate, possibly leading to clogging of the injectors. According to a study by I. Gaissinski et al. [163]: “*soot particles can play a critical role in the characteristics of the infrared radiation emission since soot radiates a continuous, near-blackbody spectrum*”.

Regenerative cooling actively cools the chamber and nozzle walls by transporting propellants along these walls by the means of tubes. These will partly take away the heat flux on the propulsion system. Regenerative cooling will also heat up the propellants before injection into the combustion chamber, increasing the efficiency of the combustion. In the case of storable propellants, especially for hydrogen peroxide, one has to be careful when using regenerative cooling techniques. The decomposition rates of hydrogen peroxide are greatly enhanced with temperature. However, Hydrogen peroxide typically runs on oxidiser rich propellant mixtures with most fuels, allowing a large amount of propellant flow rate to be used as a coolant. This results in a lower propellant temperature rise with regenerative cooling [164]. Regenerative cooling has been performed with 90% hydrogen peroxide as a coolant for the main combustion chamber in the Rocketdyne AR2-3 and the Reaction Motors LR-40 engines [164]. The decomposition rates of hydrogen peroxide are greatly enhanced with temperature. Furthermore, Miller et al. [22] showed promising results in the ability to film cool a combustion chamber and nozzle using JP-8 fuel in combination with hydrogen peroxide.

In terms of propulsion system design the following developments for the application of green storable propellants have been identified by D. Heaseler et al. [9]:

- Cooling characteristics and coking (deposition) of new fuels
- Material compatibility, film-cooling and thermal barrier coatings
- Materials and coatings in a hot oxygen rich environment

- Oxygen rich gas generator injection and preburner gas injection (staged combustion), sooting
- Brazing of combustion structures

From the research conducted by B. Zandbergen [102] it can be concluded that storable engines are often heavier and larger than the cryogenic propulsion systems. It is, however, important to note that there has been done notably more research and development into cryogenic engines in the last three decades. The storable engines that have been taken into consideration for Zandbergen's research were on average much older than the cryogenic engines. Furthermore, the thrust level of the storable propulsion units is often an order of magnitude larger than the thrust produced by the average cryogenic engine [102]. Adding to the structural mass of the engine. It is expected that more *R&D* in the field of storable propulsion systems will reduce the mass and consequently the cost of these systems. The thrust level of storable engines of the past is typically very large. For upper stage designs this is not required. By lowering the mass flow rate the thrust can be lowered, having the beneficial side effect that less pump power is required. Especially because of the inherently less complex design of storable engines. Furthermore, the longer combustion chamber lengths for storable engines (needed for hypergolic combustion) can be reduced by the findings presented by G. Rarata et al. [162].

Throughout the analysis conducted the expansion ratio of the nozzle was kept fixed. This was done to limit the complexity of the research analysis. It was found by Y. Moon et al. [14] that the expansion ratio can have a significant effect on the effectiveness and efficiency of the propulsion system. This could be further investigated in future research.

10.2.1. Propellant Pump Design

Although hydrolox powered propulsion systems are very popular, they come with some disadvantages. Hydrolox powered spacecraft are often heavier in terms of dry mass due to the low average density propellants [16]. This effect does not solely come from the larger required propellant tanks.

The low-density liquid hydrogen requires extra measures to be pumped into the engine. This can be done by means of a gas generator cycle, expander cycle and (full-flow) staged combustion cycles. The conventional upper stage engine used in the Ariane 6 upper stage is the Vinci engine, which is an expander cycle. For all types of power cycles the combustion chamber has to be fed with enough propellants to generate the required mass flow rate. To do this, without relying on highly pressurised propellant tanks, turbo-pumps are being used. The use of liquid hydrogen and liquid oxygen in hydrolox propulsion systems makes these turbo-pump designs inherently complex. To limit the heat generation in the combustion chamber the hydrolox propellant mixture typically runs fuel rich. In this case, some of the liquid hydrogen fuel is used to cool the combustion chamber and nozzle. Because of this and the significantly lower density of liquid hydrogen the turbo-pumps for the fuel and oxidiser cannot run on a single shaft [54], [165]. Apart from the added complexity of having two separate shafts to drive the fuel and oxidiser turbo-pumps, also two individual preburners are needed. Making the system increasingly more complex. To operate these preburners some of the low-density liquid hydrogen has to be fed into the preburners. This is dangerous for many reasons. The main reason being that liquid hydrogen is hard to contain (especially under high pressure) because of its low-density. Leaking liquid hydrogen uncontrollable into the preburner could lead to catastrophic failure of the entire system. To prevent this, purge seals are being used. These seals use the inert helium to generate an active barrier between the high pressure liquid oxygen and liquid hydrogen propellant feed lines [165]. All in all the design and steady-state operation of hydrolox propulsion systems are very complex, heavy and costly.

Since the proposed storable propellants have similar density and pressures at which they are stored and operated this complex turbo-pump and preburner situation is avoided. The larger average density of the storable propellant combination results in a lower propellant volume that has to be pumped to the combustion chamber to reach the required mass flow. This allows to further simplify the propulsion system by replacing the turbo-pump installation by electrical pumps. Electric pumps are becoming more popular in new propellant feed system designs. It was found by H.D. Kwak et al. [166] that the electric pump cycle is quite an attractive solution for low thrust level rocket engines as this cycle saves costs and cuts the cost per unit payload due to the simplicity of the design. Moreover, H.D. Kwak et al. state; "A dual motor configuration would greatly expand the flexibility of the engine because it can introduce a larger operating range by adjusting the O/F ratio, combustion pressure, and thrust level. This means

that the ElecPump cycle can accommodate the various mission requirement” [166]. During detailed analysis it was found that under the same operating conditions, currently the electric pump cycle has a reduced payload capability to LEO mission orbits of 2.1% to 3.1% compared to Gas Generator cycles [166]. This is primarily due to the mass of the battery pack and motor. It is expected that high-density energy storage technology can reduce this mass burden and become superior to conventional power cycles. Electric pump powered propulsion systems are currently being tested by multiple companies for various types of launchers [167].

Due to the simplicity of the storable propulsion system and the easier propellant handling of storable propellants compared to cryogenics, electric pumps can be a logical solution to further reduce complexity of the system. This reduced complexity ensures higher reliability of the system.

10.2.2. Reliability Analysis

Since the propulsion system is one of the most complex and pronounced subsystem in the upper stage module it carries a significant responsibility in terms of reliability. In this section, a brief reliability analysis of the propulsion unit is performed. Z. Huang et al. [168] investigated the most important reliability drivers that come to play to quantify the reliability of propulsion systems. The reliability drivers that were identified to be most significant to go from a cryogenic propulsion system to a storable propulsion system are listed below [168]:

- **Number of liquid propulsion engines per stage**

Although this might look trivial, the number of liquid propulsion engines that are present per stage describes more than just redundancy. Multiple smaller engines can have a higher reliability than one large engine. The total reliability depends on detailed design, application needs and physical constraints. This can include thrust size, total impulse and engine-out design [168].

- **Single engine total reliability**

The reliability of the engine itself is the main product of total propulsion system reliability. The complexity and inherent engine design together with manufacturing and operation determine the rate of failure or malfunctions [168]. In this scenario, the simpler storable engine design is favoured in terms of single engine total reliability. Smaller injector plates, propellant hypergolicity and less complex power cycles result in a smaller number of single-point failures. Through extensive development of cryogenic engines the achievable reliability is significant. The inherently simple design of storable propellants will probably amount to similar or even higher reliability levels.

- **Engine operation duration**

Longer run times of propulsion systems amount to a higher risk of failure. Therefore, reliability is directly related to the operation duration of the propulsion systems [168]. The upper stage propulsion system typically operates for a longer duration than the first stage “boost” stage to allow for orbital injection and trajectory control. From this logic it can be derived that the upper stage propulsion system has a high required reliability. It is important to note that the reliability depends on the thrust level during this burn too.

- **Reusability**

If an engine will be reused multiple times the reliability is greatly affected. More stringent life requirements are in place for reusable engines [168]. Fatigue related failure modes and causes should be closely analysed and monitored. Also during post-flight refurbishment a significant amount of inspections have to be in place to identify possible errors on time. In terms of refurbishment less complex engines are in favour. This makes a great case for storable propulsion systems over the relatively more complex hydrolox system [54], [168].

- **Propellant-specific hazards**

Not only the reliability of the entire integrated system but also the reliability of the propulsion system is affected by the type of propellants used. The propellants that are selected for combustion are bringing in propellant-specific hazards. In terms of hydrolox systems these hazards can, for example, be hydrogen embrittlement, thermal stress effect and material compatibility with liquid

and gaseous oxygen [168]. Storable propellants typically introduce fewer potential hazards into the system as the propellants do not have very stringent thermal requirements, compared to liquid hydrogen and liquid oxygen.

- **Engine combustion cycles**

For pump-fed engines the used combustion cycle influences the inherent reliability of the engine. The main reason is the large number of moving parts and high pressures involved. The combustion cycle is often referred to as the most complex and challenging part of engine design. The reliability of combustion cycles is affected by *“the complexity, controllability and operating stress, pressure and temperature”* [168]. Z. Huang et al. also found that reducing the complexity of the combustion cycle does not directly result in higher reliability.

- **Altitude start (first start)**

In the case of multistage rockets, upper stage modules are required to start at altitude. Typically under (near) vacuum conditions. According to Z. Huang et al. [168], this is beneficial to potential hydrogen leakages. However, they state that the cons outweigh the pros. The two main reasons for this statement are; *“no effective launch commit check can be performed due to the lack of a ‘hold down period’ at the launch site”* and *“it is not easy for development tests to simulate and address in-flight altitude start failure”*. Furthermore, they state that propellant conditioning is challenging during coasting and altitude starts [168]. The potential reliability benefit of storable propellants is hypergolicity. An altitude start is much more reliable if the propellants are inherently hypergolic. Adding to the overall reliability of the engine.

- **Multiple altitude start (>1 start)**

Same as the previous point, but in this case more restarts are considered at altitude. In the case of the Ariane 6 upper stage module this is very much the case to allow for orbit insertion and trajectory control. The Ariane 6 ULPM is designed to do multiple restarts, depending on the mission at hand [11]. During development testing, the Vinci engine is fired three consecutive times during static hot-firing tests [91]. During these tests, a variety of thrust levels and burn durations were tested. This restartability is paramount to delivering payloads to different orbits and inclinations. The Merlin 1D upper stage engines that are fitted into the falcon 9 upper stage has to be restarted 4 times during flight (depending on the mission and payload). These ignitions are done by the use of the pyrophoric mixture Triethylaluminium-Triethylborane (TEA-TEB) [169]. TEA-TEB is extremely toxic, corrosive and dangerous to handle. It is very flammable and is hard to contain safely for extended periods of time [170]. TEA-TEB has to be stored somewhere in the rocket where the LOX boil-off does not freeze the feed lines, adding additional complexity and reliability hazards. For redundancy 2 TEA-TEB tanks are added to the Falcon 9 launch vehicle [169]. To allow for altitude restarts TEA-TEB is used to induce ignition. If the TEA-TEB is consumed or, due to a malfunction, not fed towards the combustion chamber the engine is unable to restart. This could lead to potential catastrophic failure of the mission, especially for reusable launch vehicles such as the Falcon 9 and upcoming Starship. This reliability consideration betters the case for storable propellants. Especially the suggested hypergolic storable propellant combinations. In this case, no external ignition source is required and inherently safe, non-limited (in terms of the number of restarts) restartability is achieved, reducing complexity, cost and increasing reliability. It is therefore argued that storable propellants are favoured in reusable launch vehicle systems.

- **Manufacturing/Ground operation support**

The level of complexity, inspectability and the number of maintenance activities during the manufacturing of the propulsion system and ground operation support affect the reliability [168]. The main driver for this consideration are the embedded human errors involved in these processes.

- **Extensiveness of development program**

The stage of development of the engine is a significant driver of the expected reliability of the system. According to Z. Huang et al. the extensiveness of the development program can be described by; *“subscale, component and subsystem development and testing, lab and hot fire testing, certification programs, design verification, reliability verification and demonstration, fail-*

ure analysis and corrective actions, and redesign” [168].

Currently, multiple studies are conducted in terms of the reliability of bi-propellant hypergolic systems. For example G. Rarata and W. Florczuk are investigating the potential hazards and reliability of running bi-propellant hypergolic systems with 98% hydrogen peroxide as oxidiser [162]. In this study multiple fuels are tested that are alternatives to the hydrazine-based propellants steady-state. They find that the reliability, performance can be synthesised' by promoting the fuels with the appropriate additives.

10.3. Propellant Storage and Feed Considerations

Pump-fed propellant storage systems shall always have a positive pressure in the propellant tanks. The reason for this is to prevent pump cavitation. The propellants shall be able to be fed into the pump inlet whilst preventing air bubbles to flow into the feed lines. These air bubbles could be potentially catastrophic during engine operation. Typical pump-fed propellant systems are pressurised between 0.68 – 3.45 bar [171]. In the case of cryogenic propellants these tank pressures are obtained by a pressurant gas in combination with heating and vaporisation of small portions of the propellants. Otherwise known as boil-off. This boil-off makes it very important to thermally control the propellants tank to prevent pressure build-up in the propellant tanks. For storable tanks, this boil-off is very limited and will not significantly contribute to the build-up of pressure in the system. This makes the storable propellant tanks more reliant on dedicated pressurisation systems. This reliance on storable propellants on a pressurant, however, results in a less complex system to operate [171]. Boil-off of cryogenics require a redundant pressure-relief system in place to actively control the pressure in the propellant tanks. In both the cryogenic and storable case, the pressurant used to pressurize the propellant tanks should not dissolve, react or condense into the propellants. Inert gasses such as helium and nitrogen are used as pressurants. Nitrogen has the tendency to dissolve in nitrogen tetroxide, liquid oxygen and hydrogen peroxide [171], [172]. In this case, helium is used. Furthermore, the pressurisation of the tank is not only in place to maintain the 'Net Positive Suction Pressure (NPSP)', it is also responsible for the structural stability requirements of the propellant tanks. This makes it very important to maintain proper tank pressures in the propellant tanks. Again, cryogenics make this more prone to errors due to their boil-off characteristic [173].

These pressurant gasses introduce potential hazards in case one deals with cryogenics. The pressurising gas is usually warmer than the cryogenic liquids. The heat transfer from the gas to the liquid will cool the gas and will increase in density; a larger mass of the gas is needed for pressurisation. During multiple restarts this can result in quick temperature changes and irregular tank pressures for cryogenic propellant storage systems [171]. The very low temperatures required to store cryogenics therefore result in a very complex fluid-mechanical and thermodynamic processes that impact the pressurisation and storage system design [174].

As mentioned before in chapter 9 storable propellants allow for innovative structural tank design. This involves the use of carbon fiber reinforced plastics (CFRP) or carbon fiber composite (CFC) in short. Looking at Figure 9.6, it is clear that the storable propellants, in combination with CFC structural tank design, can have significant geometrical advantages over cryogenic designs. This innovative tank design can be considered for storable propellants since they are easier to handle/store under normal conditions. Cryogenic storage system designs are driven by the cryogenic nature of the propellants; the propellant tanks should be able to cope with large thermal stresses [16], [74]. The vapour pressure and boil-off that comes with cryogenic propellants requires a higher strength/ thickness of the tanks [171]. ArianeGroup and MT Aerospace are working together on an upper stage design iteration focused on constructing the propellant tanks of the upper stage out of carbon fiber composite material [74], [75], [156]. The development project PHOEBUS (Prototype Highly OptimizEd Black Upper Stage) is focused on designing a cryogenic carbon fiber composite upper stage called ICARUS (Innovative Carbon ARiane Upper Stage) [157]. Although there are promising test results for the cryogenic tank pressure tests it is a challenge to make the tanks withstand the extremely cold temperatures and high cryogenic pressures while maintaining them to be leak-free and preventing them from embrittlement. To ensure the tank from leaking and catastrophic failure the development team came up with a metal

liner that was added to the carbon fiber composite (CFC) tanks. This liner would serve as a very thin protective layer between the cryogenic propellants and the carbon fiber composite material. Adding this metal liner will however make the system more expensive to manufacture and will potentially reduce the net benefit of the lighter composite material [75].

The development of carbon fiber structures for cryogenic upper stage design is very promising, however, the hydrolox system still introduces a lot of challenges that must be overcome in the future to allow these designs to be used. To solve these issues, more safety and peripheral equipment should be added. Potentially making the PHOEBUS and ICARUS design complex and less reliable. Currently, SpaceX is developing a carbon fiber propellant tank to carry cooled liquid methane and liquid oxygen for their Starship fully re-usable orbital-class rocket. During the development, Founder, CEO and Chief Engineer of SpaceX, Elon Musk said that this poses a lot of challenges and difficulties; “Even though carbon fiber has incredible strength-to-weight, when you want one of them put super-cold liquid oxygen and liquid methane - particularly liquid oxygen - in the tank, it’s subject to cracking and leaking and it’s a very difficult thing to make” [175].

Storable propellants, on the contrary, are easy to store under normal room temperatures, while having a limited boil-off and advantageous low vapour pressure. Furthermore, it is found in Table 7.23 that most fuels under consideration are compatible with plastics and reinforced plastic composites. Highly concentrated hydrogen peroxide is compatible with aluminium (Appendix B [16]) and can be made compatible with carbon fiber composite as well. To make HTP compatible with carbon fiber, however, some modifications have to be made. These modifications are comparable to the ones used to store cryogenic liquids described above [74], [75]. However, they are fabricated with a different procedure as these tanks do not have to incorporate insulation to prevent boil-off or to deal with the high cryogenic thermal stresses [158]. Hydrogen peroxide is not suitable for storage on pure carbon fiber composite structures as rapid decomposition could occur. To prevent this, a liner material (fluorinated ethylene/propylene (FEP)) is incorporated into the tanks and fittings. This liner material protects the carbon fiber composite, that carries the crucial hoop-stresses, from the highly concentrated hydrogen peroxide [158]. Both Aluminium and FEP showed to be the best materials for storage of hydrogen peroxide during experimental tests. Other thermoplastic liner materials that are suitable for some applications include nylon 6 and polyethylene [158]. These liner materials can also be applied to make valves and fittings compatible with highly concentrated hydrogen peroxide.

To conclude, introducing storable propellants into the upper stage design opens up the possibility to conveniently use carbon fiber composite structures for the propellant tank.

10.4. Thermal Control Considerations

The cryogenic propellants are kept at extremely cold temperatures to maintain them in their liquid form. The propellants are stored in cryogenic storage containers on the launch platform before they are loaded into the launch vehicle. When dealing with hydrolox systems the propellants have to be stored in the tanks with temperatures below 20.28 K (-252.8°C) for liquid hydrogen and below 90.19 K (-183°C) for liquid oxygen. The thermal footprint of these cold propellant temperatures is clearly visible in Figure 10.1.

Figure 10.1 shows the temperature distribution of the Ariane 6 ULPM shortly after engine cut-off. The great variation in upper stage temperature is clearly visible. The coldest elements are, as expected, the cryogenic propellant tanks. The hottest part of the upper stage design will be the combustion chamber/throat area where the temperatures will reach around 841°C . This thermal distribution plot is indicative to understand the value of good thermal control of the upper stage spacecraft.

Due to the cold cryogenic propellants the tank wall temperature falls well below the ambient air temperature. These cold tank wall temperatures result in condensation of the ambient humid air on the rocket structure. In Figure 10.1 these outer tank wall temperatures range between -47.95°C and -116.31°C . This condensation quickly solidifies into ice. The formation of ice on the exterior side of the upper stage is unfavourable. In the period prior to launch the ice formation adds to the launch vehicle inert mass, it can cause valves to malfunction and it can make structural components brittle or weaker

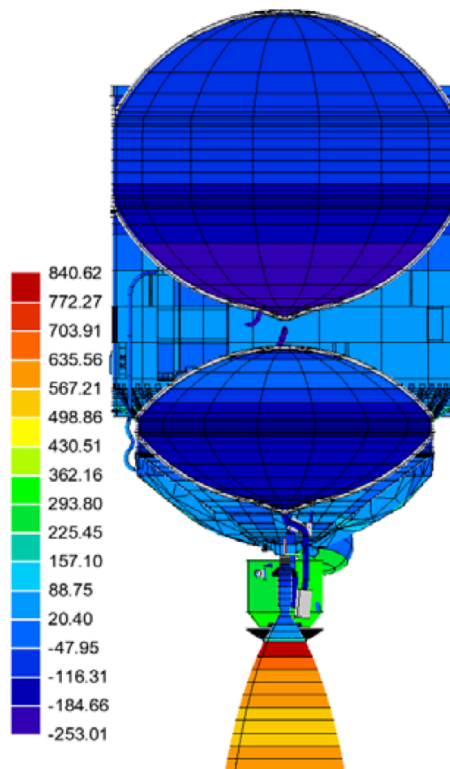


Figure 10.1: Temperature Distribution (in Celsius) of Ariane 6 ULPM [88]

to a point where the launch loads and vibrations cannot be sustained [171]. During the launch, these pieces of ice can damage the vehicle when shaken off. One catastrophic example is the final Columbia Space Shuttle flight, where the interface between the foam and the aluminium substrate experienced stresses due to differences in how much the aluminium and the foam contract when subjected to cryogenic temperatures. This stress made the seal fail between the insulation layer and the aluminium structure. Ice formation inside the insulation layer resulted in the loss of the thermal foam tile that hit the thermal protection layer of the space shuttle orbiter. Upon re-entry this puncture resulted in the disintegration of the vehicle, killing all people onboard [176].

To prevent such accidents from happening, extensive thermal insulation, passive/ active thermal control and thermal barriers have to be put in place. Looking at the Columbia disaster the porous external insulation layers need to be sealed to prevent moisture condensation from building up in the insulation layer [171], [176]. To prevent propellant loss and pressure build-up due to boil-off and evaporation, the inside of the propellant tanks have to be thermally insulated too. Different types of thermal insulation layers are used. The layers can be wrapped around the structures. This is mostly done with Multi-Layer Insulation (MLI) material. More popular nowadays is spray-on insulation material. This kind of insulation material is sprayed upon the structure such that it is evenly distributed even in hard-to-reach places. A significant disadvantage to cryogenic propellants is the boil-off is very hard to completely prevent from occurring. For long-duration storage of cryogenics, for example for deep space missions or long thrust scenarios, cryo-coolers are required to re-condense the vapors, minimize evaporation losses and limit the amount of boil-off pressure [177]. Other ways to maintain the thermal envelope of the propellants is to use the coldest propellant (in hydrolox systems this is liquid hydrogen) to take some heat away. This heat results in some boil-off of the propellant which will be vented off into space, which was done for the Saturn V or will be used for active station-keeping [177]. Just before launch the pressure in the cryogenic propellant tanks is increased to raise the boiling point slightly such that heat transferred during the rocket firing can be absorbed [171]. Again, a complex and expensive procedure that is not required in case storable propellants are used.

These considerations show the benefit that lies in the use of storable propellants. With storable

propellants very limited thermal control is required. The propellants are stored under ambient temperatures and require a limited amount of pressure to fulfil the Net Positive Suction Pressure.

In conclusion, storable propellants need less extreme temperature control, leak less easily, require non-complex metallurgy and has a larger material thermal compatibility. The use of storable propellants results in a relatively simple thermal control design and cost.

10.5. Structural Considerations

Although most of the upper stage is comprised of propellant tanks there still are several key structural components. The engines are mounted to the aft end of the propellant tank structure by means of a dedicated thrust frame. This thrust frame is in place to exert the loads and stresses from the propulsion system. The tanks are connected with thin-walled cylinders that are called 'skirts', 'interstages' and 'intertanks'. Structural components such as ribs and stiffeners are applied to carry the loads and stresses within the design envelope [73]. Typically a variety of aluminium alloys is used to make these structural elements. The most important characteristics of Launch Vehicle materials are [54]:

- Material strength
- Material stiffness
- Mass density
- Nature of failure modes
- Ability to tolerate small-scale damage
- Mechanical and chemical compatibility with nearby materials

It is important to note that long-term damage and resistance or durability is not a very important design criterion for expendable launch vehicles but is of much importance for reusable ones.

As mentioned earlier, multiple companies and agencies investigate the possibility to use carbon fiber reinforced plastics (CFRP) to construct these elements. CFRP is able to take approximately four times the loads of aluminium due to the very high strength levels it can take. Furthermore, the stiffness is approximately 1.8 times higher for CFRP compared to aluminium. The best characteristic of CFRP is the low specific density the material has. This makes it possible to have significant mass savings when applied to structural components. This is the main reason why multiple companies are investigating the application of CFRP in intertank and interstage structures [74], [75], [157].

For propellant tanks a special inner liner has to be inserted to ensure material compatibility. In the case of cryogenic propellants a metal liner is required and a FEP liner is required to make the CFRP material compatible with most storable propellants [135]. Currently, the specific impulse of storable propellant combinations is still inferior to cryogenic propellant combinations. If no design iterations have been performed or the payload capability was unchanged this can have the indirect effect of a larger wet mass, as was found in previous chapters. This means that the thrust-to-weight ratio of the launch vehicle might change. New load paths, stress levels and fatigue modes have to be investigated in this case to make sure the structural strength of the vehicle maintains within the design envelope.

The aluminium structural elements for the Ariane 6 are produced by MT Aerospace. The main manufacturing technique that is applied by MT Aerospace are forming processes, shoot peen forming being the baseline forming process for the cylindrical panels of the structures [73]. For the ribs and stiffeners forging techniques are also applied. It is found that the shoot peening process reached a TRL of 6 for the configurations that apply to the Ariane 6 stages (diameter, thickness, etc.). The elements are connected by the means of friction stir welding (FSW). Friction stir welding is a technique where typically two identical metals are welded together by the application of friction. The friction between the rotating weld head and the material will melt the parts together in a relatively clean weld seam. During this process no material is consumed by the tool and the work pieces are essentially welded together by locally melting the material and pressing them together. This welding technique is applied for flange welds, circumferential welds, meridional welds and longitudinal welds [73]. This friction stir welding is an innovative way of reducing the complexity of the structure and limiting the number of welds required. Additive manufacturing can also be a promising manufacturing technique.

The introduction of CFRP material calls for new manufacturing techniques. When a carbon/glass fiber, or any other carbon composite material for that matter, is applied this is regularly done by a composite layup technique. Depending on the use case the carbon composite fibers can be sprayed, mixed

with a resin, on top of a mall or can be wrapped around a mall (a vessel or tank structure for example). In multiple steps this structure will be hardened at elevated temperatures and pressures. This technique can be used to produce relatively strong but light pressure vessels, for example propellant tanks.

The emerging market of commercial space flight requires massive cost reductions to make spacecraft designs economically viable. Reducing cost is strongly related to reducing the mass of spacecraft components. Additive manufacturing (AM) is a new manufacturing technique that can efficiently produce optimised designs, reducing cost/mass while maintaining the required performance. The projected reduction in cost and schedule risk make AM a very attractive manufacturing technique [16], [72]. Additive manufacturing is often better known by the term '3D printing' and is a fairly new manufacturing technique. In order to additive manufacture a part, first a model of the part should be uploaded to a designated design software tool. This tool will make it possible to describe the lay-up process and communicate this to the production facility. Then the part will be built up layer by layer. This process is often a very time-consuming operation but will (depending on the quality of the machine and coarseness of the lay-up material) result in very accurate product [16], [178]. However, the projection is that this manufacturing technique will become much faster and more economical in the future. Additive manufacturing can be done in a lot of ways with different methods for different design objectives and materials.

The AM machines offer production flexibility while maintaining the quality. Another advantage of additive manufacturing compared to 'subtractive' manufacturing is that there is less waste of production material. For aerospace engineering applications additive manufacturing allows for the production of complex designs that previously were impossible to manufacture, combining (normally) multiple parts into one additive manufactured component [16], [178].

The European Space Agency is looking into ways to use additive manufacturing to cost-effectively and rapidly produce semi-storable rocket engines in the Prometheus program [156]. Prometheus is an ultra-low cost reusable rocket engine demonstrator that is operating on liquid methane and liquid oxygen. The Prometheus engine aimed to be used on core, booster and upper stages of the future European launch vehicles [156]. The research conducted showed that additive layer manufacturing can cut down the number of parts and can speed up the production process and reduces waste. Preliminary cost estimation showed that a tenfold cost reduction can be obtained compared to the Ariane 5 Vulcain 2 engine [156].

Lastly, due to the use of storable propellants, it is possible to reduce the dimension of the upper stage, as was discussed in chapter 9. Due to the smaller propellant tanks the length of the entire upper stage is reduced quite significantly. This is schematically depicted in Figure 9.6. This is useful for attitude control in-space but also during the manufacturing phase it is useful as smaller jigs and support structures are required to assemble, test and integrate the subsystems. This will drastically cut-down the manufacturing cost and development time. Lighter structures are also easier to manipulate during construction.

10.6. Ground Operations and Handling

The European Union started the program GRASP to identify (new) storable fuels that are safe to work with, easy to store and are non-toxic nor carcinogenic [122]. In two uncorrelated research works by G. Rarata et al. [162] and M. Ventura et al. [164] it was found that hypergolic fuels with highly concentrated hydrogen peroxide can "seriously" reduce the costs and risks related to the safety and services procedures on the ground segment. The largest risk that was identified for handling 98% concentrated hydrogen peroxide was connected to possible human errors and material failures. Hydrogen peroxide is argued to offer excellent and unique opportunities; "it is an environmentally and personnel friendly, non-cryogenic and almost non-volatile strong, liquid rocket oxidiser that is next after liquid oxygen (LOX)" [162]. Often, storable fuels have similar characteristics making the storable propellants inherently cost-effective for ground operations and handling. For cryogenic propellants, it is important to have safe methods in place for fuelling and defuelling processes. Due to the extremely low temperatures and potential rapid boil-off these ground operations and handling sequences require a lot of risk mitigation strategies and peripheral equipment [91]. Before cryogenic propellants can be loaded into

the launch vehicle propellant tanks it is very important to make sure that no air or moisture is present in the tanks, feed lines or valves. Otherwise solid air particles or ice could be formed, potentially leading to blockages or plugging injectors [171]. Furthermore, the ground operations and handling for cryogenic propellants into the launch vehicle are getting even more complex as the propellant tanks, feed lines, valves and piping should be chilled or cooled down prior to on-boarding of the propellants. This is done to prevent excessive bubbling of the cryogenic liquid due to boil-off. Cooling down the feed lines, propellant tanks and valves is done by initial cryogenic liquids that will absorb the heat from the relatively warm hardware. This initial liquid will vaporise and vented out of the system by the means of appropriate valves [171]. As discussed earlier, storing cryogenic propellants for extended periods will result in the heating of the cryogenic propellants. Due to the ambient-temperature of the exterior hardware the cryogenic liquid will slowly vaporise/ boil-off, leading to significant pressures in the storage container (which can be the propellant tank or ground storage tank). If there are no pressure safety devices present on the launch vehicle or on the ground equipment these pressures can result in catastrophic failure of the system. This directly points out the complexity that is added to the ground and on-board systems to handle and store cryogenic propellants. Pressure Safety devices can, for example, be pressure relief valves, burst diaphragms, self-regulated cryo-coolers etc. [171].

Storing propellants that are liquid at ambient temperatures and pressure and are nearly non-vaporising under normal conditions do not require such complex ground and handling equipment. This forecasts reduced complexity and added reliability, trickling down to a lower operation cost during pre-launch and post-launch operations. The main cost-driver for the ground operations and handling sector are the potential compatibility issues with the new storable propellants. According to O. Frota et al. [8], the development of new materials for tanks, bladders, ground support equipment, etc. is necessary to overcome these potential compatibility issues.

Since this research was focused on hydrogen peroxide being the designated oxidiser for storable bi-propellant propulsion systems, considerations regarding the production, handling and storage of hydrogen peroxide will be briefly discussed below.

Producing Hydrogen Peroxide

Although there are various ways of producing hydrogen peroxide, it is often produced using the anthraquinone process. This production process is a cyclic operation that consists of sequentially performing hydrogenation, filtration oxidation and extraction methods. In this process, as the name suggests, alkylanthraquinone is used. During the first step, hydrogenation is used to transform the alkylanthraquinone to tetrahydroalkyl-anthrahydroquinone [179]. This is done by ensuring that the temperature of the environment is maintained at 45°C and using a palladium catalyst. When this process is finished, still a lot of traces of the catalyst are present in the solution. Through filtration, the catalyst is removed and stability of the hydrogen peroxide is ensured. After the filtration phase, oxidation will be used to oxidise the tetrahydroalkyl-anthrahydroquinone. During this process, hydrogen peroxide is formed in an organic phase, no catalyst is necessary because of this auto-oxidation [179]. After the hydrogen peroxide is produced it has to be extracted. This happens in the last step where demineralised water is used in an extraction column to extract the hydrogen peroxide from the solution. The hydrogen peroxide is collected at the bottom of the extractor column in an aqueous solution with water. Through subsequent purifying and vacuum distilling the hydrogen peroxide concentration of the solution can be brought up [179].

The technique described above is used most often in the industry. The cost-effectiveness of this production technique depends on the ability to extract and recycle the anthraquinone components to be reused in the process as these chemicals are expensive. When higher concentrations of hydrogen peroxide are required the number of steps that have to be taken in the process increases, bringing up the price. The anthraquinone process also takes a lot of energy consumption (31.06 mega joules per kg). On average a kilogram of hydrogen peroxide (98%) costs about 3.76 € [53].

SolvGE is trying to drastically reduce the cost of high concentration hydrogen peroxide by reducing the complexity of production and making it possible to produce the hydrogen peroxide on-site, mitigating the transportation risks and cost. SolvGE developed a hydrogen peroxide printer that can produce

hydrogen peroxide up to a concentration of 99.5% using innovative patented technology that allows the production of hydrogen peroxide through a safe and scalable passive production technique [15]. This hydrogen peroxide printer is able to passively increase the concentration of the input hydrogen peroxide from around 20 to 30% to around 98%. This process does not affect the purity. Secondly, SolvGE also produced an electro-chemical production process that can combine hydrogen and oxygen (without electrolytes) to produce hydrogen peroxide. This production facility is currently able to produce 1 to 20 kg in one day. Since the production and concentration system scale linearly the system can be stacked to increase the production to several tons hydrogen peroxide in the future. When this production rate is met the expected production price of hydrogen peroxide will be around 0.80 € per kg. SolvGE's production and concentration process combined has an approximate energy consumption of 16.74 mega joules per kg. This is around half the amount of required energy as what is used during the anthraquinone process.

Note: the information presented about the concentration and production systems of SolvGE was given by the SolvGE Production Team and was cleared for the public by SolvGE Management.

Handling Hydrogen Peroxide

The inherent extra safety of the “new” hypergolic propellants can greatly reduce the cost and risks involved with handling and service procedures on the ground segment [162]. Hydrogen peroxide proved itself over the last decades of being able to be produced relatively safe without having a big impact on the environment [164], [180].

Some of the most notable hazards and risks that were identified are the following [162]:

- Uncontrolled ignition/decomposition
- Contamination of the external environment
- Oxidiser corrosivity with typical construction materials
- Accumulation of vapours in the storage device
- Incompatibility of seal material for long term storage
- Incompatible protective equipment

Good handling protocols and regular checks can help mitigate these identified hazards and risks. Often these protocols are suggested by manufacturing companies or by governmental watchdogs.

Transport and storage of hydrogen peroxide generally is a very time-consuming and expensive operation [180]. Especially the transport of High Test Peroxide (HTP) with concentrations above 90% is heavily regulated and special shipment methods and regulations are required to be able to transport this substance [181]. Hydrogen peroxide with concentrations of more than 8% are considered hazardous materials by the U.S. Department of Transportation (DOT). This category is required to use specialised railcars or tank trucks that have high-purity aluminium or steel storage containers with dedicated filter vents [72], [181]. This high transportation cost and long storage periods can be mitigated by the production facility offered at SolvGE. Using their passive production technique highly concentrated hydrogen peroxide can be produced on-site at high production volumes for a fraction of the cost.

Storing Hydrogen Peroxide

To prevent a lot of vapour gas from accumulating at the top of the storage tank it is recommended to make the vessels atmospheric by incorporating a vent to release the built up of liberated oxygen [72]. Furthermore, it is unacceptable to use the following materials [72]:

- Brass
- Copper
- Nickel
- Iron and mild steel
- Bronze
- Synthetic rubbers
- Polypropylene
- Zinc

The materials that are recommended consist mainly of aluminium and stainless steel. Other acceptable materials are:

- Chemical glass
- Chemical Ceramic
- Polytetrafluoroethylene (PTFE; Teflon®1)
- Fluorinated Ethylene Propylene (FEP)
- Polyethylene
- Viton®, Kelf®, Tygon®
- PVC

Hydrogen peroxide should be stored in low temperatures and kept from UV light to ensure stability [181]. For storage, it is important to regularly check the storage container for possible contaminants. Contaminants can result in uncontrollable decomposition of hydrogen peroxide. Metallic flakes (due to faulty maintenance of the container) can act as a catalytic reaction but also airborne contamination and contaminated hydrogen peroxide that return to the storage container can result in rapid decomposition of hydrogen peroxide, making the ambient temperature of the container rise, resulting in an even faster decomposition reaction [72]. Furthermore, large piping runs should be avoided and the number of valves and fittings should be minimised.

In general, highly concentrated hydrogen peroxide is easy to store, safe to handle and becoming easier to produce. Taking into account the right environmental conditions and materials of the storage tanks and handling equipment, the risk on decomposition of hydrogen peroxide can be greatly reduced [182].

10.7. Re-Design Potential Cost Impact

All the subsystem considerations discussed above can be considered recommendations for future research and development. A lot of subsystems that were designed for the use of storable propellants are outdated. The development in storable propellants slowed down after the '70s due to the increasing interest in non-toxic, non-carcinogenic cryogenic liquids. The introduction of green storable propellants and their potential cost benefit will spark interest in storable oriented subsystems once again. Since, a lot of development is required it is expected that this will introduce a significant development cost impact. Development in material compatibility, propellant engineering and steady-state injection and combustion will be most pronounced. It is hard to estimate the potential cost burden of this development phase. It is however expected that the inherently less complex systems (as discussed in this chapter) will eventually result in rapid development and lower development cost compared to hydrolox systems.

Over the long haul, it is expected that the simpler (sub)systems design, the ease of operation and safe storage and handling, that come to play with storable propellants, will result in lower operation and development costs. Furthermore, due to the energy-dense propellants, stages filled with storable propellants can become more condensed. Smaller dimensions are required to take up the required propellants. This results in lighter structures. Furthermore, storable propellants allow the use of a variety of lightweight materials that can be used in structural components and propellant storage designs. Lighter and more condensed stages are easier to handle, maintain and transport before launch, they are easier to actively control during in-space operation and they introduce better aerodynamic flight performance.

Although it is hard to quantify the possible cost impact, the following can be concluded from the preceding sections on subsystem considerations:

- **Propulsion Subsystem**

The propulsion subsystem will be less complex and easier to operate due to the simpler turbo-pump design. Due to hypergolicity, inherent reliability is introduced into the system resulting in fewer redundant systems and safety margins introduced into the design. The development will

have a significant mass burden but the manufacturing cost and operation cost of storable propulsion subsystems is expected to be at least comparable to hydrolox systems.

- **Propellant Storage and Feed Subsystem**

The storable propellants are easier to store at ambient temperature and pressure. Development of storable propellant storage systems is well underway and is not expected to create a significant development cost burden. Furthermore, the cost of operation and manufacturing is expected to decrease due to the simpler and smaller design.

- **Thermal Control Subsystem**

The thermal control subsystem is also simpler for storable upper stage designs. In the pre-launch phase and during launch less thermal control is required to keep the propellants safe. Less mass is attributed to thermal control. This will have a significant cost reduction impact on the overall system.

- **Structural Subsystem**

Storable propellants introduce more design options in terms of material compatibility. The structural design is not expected to drastically change. New manufacturing techniques have been discussed that over the life-cycle of the project can reduce the manufacturing cost significantly while allowing for higher precision and accuracy. The initial cost impact of changing the manufacturing process is expected to be significant. It is however important to note that these processes can also be applied to cryogenic designs.

- **Ground Operation and Handling**

It is expected that the inherently safe and easy use of storable propellants will significantly reduce the ground operation and handling cost in pre- and post-launch processes, as predicted by GRASP [121]. The safe processes will result in less expensive ground equipment required, bringing down the operation cost per flight. This can be especially important for future reusable launch vehicle designs.

The simpler subsystems and lower ground operation and handling cost will be a great benefit of using storable propellants especially in reusable launch vehicles. In this case, the main contributors to the cost-per-flight figure are the refurbishment cost and operation cost. If the launch vehicle systems operate on inherently simple storable propulsion systems the refurbishment effort will be less. Fewer components have to be checked after the flight and due to the high reliability (e.g. restartability of the propulsion system) less redundant systems have to be verified and validated on their status post-flight. The ease of storage and operation of storable propellants makes it possible to provide cost-effective rapid reusability. Rapid reusability describes the case when more launches are required in far smaller time intervals compared to what is currently done. For reusable systems it is required that the stages land back on earth or other planetary body in order to be inspected, refuelled and relaunched. To do this landing manoeuvre, the system is very much reliant on the propulsion system. This propulsion system has to restart multiple times to do retro- and landing burn sequences.

10.8. Executive Chapter Summary

In this chapter, subsystems were discussed that are significantly impacted by the implementation of storable propellants. Furthermore, the re-design considerations that are described also serve as future work recommendations. These are the propulsion subsystem, propellant storage and feed subsystem, thermal control and structural subsystem. Also, the ground operation and handling process were discussed. The pre- and post-launch ground operations are much different between storable and cryogenic propellants.

For the propulsion subsystem, re-design considerations were discussed. It was found that the injection dynamics and injector plate design for storable propellants are very important to take into account. The injection behaviour of (gelled) storable fuels can improve performance, reduce the complexity and increase reliability. Especially viscosity and viscoelastic properties play a vital role in injection and mixing. The combustion chamber length is dependent on the ignition delay time (IDT) of the storable

propellant combination. The IDT can be tweaked (with appropriate additives) such that it can be optimised for the injector plate and the combustion chamber length. The combustion chamber temperature is dependent on the mixture ratio of the propellants. The temperature in the combustion chamber can be impacted by possible depositions of combustion products. To maintain the combustion chamber within the operational temperature envelope different cooling techniques are described. Film cooling and regenerative cooling is currently under development for highly concentrated hydrogen peroxide. It is argued that storable propellant engines are inherently less complex due to the hypergolic behaviour of the propellants. It is expected that the simple engine design will flow down into a lighter and cheaper propulsion system in the future. Due to the relatively dense storable propellants the pump design and feed system can be much simpler than what is seen for cryogenic propellants. The cryogenic propellants required dedicated turbo-shafts and purge seals to pump the low-density liquid hydrogen around. This adds considerably to the complexity of the cryogenic propellant design. The simpler design for storable propellants increases the reliability of the system.

In terms of reliability, it is found that storable engines are preferred over cryogenic engines, mainly due to the less complex designs. The hypergolic behaviour of the storable propellants enhances the reliability of upper stage designs as multiple altitude starts are ensured with a higher probability. Cryogenic systems need the dedicated pyrophoric mixture TEA-TEB to restart the engine mid-flight. If this extremely toxic and corrosive material is depleted or not fed to the engine the engine is lost. Storable engines depend on the hypergolic combustion of the propellants to restart the engine. This way the restartability is easier to obtain during normal operation. Furthermore, the propellant-specific hazards, and reusability favour storable types of propellants. Currently, multiple studies are conducted to quantify reliability factors for bi-propellant hypergolic systems.

It was found that the complexity of storage and feeding propellants is mainly determined by the chemical and physical characteristics of the propellants. Cryogenic propellants have significant boil-off due to their low vapour pressure. This boil-off can introduce large pressures and stresses into the design. Dedicated pressure-relief systems have to be in place to make sure that the propellant tanks and propellants remain in their operational envelope. This adds to the complexity and cost of the subsystem. A lot of *R&D* is currently conducted to investigate the possibility of using carbon fiber composite material for structural components. Although this development shows promising results it is significantly harder to develop composite cryogenic propellant tanks than composite storable propellant tanks. This is mainly due to the high pressures and thermal footprint cryogenic propellants inherently have. Both for the cryogenic and storable propellants, a dedicated liner material is added to the interior of the propellant tanks to make the tank compatible with the propellants. This liner is made from metal for cryogenics. A FEP liner is proposed for highly concentrated peroxide. All considered, it was concluded that storable propellants have distinct advantages over cryogenics in terms of storage and feed systems in launch vehicle designs. Novel carbon fiber composite structures are eminently interesting for storable-based designs.

In terms of thermal control, it was concluded that storable fuels and oxidisers require less complex and costly solutions to keep the propellants within their design constraints. For cryogenic systems, it was found that proper insulation solutions have to be proposed to prevent (semi-)exterior ice formation, allow for safe propellant feed operation and to prevent catastrophic boil-off. Furthermore, storable propellants are less prone to thermal leaks, require simple metallurgy and have larger material thermal compatibility. In terms of structural considerations, it was found that new manufacturing techniques can reduce the complexity and cost of the overall design. This is both the case for cryogenic and storable designs. Additive manufacturing shows great promise in the production of both aluminium and CFRP materials. It was found that additive layer manufacturing can cut down the number of parts and can speed up the production process while reducing waste. These techniques can be applied in all structural fields of launch vehicle design. Lastly, the condensed design of storable upper stages (due to the smaller propellant tanks) can reduce manufacturing and development cost and time significantly. Because smaller support structures are required, making them easier to manipulate during construction.

The ground operation and handling of storable propellants are expected to be less expensive than cryogenic propellants. The main reasons are; safer handling, less complex ground support structures,

easier manufacturing/storage/feeding and less costly procurement. Through a novel production method hydrogen peroxide can be produced on-site safely and cost-effectively. This will extend the possible use cases and availability of hydrogen peroxide even further. Under the right precautions, hydrogen peroxide is safe to handle and store. Furthermore, hydrogen peroxide is compatible with a wide range of materials.

To conclude, it was found that storable propellants lead to simpler, more reliable, safer, and cost-effective subsystem re-designs. Mainly the simpler and safer operation of storable propulsion systems, storage systems, and thermal control is expected to lead to significant cost savings in the future. Bringing down the cost-per-flight further and bringing up the payload performance of the storable "Prototype X" design concept. Especially future reusable launch systems operating on storable propellants can benefit from these cost considerations and added reliability.

11

Conclusion

In this chapter, the main conclusions, from the work presented in this thesis work, will be discussed. This thesis research aimed to narrow down the research gap on storable upper stage designs. Recommendations for future work are given to further aid in this goal, and close the research gap.

The research discussed in this thesis work investigated the cost-effectiveness and feasibility of 'green' storable upper stage design concepts. First, dedicated models were developed to study the behaviour, in terms of performance, mass and cost, of the upper stage design concepts. These models gave insight into design impacts of optimisation solutions. A selection of promising 'green' storable propellants was made to further analyse their design benefits and constraints. The most promising storable propellants were subject to detailed mass and cost analysis to investigate the cost-per-flight (CpF) and payload performance of each optimised storable design. Next to these developed propellants, a comprehensive cross-over analysis was performed to study the effects of storable propellants at different performance levels. A brief discussion on subsystem re-design considerations pointed out the benefits of the storable concepts compared to conventional cryogenic designs. The process described above provided a lot of valuable data that now enables to formulate an answer to the research questions coming forth from the research goal:

Investigate the cost-benefit, payload performance and technical feasibility of green storable upper stage design concepts, compared to a conventional cryogenic upper stage design

The combined data collection this thesis work produced shows that this goal is achieved. Achieving this goal allows to formulate a conclusion on the work described in this thesis:

Although current 'green' storable propellants can reduce the cost-per-flight of the upper stage by 8.9%, their wet mass burden reduces the payload performance by at least 308.09%. Making them not cost-effective in the current medium/heavy launch vehicle market. However, further development in storable propellant engineering can improve the payload performance of the storable upper stage concept by +37.79% for the same wet mass, compared to the cryogenic design, while reducing the geometrical dimensions of the upper stage concept by roughly 33%. Storable 'green' propellants significantly reduce complexity and add reliability and safety to the system, potentially improving the payload performance even further. Calculations suggest that a hybrid launch vehicle, comprised of a cryogenic first stage and a 'green' storable upper stage, would be the most cost-effective expendable launch vehicle in the West having a payload performance of 3.80 k€/kg. However, taking into account the added safety, higher reliability and reduced complexity of the storable systems, it is expected that the proposed hybrid launch vehicle (either expendable or reusable) will outperform all medium to heavy launch vehicles on the market today (Figure 9.7).

This thesis describes the cost-benefit of various storable design concepts together with their corresponding payload performance. The technical feasibility of these concepts is also discussed in great detail. This allows to answer the research questions:

A variety of 'green' fuels were investigated as potential candidates for a propellant combination with highly concentrated hydrogen peroxide. For this propellant selection it was required that the fuels had a classification of being 'green'. Through extensive propellant analysis it could be concluded that the dry mass for storable designs was reduced by approximately 20% on average. However, it was found that the wet mass increase significantly due to the higher density of the fuels and their reduced specific impulse. This wet mass burden was ranging between +38.32% and +62.84%, depending on the propellant combination. Due to this wet mass burden, the payload capability was significantly reduced for storable concepts.

Optimised specific impulse characteristics for each combination, together with their respective combustion conditions, were used as input to the detailed mass and cost analysis. The mass and cost analysis showed significant cost reductions in development and manufacturing, in the range of 13.8–13.3%. The operating cost was increased by approximately 2.0 to 2.7%. On average the cost-per-flight was reduced by 8.4 – 8.9% for the "Prototype X" storable concepts. The reduced cost-per-flight figure that was found for storable designs does not correct for the reduced payload mass that can be carried. The most promising storable concept had a payload capability reduction of 70.3%, bound for LEO. This calculation was based on the combination H₂O₂/DMAZ having the largest variety in mission characteristics, with missions to LEO, SSO, Polar Orbit, and can do ISS servicing missions. Combining the payload capability with the CpF for the various storable designs showed that all "Prototype X" concepts were subject to a significant payload performance reduction. The minimum cost-per-kg increment was found for the H₂O₂/DMAZ combination and was estimated to be +308.09%.

From a market outlook analysis it could be concluded that none of the storable "Prototype X" concepts were deemed commercially attractive to be used in the current launch vehicle. The wet mass burden, as a result of lower propellant efficiency, resulted in a smaller payload capability. The reduced payload capability diminished the advantage of a lower CpF and a simpler system design.

A cross-over analysis was conducted for the "Prototype X" storable design concept. Here the focus was on finding the required performance of a hypothetical "Fuel X" that would make the storable concept more economically attractive. It helped to point out what is necessary for storable propellants to make them competitive with the conventional cryogenic propellants. DMAZ served as a benchmark for the hypothetical "Fuel X". The density, optimum mixture ratio and combustion chamber pressure were kept fixed at the values that were found for DMAZ. First, the cross-over analysis focused on finding the specific impulse where the wet mass of the storable design concept was limited to what was found for the ULPM. This analysis was performed for the aluminium storable concept and for a carbon fiber composite storable concept. In the latter, the interstage, intertank and propellant tanks of the "Prototype X" were constructed from carbon fiber composite material, essentially adding a structural design variable. Storable 'green' propellants inherently have significant advantages over cryogenic propellants in terms of handling and storage. A carbon fiber composite upper stage design thus can have significant mass and cost-saving advantages.

In the cross-over analysis it was found that the aluminium "Prototype X" concept had a cross-over point at a specific impulse of $I_{sp} = 433.5 s$. Here, the wet mass of the storable concept was in the same range as the cryogenic design. The dry mass, however, was 22% less for the aluminium ULPM. It was found that the CpF for the aluminium "Prototype X" was reduced by 10.6% compared to the conventional Ariane 6 ULPM. Here all three cost contributors experienced a cost reduction. The carbon fiber composite "Prototype X" concept got to this cross-over point when "Fuel X" reaches a specific impulse of $I_{sp} = 407.1 s$. The dry mass was reduced by approximately 42%. Compared to the conventional cryogenic design the composite "Prototype X" vehicle was 19.1% cheaper in CpF. The conventional payload capability in this cross-over analysis was maintained. A second analysis was performed to investigate the design concepts in case the "Fuel X" could produce cryogenic levels of performance with hydrogen peroxide. It was found that the CpF was reduced by 11.2% and 19.8% for the aluminium and composite concept, respectively. To understand the impact of the reduced CpF, found for these four concepts, the payload performance was calculated. The cross-over designs maintained the conventional payload capability, whereas the designs with cryogenic level performance had an improved payload capability of 15% and 29% for the aluminium and composite concept, respectively. The aluminium conceptual designs reduced the payload performance by 10.52% and 22.78% respectively. The two composite design concepts achieved the best CpF. The composite concepts reduced the pay-

load performance by 19.01% and 37.79% respectively. It was found that the composite “Prototype X” concepts potentially can reduce the geometrical dimensions of the upper stage by roughly 33%. The smaller propellant tanks and intertank make the upper stage structure more condensed. It is important to note that the specific impulse characteristics assumed here are currently not achieved yet for ‘green’ storable combinations. It is, however, argued that the relative performance gap, in terms of specific impulse, can be overcome in the future.

By market analysis it was found that an increased payload performance was found for all proposed “Prototype X” concepts. These improvements range from 2.64% to 26.27% of payload performance increase. Compared to other medium/heavy launch vehicles the hybrid design promised to be the most cost-effective expendable launch vehicle in the west. However, it is expected that the simpler, more reliable, safer, and more cost-effective subsystem re-designs for ‘green’ storable designs can make the “Prototype X” concept outperform all current medium to heavy expendable launch vehicles (Figure 9.7). Mainly the simpler and safer operation of storable propulsion systems, storage systems, and thermal control is expected to lead to significant cost-savings in the future. Bringing down the cost-per-flight further and bringing up the payload performance of the storable “Prototype X” design concept. Applied to reusable launch systems the effect of storable propellants on the payload performance will be even more pronounced. Due to their reduced operation and refurbishment cost burden, reusable storable stages are expected to outperform current reusable systems on the market, while reducing complexity and adding reliability and safety.

Future Work Recommendations

Throughout this thesis research various storable upper stage concepts have been discussed. The first three concepts were designed for the most promising fuels in combination with hydrogen peroxide. These are DMAZ, Ethanol and Dimethylamine. Next, the cross-over analysis was performed. In this analysis the conventional aluminium and novel carbon fiber composite upper stage structures were analysed on their required specific impulse to have the same payload capability as the cryogenic upper stage. Lastly, the specific impulse of the hypothetical storable propellants was boosted to the level of hydrolox combinations. The payload performance of all these seven concepts have been calculated and are graphically shown in Figure 11.1.

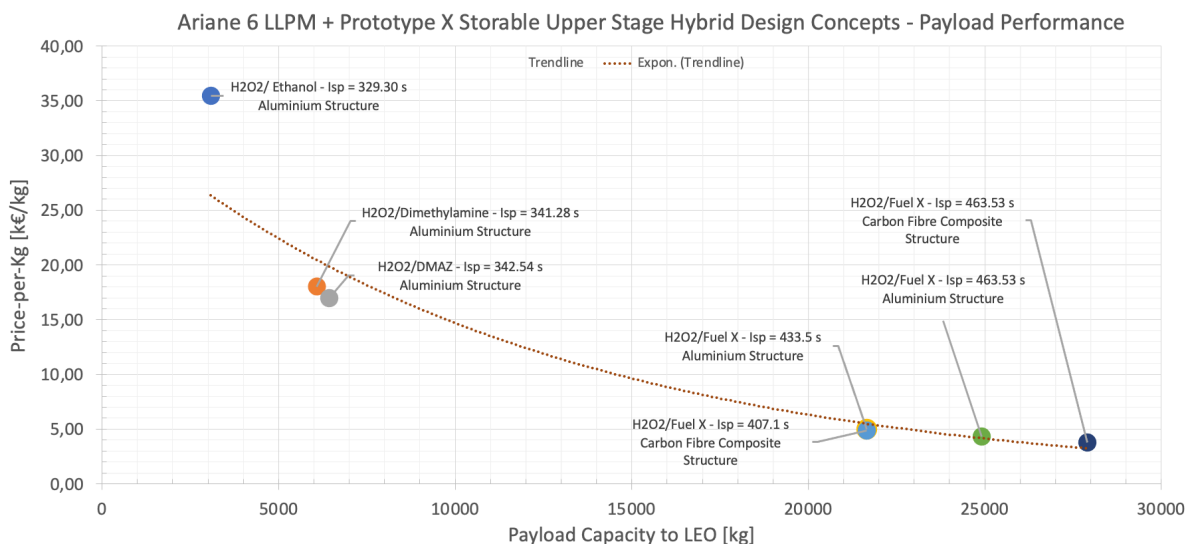


Figure 11.1: Calculated Payload Performance for Various Prototype X Design Concepts Integrated with Ariane 6 First Stage

In this section, recommendations are provided to describe the aspects of this research that should be investigated in the future.

- This research thesis serves as a preliminary feasibility study into storable upper stage designs. During this research the necessary assumptions and estimations have been made to set up the models and/or to allow for comparison. In chapter 8 the analysis was limited to only changing the type of storable propellants. No further design iterations (in terms of the type of material, number of elements or dimensions) have been performed. This allows to compare the cost and performance estimates of the storable concepts one-to-one with the modelled cryogenic upper stage design. In chapter 9, however, also design iterations in terms of materials and dimensions have been performed. Carbon fiber composite materials were introduced and their effect on mass and cost of the upper stage design was investigated. It is recommended for future research to investigate the impact of carbon fiber composite materials on these cost estimating relationships. It is important to understand how the development and manufacturing cost is affected by these new materials. Also, the discussed error margins of $\pm 20\%$ will probably change due to the introduction of CFC material. These updated error margin have to be investigated and calculated in future research. Furthermore, it is recommended to make the operation cost model more detailed, such that it combines a wider variety of ground operation aspects.
- The integration of the proposed hybrid launch vehicle (cryogenic first stage and storable upper stage) could be investigated more extensively. During this research the boosters have not been taken into account for the cost estimate. It is recommended to do further cost analysis on these boosters and their integration with the hybrid launch vehicle concept. Moreover, this research was focused on the upper stage design of the launch vehicle. The storable upper stage design concepts have been compared to the conventional cryogenic counterpart. It is however much recommended to investigate the estimated payload performance for a fully storable launch vehicle. The design benefits of storable first stage designs could be further investigated in this way. This would provide a better estimate of total payload performance and allows to better compare this with competitor launch vehicles. Therefore it is recommended to do similar research into storable first stage concepts.
- During the cross-over analysis performed in this chapter, performance characteristics for storable propellants have been suggested. It is important to investigate the feasibility of these performance characteristics for current propellant combinations. This research can lead to specific design suggestions to synthesise a propellant combination that meets the proposed performance characteristics. In terms of propellants, the following development is necessary [9]:
 - Increase performance in terms of specific impulse, storability and low total volume for high total impulse missions.
 - Reduce overall life cycle costs in terms of hardware and ground operations for high and low total impulse missions.
 - Exploit common propellant storage with main propulsion for attitude control when utilising bi-propellant systems.
- Since the launch vehicle market is shifting towards a higher level of reusability, it is useful and meaningful to investigate the added benefit of storable propellants for reusable launch vehicle stages. The reusability of rocket stages will drastically impact the cost-per-flight. The manufacturing cost and development cost will be distributed over more launches while fewer systems have to be built. Following this logic, the operation cost will become more pronounced together with the added cost of refurbishment and maintenance. The use of storable propellants will reduce the complexity of the overall propulsion system and storage/feed system. Furthermore, the proposed hypergolic propellant combinations adds to the reliability of the entire system. Especially important for reusable launch vehicle systems as these typically rely on multiple firings of the propulsion units for re-entry and retro-landing burns. The propellant cost, dependent on the level of reusability, will have a more pronounced effect on the cost-per-flight estimate. It is thus recommended to investigate what impact storable propellants have on the cost of reusable launch vehicles.

Bibliography

- [1] F. Koch. (2021). "Ariane 6 complete upper stage," [Online]. Available: https://www.esa.int/ESA_Multimedia/Images/2021/01/Ariane_6_complete_upper_stage4 (visited on 04/20/2022).
- [2] Federal Aviation Administration. (2020). "Commercial Space Data," [Online]. Available: https://www.faa.gov/data_research/commercial_space_data/launches/ (visited on 06/15/2021).
- [3] E. ESTEC. (2001). "Green propellant for space propulsion," [Online]. Available: http://www.esa.int/Applications/Observing_the_Earth/Green_Propellant_for_Space_Propulsion (visited on 06/15/2021).
- [4] M. Ross and J. Vedda, "The policy and science of rocket emissions," *The Aerospace Corporation*, 2018.
- [5] I. W. C.S. Dorbian P.J. Wolfe, "Estimating the climate and air quality benefits of aviation fuel and emissions reductions," *Atmospheric Environment*, vol. 45, no. 16, pp. 2750–2759, 2011.
- [6] D. F. Letizia, "Space debris environment report," *AMOS 2019*, 2021. [Online]. Available: <https://sdup.esoc.esa.int/discosweb/statistics/> (visited on 08/03/2021).
- [7] S. G. J. Silverman, "Current trends in storable propellants," *SAE Transactions*, vol. 68, pp. 282–287, 1960.
- [8] M. F. O. Frota B. Mellor, "Proposed selection criteria for next generation liquid propellants," *Proceedings of the 2nd International Conference on Green Propellants for Space Propulsion*, 2004.
- [9] D. H. et al., "Green propellant propulsion concepts for space transportation and technology development needs," *Proceedings of the 2nd International Conference on Green Propellants for Space Propulsion*, 2004.
- [10] S. K. H. Kang, "Green hypergolic combination: Diethylenetriamine-based fuel and hydrogen peroxide," *Acta Astronautica*, vol. 137, pp. 25–30, 2017.
- [11] A. Group, "Ariane 6 user's manual," *Ariane Space*, vol. 1, 2018.
- [12] G. R. et al., "Near future green propellant for space transportation," *VIII International Scientific Conference*, 2013.
- [13] A. C. et al., "Development of hydrogen peroxide monopropellant rockets," *American Institute of Aeronautics and Astronautics*, vol. 42, 2012. DOI: 10.2514/6.2006-5239.
- [14] e. a. Y. Moon C Park, "Design specifications of h₂O₂/kerosene bipropellant rocket system for space missions," *Elsevier Aerospace Science and Technology*, vol. 33, no. 1, pp. 118–121, 2014. DOI: 10.1016/j.ast.2014.01.006.
- [15] SolvGE. (2021). "Solvge website," [Online]. Available: <http://www.solvge.com> (visited on 06/15/2021).
- [16] P. Elferink, "Launcher upper stage cost optimization through green propulsion - a comprehensive literature review," M.S. thesis, Delft University of Technology, 2021.
- [17] S. Jain, "Self-igniting fuel-oxidizer systems and hybrid rockets," *Journal of Scientific and Industrial Research*, vol. 62, pp. 293–310, 2003.
- [18] e. a. A. Okninski B. Bartkowiak, "Development of a small green bipropellant rocket engine using hydrogen peroxide as oxidizer," *Propulsion and Energy Forum*, vol. 50, 2014.
- [19] C.W.Jones and J. H. Clark, Eds., *Applications of Hydrogen Peroxide and Derivatives*. The Royal Society of Chemistry, 1999, pp. 1–36, ISBN: 0-85404-536-8.

- [20] e. a. R. Ross D. Morgan, "Upper stage flight experiment 10k engine design and test results," *36th AIAA/ASME/SAE/ASEE Joint Propulsion Conference*, 2000.
- [21] e. a. J.C. Sisco B.L. Austin, "Autoignition of kerosene by decomposed hydrogen peroxide in a dump-combustor configuration," *Propulsion and Power*, vol. 21, no. 3, 2005.
- [22] e. a. K.J. Miller J.C. Sisco, "Design and ground testing of a hydrogen peroxide/kerosene combustor for rbcc application," *39th AIAA/ASME/SAE/ASEE Joint Propulsion Conference and Exhibit*, vol. 39, 2003.
- [23] W. A. B.L. Austin S.D. Heister, "Characterization of pintle engine performance for nontoxic hypergolic bipropellants," *Propulsion and Power*, vol. 21, no. 4, 2005.
- [24] e. a. Y. Moon C. Park, "Design specifications of h₂O₂/kerosene bipropellant rocket system for space missions," *Aerospace Science and Technology*, vol. 33, pp. 118–121, 2014.
- [25] K. I. G. Da Silva, "Hypergolic systems: A review in patents," *Journal of Aerospace Technology and Management*, vol. 4, no. 4, pp. 407–412, 2012.
- [26] e. a. M.S. Naseem B.V.S. Jyoti, "Hypergolic studies of ethanol base gelled bi-propellant system for propulsion application," *Propellant, Explosives, Pyrotechnics*, vol. 42, no. 6, pp. 1–8, 2017.
- [27] e. a. A.S. Gohardani J. Stanojev, "Green space propulsion: Opportunities and prospects," *Progress in Aerospace Sciences*, vol. 71, pp. 128–149, 2014.
- [28] M. G. B.M. Melof, "Investigation of hypergolic fuels with hydrogen peroxide," *37th Joint Propulsion Conference and Exhibit*, vol. 37, 2012.
- [29] R. J. Lewis, Ed., *Hazardous Chemicals Desk Reference*. Wiley & Sons, 1997, ISBN: 978-0-470-18024-2.
- [30] J. R. J.E. Funk, "Assessment of united states navy block 0 nhmf/rghp propellants," *Proceedings: Second International Hydrogen Peroxide Propulsion Conference*, vol. 2, 1999.
- [31] N. P. C.J. Meade B.M. Lormand, "Status of non-toxic hypergolic miscible fuel development at nawc wd china lake," *Proceedings: Second International Hydrogen Peroxide Propulsion Conference*, vol. 2, 1999.
- [32] e. a. B.L. Austin, "Characterisation of non-toxic hypergolic bi-propellants," *Proceedings: Second International Hydrogen Peroxide Propulsion Conference*, vol. 2, 1999.
- [33] W. F. G. Rarata, "Novel liquid compounds as hypergolic propellants with htp," *KONES Powertrain and Transport*, vol. 23, 2016.
- [34] S. K. H. Kang D. Jang, "Demonstration of 500 n scale bipropellant thruster using non-toxic hypergolic fuel and hydrogen peroxide," *Aerospace Science and Technology*, vol. 49, pp. 209–2014, 2016.
- [35] e. a. R. Mahakali, "Development of reduced toxicity hypergolic propellants," *AIAA-2011-5631*, vol. 47, 2011.
- [36] J. Yamamoto, "Sodium borohydride digest," *Rohm and Haas Company*, 2013.
- [37] S. K. H. Kang, "Experiment and speculations on nontoxic hypergolic propulsion with hydrogen peroxide," *Journal of Spacecraft and Rockets*, vol. 55, 2018.
- [38] e. a. Sh. L. Guseinov S.G. Fedorov, "Hypergolic propellants based on hydrogen peroxide and organic compounds: Historical aspect and current state," *Russian Chemical Bulletin*, vol. 67, pp. 1943–1954, 2018.
- [39] e. a. V.K. Bhosale J. Jeong, "Additive-promoted hypergolic ignition of ionic liquid with hydrogen peroxide," *Combustion and Flame*, vol. 214, pp. 426–436, 2020.
- [40] X. Z. C. Sun S. Tang, "Hypergolicity evaluation and prediction of ionic liquids based on hypergolic reactive groups," *Combustion and Flame*, vol. 205, pp. 441–445, 2019.
- [41] S. K. V.K. Bhosale J. Jeong, "Ignition of boron-based green hypergolic fuels with hydrogen peroxide," *Fuel*, vol. 255, 2019.
- [42] e. a. J. Li, "The ignition process measurements and performance evaluations for hypergolic ionic liquid fuels: [emim][dca] and [bmim][dca]," *Fuel*, vol. 215, pp. 612–618, 2018.

- [43] e. a. S.V. Stovbun, "Synthesis and testing of hypergolic ionic liquids for chemical propulsion," *Acta Astronautica*, vol. 135, pp. 110–113, 2017.
- [44] J. S. Q. Zhang, "Energetic ionic liquids as explosives and propellant fuels: A new journey of ionic liquid chemistry," *Chemical Reviews*, vol. 114, no. 20, pp. 10 527–10 574, 2014.
- [45] G. R. W. Florczuk, "Performance evaluation of hypergolic green propellants based on htp for a future next generation spacecraft," *53rd AIAA/SAE/ASEE Joint Propulsion Conference*, vol. 53, 2016.
- [46] *Chemical book*, <https://www.chemicalbook.com/>, Accessed: 2021-09-10.
- [47] T. Economics. (2022). "Ethanol," [Online]. Available: <https://tradingeconomics.com/commodity/ethanol> (visited on 02/02/2022).
- [48] ChemAnalyst. (2022). "Pyridine price trend and forecast," [Online]. Available: <https://www.chemanalyst.com/Pricing-data/pyridine-1172> (visited on 02/02/2022).
- [49] C. Book. (2022). "Diethylenetriamine (deta)," [Online]. Available: <https://www.chemicalbook.com/Price/Diethylenetriamine.html> (visited on 02/02/2022).
- [50] —, (2022). "Isoamyl alcohol price," [Online]. Available: https://www.chemicalbook.com/ProductList_En.aspx?kwd=isoamyl (visited on 02/02/2022).
- [51] D. L. Agency. (2021). "Market prices of bulk spacecraft materials," [Online]. Available: https://www.dla.mil/Portals/104/Documents/Energy/Standard%5C%20Prices/Aerospace%5C%20Prices/E_2017Oct1AerospaceStandardPrices_170913.pdf?ver=2017-09-13-145335-477 (visited on 09/10/2021).
- [52] —, (2021). "Market prices of bulk spacecraft propellants (new version)," [Online]. Available: https://www.dla.mil/Portals/104/Documents/Energy/Standard%5C%20Prices/Aerospace%5C%20Prices/E_2017Oct1AerospaceStandardPrices_170913.pdf?ver=2017-09-13-145335-477 (visited on 09/10/2021).
- [53] —, (2021). "Market prices of bulk spacecraft propellants," [Online]. Available: https://www.dlislis.dla.mil/webflis/pub/pub_search.aspx (visited on 09/06/2021).
- [54] B. Zandbergen, Ed., *Thermal Rocket Propulsion (Version 2.08)*. TU Delft, 2020, pp. 41–45.
- [55] G. M. N. U.R. Rao S.C. Gupta and D. N. Moorthi, "Pslv-d1 mission," *Current Science*, vol. 65, no. 7, pp. 522–528, 1993.
- [56] m. R. S. Krishnamurthy, "Pslv second stage successfully tested," *SPACE India*, vol. 1, pp. 2–6, 1990.
- [57] E. Kyle. (2021). "Space launch report: Ariane 5 data sheet," [Online]. Available: <https://www.spacelaunchreport.com/ariane5.html> (visited on 09/02/2021).
- [58] E. S. Agency. (2021). "Ariane-5," [Online]. Available: <https://www.esa.int/esapub/achievements/Sc72s6.pdf> (visited on 09/02/2021).
- [59] P. Blau, "Gslv mk. ii launch vehicle," *Spaceflight101.com*, 2021.
- [60] U. S. G. A. Office, "Surplus missile motors - sale price drives potential effects on dod and commercial launch providers," *United States Government Accountability Office*, pp. 29–30, 2017.
- [61] OFOISR, "Proton launch system description and history," *Proton Launch System Mission Planner's Guide*, vol. 7, 2009.
- [62] A. Group, "Soyuz user's manual," *Ariane Space*, vol. 2, 2018.
- [63] A. Zak. (2020). "Fregat upper stage," [Online]. Available: <http://www.russianspaceweb.com/fregat.html> (visited on 09/02/2021).
- [64] SpaceX, "Falcon user's guide," *SpaceX*, 2020.
- [65] A. Isselhorst, "Hm7b simulation with espss tool on ariane 5 esc-a upper stage," *46th AIAA/ASME/SAE/ASEE Joint Propulsion Conference and Exhibit*, vol. 46, 2010.
- [66] E. S. Agency. (2021). "Ariane 5 eca," [Online]. Available: https://www.esa.int/Enabling_Support/Space_Transportation/Launch_vehicles/Ariane_5_ECA2 (visited on 09/02/2021).

- [67] R. A. Braeunig. (2021). "The ariane family," [Online]. Available: <http://www.braeunig.us/space/specs/ariane.htm> (visited on 11/16/2021).
- [68] —, (2021). "The delta family," [Online]. Available: <http://www.braeunig.us/space/specs/delta.htm> (visited on 11/16/2021).
- [69] S. 101. (2021). "Atlas v 551," [Online]. Available: <https://spaceflight101.com/spacerockets/atlas-v-551/> (visited on 11/16/2021).
- [70] M. Wade. (2021). "Delta k," [Online]. Available: <https://web.archive.org/web/20080505082051/http://www.astronautix.com/stages/deltak.htm> (visited on 11/16/2021).
- [71] C. B. J.A. Halchak J.L. Cannon, "Materials for liquid propulsion systems," *NASA Marshall Space Flight Center*, 2020.
- [72] I. Solvay Chemicals, "Hydrogen peroxide - safety and handling, technical data sheet," *Solvay*, 2019.
- [73] e. a. J. merino A. Patzelt, "Ariane 6 - tanks and structures for the new european launcher," *Deutscher Luft- und Raumfahrtkongress*, 2017.
- [74] C. Henry. (2019). "Prototype ariane 6 carbon-composite upper stage gets esa funding," [Online]. Available: <https://spacenews.com/prototype-ariane-6-carbon-composite-upper-stage-gets-esa-funding/> (visited on 08/13/2021).
- [75] A. Tomaswick. (2021). "Lightweight carbon fiber reinforced plastic fuel tanks pass a critical test, and could knock a lot of weight off a rocket's dry mass," [Online]. Available: <https://www.universetoday.com/152035/lightweight-carbon-fiber-reinforced-plastic-fuel-tanks-pass-a-critical-test-and-could-knock-a-lot-of-weight-off-a-rockets-dry-mass/> (visited on 08/13/2021).
- [76] P. S. Technologies. (2015). "H2o2 handling safety overview," [Online]. Available: http://maenas.eng.usu.edu/Peroxide_Web_Page/documents/H2O2%5C%20Material%5C%20Compatibility%5C%20Overview.pdf (visited on 09/06/2021).
- [77] INCOSE. (2021). "What is systems engineering," [Online]. Available: <https://www.incose.org/systems-engineering> (visited on 09/08/2021).
- [78] V. G. E. Caillaud B. Rose, "Research methodology for systems engineering: Some recommendations," *IFAC-PapersOnLine*, vol. 49, no. 12, pp. 1567–1572, 2016.
- [79] P. D. E. Gill, *Model-based systems engineering*, University Lecture, 2020.
- [80] L. Hart, *Introduction to model-based system engineering (mbse) and sysml*, Presentation Slides INCOSE Chapter Meeting, 2015.
- [81] P. D. E. Gill, *Introducing systems engineering*, University Lecture, 2020.
- [82] D. E. Koelle, "Handbook of cost engineering and design of space transportation systems," *TransCostSystems (TCS)*, *Ottobrunn Germany*, 8.2 edition, 2013.
- [83] N. Drenthe, "Solstice - small orbital launch systems, a tentative initial cost estimate," M.S. thesis, Delft University of Technology, 2016.
- [84] M. Balesdent, "Multidisciplinary design optimization of launch vehicles," *École Centrale de Nantes*, 2011.
- [85] M. van Kesteren, "Air launch versus ground launch: A multidisciplinary design optimization study of expendable launch vehicles on cost and performance," *Delft University of Technology*, 2013.
- [86] C. H. Y. F. Biscani D. Izzo, "A global optimisation toolbox for massively parallel engineering optimisation," *European Space Agency*, 2010.
- [87] G. Muller, "Systems engineering research methods," *Procedia Computer Science*, 2013.
- [88] A. A. e. A. R. Burrow D. Just, "Thermal control of the cryogenic upper stage of ariane 6," *International Conference on Environmental Systems*, vol. 49, 2019.
- [89] E. S. Agency, "N° 43–2014: Media backgrounder for esa council at ministerial level," *C/M 14*, 2014. [Online]. Available: https://www.esa.int/For_Media/Press_Releases/Media_backgrounder_for_ESA_Council_at_Ministerial_Level (visited on 08/05/2021).

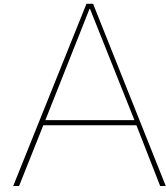
- [90] D. Gallois, "Ariane 6, un chantier européen pour rester dans la course spatiale," *Le Monde*, 2014. [Online]. Available: https://www.lemonde.fr/economie/article/2014/12/01/les-europeens-s-appretent-a-mettre-ariane-6-en-chantier_4532259_3234.html (visited on 08/05/2021).
- [91] D. Z. für Luft- und Raumfahrt. (2021). "Ariane 6 - dlr ready to test first upper stage," [Online]. Available: https://www.dlr.de/content/en/articles/news/2021/01/20210213_ariane-6-dlr-ready-to-test-first-upper-stage.html (visited on 08/05/2021).
- [92] A. Group. (2019). "Vinci engine - propulsion solutions for launchers," [Online]. Available: https://www.ariane.group/wp-content/uploads/2020/06/VINCI_2020_04_DS_EN_Eng_Web.pdf (visited on 08/13/2021).
- [93] S. Snecma. (2011). "Space propulsion - vinci," [Online]. Available: <https://forum.nasaspacesflight.com/index.php?action=dlattach;topic=27843.0;attach=363518> (visited on 11/18/2021).
- [94] J. Vandamme, "Assisted-launch performance analysis - using trajectory and vehicle optimization," M.S. thesis, Delft University of Technology, 2012.
- [95] A. Ponomarenko. (2010). "Rpa: Tool for liquid propellant rocket engine analysis c++ implementation," [Online]. Available: http://w.lpre.de/downloads/1.0/docs/RPA_LiquidRocketEngineAnalysis_II.pdf (visited on 12/21/2021).
- [96] —, (2013). "Assessment of delivered performance of thrust chamber," [Online]. Available: https://www.rocket-propulsion.com/downloads/pub/RPA_AssessmentOfDeliveredPerformance.pdf (visited on 12/21/2021).
- [97] G. Sutton, *Rocket Propulsion Elements*, 7th ed. John Wiley and Sons Inc., 2001, ISBN: 0-471-32642-9.
- [98] H. V. J.C. Oglebay G.D. Sagerman, "Analytical evaluation of space storable propellants for unmanned jupiter and saturn orbiter missions," *Nasa Technical Memorandum - Lewis Research Center*, vol. 1, 1969.
- [99] F. Castellini, "Multidisciplinary design optimization for expendable launch vehicles," M.S. thesis, Politecnico Di Milano, 2012.
- [100] B. G. R. A.V. Barderas, "How to calculate the volumes of partially full tanks," *International Journal of Research in Engineering and Technology*, vol. 5, 2016.
- [101] W. L. R.W. Humble G.N. Henry, *Space Propulsion Analysis and Design*, 1st ed. The McGraw-Hill Companies, Inc. Primis Custom Publishing, 1995, ISBN: 0-07-031320-2.
- [102] B. Zandbergen, "Simple mass and size estimation relationships of pump fed rocket engines for launch vehicle conceptual design," *6TH EUROPEAN CONFERENCE FOR AERONAUTICS AND SPACE SCIENCES (EUCASS)*, 2015.
- [103] R. Ernst, "Liquid rocket analysis (lira) - development of a liquid bi-propellant rocket engine design, analysis and optimization tool," M.S. thesis, Delft University of Technology, 2014.
- [104] S. Contant, "Design and optimization of a small reusable launch vehicle using vertical landing techniques," M.S. thesis, Delft University of Technology, 2019.
- [105] R. Rohrschneider, "Development of a mass estimating relationship database for launch vehicle conceptual design," M.S. thesis, Georgia Institute of Technology, 2002.
- [106] M. G. J.W. Marvin C.Y. Laporte, "Verification and validation deployment package," *International Council on Systems Engineering (INCOSE)*, vol. 1, 2012.
- [107] E. G. M. Calabro, "Launcher analysis and cost benefits," *European Union's Horizon 2020 Research and Innovation Programme*, vol. 1, 2018.
- [108] S. L. Report. (2021). "Ariane 5," [Online]. Available: <http://www.spacelaunchreport.com/ariane5.html> (visited on 11/16/2021).
- [109] S. Insider. (2021). "SpaceX falcon 9 v1.1," [Online]. Available: <https://www.spaceflightinsider.com/hangar/falcon-9/> (visited on 11/16/2021).

- [110] R. J. D.E. Koelle, "Development and transportation costs of space launch systems," *Presentation DLR*, 2007.
- [111] D. E. Koelle, "Transcost statistical-analytical model for cost estimation and economical optimization of space transportation systems," *TransCostSystems (TCS)*, Otto-brunn Germany, 6.2 edition, 1998.
- [112] —, "The transcost-model for launch vehicle cost estimation and its application to future systems analysis," *Acta Astronautica*, vol. 11, no. 12, pp. 803–817, 1984.
- [113] M. v. P. N.T. Drenthe B.T.C. Zandbergen, "Cost estimating of commercial smallsat launch vehicles," *European Conference for Aeronautics and Space Sciences*, vol. 7, 2017.
- [114] H. J. D. Greves, Ed., *Cost Engineering for Cost-Effective Space Programmes*. ESTEC, Noordwijk, The Netherlands, 2003.
- [115] OECD. (2021). "Oecd consumer price index inflation data," [Online]. Available: <https://data.oecd.org/price/> (visited on 10/22/2021).
- [116] E. C. E. Team, "Tec-syc cost risk procedure," *European Space Agency*, 2010.
- [117] B. A. B. Fox K. Brancato, *Guidelines and Metrics for Assessing Space System Cost Estimates*, 1st ed. RAND Corporation, 2008, ISBN: 978-0-8330-4023-7.
- [118] N. Aeronautics and S. Administration, "Nasa cost estimating handbook," *Washington, DC*, 4.0 edition, 2015.
- [119] A. Parsonson. (2020). "Esa requests €230 million more for ariane 6 as maiden flight slips to 2022," [Online]. Available: <https://spacenews.com/esa-request-230-million-euros-more-for-ariane-6-as-maiden-flights-slips-to-2022/> (visited on 01/06/2022).
- [120] N. I. of Standards and Technology. (2022). "Nist chemistry webbook," [Online]. Available: <https://webbook.nist.gov/chemistry/> (visited on 01/19/2022).
- [121] C. E. Commission. (2011). "Final report summary - grasp (green advanced space propulsion)," [Online]. Available: <https://cordis.europa.eu/project/id/218819/reporting> (visited on 01/20/2022).
- [122] A. Tomaswick. (2007). "Grasp—green advanced space propulsion: Let's make spacecraft green," [Online]. Available: <https://cordis.europa.eu/project/id/218819> (visited on 08/23/2021).
- [123] B. Mellor, "A preliminary technical review of dmaz: A low-toxicity hypergolic fuel," *Proceedings of the 2nd International Conference on Green Propellants for Space Propulsion*, 2004.
- [124] M. McQuaid, "The structure of secondary 2-azidoethanamines: A hypergolic fuel vs. a nonhypergolic fuel," *Army Research Laboratory*, 2004.
- [125] B. J. et al., "Hypergolicity and ignition delay study of gelled ethanolamine fuel," *Combustion and Flame*, vol. 183, pp. 102–112, 2017.
- [126] S. Shimizu, "Pyridine and pyridine derivatives," *Ullmann's Encyclopedia of Industrial Chemistry*, 2000.
- [127] B. V. et al., "Alkylation," *Kirk-Othmer Encyclopedia of Chemical Technology*, 2003.
- [128] D. DeSantis, "Satellite thruster propulsion: H₂O₂ bipropellant comparison with existing alternatives," *Ohio State University, Department of Space Technologies*, 2014.
- [129] W. A. M. Van Gysel, "Methylamines," *Ullmann's Encyclopedia of Industrial Chemistry*, 2000.
- [130] E. F. et al., "Methanol," *Ullmann's Encyclopedia of Industrial Chemistry*, 2005.
- [131] A. Papa, "Propanols," *Ullmann's Encyclopedia of Industrial Chemistry*, 2000.
- [132] J. K. L.J. Kapusta L. Boruc, "Pressure and temperature effect on hypergolic ignition delay of triglyme-based fuel with hydrogen peroxide," *Fuel*, vol. 287, 2021.
- [133] T. Saaty, "Analytical hierarchy process trade-off tool users manual," *Dutch Space B.V. and Technical University Delft*,

- [134] U. E. I. Administration. (2021). "Use and supply of ethanol," [Online]. Available: <https://www.eia.gov/energyexplained/biofuels/use-and-supply-of-ethanol-supply.php> (visited on 02/02/2022).
- [135] Graco, "Chemical compatibility," *Graco Inc.*, 2013.
- [136] M. N. S.G. Pakdehi, "Shelf life prediction of a novel liquid fuel, 2-dimethylaminoethyl azide (dmaz)," *Central European Journal of Energetic Materials*, 2017.
- [137] L. Hebei Yanxi Chemical Co. (2022). "Ethanamine," [Online]. Available: <https://hbyanxi.en.made-in-china.com/> (visited on 02/02/2022).
- [138] Research and Markets. (2018). "Ethanamines: Worldwide markets, 2023 - the growing demand for glyphosate is fueling the market," [Online]. Available: <https://www.prnewswire.com/news-releases/ethanamines-worldwide-markets-2023---the-growing-demand-for-glyphosate-is-fueling-the-market-300760739.html> (visited on 02/02/2022).
- [139] G. Glycol. (2018). "Technical data sheet monoethanolamine," [Online]. Available: https://www.gcglycol.com/toccms/upload/ckupload/files/Technical20Data20Sheet_MEA20REV01.pdf (visited on 02/02/2022).
- [140] G. Rand, *Fundamentals Of Aquatic Toxicology: Effects, Environmental Fate And Risk*, 2nd ed. Taylor and Francis Group, 2003, ISBN: 1-56032-091-5.
- [141] U. E. I. Administration. (2012). "Petroleum and other liquids," [Online]. Available: https://www.eia.gov/dnav/pet/hist/LeafHandler.ashx?n=PET&s=8_NA_8PIO_NUS_BSD&f=A (visited on 02/02/2022).
- [142] Reagents. (2021). "2,2,4 - trimethylpentane acs," [Online]. Available: <https://www.reagents.com/2300186/Product/2-2-4-Trimethylpentane> (visited on 02/02/2022).
- [143] ChemAnalyst. (2022). "Dimethyl amine price trend and forecast," [Online]. Available: <https://www.chemanalyst.com/Pricing-data/dimethylamine-dma-1180> (visited on 02/02/2022).
- [144] —, (2022). "Methanol price trend and forecast," [Online]. Available: <https://www.chemanalyst.com/Pricing-data/methanol-1> (visited on 02/02/2022).
- [145] —, (2022). "Isopropyl alcohol (ipa) price trend and forecast," [Online]. Available: <https://www.chemanalyst.com/Pricing-data/isopropyl-alcohol-31> (visited on 02/02/2022).
- [146] Statista. (2020). "Market volume of isopropyl alcohol worldwide from 2015 to 2020, with a forecast for 2021 to 2026," [Online]. Available: <https://www.statista.com/statistics/1245200/isopropyl-alcohol-market-volume-worldwide/> (visited on 02/02/2022).
- [147] C. I. Ltd. (2021). "Isoamyl alcohol," [Online]. Available: <https://www.chemoxy.com/wp-content/uploads/2019/12/TDS-Isoamyl-Alcohol.pdf> (visited on 02/02/2022).
- [148] T. N. K. Wilson A. Tome, "Actual and potential uses of fourteen selected glymes," *Environment and Resources Division, Abt Associates Inc.*, 2009.
- [149] Braeuning. (2012). "Basic of space flight: Rocket propellants," [Online]. Available: <http://www.braeunig.us/space/propuls.htm> (visited on 02/10/2022).
- [150] H. Jones, "The recent large reduction in space launch cost," *International Conference on Environmental Systems*, vol. 38, 2018.
- [151] U. L. Alliance. (2022). "Atlas v - ula," [Online]. Available: <https://www.ulalaunch.com/rockets/atlas-v> (visited on 02/16/2022).
- [152] —, "Delta iv user guide," *United Launch Alliance*, vol. 1, 2013.
- [153] I. L. Services, "Proton launch system mission planner's guide," *International launch Services*, vol. 1, 2009.
- [154] S. Clark. (2020). "Russia's angarra a5 rocket succesful in second test flight," [Online]. Available: <https://spaceflightnow.com/2020/12/14/russias-angara-a5-rocket-succesful-in-second-test-flight/> (visited on 02/16/2022).

- [155] e. a. RS. Praveen N.Jayan, "Development of cryogenic engine for gslv mkiii: Technological challenges," *Materials Science and Engineering*, vol. 171, 2017.
- [156] E. S. Agency. (2021). "New esa contracts to advance prometheus and phoebus projects," [Online]. Available: https://www.esa.int/Enabling_Support/Space_Transportation/New_ESA_contracts_to_advance_Prometheus_and_Phoebus_projects (visited on 09/03/2021).
- [157] M. Aerospace. (2021). "Mt aerospace and ariane group sign prototype development contract for optimized ariane 6 upper stage," [Online]. Available: <https://www.mt-aerospace.de/news-details-en/mt-aerospace-and-arianegroup-sign-prototype-development-contract-for-optimized-ariane-6-upper-stage.html> (visited on 02/23/2022).
- [158] T. K. DeLay, "Composite-material tanks with chemically resistant liners," *Marshall Space Flight Center, Alabama*, 2004.
- [159] A. Zak. (2022). "Tangara-5 to replace proton," [Online]. Available: <http://www.russianspaceweb.com/angara5.html> (visited on 03/31/2022).
- [160] T. Edwards, "Liquid fuels and propellant for aerospace propulsion," *Journal of Propulsion and Power*, vol. 19, no. 6, pp. 1089–1107, 2003.
- [161] T. Borsboom, "The design and testing of an injector for an advanced hypergolic dual-mode propulsion system," M.S. thesis, Delft University of Technology, 2021.
- [162] W. F. G. Rarata, "The handling hazards of propellant hypergolic with hydrogen peroxide," *Conference: XIV Międzynarodową Konferencję Naukową IPOEX 2017*, vol. 14, 2017.
- [163] I. G. et al., "Effect of soot particles on supersonic rocket plume properties," *International Journal of Turbo and Jet Engines*, vol. 29, no. 2, pp. 89–110, 2012.
- [164] S. Y. M. Ventura S. Heister, "Rocket grade hydrogen peroxide (rghp) for use in propulsion and power devices - historical discussion of hazards," *43rd IAA/ASME/SAE/ASEE Joint Propulsion Conference and Exhibit, Cincinnati*, vol. 43, 2007.
- [165] T. Dodd. (2019). "Is spacex's raptor engine the king of rocket engines?" [Online]. Available: <https://everydayastronaut.com/raptor-engine/> (visited on 03/10/2022).
- [166] C. C. H.D. Kwak S. Kwon, "Performance assessment of electrically driven pump-fed lox/kerosene cycle rocket engine: Comparison with gas generator cycle," *Aerospace Science and Technology*, vol. 77, pp. 67–82, 2018.
- [167] G. N. Jr. F. Moring. (2015). "Rocket lab unveils battery-powered turbomachinery," [Online]. Available: <http://aviationweek.com/space/rocket-lab-unveils-battery-powered-turbomachinery> (visited on 09/03/2021).
- [168] J. F. Z. Huang and F. Kuck, "Key reliability drivers of liquid propulsion engines and a reliability model for sensitivity analysis," *American Institute of Aeronautics and Astronautics*, 2005.
- [169] S. Clark. (2010). "Live coverage of the inaugural falcon 9 rocket launching a dragon test unit on a demonstration flight," [Online]. Available: <https://spaceflightnow.com/falcon9/001/status.html> (visited on 03/15/2022).
- [170] R. B. et al., "Borone compounds," *Ullmann's Encyclopedia of Industrial Chemistry*, 2000.
- [171] O. B. G.P. Sutton, Ed., *Rocket Propulsion Elements*. JOHN WILEY and SONS, INC., 2001, ISBN: 0-471-32642-9.
- [172] A. G. et al., "Oxidation of molecular nitrogen with hydrogen peroxide," *Izvestiya Akademii Nauk. Seriya Khimicheskaya*, vol. 1, no. 3, pp. 733–735, 2003.
- [173] e. a. J.S. Mok W.E. Anderson, "Thermal decomposition of hydrogen peroxide, part i: Experimental results," *Journal of Propulsion and Power*, vol. 21, no. 5, pp. 942–953, 2005.
- [174] V. Clark, "Modelling of propellant management systems in early-phase launcher development," *6th European Union Conference for Aerospace Sciences*, 2015.

- [175] D. Mosher. (2016). "The 'trickiest' part of elon musk's mars spaceship — a giant black orb — just passed a critical test," [Online]. Available: <https://www.businessinsider.nl/spacex-carbon-fiber-fuel-tank-ocean-ship-test-2016-11?international=true&r=US> (visited on 03/17/2022).
- [176] H. G. et al., "Columbia - accident investigation board," *Columbia Accident Investigation Safety Board*, vol. 1, 2003.
- [177] B. K. e. a. J.A. Goff, "Realistic near-term propellant depots: Implementation of a critical space-faring capability," *American Institute of Aeronautics and Astronautics*, 2009.
- [178] J. P. T. Pereira J.V. Kennedy, "A comparison of traditional manufacturing vs additive manufacturing, the best method for the job," *Procedia Manufacturing*, vol. 30, pp. 11–18, 2019.
- [179] N. Z. I. of Chemistry. (2021). "The manufacture of hydrogen peroxide," [Online]. Available: <https://nzic.org.nz/app/uploads/2017/10/1E.pdf> (visited on 09/06/2021).
- [180] U. Gotzig, "Challenges and economic benefits of green propellants for satellite propulsion," *7th European Conference for Aeronautics and Space Sciences*, vol. 7, 2015.
- [181] N. L. of Medicine. (2021). "Hydrogen peroxide - shipment methods/regulations," [Online]. Available: <https://webwiser.nlm.nih.gov/substance?substanceId=322> (visited on 09/06/2021).
- [182] D. M. Jeff, "Hydrogen peroxide - the safe supply and handling of htp," *Solvay Interlox, Inc.*, 2019.



Inflation Charts

The inflation rates of the European Union since 2015 is graphically shown in Figure A.1. This helps to find the required inflation correction factor for the cost estimation in chapter 6. The EU values are obtained from the Organisation for Economic Co-Operation and Development (OECD) [115].

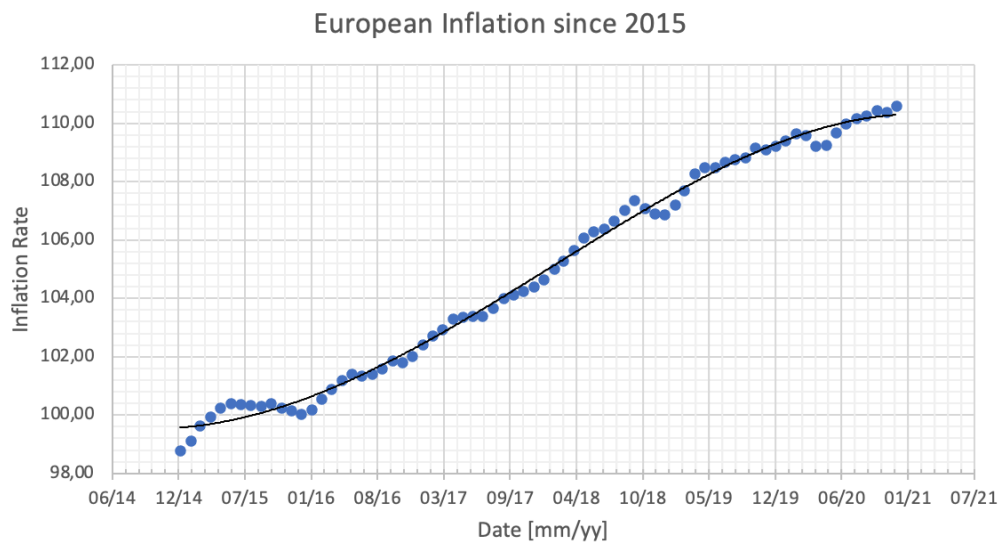


Figure A.1: Average Monthly Inflation since 2015 in the European Union [115]

B

Hydrogen Peroxide Material Compatibility

Hydrogen Peroxide Material Compatibility Chart

All wetted surfaces should be made of materials that are compatible with hydrogen peroxide. The wetted area or surface of a part, component, vessel or piping is a surface which is in permanent contact with or is permanently exposed to the process fluid (liquid or gas).

Less than 8% concentration H₂O₂ is considered a non-hazardous substance. Typically encountered versions are baking soda-peroxide toothpaste (0.5%), contact lens sterilizer (2%), over-the-counter drug store Hydrogen Peroxide (3%), liquid detergent non-chlorine bleach (5%) and hair bleach (7.5%).

At 8% to 28% H₂O₂ is rated as a Class 1 Oxidizer. At these concentrations H₂O₂ is usually encountered as a swimming pool chemical used for pool shock treatments.

In the range of 28.1% to 52% concentrations, H₂O₂ is rated as a Class 2 Oxidizer, a Corrosive and a Class 1 Unstable (reactive) substance. At these concentrations, H₂O₂ is considered industrial strength grade.

Concentrations from 52.1% to 91% are rated as Class 3 Oxidizers, Corrosive and Class 3 Unstable (reactive) substances. H₂O₂ at these concentrations are used for specialty chemical processes. At concentrations above 70%, H₂O₂ is usually designated as high-test peroxide (HTP).

Concentrations of H₂O₂ greater than 91% are currently used as rocket propellant. At these concentrations, H₂O₂ is rated as a Class 4 Oxidizer, Corrosive and a Class 3 Unstable (reactive) substance.

Material	Compatibility 10% H ₂ O ₂	Compatibility 30% H ₂ O ₂	Compatibility 50% H ₂ O ₂	Compatibility 100% H ₂ O ₂ (HTC)
Chemical resistance data is based on 72° F (22° C) unless otherwise noted				
A- Suitable				
B - Good, minor effect, slight corrosion or discoloration				
F - Fair, moderate effect, not recommended for continuous use;				
softening, loss of strength, and/or swelling may occur				
X - Do Not Use - severe effect, not recommended for ANY use				
NA - Information Not Available				
304 stainless steel	B ¹	B ¹	B ¹	B ¹
316 stainless steel	B	B	A ¹	A ¹
416 stainless steel	B	B	F	X
440C stainless steel	B	B	A	X
ABS plastic	A	A	A	A

It is the sole responsibility of the system designer and user to select products suitable for their specific application requirements and to ensure proper installation, operation, and maintenance of these products. Material compatibility, product ratings and application details should be considered in the selection. Improper selection or use of products described herein can cause personal injury or product damage. In applications where exposure to harmful chemicals is frequent, of long duration or in high concentrations, additional testing is recommended.



End your search, simplify your supply chain
ISO 9001:2015 Certified Companies

4091 S. Eliot St., Englewood, CO 80110-4396
Phone 303-781-8486 | Fax 303-761-7939
Ismedspec.com

© Copyright 2020 IS MED Specialties

Hydrogen Peroxide Material Compatibility Chart

ver 09-Jul-2020

Material	Compatibility 10% H ₂ O ₂	Compatibility 30% H ₂ O ₂	Compatibility 50% H ₂ O ₂	Compatibility 100% H ₂ O ₂ (HTC)
----------	--	--	--	---

Chemical resistance data is based on 72° F (22° C) unless otherwise noted

A - Suitable

B - Good, minor effect, slight corrosion or discoloration

F - Fair, moderate effect, not recommended for continuous use;

softening, loss of strength, and/or swelling may occur

X - Do Not Use - severe effect, not recommended for ANY use

NA - Information Not Available

1 - Satisfactory to 120°F (48° C)

2 - Satisfactory for O-rings, diaphragms or gaskets

3 - Temporary use only

Acetal (Delrin®)	X	X	X	X
Acrylic (PMMA)	B	F	NA	X
Alloy 20 (Carpenter 20)	F	B	B	X
Aluminum	A	A	A	A
Brass	X	X	X	X
Bronze	B	B	B	B
Buna N (Nitrile)	X	X	X	X
Carbon graphite	F	F	F	F
Carbon steel	X	X	X	X
Cast iron	F	X	X	X
Ceramic Al ₂ O ₃	A	A	A	A
Ceramic magnet	A	A	A	A
Copper	X	X	X	X
CPVC	A	A	A	A
EPDM	A	B	B	X
Epoxy (epoxide polymers)	F	B	B	X
FKM (fluoroelastomers, Viton®)	A	A	A	A
Hastelloy-C®	A	A	A	A
HDPE	A	A	A	X
Hypalon®	X	X	X	X
Hytre® (polyester elastomer)	X	X	X	X
LDPE	A	F ¹	F ¹	F ¹
Natural rubber	B	F	F	F
Neoprene	X	X	X	X
NORYL®	A ¹	A ¹	A	A

It is the sole responsibility of the system designer and user to select products suitable for their specific application requirements and to ensure proper installation, operation, and maintenance of these products. Material compatibility, product ratings and application details should be considered in the selection. Improper selection or use of products described herein can cause personal injury or product damage. In applications where exposure to harmful chemicals is frequent, of long duration or in high concentrations, additional testing is recommended.



End your search, simplify your supply chain
ISO 9001:2015 Certified Companies

4091 S. Eliot St., Englewood, CO 80110-4396
Phone 303-781-8486 | Fax 303-761-7939
Ismedspec.com

© Copyright 2020 IS MED Specialties

Hydrogen Peroxide Material Compatibility Chart

ver 09-Jul-2020

Material	Compatibility 10% H ₂ O ₂	Compatibility 30% H ₂ O ₂	Compatibility 50% H ₂ O ₂	Compatibility 100% H ₂ O ₂ (HTC)
Chemical resistance data is based on 72° F (22° C) unless otherwise noted				
A- Suitable				
B - Good, minor effect, slight corrosion or discoloration				
F - Fair, moderate effect, not recommended for continuous use;				
softening, loss of strength, and/or swelling may occur				
X - Do Not Use - severe effect, not recommended for ANY use				
NA - Information Not Available				
Nylon (polyamides)	F	X	X	X
PCTFE (Kel-F® and Neoflon®)	A ¹	A ¹	A ¹	X
PFA (perfluoroalkoxy alkanes)	A	A	A	A
Polycarbonate	A ¹	A ¹	A ¹	A
Polypropylene	A	B	B	B
PP-363 (plasticized vinyl) ²	A	A	A	X
PPS (Ryton®)	A	A	F	F
PTFE (Garlock Glyon® 3500) ²	A	A	A	X
PTFE (Teflon®), virgin ²	A	A	A	A
PVC	A	A	A	A
PVDF (Hylar®)	A ¹	A ¹	X	X
PVDF (Kynar®)	A	A	A	A
PVDF (Solef®)	A ¹	A ¹	X	X
Silicone	A	B	B	B
SPR (styrene butadiene rubber)	X	X	X	X
Thiokol™ (polysulfide polymers)	X	X	X	X
Titanium ³	A	B	B	B
TPE (thermoplastic elastomers)	X	X	X	X
TPU (thermoplastic polyurethanes)	X	X	X	X
Tygon®	B	B	B	B
Tungsten carbide	X	X	X	X
Viton® A ²	A	A	A	A

It is the sole responsibility of the system designer and user to select products suitable for their specific application requirements and to ensure proper installation, operation, and maintenance of these products. Material compatibility, product ratings and application details should be considered in the selection. Improper selection or use of products described herein can cause personal injury or product damage. In applications where exposure to harmful chemicals is frequent, of long duration or in high concentrations, additional testing is recommended.



End your search, simplify your supply chain
ISO 9001:2015 Certified Companies

4091 S. Eliot St., Englewood, CO 80110-4396
Phone 303-781-8486 | Fax 303-761-7939
Ismedspec.com

© Copyright 2020 IS MED Specialties